Recovery dynamics of ants in the Ecuadorian Chocó

vom Fachbereich Biologie
der Technischen Universität Darmstadt
zur Erlangung des Grades
Doktor rerum naturalium
(Dr. rer. nat.)

Dissertation von
Philipp Otto Hönle
aus Leonberg, Deutschland

Erstgutachter: Prof. Dr. Nico Blüthgen
Zweitgutachter: PD Dr. Michael Heethoff

Darmstadt 2022

Hönle, Philipp Otto: Recovery dynamics of ants in the
Ecuadorian Choco.
Darmstadt, Technische Universität Darmstadt.

Queen of the ant Ectatomma tuberculatum from the Reserva Rio Canandé, Ecuador.

Contents

SUMMARY

A question of global importance is if, and how fast, ecosystems can naturally recover to regain their previous biodiversity and ecosystem functions. Given the decrease of old-growth forest cover in tropical landscapes, previously disturbed forests and their ability to recover are gaining importance. This is especially relevant for biodiversity hotspots, which are areas with many endemic species under severe threat through human activities. However, current knowledge on the recovery potential and underlying processes is limited, especially for animals. Ants constitute one of the most abundant insects in tropical ecosystems and are of paramount importance for ecosystem functioning, making them ideal indicators for disturbance and recovery processes.

In my thesis, I therefore investigated the recovery of ant communities in the Ecuadorian Chocó, which is part of the Tumbes-Chocó-Magdalena biodiversity hotspot. By using a chronosequence approach spanning 0 – 34 years of recovery, I explored the recovery of ant communities after forest clearance for agriculture, and if legacy effects from past land-use (cacao plantations and pastures) affect the recovery. In my first study, I found that ant communities recover quickly in approximately less than four decades, with former cacao plantations having a slight advantage over former pastures.

My second study is devoted to stratification patterns during recovery, as stratification strongly affects insect communities and abundance. For instance, ant communities in the leaf litter constitute different sets of species than those on tree trunks. However, the role of such stratification patterns during recovery is barely known. I sampled ants in three strata (ground, leaf litter, lower tree trunk) and assembled a comprehensive dataset with a total of 183 assemblages (three strata in 61 plots, comprising 283 species). I assessed the ants' species composition, 13 morphological traits (measured from over 600 specimens), and functional and phylogenetic diversity to compare their recovery trajectories. My results supported the hypothesis that the ants' reassembly is influenced by recovery age and, most importantly, differs among strata.

By providing a curated ant collection of the Chocó region, my research represents a valuable resource for future work of this underexplored region. The collecting effort resulted in the description of two new trap-jaw ant species, *Odontomachus davidsoni* (third study) and *Strumigenys ayersthey* (fourth study). These species are morphologically outstanding, and possibly endemic to the Chocó. The discovery of new, conspicuous species highlights the biological relevance of the Chocó as threatened biodiversity hotspot. Most importantly, my study demonstrated that the small-scale agricultural areas in the region have a high recovery potential, suggesting that conservation measures in the area have good chances to succeed in preserving biodiversity.

ZUSAMMENFASSUNG

Es ist von globaler Bedeutung wie schnell sich Ökosysteme nach einer Störung regenerieren, und dabei ihre vorige Biodiversität und Ökosystemfunktionen erreichen. Angesichts der stetigen Abnahme von Primärwaldflächen in tropischen Landschaften steigt die Bedeutung des Regenerationspotenzial von degradierten Habitaten. Besonders wichtig ist dies für sogenannte Biodiversitäts-Hotspots, also Regionen mit hohen Vorkommen an endemischen Arten die gleichzeitig in ihrer Existenz durch menschliche Habitatdegeneration bedroht sind.

In dieser Dissertation untersuche ich daher die Regenerationsprozesse von Ameisengemeinschaften im ecuadorianischen Chocó, welcher zu dem Tumbes-Chocó-Magdalena Biodiversitäts-Hotspot gehört. Ameisen gehören zu den häufigsten Insekten in tropischen Habitaten, und erfüllen eine Vielzahl von unersetzlichen Ökosystemfunktionen. Dies macht sie daher zu idealen Indikatoren für Störungs- und Regenerationsprozessen. Um die Ameisenregeneration zu erforschen, nutze ich in meiner ersten Studie eine Chronosequenz welche 0 – 34 Jahre von natürlicher Regeneration abdeckt, und betrachte wie schnell die Ameisengemeinschaften das Primärwaldniveau erreichen und ob die ehemalige Landnutzung auf diesen Flächen (Kakaoplantagen und Weiden) eine Rolle in ihrer Regeneration spielt. Tatsächlich zeige ich, dass die Ameisen relativ schnell in weniger als 4 Jahrzehnten das Primärwaldniveau erreichten, wobei ehemalige Kakaoplantagen tedenziell schneller sind als Weiden.

Meine zweite Studie widmet sich der Stratifizierung während der Regeneration. Stratifizierung hat großen Einfluss auf Insektengemeinschaften: In der Streuschicht des Waldes leben beispielsweise andere Ameisenarten als auf Baumstämmen. Allerdings ist nur wenig bekannt, welche Rolle diese Stratifizierung in der Regeneration spielt. Ich sammelte daher Ameisen aus drei unterschichtlichen Strata (Boden, Streuschicht, unterer Baumstamm), und stellte ein umfassendes Datenset mit 183 Ameisengemeinschaften zusammen (drei Strata in 61 Plots, ingesamt 283 Arten). Dabei wurde die Artkomposition, 13 morphologische Eigenschaften (gemessen an über 600 Individuen) und funktionelle und phylogenetische Diversität der Ameisen erfasst, und anschließend ihre Regenerationsdynamiken betrachtet. Meine Ergebnisse unterstützen die Hypothese, dass die Regeneration der Ameisengemeinschaften sowohl durch das Regenerationsalter als auch durch die Stratifizierung beeinflusst wird.

Meine Arbeit stellt eine wichtige Ressource für künftige Forschungsarbeiten dar, da zusätzlich zu meinen quantitativen Forschungsarbeiten eine kurierte Ameisensammlung der bislang nur wenig erforschten Chocó-Region aufgebaut wurde. Dies führte auch zu der Entdeckung und Beschreibung von zwei neuen Schnappkieferameisenarten, *Odontomachus davidsoni* (dritte Studie) und *Strumigenys ayersthey* (vierte Studie). Die neuen Arten sind morphologisch außergewöhnlich, und wahrscheinlich endemisch im Chocó. Dies zeigt die Relevanz und das Potenzial des Chocó als Biodiversitäts-Hotspot. Die bedeutendste Erkenntnis meiner Forschung ist, dass die kleinen, lokalen Agrikulturflächen ein hohes Regenerationspotenzial besitzen, und damit Umweltschutzmaßnahmen in der Region gute Chancen auf Erfolg in der Erhaltung der Biodiversität besitzen.

1 GENERAL INTRODUCTION

More than two centuries after the first pioneering research of explorers such as Alexander von Humboldt and Charles Darwin, Ecuador's tropical rainforests remain vastly underexplored. In popular perception, Ecuador is the epitome of a pristine place, inspiration to some of the most important biological theories such as evolution (Darwin 1872). While it is true that Ecuador hosts some of the most impressive biodiversity on earth, it is unfortunately also threatened by human activities (Dinerstein 1995). Surveying the species-rich insect communities of tropical forests will remain a scientific challenge for many decades, if not centuries, of human discovery. As deforestation takes heavy tolls, time runs out, as more and more species face threats of extinction even before being discovered.

Since early ages of exploration, biological research has expanded from merely describing species to seeking an understanding of how an ecosystem can host so many species, and how these species are assembled into such complex tropical communities. A central aim of ecology is to extract the underlying rules that lead to this assembly. The complexity and diversity of a tropical ecosystem drives curiosity, but also poses a challenge: it is necessary to break the complex system into many smaller components, which finally come together to produce a coherent picture. As tropical rainforests are facing large-scale environmental threats, faunistic and ecological knowledge on the capability of forest regeneration, including the reassembling process of species communities after disturbance (e.g., logging) is more important than ever. Knowledge on the generally applicable rules of species assembly is a central theme for ecological theory and can inform conservation measures. Gaining a better knowledge of the recovery potential of tropical forests is crucial for future conservation management and it thus an aspect that will define the future of human land-use.

In this thesis, I hope to contribute to the understanding of a small, but vital part of any tropical ecosystem - the ant fauna. Ants are among the most abundant animals in tropical ecosystems, and no tropical research would be exhaustive without considering them. In the present thesis, I studied the communities of ants in an Ecuadorian rainforest to better understand how tropical ecosystems re-assemble after disturbance, and how long the process takes. My efforts also resulted in an extensive research collection of the local ant fauna, including the discovery of several new endemic species, two of which I will describe here.

1.1 FOREST RECOVERY AND (RE)ASSEMBLY

A main aspect of my PhD thesis was to investigate the recovery and reassembly process of tropical forests after disturbance. Tropical forests host a large part of global biodiversity. However, many tropical regions experience unsustainable rates of deforestation, and natural landscapes are in decline (Hansen et al. 2013, Potapov et al. 2017, Curtis et al. 2018). In recent years there have been several countering trends, driven by both an increased protection of the remaining habitats as well as an increase in urbanization coupled with rural exodus. Former agricultural areas and other disturbed forests are now on their path to recover, and these areas now represent one the most common type of forest globally (Chazdon 2003, Benayas et al. 2007, Meli et al. 2017). The future of recovering forests will define the success of conservation measures, climate mitigation and the global effort to preserve biodiversity (Curran et al. 2014, Crouzeilles et al. 2016, Lennox et al. 2018, Chazdon et al. 2020). How well the recovering forests act as carbon stocks or habitats for threatened species is much debated, and effective policy decisions rely on scientific consensus. On one hand, undisturbed 'primary' forests are deemed to be irreplaceable, as many organisms struggle to survive within disturbed areas, giving relatively less conservation value to disturbed forests (Gibson et al. 2011). On the other hand, disturbed forests can host an impressive reservoir of animal and plant species (Chazdon et al. 2009). Further, if left undisturbed for long enough, disturbed forest habitats may eventually converge and host the same complex tropical diversity as 'primary' forests. The duration of this process is, however, unclear. Estimations of recovery time to reach the prior old-growth state can span from hundred years to thousands, depending on the surrounding landscape and prior land-use, among other factors (Gibson et al. 2011, Curran et al. 2014, Lennox et al. 2018).

Humans have shaped forest ecosystems, such as the Amazon rainforest, since thousands of years, which is still visible in vegetation structure today (Chazdon 2014, Maezumi et al. 2018). Similarly, the recent human footprint of modern times is, and will be for a long time, visible in recovering forests, where remnants of our past land-use is shaping forest structure and potentially influence the recovery (Pascarella et al. 2000, Bowen et al. 2007, Meli et al. 2017, Chazdon et al. 2020).

Conservation goals should not only include protection of the habitat, but accommodate for the needs of humans, with potentially sustainable use of the ecosystem (Chazdon et al. 2020). The extent and type of land-use determines forest recovery times, which can substantially vary from one place to another (Crouzeilles et al. 2016, Chazdon et al. 2020). Hence, studies addressing the recovery time in specific geographic areas are important to assess the recovery potential of locally occurring forest landscapes.

The forest recovery process can be divided into various sub-processes. For instance, ecologists often differentiate between an ecosystem's resistance and its resilience. In short, resistance describes the disturbance conditions relative to old-growth forest and resilience the rate of recovery relative to its loss. (Pimm 1984, Pimm et al. 2019). A forest with a high resistance can sustain high levels of biodiversity during (e.g. human-induced) disturbance, such as implementing agriculture. A forest with high resilience might have lower levels of biodiversity during human disturbance, but as soon as this disturbance ends, it quickly regains its former level. A forest that is neither resilient nor resistant will inevitable succumb to disturbance.

In my present thesis, I evaluated the resistance and resilience of a tropical rainforest in a biodiversity hotspot - the Ecuadorian Chocó, a region under heavy human land-use pressure. Within this context, I also compared different strata in their recovery trajectory to gain a more complete picture of the recovery process. Forests are complex, three-dimensional habitats, with profoundly different animal communities along their vertical spatial configuration (Schulze et al. 2001, Fermon et al. 2005, Basset et al. 2015). Each of the strata along this axis potentially follows a distinct recovery trajectory. Subsequently, some strata are more likely to be threatened or slower in the recovery process than others (Whitworth et al. 2016, 2019).

Species in local communities do not represent a random subset of species from a larger regional species pool but are the result of a selection process. In the present thesis, the recovery axis (through time) and horizontal axis (through space, i.e., different forest strata) can be interpreted as selective filters on the local species pool. This selection process is also known as environmental filtering (in the widest sense; Kraft et al. 2015, Cadotte and Tucker 2017). The filtering of each species is based on ecologically relevant attributes, so-called functional traits (Kraft et al. 2015, Wong et al. 2019). Thus, the incorporation of functional traits allows for a better understanding of filtering processes across different sets of species (de Bello et al. 2021). Functional traits represent attributes that are connected to specific behaviors or that characterize the ecological role of a species. For instance, eye size is associated with a more subterranean lifestyle in ants, so if it decreases along the chronosequence, light availability is the environmental filter. While environmental filters have been extensively studied, to the best of my knowledge nothing is known about possible interactions between functional filters and recovery processes. For instance, its possible that each functional trait is stratum-specifically filtered during forest recovery.

1.2 STUDY SITE: CHOCÓ, AN ECOSYSTEM UNDER THREAT

Fig. 1.1 Truck loaded with freshly logged tree stems crossing the Río Canandé. The wood is harvested from selectively logged areas around the study area.

My research took place in Ecuador, which belongs to the most species-rich countries in the world. The country, despite its moderate size, is home to a large variety of endemic species (Myers et al. 2000, Jenkins et al. 2013). The high levels of endemism are caused by the country's diverse habitats, which encompasses two of the worlds most species-rich rainforest biomes, the Amazon and the Chocó, which are divided by the Andes. However, while the Amazon traditionally received a lot of scientific attention, the Chocó has almost been neglected.

The study site is in the lowland Chocó (150 - 650 m. a.s.l.), which is an evergreen tropical rainforest in the North-West of Ecuador. It is characterized by high precipitation (at the study site: 2095 mm), which fades away into the dry forests of the Tumbes towards the South. In the West, it stretches to the Pacific Oceans, spawning considerable mangrove growth. Towards the East, it creeps up the Andes, encompassing cloud forests reaching heights above 3000 meters in altitude. Towards the North, it continues through Colombia, connecting to the Chocó-Darién-Magdalena tropical moist rainforest areas that eventually connect to the Panamanian Darien Gap to the Mesoamerican forest biome. This influences its fauna and flora, which overall has more species overlap with Mesoamerican forests than for example the geographically closer Amazon.

Throughout its range, the Chocó is severely altered by human influence, mainly through logging, mining, and diverse forms of agriculture such as oil palm and cattle ranches (Fig 1.1, Critical Ecosystem Partnership Fund 2005). The loss of old-growth rainforest is not equally distributed among its range, and while the Northern Colombian parts remain largely intact, the southern tip of the Chocó has been subjected to heavy deforestation. Here, only 2% of the former forested area consists of undisturbed old-growth forest, and its lowland parts are most vulnerable because almost no national parks provide protection (Critical Ecosystem Partnership Fund 2005).

What happens to the Chocó in the coming decade will determine the survival of many endemic species. Protection of the remaining tropical rainforest fragments alone might be insufficient, as there is not much old-growth forest area left. The remaining forests are fragmented and could potentially suffer from a process called ecosystem decay – in which isolated fragments are no longer able to sustain a high level of biodiversity (Laurance et al. 2002). A viable option is to incorporate regenerating agriculture areas, connecting otherwise isolated forest fragments. Further, the agricultural patches themselves have potential to become old-growth forests if given enough time. Hence, knowledge about the speed and efficiency of forest recovery in former agricultural areas is central in the understanding of threatened areas like the Chocó. In my thesis, I explored the forest recovery of two locally common land-use types – i.e. cacao plantations and livestock pastures. My study design is based on a chronosequence, i.e. a space-for-time replacement, which allows studying recovery dynamics without actually observing long-term changes. My colleagues and I selected several patches of former agricultural land of different recovery ages, which were then stitched together in the data analysis to represent a timeline. While chronosequence approaches have known limitations, they provide a framework to study forest recovery in a feasible period of time (Johnson and Miyanishi 2008, Walker et al. 2010).

Two reserves within the Chocó area were surveyed in my thesis, the 'Reserva Río Canandé' (0.5263 N, -79.2129 E) and the adjacent 'Tesoro Escondido' (0.54111 N, -79.14361 E). They are managed by the NGO 'Jocotoco', which purchased them from a mixture of former smallholder farms and forests. Therefore, the reserves and surrounding areas constitute a mosaic landscape of old-growth rainforests, selectively logged forests (Fig. 1), recovering secondary forests on former pastures or cacao plantations, and currently used pastures and cacao plantations. This landscape configuration makes the reserve and surrounding area ideal for the study of recovery dynamics, which I will outline in more detail in the coming chapter.

1.3 ANT ECOLOGY AND TAXONOMY

The biodiversity inventory and the rainforest recovery study presented in the present thesis were based on a survey of the local ant communities. Ants are not just outstanding organisms because of their social nature and exceptional morphology, but also constitute one of the most abundant groups of terrestrial insects and are thus key elements of almost every terrestrial ecosystem (Lach et al. 2010).

The first ants evolved more than 100 mya years ago and, in contrast to their present abundance, were rare insects (Barden 2017). However, since the end of the Cretaceous (ca. 60 mya), a period where angiosperm forests started to dominate, ants became ecologically dominant and now constitute approximately 60% the total insect abundance in tropical ecosystems (Barden 2017). Their life is not confined to the ground, but they live everywhere from deeper soils up to the highest canopies, making them ideal for the study of community stratification (Klimes et al. 2012, Basset et al. 2015, Wong and Guénard 2020). Further, ants occupy a vast range of trophic levels, ranging from herbivorous diet up to top predators (Lach et al. 2010). Due to their social nature, they are capable of subduing preys many times larger than themselves, and their interactions with other organisms significantly influence whole ecosystems. For instance, the Neotropical army ant *Eciton burchellii* is a keystone species in tropical rainforests (Gotwald Jr 1995). The massive swarm raids of this species feast on a large range of different arthropod prey (Kaspari et al. 2011, Hoenle et al. 2019). Besides its key role as arthropod predator, *E. burchellii* colonies also attracts over a hundred of different animal species ranging from army ant birds to symbiotic mites (Rettenmeyer et al. 2011, von Beeren et al. 2021).

The recovery of forests and that of ants is strongly intertwined, resulting in complex interdependent relationships. This is apparent, for instance, during the early succession in Ecuador's rainforests: *Cecropia* trees are one of the most important successional plants, dominating typical plant communities early in succession and providing various animals with nutrition-rich fruits (Longino 1989, Chazdon 2014). In most of the trees live symbiotic *Azteca* ants, which fend off herbivores and, in turn, are provided with shelter and food by the tree (Fig. 1.2, Longino 1989, 2007).

Ants are found from agricultural areas to old-growth forests, since they are adapted to many different environmental conditions (Lach et al. 2010). The communities, however, often differ strikingly: Human-modified landscapes harbor different sets of species than nearby old-growth forests (Dunn 2004, Gomes et al. 2014, Hethcoat et al. 2019). Ant species turnover is therefore prominent along recovery gradients, making them ideal indicator taxa to study recovery processes (Alonso and Agosti 2000, Schmidt et al. 2013, Tiede et al. 2017). However, there are still large gaps in the understanding of ant community turnover in recovering forests. Research is sparse and often suffers from low replication (Bowen et al. 2007). Estimations of community recovery time are uncommon, and previous studies found that ants had not reached old-growth species diversity levels after more than 50 years (Brazil Atlantic rainforest: Bihn et al. 2008, 2010). Notably, Dunn (2004) estimates that the recovery to reach ant species richness of old-growth forests alone takes approximately 20-40 years, and recovery of species communties are expected to take even longer. Further, the effects of prior land-use are barely known (Debinski et al. 2011).

Fig. 1.2 When disturbed, *Azteca* ants hurringly leave their nest in their living *Cecropia* plant, ready to attack any intruder.

In this thesis, I investigated the process of forest recovery by not only considering species richness and community composition, but also by applying a trait-based approach, which allows untangling filter mechanisms more directly. For ants, an exhaustive trait-database is publicly available (Bishop et al. 2016, Parr et al. 2017, Gibb et al. 2018). Still, the functional reassembly of ants is poorly understood and existing studies are limited to a few regions (e.g., Bihn et al. 2010, Gibb and Cunningham 2013). I therefore assessed the ants' functional recovery in two different land-use legacies, as well as across three forest strata.

Studying the recovery potential of these tropical rainforests entailed that I collected many thousands of ant specimens that needed to be identified, best to the species level. Species-level knowledge is of paramount importance in ecological studies, because without this knowledge, studies are neither replicable nor comparable, and biodiversity conservation is severely impaired

(Wilson 2017). As a tropical ecosystem, the current study was particularly challenging, as the Chocó encompasses an enourmous and poorly-known species diversity. Ecological investigations inevitably lead to the discovery of previously unknown species, and taxonomic follow-up studies are needed.

In the Neotropics, ants belong to the taxa with reasonably good species level knowledge (Fernández et al. 2019). Nonetheless, many species groups remain to be resolved. The ant diversity of Ecuador is considerable, with currently 783 species recorded (Guenard et al. 2017), many of which are endemic (Salazar et al. 2015). However, given the lack of larger inventories, this number is likely to be a large underestimate, especially for the Chocó. From all ant records combined, only about 10% are from the Coastal region (which includes the Chocó), while 70% are from the Amazon (Salazar et al. 2015). While the Amazonian parts of Ecuador were subjected to at least a few ecological ant studies (e.g. Wilkie et al. 2009, 2010), the ant fauna of lowland Chocó remained mostly unstudied (Salazar et al. 2015). However, higher elevation ranges of the Chocó have received scientific exploration, foremost in the Ocosingo reserve (Donoso and Ramón 2009, Donoso 2017). Most importantly, this includes one of the only long-term studies on tropical ant communities (Donoso 2017). Thus, our study in the Chocó adds important knowledge on the ant distribution of Ecuador, resulting in both new species records for the country and also in species completely unknown to science.

Indeed, I described two new ant species from the Chocó as part of this thesis. Both species seem to be endemic and thus under threat of extinction. Both belong to the morphologically unusual group of trap-jaw ants. Trap-jaws are spring-loaded mandibular systems, akin to a mousetrap, that can close with enormous speed (Gronenberg et al. 1993, Gronenberg 1996). The ants use them to capture swiftly moving prey such as springtails, or even for self-defense purposes. Trap jaws convergently evolved many times among ants (Ward et al. 2015, Booher et al. 2021), and the two discovered species are unrelated members of the genera *Odontomachus* and *Strumigenys*. *Odontomachus* ants are relatively large and conspicuous. Since the end of the 70ies no new species were discovered in the genus in South America, which makes this species a rather spectacular new addition to the Ecuadorian ant fauna (Hoenle et al. 2020). Together with the expert Doug Booher, I described an unusual species of *Strumigenys* (Booher and Hoenle 2021). Detecting a new *Strumigenys* species is not surprising to a myrmecologist, as there are 854 species described globally, and since there is already a long list of endemic *Strumigenys* known from Ecuador (Salazar et al. 2015). However, its morphology is unique and an outlier amongst hundreds of other *Strumigenys* species, which led us to erect a new subgenus. Its description has a special focus on its odd-looking mandibular morphology that is involved in the trap-jaw functioning (Booher and Hoenle 2021).

1.4 STRUCTURE OF THE THESIS

My PhD thesis is divided in six chapters, where the **first chapter** served as general introduction and **the last chapter** as a general discussion. Each of the chapters two to five represent scientific publications or manuscripts to be published:

My **second chapter** focuses on the recovery process of ant communities, including the question of how long communities need until old-growth conditions are reached. To achieve this, we implemented a chronosequence with rainforest plots from 0 to 34 years of recovery. The study includes two types of land-use legacies, cacao plantations and pastures. We assessed multiple ecological metrics of the ant fauna, including species richness, species composition and functional traits, and compared their recovery trajectories. This then allowed us to estimate the resistance and resilience of each ecological attribute and further allowed for a comparison between recovery outcomes of the two land-use legacies.

Publication: Philipp O. Hoenle, David A. Donoso, Adriana Argoti, Michael Staab, Christoph von Beeren, Nico Blüthgen (accepted). Rapid ant community re-assembly in a Neotropical forest: recovery dynamics and land-use legacy. Ecological Applications.

In my **third chapter**, I conducted a more fine-scaled analysis addressing the reassembly process of functional ant traits. To achieve this, with the help of my collegues I surveyed ant communities of three different strata: leaf litter, ground, and lower tree trunks. I investigated the species turnover between the strata, as well as their functional and phylogenetic structure. Of special interest are the combined effects of environmental filters that lead to stratification of traits along the vertical axis (strata) and time axis (recovery). Finally, I extracted general re-assembly patterns among the multitude of investigated functional traits.

Philipp O. Hoenle (publication in prep.). Stratification and recovery time jointly shape ant functional re-assembly in a Neotropical forest.

In my **fourth chapter**, we describe a new *Odontomachus* trap-jaw ant species from the Chocó, *O. davisoni*. This includes not only detailed pictures and a morphological description, but also life-history observations and DNA barcodes for molecular species identification. Further, for the first time the DISC3D (Darmstadt Insect Scanner 3D) is used in a taxonomic species description. The scanner allowed us to provide a photogrammetric 3D model of the new ant species, allowing other researchers to easily screen for morphological characters, and to perform morphometric measurements.

Publication: Philipp O. Hoenle, John E. Lattke, David A. Donoso, Christoph von Beeren, Michael Heethoff, Sebastian Schmelzle, Adriana Argoti, Luis Camacho, Berhard Ströbel, Nico Blüthgen. 2020. *Odontomachus davidsoni* sp. nov. (Hymenoptera, Formicidae), a new conspicuous trap-jaw ant from Ecuador species. Zookeys 948:75–105

In the **fifth chapter**, we describe another trap jaw ant species, *Strumigenys ayersthey*. Through µCT scanned images, my colleague and I examined the mandibular morphology of the new species in a comparative framework, and for the first time described proper articulations between the mandibles and clypeus, and the labrum and clypeus. Potentially, they are unique morphological characters of the new species.

Publication: Douglas B. Booher, Philipp O. Hoenle (2021): A new species group of *Strumigenys* (Hymenoptera, Formicidae) from Ecuador, with a description of its mandible morphology. Zookeys 1036:1–9

1.5 REFERENCES

Alonso, L. E. and Agosti, D. 2000. Biodiversity studies, monitoring and ants: An overview. In D. Agosti, J. D. Majer, L. E. Alonso, & R. Shultz (Eds.), Ants. Standard Methods for Measuring and Monitoring Biodiversity (pp. 1– 8). Washington, DC: Smithsonian Institution Press.

Basset, Y., L. Cizek, P. Cuénoud, R. K. Didham, V. Novotny, F. Ødegaard, T. Roslin, A. K. Tishechkin, J. Schmidl, N. N. Winchester, D. W. Roubik, H.-P. Aberlenc, J. Bail, H. Barrios, J. R. Bridle, G. Castaño-Meneses, B. Corbara, G. Curletti, W. Duarte da Rocha, D. De Bakker, J. H. C. Delabie, A. Dejean, L. L. Fagan, A. Floren, R. L. Kitching, E. Medianero, E. Gama de Oliveira, J. Orivel, M. Pollet, M. Rapp, S. P. Ribeiro, Y. Roisin, J. B. Schmidt, L. Sørensen, T. M. Lewinsohn, and M. Leponce. 2015. Arthropod Distribution in a Tropical Rainforest: Tackling a Four Dimensional Puzzle. PLOS ONE 10:e0144110.

von Beeren, C., N. Blüthgen, P. O. Hoenle, S. Pohl, A. Brückner, A. K. Tishechkin, M. Maruyama, B. V. Brown, J. M. Hash, W. E. Hall, and D. J. C. Kronauer. 2021. A remarkable legion of guests: Diversity and host specificity of army ant symbionts. Molecular Ecology 30:5229-5246.

Benayas, J. R., A. Martins, J. M. Nicolau, and J. J. Schulz. 2007. Abandonment of agricultural land: an overview of drivers and consequences. CAB reviews: Perspectives in Agriculture, Veterinary Science, Nutrition and Natural Resources 2:1–14.

Bihn, J. H., G. Gebauer, and R. Brandl. 2010. Loss of functional diversity of ant assemblages in secondary tropical forests. Ecology 91:782–792.

Bihn, J. H., M. Verhaagh, M. Brändle, and R. Brandl. 2008. Do secondary forests act as refuges for old growth forest animals? Recovery of ant diversity in the Atlantic forest of Brazil. Biological Conservation 141:733–743.

Bishop, T. R., M. P. Robertson, H. Gibb, B. J. Van Rensburg, B. Braschler, S. L. Chown, S. H. Foord, T. C. Munyai, I. Okey, and P. G. Tshivhandekano. 2016. Ant assemblages have darker and larger members in cold environments. Global Ecology and Biogeography 25:1489–1499.

Booher, D. B., J. C. Gibson, C. Liu, J. T. Longino, B. L. Fisher, M. Janda, N. Narula, E. Toulkeridou, A. S. Mikheyev, A. V. Suarez, and E. P. Economo. 2021. Functional innovation promotes diversification of form in the evolution of an ultrafast trap-jaw mechanism in ants. PLOS Biology 19:e3001031.

Booher, D. B., and P. O. Hoenle. 2021. A new species group of Strumigenys (Hymenoptera, Formicidae) from Ecuador, with a description of its mandible morphology. ZooKeys 1036:1–19.

Bowen, M. E., C. A. McAlpine, A. P. House, and G. C. Smith. 2007. Regrowth forests on abandoned agricultural land: a review of their habitat values for recovering forest fauna. Biological Conservation 140:273–296.

Cadotte, M. W., and C. M. Tucker. 2017. Should Environmental Filtering be Abandoned? Trends in Ecology & Evolution 32:429–437.

Chazdon, R. L. 2003. Tropical forest recovery: legacies of human impact and natural disturbances. Perspectives in Plant Ecology, Evolution and Systematics 6:51–71.

Chazdon, R. L., C. A. Harvey, O. Komar, D. M. Griffith, B. G. Ferguson, M. Martínez-Ramos, H. Morales, R. Nigh, L. Soto-Pinto, and M. Van Breugel. 2009. Beyond reserves: A research agenda for conserving biodiversity in human-modified tropical landscapes. Biotropica 41:142–153.

Chazdon, R. L. 2014. Second Growth. Chicago: University of Chicago Press.

Chazdon, R. L., D. Lindenmayer, M. R. Guariguata, R. Crouzeilles, J. M. Rey Benayas, and E. Lazos Chavero. 2020. Fostering natural forest regeneration on former agricultural land through economic and policy interventions. Environmental Research Letters 15:043002.

Crouzeilles, R., M. Curran, M. S. Ferreira, D. B. Lindenmayer, C. E. V. Grelle, and J. M. Rey Benayas. 2016. A global meta-analysis on the ecological drivers of forest restoration success. Nature Communications 7:11666.

Curran, M., S. Hellweg, and J. Beck. 2014. Is there any empirical support for biodiversity offset policy? Ecological Applications 24:617–632.

Curtis, P. G., C. M. Slay, N. L. Harris, A. Tyukavina, and M. C. Hansen. 2018. Classifying drivers of global forest loss. Science 361:1108–1111.

Darwin, C.R. 1872. The Origin of Species by Means of Natural Selection. London: John Murray.

Debinski, D. M., R. A. Moranz, J. T. Delaney, J. R. Miller, D. M. Engle, L. B. Winkler, D. A. McGranahan, R. J. Barney, J. C. Trager, and A. L. Stephenson. 2011. A cross-taxonomic comparison of insect responses to grassland management and land-use legacies. Ecosphere 2:1–16.

De Bello, F., C. P. Carmona, A. T. Dias, L. Götzenberger, M. Moretti, and M. P. Berg. 2021. Handbook of Trait-Based Ecology: From Theory to R tools. Cambridge University Press.

Donoso, D. A. 2017. Tropical ant communities are in long-term equilibrium. Ecological Indicators 83:515–523.

Donoso, D. A., and G. Ramón. 2009. Composition of a high diversity leaf litter ant community (Hymenoptera: Formicidae) from an Ecuadorian pre-montane rainforest. Annales de la Société Entomologique de France, 45:487-499.

Dinerstein, E.A. .1995. Conservation Assessment of the Terrestrial Ecoregions of Latin America and the Caribbean. Washington, D.C.: World Bank.

Dunn, R. R. 2004. Recovery of faunal communities during tropical forest regeneration. Conservation Biology 18:302–309.

Fermon, H., M. Waltert, R. I. Vane-Wright, and M. Mühlenberg. 2005. Forest use and vertical stratification in fruit-feeding butterflies of Sulawesi, Indonesia: impacts for conservation. Biodiversity and Conservation 14:333–350.

Fernández, F., R. J. Guerrero, and T. Delsinne. 2019. Hormigas de Colombia. Univ. Nacional de Colombia.

Gibb, H., and S. A. Cunningham. 2013. Restoration of trophic structure in an assemblage of omnivores, considering a revegetation chronosequence. Journal of Applied Ecology 50:449–458.

Gibb, H., N. J. Sanders, R. R. Dunn, X. Arnan, H. L. Vasconcelos, D. A. Donoso, A. N. Andersen, R. R. Silva, T. R. Bishop, and C. Gomez. 2018. Habitat disturbance selects against both small and large species across varying climates. Ecography 41:1184–1193.

Gibson, L., T. M. Lee, L. P. Koh, B. W. Brook, T. A. Gardner, J. Barlow, C. A. Peres, C. J. Bradshaw, W. F. Laurance, and T. E. Lovejoy. 2011. Primary forests are irreplaceable for sustaining tropical biodiversity. Nature 478:378–381.

Gomes, E. C. F., G. T. Ribeiro, T. M. da Silva, and L. Sousa-Souto. 2014. Ant assemblages (Hymenoptera: Formicidae) in three different stages of forest regeneration in a fragment of Atlantic Forest in Sergipe, Brazil. Sociobiology 61:250–257.

Gotwald Jr, W. H. 1995. Army ants: the biology of social predation. Cornell University Press.

Gronenberg, W. 1996. The trap-jaw mechanism in the dacetine ants *Daceton armigerum* and *Strumigenys* sp. Journal of Experimental Biology 199:2021–2033.

Gronenberg, W., J. Tautz, and B. Hölldobler. 1993. Fast trap jaws and giant neurons in the ant *Odontomachus*. Science 262:561–563.

Guenard, B. S., M. D. Weiser, K. Gomez, N. Narula, and E. P. Economo. 2017. The Global Ant Biodiversity Informatics (GABI) database: synthesizing data on the geographic distribution of ant species (Hymenoptera: Formicidae). Myrmecological News 24:83-89.

Hansen, M. C., P. V. Potapov, R. Moore, M. Hancher, S. A. Turubanova, A. Tyukavina, D. Thau, S. V. Stehman, S. J. Goetz, and T. R. Loveland. 2013. High-resolution global maps of 21st-century forest cover change. Science 342:850–853.

Hethcoat, M. G., B. J. King, F. F. Castiblanco, C. M. Ortiz-Sepúlveda, F. C. P. Achiardi, F. A. Edwards, C. Medina, J. J. Gilroy, T. Haugaasen, and D. P. Edwards. 2019. The impact of secondary forest regeneration on ground-dwelling ant communities in the Tropical Andes. Oecologia 191:475–482.

Hoenle, P., J. Lattke, D. Donoso, C. von Beeren, M. Heethoff, S. Schmelzle, A. Argoti, L. Camacho, B. Ströbel, and N. Blüthgen. 2020. *Odontomachus davidsoni* sp. nov. (Hymenoptera, Formicidae), a new conspicuous trap-jaw ant from Ecuador. ZooKeys 948:75–105.

Hoenle, P. O., N. Blüthgen, A. Brückner, D. J. Kronauer, B. Fiala, D. A. Donoso, M. A. Smith, B. Ospina Jara, and C. von Beeren. 2019. Species-level predation network uncovers high prey specificity in a Neotropical army ant community. Molecular Ecology 28:2423–2440.

Jenkins, C. N., S. L. Pimm, and L. N. Joppa. 2013. Global patterns of terrestrial vertebrate diversity and conservation. Proceedings of the National Academy of Sciences 110:E2602–E2610.

Johnson, E. A., and K. Miyanishi. 2008. Testing the assumptions of chronosequences in succession. Ecology Letters 11:419–431.

Kaspari, M., S. Powell, J. Lattke, and S. O'Donnell. 2011. Predation and patchiness in the tropical litter: do swarm-raiding army ants skim the cream or drain the bottle? Journal of Animal Ecology 80:818–823.

Klimes, P., C. Idigel, M. Rimandai, T. M. Fayle, M. Janda, G. D. Weiblen, and V. Novotny. 2012. Why are there more arboreal ant species in primary than in secondary tropical forests? Journal of Animal Ecology 81:1103–1112.

Kraft, N. J. B., P. B. Adler, O. Godoy, E. C. James, S. Fuller, and J. M. Levine. 2015. Community assembly, coexistence and the environmental filtering metaphor. Functional Ecology 29:592–599.

Lach, L., C. Parr, and K. Abbott. 2010. Ant Ecology. Oxford, Oxford university press.

Laurance, W. F., T. E. Lovejoy, H. L. Vasconcelos, E. M. Bruna, R. K. Didham, P. C. Stouffer, C. Gascon, R. O. Bierregaard, S. G. Laurance, and E. Sampaio. 2002. Ecosystem decay of Amazonian forest fragments: a 22-year investigation. Conservation Biology 16:605–618.

Lennox, G. D., T. A. Gardner, J. R. Thomson, J. Ferreira, E. Berenguer, A. C. Lees, R. Mac Nally, L. E. O. C. Aragão, S. F. B. Ferraz, J. Louzada, N. G. Moura, V. H. F. Oliveira, R. Pardini, R. R. C. Solar, F. Z. Vaz-de Mello, I. C. G. Vieira, and J. Barlow. 2018. Second rate or a second chance? Assessing biomass and biodiversity recovery in regenerating Amazonian forests. Global Change Biology 24:5680–5694.

Longino, J. T. 1989. Geographic variation and community structure in an ant-plant mutualism: Azteca and Cecropia in Costa Rica. Biotropica:126–132.

Longino, J. T. 2007. A taxonomic review of the genus Azteca (Hymenoptera: Formicidae) in Costa

Rica and a global revision of the aurita group. Zootaxa 1491:1–63.

Maezumi, S. Y., D. Alves, M. Robinson, J. G. de Souza, C. Levis, R. L. Barnett, E. Almeida de Oliveira, D. Urrego, D. Schaan, and J. Iriarte. 2018. The legacy of 4,500 years of polyculture agroforestry in the eastern Amazon. Nature Plants 4:540–547.

Meli, P., K. D. Holl, J. M. Rey Benayas, H. P. Jones, P. C. Jones, D. Montoya, and D. Moreno Mateos. 2017. A global review of past land use, climate, and active vs. passive restoration effects on forest recovery. PLOS ONE 12:e0171368.

Myers, N., R. A. Mittermeier, C. G. Mittermeier, G. A. Da Fonseca, and J. Kent. 2000. Biodiversity hotspots for conservation priorities. Nature 403:853–858.

Parr, C. L., R. R. Dunn, N. J. Sanders, M. D. Weiser, M. Photakis, T. R. Bishop, M. C. Fitzpatrick, X. Arnan, F. Baccaro, and C. R. Brandão. 2017. GlobalAnts: A new database on the geography of ant traits (Hymenoptera: Formicidae). Insect Conservation and Diversity 10:5–20.

Pascarella, J. B., T. M. Aide, M. I. Serrano, and J. K. Zimmerman. 2000. Land-Use History and Forest Regeneration in the Cayey Mountains, Puerto Rico. Ecosystems 3:217–228.

Pimm, S. L. 1984. The complexity and stability of ecosystems. Nature 307:321–326.

Pimm, S. L., I. Donohue, J. M. Montoya, and M. Loreau. 2019. Measuring resilience is essential to understand it. Nature Sustainability 2:895–897.

Potapov, P., M. C. Hansen, L. Laestadius, S. Turubanova, A. Yaroshenko, C. Thies, W. Smith, I. Zhuravleva, A. Komarova, and S. Minnemeyer. 2017. The last frontiers of wilderness: Tracking loss of intact forest landscapes from 2000 to 2013. Science Advances 3:e1600821.

Rettenmeyer, C. W., M. E. Rettenmeyer, J. Joseph, and S. M. Berghoff. 2011. The largest animal association centered on one species: the army ant Eciton burchellii and its more than 300 associates. Insectes Sociaux 58:281–292.

Salazar, F., F. Reyes-Bueno, D. Sanmartin, and D. A. Donoso. 2015. Mapping continental Ecuadorian ant species. Sociobiology 62:132–162.

Schmidt, F. A., C. R. Ribas, and J. H. Schoereder. 2013. How predictable is the response of ant assemblages to natural forest recovery? Implications for their use as bioindicators. Ecological Indicators 24:158–166.

Schulze, C. H., K. E. Linsenmair, and K. Fiedler. 2001. Understorey versus canopy: patterns of vertical stratification and diversity among Lepidoptera in a Bornean rain forest. Pages 133–152 *in* K. E. Linsenmair, A. J. Davis, B. Fiala, and M. R. Speight, editors. Tropical Forest Canopies: Ecology and Management. Springer Netherlands, Dordrecht.

Tiede, Y., J. Schlautmann, D. A. Donoso, C. I. Wallis, J. Bendix, R. Brandl, and N. Farwig. 2017. Ants as indicators of environmental change and ecosystem processes. Ecological Indicators 83:527–537.

Walker, L. R., D. A. Wardle, R. D. Bardgett, and B. D. Clarkson. 2010. The use of chronosequences in studies of ecological succession and soil development: Chronosequences, succession and soil development. Journal of Ecology 98:725–736.

Ward, P. S., S. G. Brady, B. L. Fisher, and T. R. Schultz. 2015. The evolution of myrmicine ants: phylogeny and biogeography of a hyperdiverse ant clade (H ymenoptera: F ormicidae). Systematic Entomology 40:61–81.

Whitworth, A., C. Beirne, R. Pillco Huarcaya, L. Whittaker, S. J. Serrano Rojas, M. W. Tobler, and R. MacLeod. 2019. Human disturbance impacts on rainforest mammals are most notable in the canopy, especially for larger-bodied species. Diversity and Distributions 25:1166–

1178.

Whitworth, A., J. Villacampa, A. Brown, R. P. Huarcaya, R. Downie, and R. MacLeod. 2016. Past Human Disturbance Effects upon Biodiversity are Greatest in the Canopy; A Case Study on Rainforest Butterflies. PLOS ONE 11:e0150520.

Wilkie, K. T. R., A. L. Mertl, and J. F. Traniello. 2009. Diversity of ground-dwelling ants (Hymenoptera: Formicidae) in primary and secondary forests in Amazonian Ecuador. Myrmecological News 12:139–147.

Wilkie, K. T. R., A. L. Mertl, and J. F. A. Traniello. 2010. Species Diversity and Distribution Patterns of the Ants of Amazonian Ecuador. PLOS ONE 5:e13146.

Wilson, E. O. 2017. Biodiversity research requires more boots on the ground. Nature Ecology & Evolution 1:1590–1591.

Wong, M. K., B. Guénard, and O. T. Lewis. 2019. Trait-based ecology of terrestrial arthropods. Biological Reviews 94:999–1022.

Wong, M. K. L., and B. Guénard. 2020. Subterranean ants. Pages 1–6 *in* C. Starr, editor. Encyclopedia of Social Insects. Springer International Publishing, Cham.

2 RAPID ANT COMMUNITY RE-ASSEMBLY IN A NEOTROPICAL FOREST: RECOVERY DYNAMICS AND LAND-USE LEGACY

This chapter was accepted for publication in the Journal ‘Ecological Applications’.

Authors:

Philipp O. Hoenle[a], David A. Donoso[b, c], Adriana Argoti[d], Michael Staab[a], Christoph von Beeren[a], Nico Blüthgen[a]

Affiliations:

[a]Ecological Networks, Department of Biology, Technical University of Darmstadt, Darmstadt, Germany.

[b]Departamento de Biología, Escuela Politécnica Nacional, Quito, Ecuador.

[c]Centro de Investigación de la Biodiversidad y Cambio Climático, Universidad Tecnológica Indoamérica, Quito, Ecuador

[d]Escuela de Ciencias Biológicas, Pontificia Universidad Católica del Ecuador, Quito, Ecuador.

Author contributions

NB, POH, CvB and MS conceived the ideas and designed methodology; PH and AA conducted the field work; PH and DD identified the ant species; PH and MS analyzed the data; PH led the writing of the manuscript; NB supervised the study. All authors contributed critically to the drafts and gave final approval for publication.

2.1 ABSTRACT

Regrowing secondary forests dominate tropical regions today, and a mechanistic understanding of their recovery dynamics provides important insights for conservation. In particular, land-use legacy effects on the fauna have rarely been investigated. One of the most ecologically dominant and functionally important animal groups in tropical forests are ants. Here, we investigated the recovery of ant communities in a forest – agricultural habitat mosaic in the Ecuadorian Chocó region. We used a replicated chronosequence of previously used cacao plantations and pastures with 1 – 34 years of regeneration time to study the recovery dynamics of species communities and functional diversity across the two land use legacies. We compared two independent components of responses on these community properties: resistance, which is measured as the proportion of an initial property that remains following the disturbance; and resilience, which is the rate of recovery relative to its loss. We found that compositional and trait structure similarity to old-growth forest communities increased with regeneration age, whereas ant species richness remained always at a high level along the chronosequence. Land-use legacies influenced species composition, with former cacao plantations showing higher resemblance to old-growth forests than former pastures along the chronosequence. While resistance was low for species composition and high for species richness and traits, all community properties had similarly high resilience. In essence, our results show that ant communities of the Chocó recovery rapidly, with former cacao reaching predicted old-growth forest community levels after 21 years and pastures after 29 years. Recovery in this community was faster than reported from other ecosystems and was likely facilitated by the low-intensity farming in agricultural sites and their proximity to old-growth forest remnants. Our study indicates the great recovery potential for this otherwise highly threatened biodiversity hotspot.

2.2 INTRODUCTION

The global cover of natural landscapes continues to decline in the 21st century, almost exclusively caused by human land use (Hansen et al. 2013, Potapov et al. 2017, Curtis et al. 2018). A substantial portion of these natural landscapes are forests, which are converted into agricultural areas, leading to habitat loss for forest-adapted species (Curtis et al. 2018). Loss is especially prevalent in the Neotropics, which are particularly vulnerable to commodity-driven deforestation (Curtis et al. 2018, Newbold et al. 2020). However, partly facilitated by rural exodus because of urbanization, a fraction of global forests with previous anthropogenic disturbances are increasingly undergoing natural succession (Benayas et al. 2007, Chazdon and Guariguata 2016, Meli et al. 2017, Chazdon et al. 2020).

Understanding the dynamics of recovering forests plays a pivotal role for future conservation efforts and management strategies (Curran et al. 2014, Moreno-Mateos et al. 2017). Indeed, a pressing issue in modern ecology is to determine ecosystems' regeneration dynamics – for instance, whether a disturbed forest is capable of reaching old-growth conditions, and how long this would take (Chazdon 2003, Gibson et al. 2011, Lennox et al. 2018). Human-induced conversion of forest is generally understood as a disturbance event, and its recovery dynamics to pre-disturbance levels are characterized by ecological concepts such as resistance, resilience and variability (Pimm 1984, Chazdon 2014, Donohue et al. 2016). These concepts are the means to understand and to predict how fast a system can return to its original state.

Previous work showed that forest recovery time is highly variable and mainly influenced by factors such as climate and distance to nearest forest fragments (Lawton et al. 1998, Bowen et al. 2007, Dent and Wright 2009, Crouzeilles et al. 2016, Meli et al. 2017, Crouzeilles et al. 2019). Further, the extent of previous disturbance influences recovery, as e.g. selectively logged forests recover faster than former agricultural areas (Chazdon 2003, Bowen et al. 2007, Meli et al. 2017). Land-use legacy effects are multi-faceted and can, for example, delay natural plant recovery through deprivation of ground nutrients by crops (Pascarella et al. 2000, Holl and Zahawi 2014).

Studying recovery is challenging, because the necessary long-term monitoring data is rarely available (but see Norden et al. 2015). To overcome this, sites with different regeneration age in a similar environment can be studied to represent a chronosequence. However, this approach comes with its own challenges, and while several studies have investigated recovery using chronosequences, important questions remain unanswered, as shortcomings such as low replication are common and recovery hard to predict (Bowen et al. 2007, Chazdon et al. 2007, Norden et al. 2015). In particular, comparisons of faunistic recovery between sites with differing land-use legacies are rare, even for well-studied faunal taxa such as birds and ants (Bowen et al. 2007, Crouzeilles et al. 2016). Ants are an exceptionally abundant group of insects and well-established, representative indicator taxa for environmental gradients and disturbance (Majer 1983, Alonso and Agosti 2000, Schmidt et al. 2013, Arnan et al. 2014, Gibb et al. 2015, Tiede et al. 2017). Understanding their recovery patterns thus allows for a better understanding of general community recovery, as they contribute in many ways to ecosystem functioning (Dunn 2004). While numerous studies have described ant recovery, research on the comparative effects of past land-use is sparse (Williams et al. 2012, Stuhler & Orrock 2016). For example, Debinski et al. (2011) showed that ant communities were affected by past land management in the United States, while in tropical forests this topic remains, to the best of our knowledge, largely unexplored (but see Vasconselos 1999).

To study community recovery dynamics, we sampled ant communities in a secondary tropical forest originating from former cacao plantations and pastures. We investigated effects of land-use legacy, through a chronosequence approach, for regenerating areas of cacao plantations and livestock pastures. We assessed different emergent properties of communities (species composition, taxonomic diversity, functional trait diversity and trait structure), which are characteristics not identifiable from individual organisms alone but arise from higher perspectives of community organization (Konopka 2009). We expected that all properties show a gradual recovery response toward pre-disturbance conditions, meaning their similarity to an old-growth forest reference increases with recovery time (Fig. 2.1). As cacao plantations have been shown to harbor a high diversity of ants, which is mediated through their structural similarity to forest such as leaf-litter and a small canopy layer (Belshaw and Bolton 1993, Delabie et al. 2007), we expected to find a comparatively faster recovery for all properties in cacao compared to pastures, indicating a higher resistance and/or resilience in cacao.

Our aim was to explicitly compare recovery times of related community properties. Because species richness and trait structure are aggregate properties emerging from species composition, but can obtain similar values with entirely different sets of species, we expected that species richness and traits could only be equal or faster than species composition in their recovery. Previous studies indicate that species composition takes often several decades longer than species diversity to recover (Dunn 2004, Curran et al. 2014, Moreno-Mateos et al. 2017), while the recovery of other community properties, such as trait structure, are less explored (Aubin et al. 2013, Barber et al. 2017, Edwards et al. 2021). In line with other studies, we expect that trait structure in agricultural environments is profoundly different from those in old-growth forest, thus resulting in a slower recovery than species richness (Bihn et al. 2010, Rocha-Ortega et al. 2018) (Fig. 2.1). Here, we investigate recovery after disturbance by breaking it into two measurable and statistically independent components: *resistance* and *resilience* (sensu Pimm 1984, Pimm et al. 2019). Resistance is measured as the proportion of an initial property that remains following the disturbance. Resilience on the other hand is a measurement of the recovery rate. We set out to understand how recovery times are influenced by the dynamics of the systems; that is, if different outcomes are primarily driven by effects of resistance or resilience, or a combination of both. As an example, in Fig. 2.1, diversity is conceptualized with a higher resistance in comparison to the other community properties, and thus recovered quicker. We expect resistance to be similar in community composition to traits, as both are tightly linked to each other.

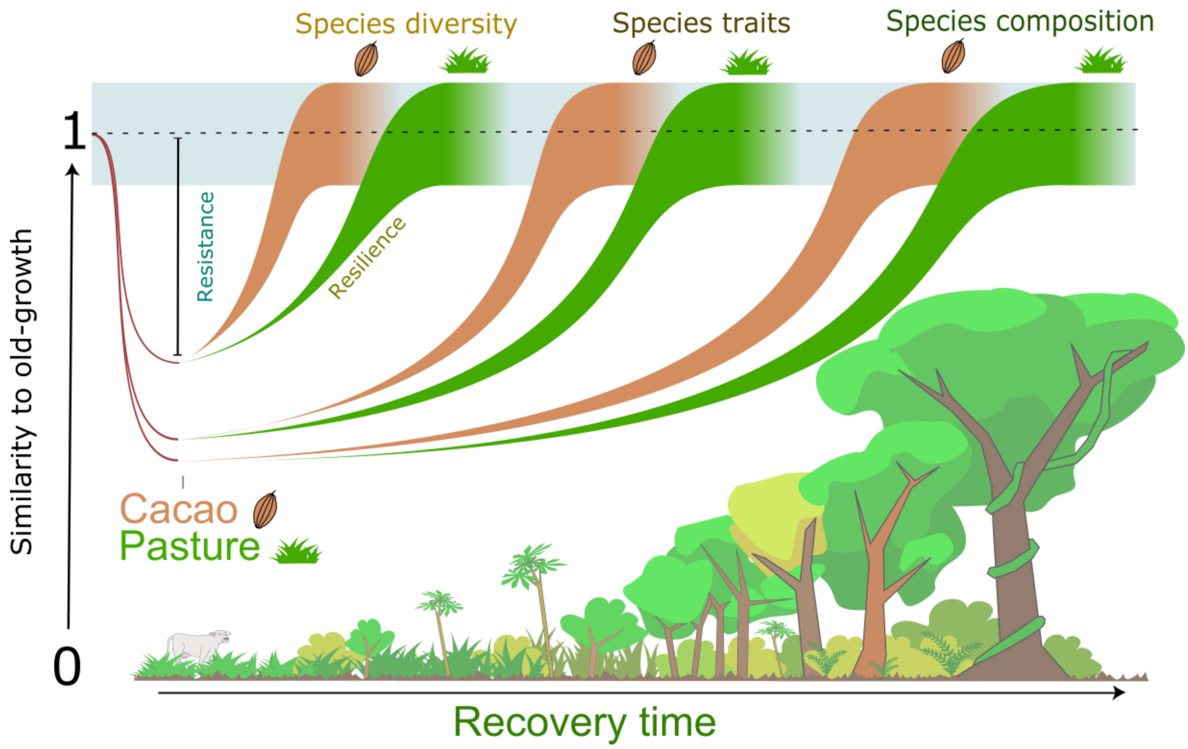

Fig. 2.1: Framework of hypothesized recovery trajectories. Disturbance is represented by deforestation and subsequent agriculture (cacao or pasture), and *resistance* describes the remaining similarity to old-growth forest after disturbance. *Resilience*, in turn, refers to the recovery rate. Old-growth forest represents the reference state (blue top layer). The y-axis therefore defines the similarity to the reference state. We expected to find different recovery times for the three community properties 'species diversity' (here assessed as species richness), 'species traits' and 'species composition', as well as faster recovery time for former cacao plantations (brown trajectories) than pastures (green trajectories). This figure was inspired by Moreno-Mateos et al. (2017).

2.3 MATERIAL AND METHODS

Study site and plot design

Our study was conducted at the Reserva Río Canandé (0.5263 N, 79.2129 W) in Ecuador (Esmeraldas Province) during the rainy season in April – June 2018 and February – May 2019. The reserve and surrounding areas contained old-growth rainforests, regenerating secondary forests that used to be either pastures or cacao plantations (henceforth referred to as regeneration areas), and currently used pastures and cacao plantations. The current land-use in this area is relatively recent, and although we do not have specific dates, interviews with farmers showed that the majority of agricultural use has been within the last 50 years. The land-use is not intensive, but mostly small-scale farming in a forest mosaic landscape. We selected a total of 61 plots, each encompassing an area of 40 m × 40 m. Our plot design included the following habitat categories: eight cacao plots, eight pasture plots, 12 cacao regeneration plots, 17 pasture regeneration plots, and 16 old-growth forest plots. Spatial dependence was minimized by haphazardly selecting locations and by keeping a minimum distance of at least 200 m among plots of the same type. Plots were located at elevations between 127 m and 615 m and showed substantial overlap in elevation (Supplement Fig. S2.1). Old-growth forests had on average the highest elevation (374 ± 30 m), followed by cacao regeneration (319 ± 35 m), pasture regeneration (308 ± 31 m), pasture (205 ± 39 m) and cacao (205 ± 58 m). To account for potential influences of elevation, we incorporated elevation as fixed effect in all our models (see below). The agricultural plots were closely located to the forest edge, the approximate distance of which was assessed with Google Earth (Version 7.3.3.7786) satellite data (mean 60 ± 17 m; range 0 to 233 m). All other plots were embedded within the forest.

The regenerating areas are under natural succession with negligible human interference. Belonging to former smallholder farms, they are distributed patchily throughout the reserve and embedded in a matrix of surrounding forest. The Fundacíon Jocotoco bought most of the farms, and integrated them into the reserve Río Canandé. A few plots were already abandoned before the installation of the reserve. We determined regeneration age by interviewing local park rangers and farmers and incorporated information of land purchase provided by the Fundación Jocotoco. Each plot was assigned the number of years it has been in succession (starting as year of abandonment, range 1 – 34 years). The age distribution and replication is approximately equal among recovery plots: Cacao recovery had seven plots that were younger and five older than 15 years, while pasture recovery had ten plots younger and seven older than 15 years. There were no obvious differences in the plot structure between older recovery plots of pasture and cacao, except for interspersed cacao trees on former cacao plantations. Agricultural areas, i.e. cacao plantations and pastures, were selected from adjacent active farms. The cacao plantations are typically monocultures and lack shade trees (sun-tolerant type). Cacao trees reached a height of approximately four meters, and a distance of four meters between trees in a row, and herbicide application was common. Pasture plots were extensively grazed by cattle, horses or donkeys. While the vegetation consisted mainly of grasses, there are typically sparse trees providing shade for livestock. The regeneration time of plots currently used as agricultural fields was defined as zero years. The two different time trajectories of cacao and pasture, which each consist of year 0 and all following regeneration ages, are referred to as land-use legacies. To facilitate comparisons, we identified 16 plots as old-growth forest that have, to the best of our knowledge, experienced no logging in recent times. These served as reference state and consequently received no regeneration age. Further information on the age and spatial distribution of the plots are given in the Supplement Fig. S2.1.

Ant sampling and identification

On each plot ants were collected with three standardized methods to cover ant diversity from different strata: leaf-litter, epigeal and tree trunk (modified from Agosti et al. 2000). To capture the leaf-litter ant community, we used Winkler extraction. We established a 20 m transect line parallel to one side of the plot. A leaf-litter sample (including topsoil) of approximately 20 cm × 20 cm was collected every 5 m along the transect. We sifted the leaf-litter (1 cm^2 mesh size) for approximately 5 minutes to remove larger twigs and leaves before transferring it into a Winkler bag. We pooled these samples per plot resulting in a total area of 0.2 m^2. Because pastures had no leaf litter, we used a spade to cut out the first five centimeters of the grass turf with the same dimensions and pooled the samples per plot. The samples were subsequently transferred to Winkler bags for 48 hours.

The ground ant community was collected by hand sampling. We used another 20 m transect parallel to the Winkler transect and placed a sampling subplot every 5 m. In each subplot, we collected ants with forceps within an area of 1 m^2 for 5 minutes. The five samples were pooled per plot. We focused on maximizing species numbers by collecting only a few individuals per species (e.g., close to a nest). While collecting, we carefully removed leaf-litter and opened small twigs to look for ant nests.

For tree trunk sampling, we located the five largest trees in each plot and collected ants at trunks for five minutes per tree. Collecting was restricted to reachable heights (0 – 2 m). We focused on collecting ants from the trunk, but also looked under epiphytes and tree bark. Because of the lack of trees on some pastures, we collected from trees directly adjacent to the plot in the same pasture, when necessary. Three of the pastures had fewer than 5 trees but at least one tree per pasture was sampled (total of n=10 missing trees).

To avoid a collector bias, the same person carried out leaf-litter sampling (AA), hand sampling (POH) and tree trunk sampling (POH). Specimens were sorted into morphospecies and identified to species level whenever possible. Detailed information on the ant identification process can be found in the Supplement S2.1 Section S1. Voucher specimens are deposited in the MEPN museum collection at Escuela Politécnica Nacional in Quito. The Ministerio de Ambiente de Ecuador issued the permits for collection (MAE-DNB-CM-2017-0068) and exportation (41-2018-EXPCM- FAU-DNB/MA and 144-2019-EXP-CM-FAU-DNB/MA).

Traits

We measured a subset of morphological traits following Parr et al. (2017). The 10 traits used have repeatedly been shown to be related to ecological attributes of ants (Sosiak & Barden 2020, Weiser & Kaspari 2006, Gibb et al. 2015, Parr et al. 2017). A table of all functional traits used in this study together with a short description of their proposed functional significance can be found in the Supplement S2.1 Table S2.1. For instance, mandible length correlates to feeding mode, with longer-mandibled ants having a more predatory lifestyle, while femur length is positively correlated with structurally more complex environments (Weiser and Kaspari 2006).

We used a Keyence VHX-5000 (Keyence Deutschland BmH, Neu-Isenburg, Germany) for taking high-resolution images and trait measurements. In total, the traits of 653 specimens belonging to 242 species were recorded (Data S1). Due to the high number of species (284 in total) and high number of uniques (99 species) in our data set, we aimed for measurements of at least three specimens per species for more common species (> 10 occurrence), and at least two specimens for rare species (> 2 incidences) except for *Paraponera clavata* (n = 1 specimen measured). On average, we measured traits on 2.7 specimens per species/morphospecies (range 1 – 12).

We measured minor workers in the polymorphic genera *Azteca*, *Pheidole*, *Tranopelta*, *Camponotus* and *Solenopsis*, because other castes were often not available. To assess the ants' color lightness, we assigned each specimen a main color, which was based on the color wheel of Parr et al. (2017). We then used the software GIMP Version 2.10.22 to extract the lightness value for each color coding using the protocol of Law et al. (2020).

All length and width measurements scale with body size. Because we were interested in trait change independent of body size, we regressed all length-measured traits with Weber's length (a surrogate of body size regularly used in ants) in linear models. Each trait was then expressed as the residuals of this model. Trait values of all specimens were averaged on the species level.

Analysis overview

The main objective of our analysis was to compare the recovery trajectories of three elemental community properties, and to break these properties down into recovery components of resistance and resilience. All measures were based on unweighted incidence (presence/absence) of each ant species per plot. The three community properties were species richness, species composition and traits (Fig. 2.1). To facilitate comparisons, all community properties were expressed as a similarity to old-growth forest.

From these similarity metrics, we assessed the *resistance* as the intercept value (recovery year ‘0’) relative to the old-growth forest mean, which we predicted from linear mixed-effects models in a regression against recovery time. This was done separately for each community property, and for each legacy type (cacao and pasture subsets).

For comparing *resilience*, we first unified scales by standardizing between the intercept as 0, and mean old-growth forest value as 1, which was necessary to compare slope values independent of the intercept. Again, we used linear mixed-effects models on the standardized data, and extracted their slopes for regeneration time, i.e., the *resilience*. Resistance and resilience could then be directly compared among each community property and each independent land-use legacy type (see Fig. 2.1). All analyses were performed with the software R (R Core Team 2018; Version 3.5.1).

Species richness

As a measure of species diversity, we calculated the species richness for each plot based on the species incidence. Species richness similarity was calculated as the richness value of each plot relative to the mean richness value across 16 old-growth forest plots as a reference.

Species Composition

For species composition, we created a non-metric multidimensional scaling plot (NMDS) using the Jaccard similarity with the R-package ‘vegan’ (Oksanen et al. 2010). We tested for differences in composition between the habitat categories with the function ‘adonis’ from vegan.

To assess species composition similarity, we summarized all 16 old-growth forest plots by the proportional occurrence p_i of each ant species *i* across all plots as a reference for a mean expected ant community composition in old-gowth forests. This proportion p_i is defined as the number of plots in which species *i* was recorded, divided by the total number of old-growth plots (n = 16). For each plot (including each old-growth plot itself), we then calculated the Bray-Curtis Similarity (1-Bray-Curtis Dissimilarity) to this reference community. Hence, the absence of an ant species in a secondary forest plot that was widespread across all old-growth forests contributes to a larger dissimilarity than the absence of a rare species only found in a single plot.

Traits

As trait measures, we distinguished between the functional diversity (FD indices) and trait structure (community weighted means). Community weighted means (CWMs) are trait averages of plots, weighted by species incidence and are representative of the trait structure. Functional diversity was expressed by a variety of indices which aim to depict multiple aspects of trait diversity: Functional Richness (FRic) is a volume measurement of the amount of functional space filled by the community, Functional Eveness (FEve) quantifies the regularity with which the functional space is filled by species, Functional Divergence (FDiv) measures the average distance of species to the centroid of the functional trait space, and Functional Dispersion (FDis) is an estimator of the dispersion of the species in the trait-dimensional space (Villéger et al. 2008, Laliberté & Legendre 2010).

Based on the averaged species traits and a species incidence matrix that excluded species without trait measurements (excluded ca. 3% of species incidences), we calculated the above-mentioned functional indices (FRic, FEve, FDiv, FDis) as well as the trait structure (CWMs) with the R-package 'FD' (Laliberté et al. 2014). Each of the FD indices, were subsequently expressed as relative values to the average old-growth forest value. We recognize that due to the limitation of using only incidence data our analysis is conservative and the actual functional diversity is potentially underestimated.

As for species richness, trait diversity similarity based on each of the FD indices (one value per plot) was expressed as proportion of the mean old-growth forest value. CWMs were computed for each of the 10 traits in each plot. The trait structural similarity to old-growth forests was then calculated as Gower similarity to the mean old-growth forest trait values.

Statistical analysis

We used linear mixed-effects models with the obtained similarity values as responses, elevation, land-use legacy (pasture or cacao plantation) and regeneration time as fixed effects, and collection year as a random effect (R packages lme4; Bates et al. 2007 and lmerTest; Kuznetsova et al. 2017). Regeneration time was square root transformed to approximately linearize the slope—a commonly used geometric average method for obtaining annual growth rates. As old-growth forest plots did not have a regeneration age, they were not part of the models. We tested for interaction between regeneration time and land-use legacy, but since these were never significant we excluded them from the final models. Residuals of all models met assumptions of normality and homogeneity of variances. We are aware that since similarity values are constrained between 0 and 1, they might in theory violate two assumptions of linear models, the normal distribution of residuals and the homoscedasticity of variances (Douma and Weedon 2019). We therefore applied an alternative beta-regression (R package 'glmmTB'; Brooks et al. 2017) to the similarity values of composition and trait structure (with otherwise identical random and fixed effects structure), and compared the model results and residuals to our LMM approach. Since the residuals showed similar distributions (Supplement Fig. S2.2, S2.3) and model results (Supplement Table S2.2), we used the LMM for the analysis.

For the similarities of each property, we used the function 'predict' to estimate the regeneration time for complete recovery based on the previous linear-mixed effects model, with the average elevation (300.3 m) and the old-growth forest mean. We obtained confidence intervals through bootstrapping with the function 'bootmer' (lme4). Potential spatial autocorrelation was assessed with a Moran's I test from the R-package 'ape' (Paradis et al. 2004) on the model residuals. We also tested whether the distance to the forest edge was correlated with any of the similarities with a Spearman correlation test. This test only included agricultural sites, as all other plots were embedded within the forest. For graphical representation, we used the package 'ggplot2' (Wickham et al. 2016) to plot linear models with 95% confidence intervals for the regeneration types 'cacao' and 'pasture', containing only regeneration time as fixed effect.

Comparison of recovery time

We were interested whether the recovery trajectories differ among functional traits, species richness and species composition (Fig. 2.1). However, claiming that property *A* fully recovers in half of the time as property *B* may imply three scenarios: (i) that *A* and *B* have dropped to a similar amount during disturbance, but *A* recovers twice as fast as *B*, (ii) that *A* has dropped to only half as far as *B* and both recover at a similar rate, or (iii) a combination of level dropped and recovery rate. Consistent with independent concepts and measurements of resistance versus resilience (Pimm 1984, Pimm et al. 2019), we interpret the level to which property *A* dropped in agricultural plots compared to the reference forest as its *resistance* and the relative rate of recovery towards the reference level as *resilience*.

Assuming a linear recovery of property *A* against squareroot-transformed time in our linear-mixed effects models, we defined its *resistance* as the proportion of the intercept (which is the prediction of the level for zero years) in relation to the mean old-growth forests value. To predict the intercept, we used the function 'predict' and average elevation as covariate. We obtained confidence intervals through bootstrapping with the function 'bootmer'. To test whether there was a significant disturbance effect compared to the references (i.e., *resistance* < 1), we used a Wald t-test on the property values of agriculture and old-growth forest.

To calculate *resilience*, each community property *A* was normalized between the intercept defined as zero and the mean old-growth forest value defined as 1, in order to make slopes comparable across properties and independent of the intercept. The resulting slope *ß* for recovery time depicts the proportional change from 0 (defined minimum) to 1 (reference stage) per square-root year.

2.4 RESULTS

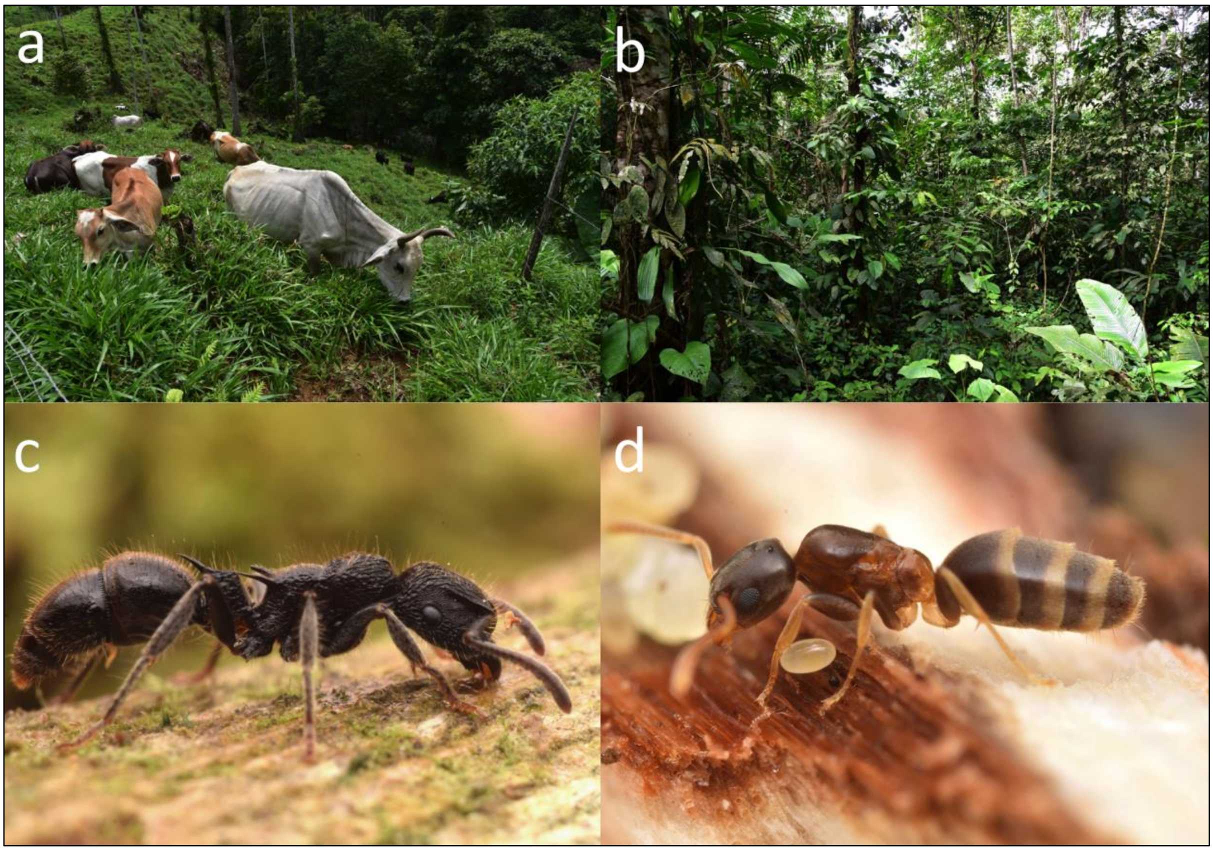

Fig. 2.2 (a) A typical extensively used pasture in the study area of Río Canandé. Picture: K. Mody. (b) Former pasture after 12 years in natural recovery. Picture: K. Mody. (c) Undescribed species of *Acanthoponera* (R. Feitosa, pers. comm.). This genus is relatively rare, and no new species has been described for half a century. (d) The queen of an undescribed species of *Tapinoma* (F.J. Guerro, pers. comm.).

Ant species richness

The Canandé hosted an extremely diverse ant fauna. We recorded a total of 284 species and morphospecies across all plots (Data S1). We found several new country records for ant species and detected several undescribed species (e.g., Fig. 2.2 C, D). Species richness was unrelated to regeneration age ($p = 0.08$; Table 2.1), but increased with elevation ($p = 0.006$; Table 2.1). There was no difference between cacao and pasture recovery ($p = 0.41$, Table 2.1; Fig. 2.3 a). The model predicted a regeneration time to complete recovery of 7.0 years (CI: 2.3 – 14.4) for cacao, and 7.9 years (CI: 2.9 – 15.4) for pasture. We detected no spatial autocorrelation (Moran's I, $p = 0.40$, $I_{(exp)} = -0.02$, $I_{(obs)} = 0.03$). Old-growth plots contained 30 species on average, while agricultural plots harbored 19 species on average, i.e. a relative richness of 63%. The resistance was significantly lower than the Null expectation (Welch t-test t = 4.23, df = 29.96, p < 0.001). The relative ant species richness was unrelated to the distance to forest edge (Spearman correlation, ρ = 0.01, p-value = 0.96).

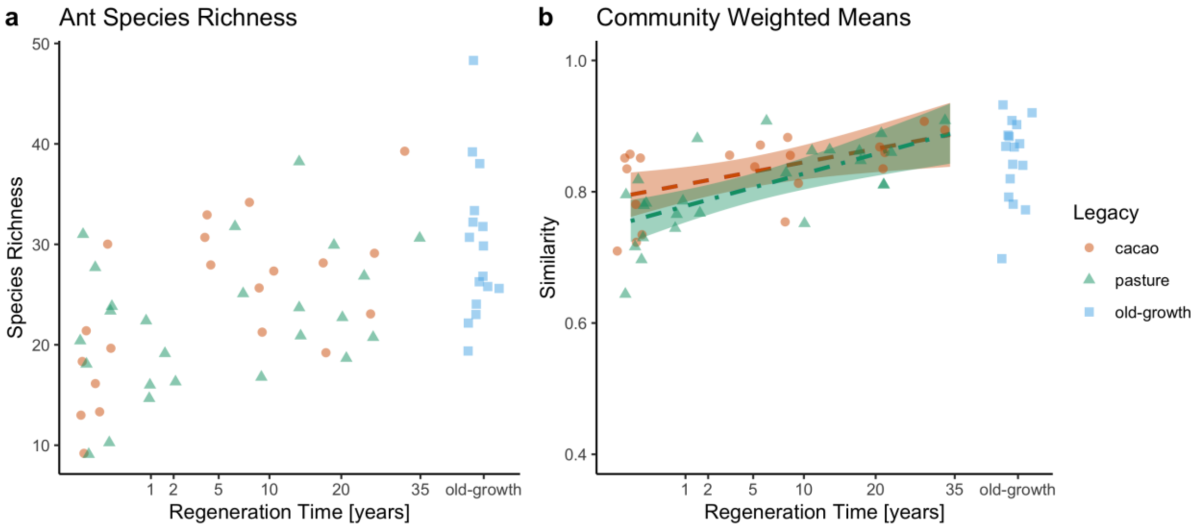

Fig. 2.3 Recovery trajectories illustrating ant species richness along the forest regeneration chronosequence (a) and the standardized similarity of trait CWMs of each plot to the average old-growth forest CWMs (b). Land-use legacy differences are highlighted with green (pasture) and red (cacao), their trajectories are predicted from a linear model with 95% CI. If no dashed lines are shown, there was no significant effect of regeneration time on the similarity (see Table 1).

Table 2.1: Linear mixed-effects model results, with elevation, land-use legacy and squareroot-transformed regeneration time as fixed factors, and collection year as random factor. Resistance is the predicted intercept relative to average old-growth forest mean, and resilience is the slope from a separate model that was standardized with intercept as 0, and old-growth forest mean as 1. Land-use legacy indicates the trajectory of pastures relative to cacao. CI shows 95% confidence intervals. Significant p-values are highlighted in bold.

	Species Diversity Similarity		
	Estimates	*95% CI*	*p*
Intercept	51.204	32.083 – 70.325	**0.003**
Elevation [km]	78.371	25.228 – 131.513	**0.006**
Land-Use Legacy [pasture]	-4.874	-16.430 – 6.681	0.408
Regeneration Time [sqrt years]	2.952	-0.396 – 6.301	0.084
Marginal R^2 / Conditional R^2	0.286 / 0.385		
Resistance [%]	72	58 – 87	**<0.001**
Resilience	0.106	-0.014 – 0.225	0.084
	Species Composition Similarity		
	Estimates	*95% CI*	*p*
Intercept	0.100	0.066 – 0.134	**<0.001**
Elevation [km]	0.206	0.092 – 0.321	**0.001**
Land-Use Legacy [pasture]	-0.038	-0.063 – -0.013	**0.005**
Regeneration Time [sqrt years]	0.025	0.018 – 0.032	**<0.001**
Marginal R^2 / Conditional R^2	0.721 / 0.721		
Resistance [%]	43	37 – 51	**<0.001**
Resilience	0.140	0.101 – 0.178	**<0.001**
	Trait [CWMs] Similarity		
	Estimates	*95% CI*	*p*
Intercept	0.748	0.710 – 0.786	**<0.001**
Elevation [km]	0.179	0.052 – 0.306	0.009
Land-Use Legacy [pasture]	-0.025	-0.053 – 0.003	0.086
Regeneration Time [sqrt years]	0.015	0.007 – 0.022	**<0.001**
Marginal R^2 / Conditional R^2	0.477 / 0.481		
Resistance [%]	**93**	**90 – 96**	**<0.001**
Resilience	0.241	0.113 – 0.368	**<0.001**

Ant species composition

Species composition was significantly different among old-growth forests, recovery plots and agriculture (Supplement S2.1 Fig. S2.4; ADONIS, df = 2, F = 3.71, $R^2 = 0.11$, $p < 0.001$). With increasing age, ant composition of regenerating forests converged toward old-growth forests (Table 2.1, Fig. 2.4). Land-use legacy affected the regeneration trajectory: as expected, communities in current and previous cacao plantations at a given age were more similar to those found in old-growth forests than communities in pastures ($p = 0.005$; Table 2.1, Fig. 2.4). The compositional species similarity was well predicted by a combination of regeneration time, elevation and land-use legacy ($R^2=0.72$, Table 2.1). We found a significant difference between agriculture and old-growth forest in compositional species similarity (Welch t-test t= -16.15, df = 15.0, $p < 0.001$). We predicted a regeneration time of 20.6 years (CI: 13.6 – 29.1) for cacao, and 28.9 years (CI: 19.2 – 40.6) for pastures until full recovery. No signs of spatial autocorrelation were detected (Moran's I, p = 0.17, $I_{(exp)} = -0.02$, $I_{(obs)} = -0.06$), and there was no correlation with distance to forest edge (Spearman correlation test, ρ =-0.004, p-value = 0.98).

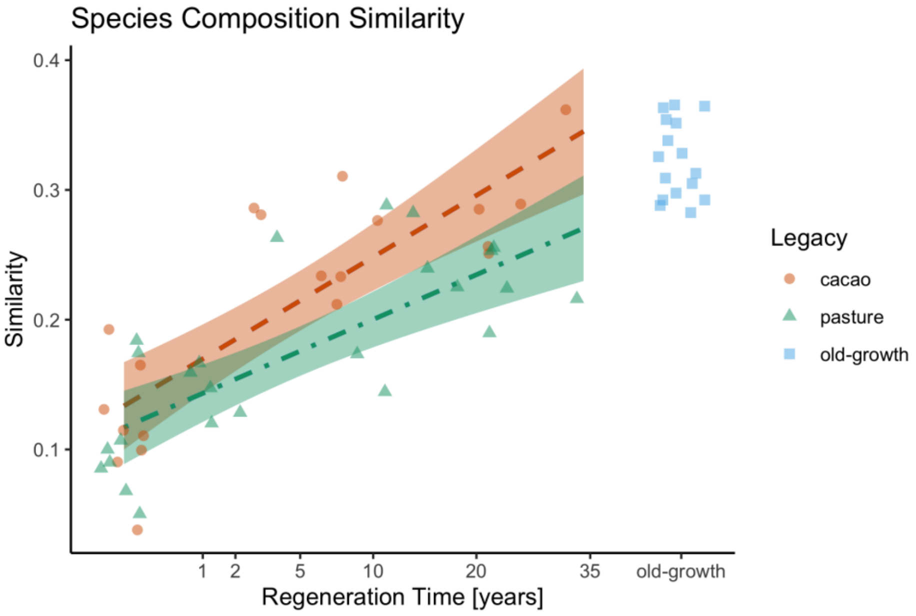

Fig. 2.4 Species composition recovery of ant communities along the chronosequence, measured as the similarity to old-growth forests. Land-use legacy differences are highlighted with green (pasture) and red (cacao), their trajectories are predicted from a linear model with 95% CI.

Functional traits

The CWM similarity increased significantly with regeneration time ($p < 0.001$; Table 2.2, Fig. 2.3 b), and was not influenced by legacy ($p = 0.09$, Table 2.1, Fig. 2.3 b). The model predicted a regeneration time of 6.2 years (CI: 2.5 – 11.3) for cacao and 8.5 years (CI: 4.0 – 14.58) for pasture until complete recovery. No spatial autocorrelation was found (Moran's I, p = 0.75, $I_{(exp)} = -0.02$, $I_{(obs)} = -0.04$), and there was no correlation with distance to the forest edge (Spearman correlation test, ρ =-0.169, p-value = 0.53). All the other functional diversity indices (FRic, FEve, FDiv, FDis) remained relatively constant in agricultural plots and over the entire chronosequence, with no detectable differences in land-use legacy (all p > 0.10). However, relative FRic values differed between agriculture vs. old-growth forest values, having lower values in agriculture (FRic: Welch t-test, t = 3.76, df = 28.78, p-value < 0.001; Supplement S2.1: Table S2.3, Fig. S2.3),

Comparative recovery dynamics

Among the assessed community properties, resistance was by far lowest in species composition with 43% (CI: 37 – 51%). Traits (CWMs) and species richness showed high resistance values with 93% (CI: 90 – 95%) and 72% (CI: 58 – 87%), respectively (Fig. 2.5). The two legacy subsets of cacao and pasture were very similar.

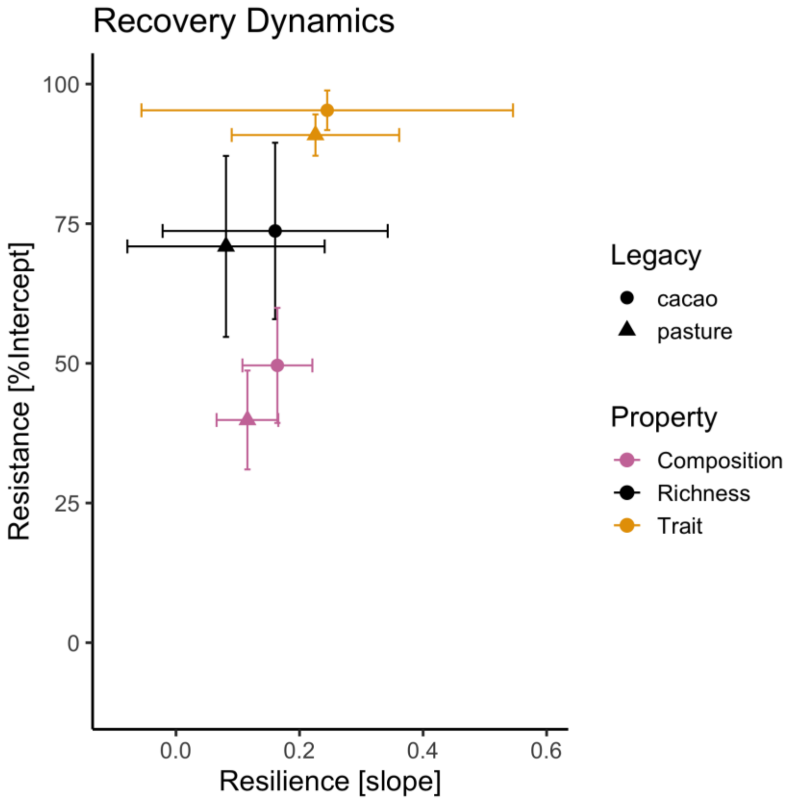

Fig. 2.5 Recovery dynamics of the three studied community properties (species richness similarity, species composition similarity, trait structure similarity), partitioned into resistance and resilience. A property needs less regeneration time the more it is situated towards the upper right, and more regeneration time the more it is situated towards the lower left.

In contrast, differences for resilience were less clear: traits (CWM) recovered fastest with 0.24 (CI: 0.11 – 0.37), followed by species composition with 0.13 (CI: 0.10 – 0.18), and finally species richness with 0.11 (CI: –0.01 – 0.23), but the CIs of the metrics were overlapping (Table 2.1; Fig. 2.5). The cacao and pasture legacy subsets were similar, although the resilience CI of cacao traits overlapped with 0 (i.e., non-significant resilience) while that of pasture traits did not.

2.5 DISCUSSION

We found a rapid recovery of ant communities and their functional traits in the Ecuadorian Chocó and provided evidence that all studied community properties will reach old-growth forest levels within less than four decades. Rapid and complete recovery was facilitated by a high resistance of species richness, trait structure and trait diversity (high similarity to old-growth forest remaining in the disturbed stage) and a similar resilience of all parameters (return rate to pre-disturbance stage). Hence, high levels of species richness occurred along the entire chronosequence, from ongoing agriculture and young secondary forests to mature forests. Whereas agricultural sites had dissimilar ant assemblages compared to old-growth and gradually approached old-growth forests with recovery, species with similar functional traits replaced one another, thus buffering overall changes in the functional trait space. The high resistance of ant communities found in agricultural sites was likely promoted by site conditions: land use was rather small in scale and relatively low in intensity and had occurred over relatively short time periods (few decades). The resilience was likely accelerated by the mosaic of secondary, selectively used and old-growth forests, promoting rapid dispersal of forest animals and plants into early recovery sites, as forest proximity generally aids natural or close-to-natural forest succession (Wijdeven and Kuzee 2000, Chazdon et al. 2009, Dent and Wright 2009).

Ant species richness. Species diversity is one of the most frequently assessed community properties. In line with the few other studies, we recorded comparatively many ant species within the Chocó area (Donoso and Ramon 2009, Donoso 2017). Several studies have linked species diversity to higher ecosystem stability, however, outcomes are mixed among studies (e.g., Oliver et al. 2015, Pennekamp et al. 2018). We found that ant species richness was remarkably constant across the chronosequence, conveying a high resistance to disturbance. However, ant richness has been reported to have idiosyncratic responses to chronosequences in the majority of studies, as some report an increase of species richness or diversity with regeneration time (Bihn et al. 2008, Rocha-Ortega et al. 2018), while others found no such relationship (Belshaw and Bolton 1993, Estrada and Fernández 1999, Schmidt et al. 2013, Staab et al. 2014, Hethcoat et al. 2019).

Ultimately, species richness changes depend on the species pool that is specialized to disturbed areas, which replace forest species during disturbance. In some regions open areas have similar species richness levels to forested areas, and thus a disturbance does not result in a decline of ant species richness (Andersen 2019).

Even though our study design aimed to reduce confounding effects of elevation, we found elevation to be moderately related to all community properties. In particular, elevation seems to be a more influential driver to species richness patterns than recovery time. Elevation increased species richness, which was expected as ant species diversity often peaks at mid-elevations in the Neotropics at around 500 m, which is within our upper boundary (Szewczyk and McCain 2016, Longino and Branstetter 2019).

Species composition. In contrast to species richness, composition accounts for a shift in species identities and often provides a stronger indication of environmental changes. As predicted, ant assemblages showed strong, consistent, and gradual changes towards the conditions found in old-growth forests, with high species turnover across sites and with forest recovery time. From highly dissimilar ant communities in agricultural areas, communities gradually converged to those found at old-growth forest level, and recovery was completed within the timeframe covered by the chronosequence, which is uncommon in chronosequence studies (Dunn 2004, Bowen et al. 2007, Crouzeilles et al. 2016). For instance, ant assemblages in the Atlantic rainforest were not recovered after 50 years of natural recovery (Bihn et al. 2008). Nevertheless, similarity of ant assemblages to old-growth forest assemblages were typically reported to be higher in older than in younger successional stages, suggesting that succession shapes ant assemblages in similar ways across ecosystems all around the globe (Estrada and Fernández 1999, Dunn 2004, Dent and Wright 2009, Neves et al. 2010, Schmidt et al. 2013, Gomes et al. 2014, Staab et al. 2014, Hethcoat et al. 2019).

In our case, abiotic conditions were probably an important driver of the high community similarity of cacao and pasture, and their low similarity to old-growth forest. In particular, early recovery stages and agricultural areas have a warmer, drier and more fluctuating microclimate due to the lack of canopy cover compared to old-growth forests (Meijide et al. 2018, Gregory et al. 2019). We found that differences shaped by land-use start to clearly emerge only in the successional stages. Communities from recovering cacao had a consistently higher similarity to old-growth forest than those derived from pastures throughout the chronosequence, which lead to faster recovery rates for previous cacao sites (ca. 21 years) than for former pastures (ca. 29 years). Our findings are consistent with studies in cacao agriculture, in particular agroforestry, which showed particularly rich ant communties, especially in the leaf-litter (Belshaw and Bolton 1993, Delabie et al. 2007), representing an advantage of recovering cacao over non-woody crops.

Functional traits. Functional traits link species to their assumed functions (Wong et al. 2019). Given that species composition showed a strong response to disturbance and thus substantial changes with recovery, it is surprising that this response is not nearly as strongly reflected in their functional diversity. While trait structure (community-weighted means) gradually approached levels of old-growth forest with increasing recovery time, they had a high resistance to disturbance. The functional diversity indices, frequently applied to describe the trait space of communities, showed no change across the chronosequence, further highlighting a high functional redundancy of ant communities. This was unexpected since several studies on ant recovery found pronounced effects of environmental change on trait functional diversity and trait structure (e.g., Mexico (Rocha-Ortega et al. 2018); Brazil (Bihn et al. 2010); Argentina (Santoandré et al. 2019); Australia (Lomov et al. 2009, Gibb and Cunningham 2013).

However, in line with our findings, there are also several studies showing that environmental degradation does not need to be associated with reductions in functional trait diversity. For instance, ant species functional dispersion of plots with low tree species diversity was similar to plots with high tree species diversity in China (Skarbek et al. 2020). Further, dung beetles and birds have also been shown to retain high levels of functional diversity even in young secondary forests in the Colombian Chocó (Edwards et al. 2021).

The influence of legacy effects on the trait structure (CWM similarity) is notable. Although only marginally significant, there appears to be a trend for environmentally selected traits that are different between the open areas of the pasture and the understory of cacao. Habitat openness can be a major environmental variable shaping the trait structure of ant assemblages (Guilherme et al. 2019, Andersen 2019). We find that with forest growth during succession, the functional similarity to old-growth forests is quickly restored.

Recovery comparison of community properties. Forest recovery outcomes are predictable by the synergistic effects of resistance and resilience of community properties (Nimmo et al. 2015). Among chronosequence studies, our study is one of few to explicitly distinguish between resistance and resilience for several community properties according to Pimm's (1984) definition. This enabled us to disentangle the separate components of the recovery. We expected different recovery times for all community properties, and that community composition would be slowest to recover, followed by trait structure and then species richness. Our data confirm the slow relative recovery of community composition, which was mediated through a much lower resistance, but similar resilience compared to the other properties. These patterns are consistent with most findings from community recovery studies as well as with theoretical expectations (Dunn 2004, Curran et al. 2014, Moreno-Mateos et al. 2017, Pimm et al. 2019). However, we did not find clear differences in recovery outcome for trait structure and species richness, which both showed high resistance and resilience in the face of disturbance. Interestingly, for all tested community properties, only resistance, but not resilience, drove differences in total recovery time. An explanation could be that community properties are biologically nested and thus computationally not independent of each other. Since species richness and trait structure are calculated from species composition, their turnover rates might be coupled, which would be worth investigating through simulations. Our result that resilience was similar among properties confirms findings on forest recovery in the Amazon, where recovery rates (resilience) of species richness in comparison to community composition of birds, plants and dung beetles were surprisingly similar (Lennox et al. 2018).

While resistance and resilience are conceptually independent, it is hard to untangle how much they are interdependent in the biological context, i.e., whether the same biological attributes that reduce impact to disturbance (resistance) are also beneficial to the recovery rates (resilience) (Nimmo et al. 2015). For instance, species attributes that correlate more to reproduction and re-colonization should increase resilience, while those that infer high physiological or behavioral plasticity should increase resistance (Shade et al. 2012; Nimmo et al. 2015). Further, resistance and resilience of the whole ecosystem is likely to be influenced by landscape configuration, with forest remnants acting as refuges (Shacklefort et al. 2018). In the landscape mosaic of our study site the community properties resistance and resilience were likely positively affected by the surrounding forest matrix. However, the distance of the plot to the forst edge was never correlated with any of the community properties. Since all plots were located rather closely to forests, future experiments in more isolated forest patches are desirable. They could shed light on the question if similar, fast recovery happens also in more fragmented areas. The two concepts of resistance and resilience could also be differentially targeted with conservation and land-use strategies. For instance, we would expect that the use of agroforestry instead of monoculture would increase resistance, as communities are more similar to forests during disturbance. Likewise, the proximity to forest remnants or active re-planting of trees during early succession should lead to an increase of resilience. Manipulative ecological experiments, which try to explicitly alter resistance independent of resilience, could greatly improve our understanding of these recovery mechanisms. While the Ecuadorian Chocó is one of the most threatened biodiversity hotspots, our study confirms a strong recovery potential for recently deforested areas, particularly since intact forests are still abundant. This knowledge is important for future development in such regions, where deforestation by logging and small-scale farming is still common. Conservation action should thus target both old-growth forests remnants as well as recovering forests, including young stages on abandoned agricultural land.

2.6 ACKNOWLEDGEMENTS

We thank the Fundacíon Jocotoco, in particular Martin Schaefer, and the associated Tesoro Escondido for logistic support and their permission to do research on their forest properties. We would like to especially acknowledge local support from the park staff in the Canandé and Tesoro Escondido reserve, which made two great field stays possible: Bryan Amayo, Alcides Zombrano, Roberto de la Cruz, Jorge Zambrano, Amado de la Cruz, Yadria Giler, Patricio Encarnación and Vanessa Moreira. Further, we thank Citlalli Morelos-Juárez, Adrian Brückner, Karsten Mody for their kind support during field work, and Matteo Trevisan and Basma Khalid for their help in measuring ant specimens. We thank John Lattke, Roberto J. Guerrero, Rodrigo Feitosa and Jack Longino for identification of ant species. We also thank Robert Collwell and Robin Chazdon for suggestions to improve the manuscript. Finally, we are very grateful for three anonymous reviewers that substantially improved our work. PH was supported by a scholarship from the German National Academic Foundation.

CvB received funding from the German Research Foundation (DFG: BE 5177/4-1). DAD thanks EPN Projects PII-ICB-02-2017 and PII-DB-2019-02. Ant collecting was supported by EPN Group Project PIGR-19-16, directed by DAD.

2.7 REFERENCES

Agosti, D., J. Majer, L. E. Alonso, and T. Schultz. 2000. Ants: Standard Methods for Measuring and Monitoring Biodiversity. Washington, DC: Smithsonian Institution Press.

Alonso, L. E. and Agosti, D. 2000. Biodiversity studies, monitoring and ants: An overview. In D. Agosti, J. D. Majer, L. E. Alonso, & R. Shultz (Eds.), Ants. Standard methods for measuring and monitoring biodiversity (pp. 1– 8). Washington, DC: Smithsonian Institution Press.

Andersen, A. N. 2019. Responses of ant communities to disturbance: Five principles for understanding the disturbance dynamics of a globally dominant faunal group. Journal of Animal Ecology 88:350–362.

Arnan, X., X. Cerdá, and J. Retana. 2014. Ant functional responses along environmental gradients. Journal of Animal Ecology 83:1398–1408.

Aubin, I., L. Venier, J. Pearce, and M. Moretti. 2013. Can a trait-based multi-taxa approach improve our assessment of forest management impact on biodiversity? Biodiversity and Conservation 22:2957–2975.

Barber, N. A., K. A. Lamagdeleine-Dent, J. E. Willand, H. P. Jones, and K. W. McCravy. 2017. Species and functional trait re-assembly of ground beetle communities in restored grasslands. Biodiversity and Conservation 26:3481–3498.

Bates, D., D. Sarkar, M. D. Bates, and L. Matrix. 2007. The lme4 package. R package version 2:74.

Belshaw, R., and B. Bolton. 1993. The effect of forest disturbance on the leaf litter ant fauna in Ghana. Biodiversity and Conservation 2:656–666.

Benayas, J. R., A. Martins, J. M. Nicolau, and J. J. Schulz. 2007. Abandonment of agricultural land: an overview of drivers and consequences. CAB Reviews: Perspectives in Agriculture, Veterinary Science, Nutrition and Natural Resources 2:1–14.

Bihn, J. H., G. Gebauer, and R. Brandl. 2010. Loss of functional diversity of ant assemblages in secondary tropical forests. Ecology 91:782–792.

Bihn, J. H., M. Verhaagh, M. Brändle, and R. Brandl. 2008. Do secondary forests act as refuges for old growth forest animals? Recovery of ant diversity in the Atlantic forest of Brazil. Biological Conservation 141:733–743.

Bowen, M. E., C. A. McAlpine, A. P. House, and G. C. Smith. 2007. Regrowth forests on abandoned agricultural land: a review of their habitat values for recovering forest fauna. Biological Conservation 140:273–296.

Brooks, M.E., Kristensen, K., van Benthem, K.J., Magnusson, A., Berg, C.W., Nielsen, A., Skaug, H.J., Maechler, M, and B. M. Bolker. 2017. glmmTMB balances speed and flexibility among packages for zero-inflated Generalized Linear Mixed Modeling. The R Journal 9:378–400.

Chazdon, R. L. 2003. Tropical forest recovery: legacies of human impact and natural disturbances. Perspectives in Plant Ecology, Evolution and Systematics 6:51–71.

Chazdon, R. L., and M. R. Guariguata. 2016. Natural regeneration as a tool for large-scale forest restoration in the tropics: prospects and challenges. Biotropica 48:716–730.

Chazdon, R. L., S. G. Letcher, M. van Breugel, M. Martínez-Ramos, F. Bongers, and B. Finegan. 2007. Rates of change in tree communities of secondary Neotropical forests following major disturbances. Philosophical Transactions of the Royal Society B: Biological Sciences 362:273–289.

Chazdon, R. L. 2014. Second growth. Chicago: University of Chicago Press.

Chazdon, R. L., D. Lindenmayer, M. R. Guariguata, R. Crouzeilles, J. M. Rey Benayas, and E. Lazos Chavero. 2020. Fostering natural forest regeneration on former agricultural land through economic and policy interventions. Environmental Research Letters 15:043002.

Chazdon, R. L., C. A. Peres, D. Dent, D. Sheil, A. E. Lugo, D. Lamb, N. E. Stork, and S. E. Miller. 2009. The potential for species conservation in tropical secondary forests. Conservation Biology 23:1406–1417.

Crouzeilles, R., F. S. M. Barros, P. G. Molin, M. S. Ferreira, A. B. Junqueira, R. L. Chazdon, D. B. Lindenmayer, J. R. C. Tymus, B. B. N. Strassburg, and P. H. S. Brancalion. 2019. A new approach to map landscape variation in forest restoration success in tropical and temperate forest biomes. Journal of Applied Ecology 56:2675–2686.

Crouzeilles, R., M. Curran, M. S. Ferreira, D. B. Lindenmayer, C. E. V. Grelle, and J. M. Rey Benayas. 2016. A global meta-analysis on the ecological drivers of forest restoration success. Nature Communications 7:11666.

Curran, M., S. Hellweg, and J. Beck. 2014. Is there any empirical support for biodiversity offset policy? Ecological Applications 24:617–632.

Curtis, P. G., C. M. Slay, N. L. Harris, A. Tyukavina, and M. C. Hansen. 2018. Classifying drivers of global forest loss. Science 361:1108–1111.

Debinski, D. M., R. A. Moranz, J. T. Delaney, J. R. Miller, D. M. Engle, L. B. Winkler, D. A. McGranahan, R. J. Barney, J. C. Trager, and A. L. Stephenson. 2011. A cross-taxonomic comparison of insect responses to grassland management and land-use legacies. Ecosphere 2:1–16.

Delabie, J. H., B. Jahyny, I. C. do Nascimento, C. S. Mariano, S. Lacau, S. Campiolo, S. M. Philpott, and M. Leponce. 2007. Contribution of cocoa plantations to the conservation of native ants

(Insecta: Hymenoptera: Formicidae) with a special emphasis on the Atlantic Forest fauna of southern Bahia, Brazil. Biodiversity and Conservation 16:2359–2384.

Dent, D. H., and S. J. Wright. 2009. The future of tropical species in secondary forests: a quantitative review. Biological Conservation 142:2833–2843.

Donohue, I., H. Hillebrand, J. M. Montoya, O. L. Petchey, S. L. Pimm, M. S. Fowler, K. Healy, A. L. Jackson, M. Lurgi, D. McClean, N. E. O'Connor, E. J. O'Gorman, and Q. Yang. 2016. Navigating the complexity of ecological stability. Ecology Letters 19:1172–1185.

Donoso, D. A. 2017. Tropical ant communities are in long-term equilibrium. Ecological Indicators 83:515–523.

Donoso, D.A. and G. Ramón. 2009. Composition of a high diversity leaf litter ant community (Hymenoptera: Formicidae) from an Ecuadorian premontane rainforest, Annales de la Société Entomologique de France 45:487–499.

Douma, J. C., and J. T. Weedon. 2019. Analysing continuous proportions in ecology and evolution: A practical introduction to beta and Dirichlet regression. Methods in Ecology and Evolution 10:1412–1430.

Dunn, R. R. 2004. Recovery of faunal communities during tropical forest regeneration. Conservation Biology 18:302–309.

Edwards, F. A., M. R. Massam, C. C. P. Cosset, P. G. Cannon, T. Haugaasen, J. J. Gilroy, and D. P. Edwards. 2021. Sparing land for secondary forest regeneration protects more tropical biodiversity than land sharing in cattle farming landscapes. Current Biology31:1284-1293.

Estrada, C., and C. Fernández. 1999. Diversidad de hormigas (Hymenoptera: Formicidae) en un gradiente sucesional del bosque nublado (Nariño, Colombia). Revista de Biología Tropical 47:189–201.

Gibb, H., and S. A. Cunningham. 2013. Restoration of trophic structure in an assemblage of omnivores, considering a revegetation chronosequence. Journal of Applied Ecology 50:449–458.

Gibb, H., N.J. Sanders, R.R. Dunn, S. Watson, M. Photakis, S. Abril, ... and C. L. Parr. 2015. Climate mediates the effects of disturbance on ant assemblage structure. Proceedings of the Royal Society B: Biological Sciences 282:20150418.

Gibb, H., J. Stoklosa, D. I. Warton, A. M. Brown, N. R. Andrew, and S. A. Cunningham. 2015. Does morphology predict trophic position and habitat use of ant species and assemblages? Oecologia 177:519–531.

Gibson, L., T. M. Lee, L. P. Koh, B. W. Brook, T. A. Gardner, J. Barlow, C. A. Peres, C. J. Bradshaw, W. F. Laurance, and T. E. Lovejoy. 2011. Primary forests are irreplaceable for sustaining tropical biodiversity. Nature 478:378–381.

Gomes, E. C. F., G. T. Ribeiro, T. M. da Silva, and L. Sousa-Souto. 2014. Ant assemblages (Hymenoptera: Formicidae) in three different stages of forest regeneration in a fragment of Atlantic Forest in Sergipe, Brazil. Sociobiology 61:250–257.

Gregory, N., R. M. Ewers, A. Y. Chung, and L. J. Cator. 2019. El Niño drought and tropical forest conversion synergistically determine mosquito development rate. Environmental Research Letters 14:035003.

Guilherme, D. R., J. L. P. Souza, E. Franklin, P. A. C. L. Pequeno, A. C. das Chagas, and F. B. Baccaro. 2019. Can environmental complexity predict functional trait composition of ground-dwelling ant assemblages? A test across the Amazon Basin. Acta Oecologica 99:103434.

Hansen, M. C., P. V. Potapov, R. Moore, M. Hancher, S. A. Turubanova, A. Tyukavina, D. Thau, S. V.

Stehman, S. J. Goetz, and T. R. Loveland. 2013. High-resolution global maps of 21st-century forest cover change. Science 342:850–853.

Hethcoat, M. G., B. J. King, F. F. Castiblanco, C. M. Ortiz-Sepúlveda, F. C. P. Achiardi, F. A. Edwards, C. Medina, J. J. Gilroy, T. Haugaasen, and D. P. Edwards. 2019. The impact of secondary forest regeneration on ground-dwelling ant communities in the Tropical Andes. Oecologia 191:475–482.

Holl, K. D., and R. A. Zahawi. 2014. Factors explaining variability in woody above-ground biomass accumulation in restored tropical forest. Forest Ecology and Management 319:36–43.

Jost, L. 2006. Entropy and diversity. Oikos 113:363–375.

Konopka, A. 2009. What is microbial community ecology?. ISME J 3:1223–1230.

Kuznetsova, A., P. B. Brockhoff, and R. H. B. Christensen. 2017. lmerTest Package: Tests in Linear Mixed Effects Models. Journal of Statistical Software 82:1–26.

Laliberté, E., and P. Legendre. 2010. A distance-based framework for measuring functional diversity from multiple traits. Ecology 91:299–305.

Laliberté, E., P. Legendre, B. Shipley, and M. E. Laliberté. 2014. Package 'FD.' Measuring functional diversity from multiple traits, and other tools for functional ecology. R package version 1.0-12.

Law, S. J., T. R. Bishop, P. Eggleton, H. Griffiths, L. Ashton, and C. Parr. 2020. Darker ants dominate the canopy: Testing macroecological hypotheses for patterns in colour along a microclimatic gradient. Journal of Animal Ecology 89:347–359.

Lawton, J. H., D. E. Bignell, B. Bolton, G. F. Bloemers, P. Eggleton, P. M. Hammond, M. Hodda, R. D. Holt, T. B. Larsen, and N. A. Mawdsley. 1998. Biodiversity inventories, indicator taxa and effects of habitat modification in tropical forest. Nature 391:72–76.

Lennox, G. D., T. A. Gardner, J. R. Thomson, J. Ferreira, E. Berenguer, A. C. Lees, R. Mac Nally, L. E. O. C. Aragão, S. F. B. Ferraz, J. Louzada, N. G. Moura, V. H. F. Oliveira, R. Pardini, R. R. C. Solar, F. Z. Vaz-de Mello, I. C. G. Vieira, and J. Barlow. 2018. Second rate or a second chance? Assessing biomass and biodiversity recovery in regenerating Amazonian forests. Global Change Biology 24:5680–5694.

Lomov, B., D. A. Keith, and D. F. Hochuli. 2009. Linking ecological function to species composition in ecological restoration: seed removal by ants in recreated woodland. Austral Ecology 34:751–760.

Longino, J. T., and M. G. Branstetter. 2019. The truncated bell: an enigmatic but pervasive elevational diversity pattern in Middle American ants. Ecography 42:272–283.

Majer, J. D. 1983. Ants: bio-indicators of minesite rehabilitation, land-use, and land conservation. Environmental Management 7:375–383.

Meijide, A., C. S. Badu, F. Moyano, N. Tiralla, D. Gunawan, and A. Knohl. 2018. Impact of forest conversion to oil palm and rubber plantations on microclimate and the role of the 2015 ENSO event. Agricultural and Forest Meteorology 252:208–219.

Meli, P., K. D. Holl, J. M. Rey Benayas, H. P. Jones, P. C. Jones, D. Montoya, and D. Moreno Mateos. 2017. A global review of past land use, climate, and active vs. passive restoration effects on forest recovery. PLOS ONE 12:e0171368.

Moreno-Mateos, D., E. B. Barbier, P. C. Jones, H. P. Jones, J. Aronson, J. A. López-López, M. L. McCrackin, P. Meli, D. Montoya, and J. M. Rey Benayas. 2017. Anthropogenic ecosystem disturbance and the recovery debt. Nature Communications 8:14163.

Neves, F. S., R. F. Braga, M. M. do Espirito-Santo, J. H. Delabie, G. W. Fernandes, and G. Sanchez-Azofeifa, A. 2010. Diversity of arboreal ants in a Brazilian tropical dry forest: effects of seasonality and successional stage. Sociobiology 56:177–194.

Newbold, T., P. Oppenheimer, A. Etard, and J. J. Williams. 2020. Tropical and Mediterranean biodiversity is disproportionately sensitive to land-use and climate change. Nature Ecology & Evolution 4:1630–1638.

Nimmo, D. G., R. Mac Nally, S. C. Cunningham, A. Haslem and A. F. Bennett. 2015. Vive la résistance: reviving resistance for 21st century conservation. Trends in Ecology & Evolution 30:516–523.

Norden, N., H. A. Angarita, F. Bongers, M. Martínez-Ramos, I. Granzow-de la Cerda, M. van Breugel, E. Lebrija-Trejos, J. A. Meave, J. Vandermeer, G. B. Williamson, B. Finegan, R. Mesquita, and R. L. Chazdon. 2015. Successional dynamics in Neotropical forests are as uncertain as they are predictable. Proceedings of the National Academy of Sciences of the United States of America 112:8013–8018.

Oliver, T. H., M.S. Heard, N.J. Isaac, D. B. Roy, D. Procter, F. Eigenbrod, ... and J.M. Bullock. 2015. Biodiversity and resilience of ecosystem functions. Trends in Ecology & Evolution 30:673–684.

Oksanen, J., F. G. Blanchet, R. Kindt, P. Legendre, R. B. O'Hara, G. L. Simpson, P. Solymos, M. H. H. Stevens, and H. Wagner. 2010. Vegan: community ecology package. R package version 1.17-4. http://CRAN. R-project. org/package= vegan.

Paradis, E., J. Claude, and K. Strimmer. 2004. APE: analyses of phylogenetics and evolution in R language. Bioinformatics 20:289–290.

Parr, C. L., R. R. Dunn, N. J. Sanders, M. D. Weiser, M. Photakis, T. R. Bishop, M. C. Fitzpatrick, X. Arnan, F. Baccaro, and C. R. Brandão. 2017. GlobalAnts: A new database on the geography of ant traits (Hymenoptera: Formicidae). Insect Conservation and Diversity 10:5–20.

Pascarella, J. B., T. M. Aide, M. I. Serrano, and J. K. Zimmerman. 2000. Land-Use History and Forest Regeneration in the Cayey Mountains, Puerto Rico. Ecosystems 3:217–228. Pennekamp, F., M. Pontarp, A. Tabi, F. Altermatt, R. Alther, Y. Choffat, ... and O. L. Petchey. 2018. Biodiversity increases and decreases ecosystem stability. Nature 563:109–112.

Pimm, S. L. 1984. The complexity and stability of ecosystems. Nature 307:321–326.

Pimm, S. L., I. Donohue, J. M. Montoya, and M. Loreau. 2019. Measuring resilience is essential to understand it. Nature Sustainability 2:895–897.

Potapov, P., M. C. Hansen, L. Laestadius, S. Turubanova, A. Yaroshenko, C. Thies, W. Smith, I. Zhuravleva, A. Komarova, and S. Minnemeyer. 2017. The last frontiers of wilderness: Tracking loss of intact forest landscapes from 2000 to 2013. Science Advances 3:e1600821.

R Core Team. 2018. R: A language and environment for statistical computing. R Foundation for Statistical Computing, Vienna, Austria. www.R-project.org.

Rocha-Ortega, M., X. Arnan, J. D. Ribeiro-Neto, I. R. Leal, M. E. Favila, and M. Martínez-Ramos. 2018. Taxonomic and functional ant diversity along a secondary successional gradient in a tropical forest. Biotropica 50:290–301.

Santoandré, S., J. Filloy, G. A. Zurita, and M. I. Bellocq. 2019. Ant taxonomic and functional diversity show differential response to plantation age in two contrasting biomes. Forest Ecology and Management 437:304–313.

Schmidt, F. A., C. R. Ribas, and J. H. Schoereder. 2013. How predictable is the response of ant assemblages to natural forest recovery? Implications for their use as bioindicators. Ecological Indicators 24:158–166.

Shackelford, N., R. J. Standish, Z. Lindo, and B.M. Starzomski. 2018. The role of landscape connectivity in resistance, resilience, and recovery of multi-trophic microarthropod communities. Ecology 99:1164–1172.

Shade, A., H. Peter, S. Allison, D.L. Baho, M. Berga, Buergmann Helmut, D. Huber, S. Langenheder, J. Lennon, J. Martiny, K. Matulich, T. Schmidt, and J. Handelsman. 2012. Fundamentals of microbial community resistance and resilience. Frontiers in Microbiology 3:417.

Skarbek, C. J., M. Noack, H. Bruelheide, W. Härdtle, G. von Oheimb, T. Scholten, S. Seitz, and M. Staab. 2020. A tale of scale: Plot but not neighbourhood tree diversity increases leaf litter ant diversity. Journal of Animal Ecology 89:299–308.

Sosiak, C. E., and P. Barden. 2020. Multidimensional trait morphology predicts ecology across ant lineages. Functional Ecology 35:139–152.

Staab, M., A. Schuldt, T. Assmann, H. Bruelheide, and A.-M. Klein. 2014. Ant community structure during forest succession in a subtropical forest in South-East China. Acta Oecologica 61:32–40.

Stuhler, J. D., and J. L. Orrock. 2016. Historical land use and present-day canopy thinning differentially affect the distribution and abundance of invasive and native ant species. Biological Invasions 18:1813–1825.

Szewczyk, T., and C. M. McCain. 2016. A systematic review of global drivers of ant elevational diversity. PLOS ONE 11:e0155404.

Tiede, Y., Schlautmann, J., Donoso, D. A., Wallis, C. I., Bendix, J., Brandl, R., & Farwig, N. 2017. Ants as indicators of environmental change and ecosystem processes. Ecological Indicators 83:527–537.

Vasconcelos, H. L. 1999. Effects of forest disturbance on the structure of ground-foraging ant communities in central Amazonia. Biodiversity and Conservation 8:407–418.

Villéger, S., N. W. Mason, and D. Mouillot. 2008. New multidimensional functional diversity indices for a multifaceted framework in functional ecology. Ecology 89:2290–2301.

Weiser, M. D., and M. Kaspari. 2006. Ecological morphospace of New World ants. Ecological Entomology 31:131–142.

Wickham, H., W. Chang, and M. H. Wickham. 2016. Package 'ggplot2.' Create Elegant Data Visualisations Using the Grammar of Graphics. Version 2:1–189.

Wijdeven, S. M., and M. E. Kuzee. 2000. Seed availability as a limiting factor in forest recovery processes in Costa Rica. Restoration Ecology 8:414–424.

Williams, E. R., D. R. Mulligan, P. D. Erskine, and K. P. Plowman. 2012. Using insect diversity for determining land restoration development: Examining the influence of grazing history on ant assemblages in rehabilitated pasture. Agriculture, Ecosystems & Environment 163:54–60.

Wong, M. K., B. Guénard, and O. T. Lewis. 2019. Trait-based ecology of terrestrial arthropods. Biological Reviews 94:999–1022.

2.8 SUPPLEMENT

Supplement for Hoenle, P. O., D. A. Donoso, A. A. Argoti, M. Staab, C. von Beeren, and N. Blüthgen. Rapid ant community re-assembly in a Neotropical forest: recovery dynamics and land-use legacy. *Ecological Applications, accepted for publication*

Section S2.1

Identification of collected ant specimens

Specimens were first sorted into morphospecies. Two individuals per morphospecies per sample were mounted. POH determined morphospecies to the species level whenever possible using primary taxonomic literature: *Acropyga* (LaPolla 2004), *Adelomyrmex* (Fernández 2003, Longino 2012), *Apterostigma* (Lattke 1997), *Brachymyrmex* (Ortiz-Sepulveda et al. 2019), *Crematogaster* (Longino 2003), *Cyphomyrmex* (Kempf and Francisco 1965), *Dolichoderus* (MacKay 1993), *Gnamptogenys* (Camacho et al. 2020), *Lachnomyrmex* (Feitosa and Brandao 2008), *Leptogenys* (Lattke 2011), *Linepithema* (Wild 2007), *Megalomyrmex* (Boudinot et al. 2013), *Neoponera* & *Pachycondyla* & *Pseudoponera* (Mackay and Mackay 2010), *Octostruma* (Longino 2013), *Pheidole* (Longino 2019), *Prionopelta* (Ladino and Feitosa 2020), *Proceratium* (Urbani and Andrade 2003), *Rasopone* (Longino and Branstetter 2020), *Sericomyrmex* (Ješovnik and Schultz 2017), *Solenopsis* (Pacheco et al. 2013), *Strumigenys* (Bolton 2000), *Wasmannia* (Longino and Fernández 2007). Due to a lack of identification literature on Ecuadorian ant species (Salazar et. 2015), we relied primarily on species keys of Costa Rican and Colombian ants, which show a reasonable degree of species overlap (Longino 2010, Fernández et al. 2019). Several ant taxonomists checked ambiguous cases (see Acknowledgements). Queens, damaged specimens, and majors of *Pheidole* and *Solenopsis* were sometimes collected but only included in the analysis if they could be clearly be associated to a species/morphospecies. In certain genera (predominantly in *Azteca*, *Solenopsis*, *Hypoponera*, *Nylanderia* and *Pheidole*) with high species diversity but poorly resolved alpha taxonomy, we relied on assigning morphologically similar specimens into morphospecies.

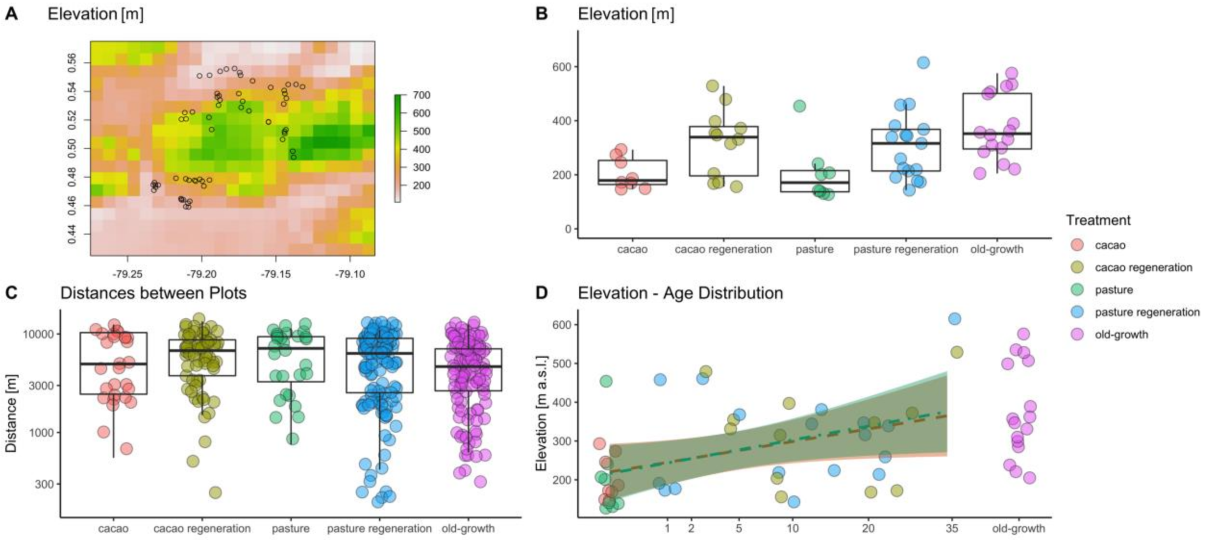

Fig. S2.1 A: Map of all plots superimposed on a height heatmap, made with the r-package 'raster' (Hijman 2011). **B**: Elevational distribution of each category. **C**: Distances between each plot within each category. The y-Axis is log-transformed. Mean ± SD distance is 5,799 ± 3,373 m. The shortest inter-category distance is 170 m, the longest is 13,403 m. **D**: Elevation along regeneration age distribution. The two variables are significantly correlated (linear model; F-value = 4.38, R^2 = 0.18, p = 0.003), and there are no differences between cacao and pasture land-use legacy (linear model; F-value = 4.38, R^2 = 0.18, p = 0.998).

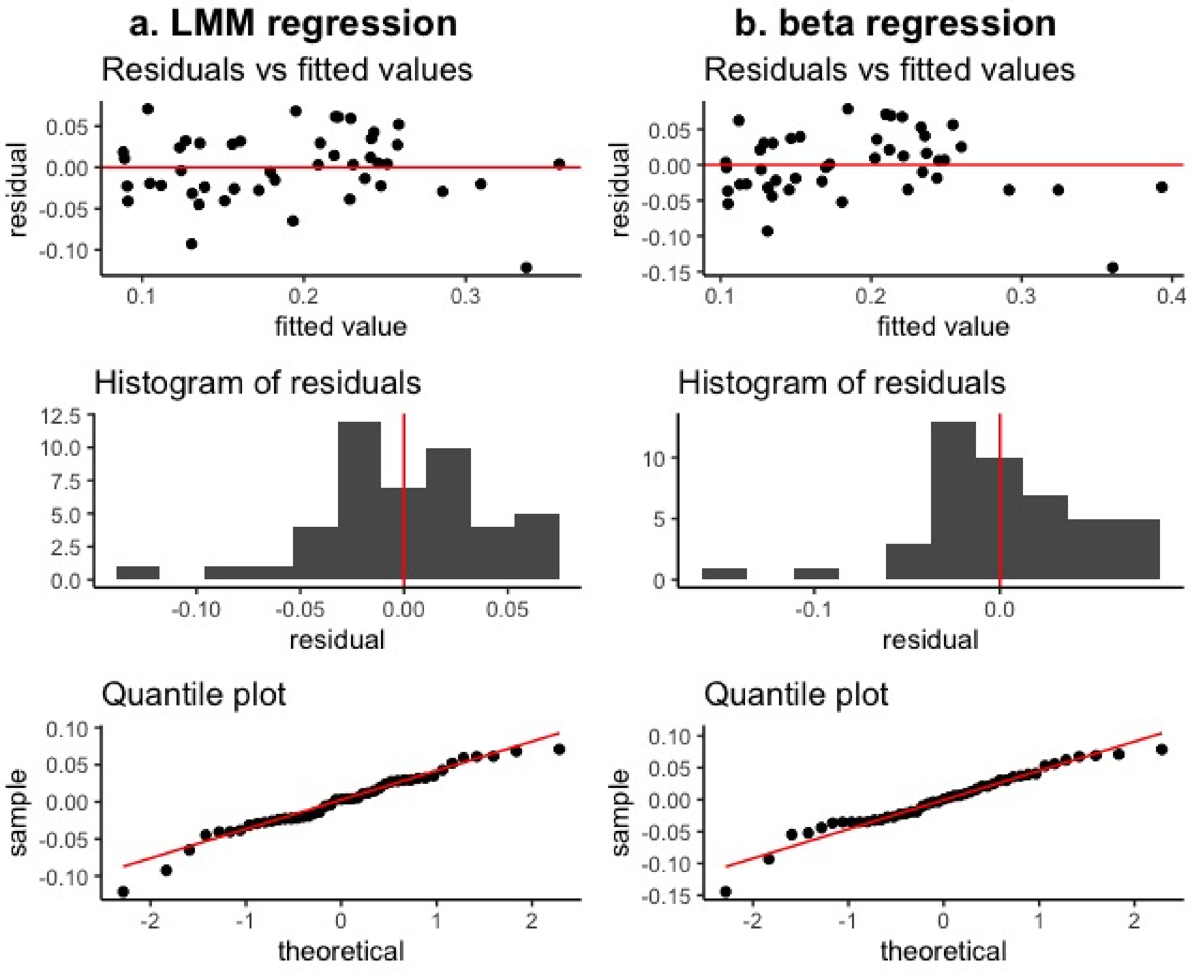

Fig. S2.2 Comparison of the residual plot diagnostics between the linear mixed effects model (a, left panels) and the beta regression (b, right panels) for the species composition similarity. The diagnostic plots indicate that residuals in both models (LMM and beta) are almost identical and indicate a normal distribution.

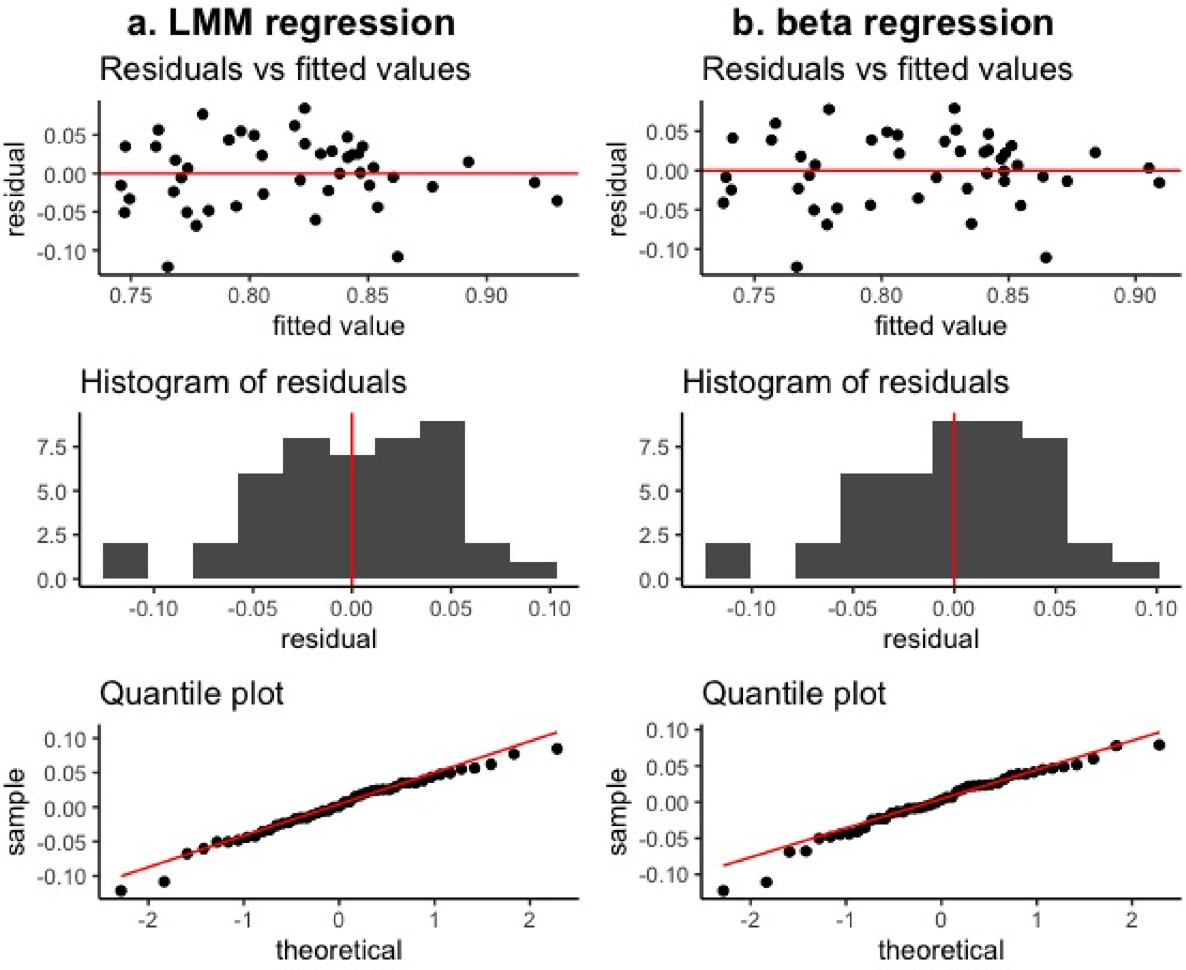

Fig. S2.3 Comparison of the residual plot diagnostics between the linear mixed effects model (a, left panels) and the beta regression (b, right panels) for the trait structure (CWM) similarity. The diagnostic plots indicate that residuals in both models (LMM and beta) are almost identical and show a normal distribution.

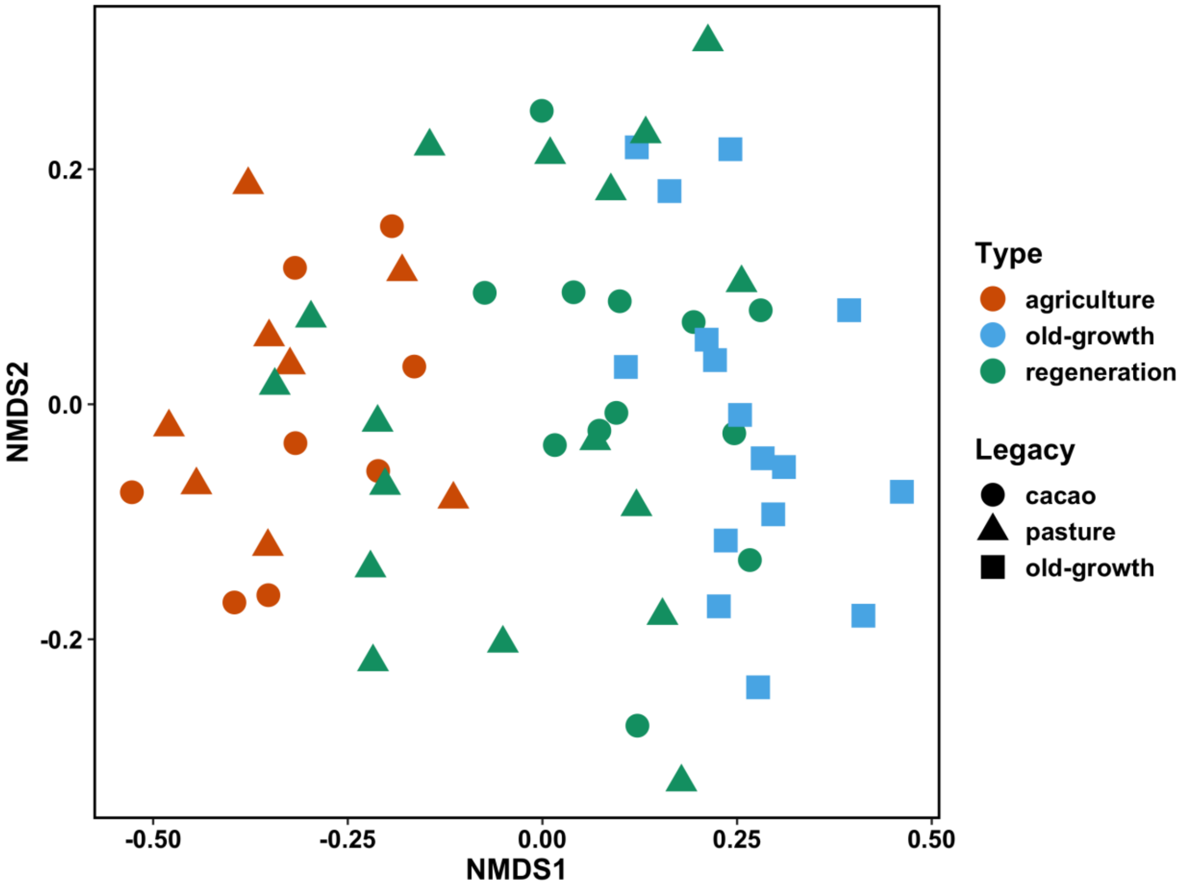

Fig. S2.4 NMDS (k = 3, stress = 0.17) depicting compositional differences in the ant communities of the category type (color) and the land-use legacy (symbols) of the 61 plots (Jaccard similarity). We increased the number of dimensions in NMDS from k = 2 to k = 3 to reduce stress, which did not influence the configuration of the first two axes (procrustes rotation 1000 permutations, $p < 0.001$). The species composition was significantly different between the category types (ADONIS, df = 2, $R^2 = 0.11$, F.Model = 3.71, $p > 0.001$).

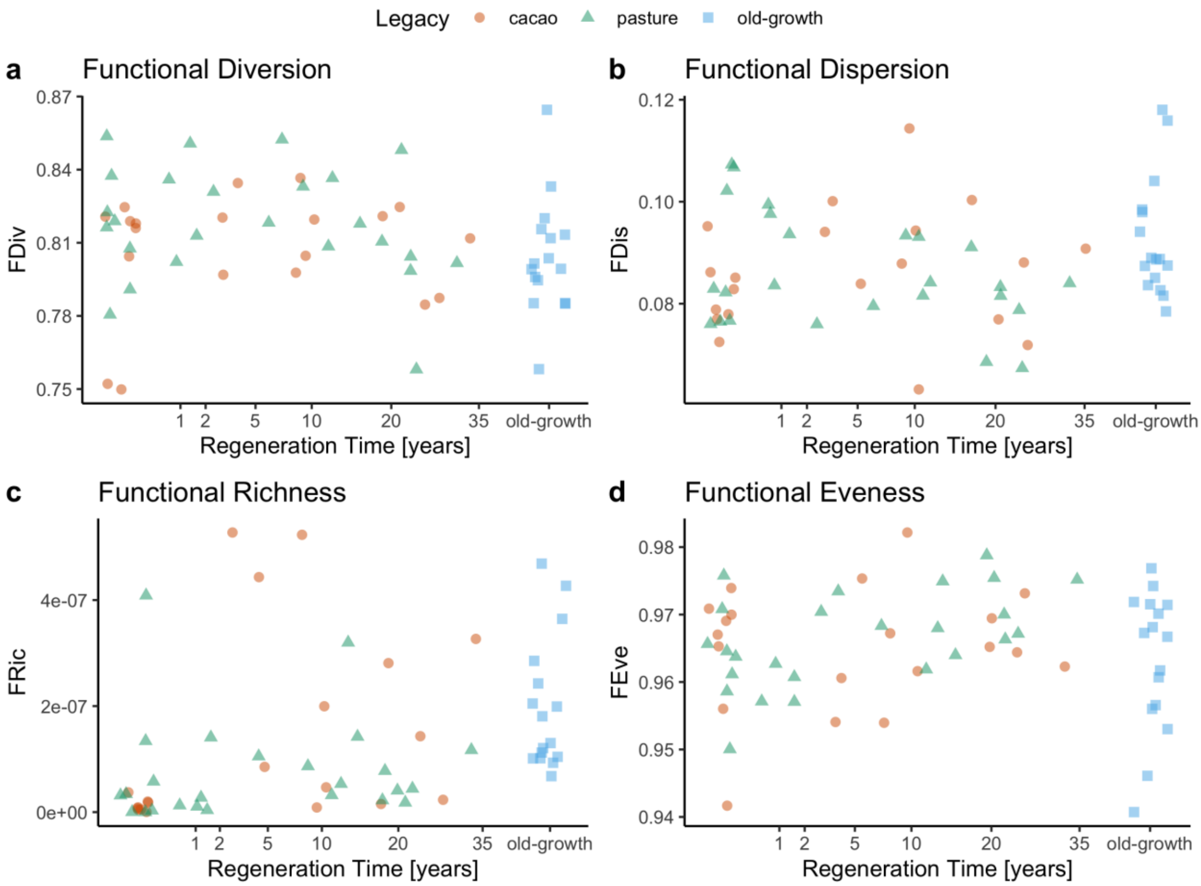

Fig. S2.5 Regression of multidimensional functional trait indices FDiv (**A**), FDis (**B**), FRic (**C**) and FEve (**D**) for each of the 61 plots to the regeneration time. In none of the indices this correlation is significant (Table S2.2).

Table S2.1. List of ant traits that were quantified in this study, and their proposed functional significance. Adapted from Parr et al. (2017).

Trait	**Proposed function**
Weber's length	Closely related to body size and linked to metabolism (Gibb et al. 2018) and microclimate (Kaspari 1993)
Head length	Indicator of diet (Weiser & Kaspari 2006)
Head width	Feeding mode (Weiser & Kaspari 2006)
Mandible length	Length of mandibles relates to diet: longer mandibles = more predatory (Gibb & Cunningham 2013)
Clypeus length	Clypeus linked to sucking ability and liquid-feeding behavior (Davidson et al. 2004)
Scape length	Sensory abilities: longer scapes facilitate following of pheromone trails (Weiser & Kaspari 2006); shorter scapes in complex environments
Pronotum width	Pronotum accommodates neck musculature which is important for digging and feeding (Peeters et al. 2020)
Femur length	Indicative of foraging speed (Feener et al. 1988); thermoregulatory strategy (Sommer &Wehner 2012)
Eye size	Eye size is indicative of food searching behaviour and activity times (Weiser & Kaspari 2006)
Eye position (=interocular width)	Related to hunting method (Fowler et al. 1991) or the component of the habitat occupied (Gibb & Parr 2013)
Color lightness	Thermoregulation, sunlight protection (Clusella-Trullaset al. 2007; Law et al. 2020); camouflage (Garcia et al. 2009)
Number of spines	Spines are defensive adaptions (Blanchard et al. 2020)
Sculpture	More sculptured cuticles increase structural integrity and dehydration tolerance (Buxton et al. 2021)

Table S2.2: Beta regression model results for species composition and trait similarity, with elevation, land-use legacy and square-root transformed regeneration time as fixed factors, and collection year as random factor. For comparison, we give the values obtained by the LMM (Table 2.1 in the main document) in parenthesis. Diagnostic plots for both are shown in Fig. S2.4 and Fig. S2.5. Significant p-values are highlighted in bold.

	Composition Similarity				**Trait Similarity**			
Predictors	*Estimate*	*Std.*	*z-value (t-value)*	*p*	*Estimate*	*Std.*	*z-value*	*p*
(Intercept)	-2.07 (0.10)	0.12 (0.02)	-17.01 (5.80)	**<0.001** **(<0.001)**	1.03 (0.75)	0.12 (0.02)	8.73 (38.62)	**<0.001** **(<0.001)**
Elevation	1.22 (0.21)	0.41 (0.06)	3.00 (3.52)	**0.003** **(0.001)**	1.36 (0.18)	0.42 (0.06)	3.23 (2.76)	**0.001** **(0.009)**
Land-use Legacy [pasture]	-0.24 (-0.04)	0.09 (0.01)	-2.64 (-2.99)	**0.008** **(0.005)**	-0.17 (-0.02)	0.09 (0.01)	-1.93 (-1.76)	0.05 (0.09)
RegenerationTime [sqrt years]	0.17 (0.03)	0.03 (<0.01)	6.65 (7.16)	**<0.001** **(<0.001)**	0.10 (0.01)	0.02 (<0.001)	3.93 (3.71)	**<0.001** **(<0.001)**
Marginal R^2 / Conditional R^2	0.797/ 0.797 (0.721 / 0.721)				1.106/ 1.106 (0.477 / 0.481)			

Table S2.3: Linear-mixed effects model results for the trait diversity indices, with elevation, land-use legacy and square-root transformed regeneration time as fixed factors, and collection year as random factor. Trait indices in the model were expressed as relative to old-growth mean. 95% confidence intervals are given. Significant p-values are highlighted in bold.

	Functional Diversion			**Functional Dispersion**		
Predictors	*Estimate*	*CI*	*p*	*Estimate*	*CI*	*p*
(Intercept)	100.52	98.13 – 102.90	**<0.001**	96.47	86.15 – 106.78	**<0.001**
Elevation	0.07	-7.99 – 8.14	0.986	-8.85	-42.04 – 24.35	0.601
Land-use Legacy [pasture]	1.33	-0.42 – 3.09	0.136	-0.28	-7.50 – 6.95	0.940
RegenerationTime [sqrt years]	-0.07	-0.56 – 0.42	0.773	-0.36	-2.42 – 1.69	0.728
Marginal R² / Conditional R²	0.050 / 0.051			0.023 / 0.023		

	Functional Richness			**Functional Eveness**		
	Estimate	*CI*	*p*	*Estimate*	*CI*	*p*
(Intercept)	18.10	-36.69 – 72.88	0.517	**99.70**	**99.01 – 100.39**	**<0.001**
Elevation	156.12	-29.56 – 341.80	0.099	1.05	-1.07 – 3.17	0.332
Land-use Legacy [pasture]	-29.92	-70.32 – 10.48	0.147	0.14	-0.32 – 0.61	0.541
Sqrt(RegenerationTime)	3.44	-7.82 – 14.69	0.549	0.08	-0.05 – 0.22	0.08
Marginal R² / Conditional R²	0.135 / 0.135			0.093 / 0.152		

References

Blanchard, B. D., A. Nakamura, Cao M. Chen, and S. T. Moreau, C. S. 2020. Spine and dine: A key defensive trait promotes ecological success in spiny ants. Ecology and Evolution, 10(12):5852–5863.

Bolton, B. 2000. The ant tribe Dacetini. Memoirs of the American Entomological Institute. 65:1–370. Lewiston, New York.

Boudinot, B. E., T. P. Sumnicht, and R. M. Adams. 2013. Central American ants of the genus *Megalomyrmex* Forel (Hymenoptera: Formicidae): six new species and keys to workers and males. Zootaxa 3732:1–82.

Buxton, J. T., K. A. Robert, A. T. Marshall, T. L. Dutka, and H. Gibb. 2021. A cross-species test of the function of cuticular traits in ants (Hymenoptera: Formicidae). Myrmecological News 31:31–46**.**

Camacho, G. P., W. Franco, and R. M. Feitosa. 2020. Additions to the taxonomy of *Gnamptogenys* Roger (Hymenoptera: Formicidae: Ectatomminae) with an updated key to the New World species. Zootaxa 4747:450–476.

Clusella-Trullas, S., J. H. van Wyk, and J. R. Spotila 2007. Thermal melanism in ectotherms. Journal of Thermal Biology 32: 235–245.

Davidson, D. W., S. C. Cook, and R. R. Snelling. 2004. Liquid-feeding performances of ants (Formicidae): ecological and evolutionary implications. Oecologia 139:255–266.

Feener, D.H., J.R.B. Lighton, and G.A. Bartholomew. 1988. Curvilinear allometry, energetics and foraging ecology: a comparison of leaf-cutting ants and army ants. Functional Ecology 2:509–520.

Feitosa, R. M., and C. R. F. Brandão 2008. A taxonomic revision of the Neotropical myrmicine ant genus *Lachnomyrmex* Wheeler (Hymenoptera: Formicidae). Zootaxa 1890:1–49.

Fernández, F. 2003. Revision of the myrmicine ants of the *Adelomyrmex* genus-group (Hymenoptera: Formicidae). Zootaxa 361:1–52.

Fernández, F., R. J. Guerreroand and T. Delsinne. 2019. Hormigas de Colombia. Univ. Nacional de Colombia.

Fowler, H.G., L. C. Forti, C. R. F. Brandão, J. H. C. Delabie, and H. L. Vasoncelos, 1999. Ecologia nutricional de formigas. Ecologia Nutricional De Insetos (ed. by A.R. Panizzi & J.R.P. Parra), pp. 131– 223. Manole, Sao Paulo, Brasil.

Garcia, T. S., D. J. Paoletti and A. R. Blaustein. 2009. Correlated trait responses to multiple selection pressures in larval amphibians reveal conflict avoidance strategies. Freshwater Biology 54:1066–1077.

Gibb, H., and S. A. Cunningham. 2013. Restoration of trophic structure in an assemblage of omnivores, considering a revegetation chronosequence. Journal of Applied Ecology 50(2):449–458.

Gibb, H. and C. L. Parr 2013. Does structural complexity determine the morphology of assemblages? An experimental test on three continents. PLOS ONE 8:e64005.

Gibb, H., N. J. Sanders, R. R Dunn, X. Arnan, H. L Vasconcelos, D. A. Donoso, A. N. Andersen, R. R. Silva, T. R. Bishop, and C. Gomez. 2018. Habitat disturbance selects against both small and large species across varying climates. Ecography 41:1184–1193.

Hijmans, R.J. 2020. raster: Geographic Data Analysis and Modeling. R package version 3.0-12. https://CRAN.R-project.org/package=raster

Ješovnik, A., and T. R. Schultz. 2017. Revision of the fungus-farming ant genus *Sericomyrmex* Mayr (Hymenoptera, Formicidae, Myrmicinae). ZooKeys 670:1–109.

Kaspari, M. 1993. Body size and microclimate use in Neotropical granivorous ants. Oecologia, 96(4):500–507.

Kempf, W. W., and C. S. Francisco. 1965. A revision of the Neotropical fungus-growing ants of the genus *Cyphomyrmex* Mayr. Part II: Group oí *rimosus* (Spinola)(Hym., Formicidae). Studia Entomologica 8:60–200.

Ladino, N., and R. M. Feitosa. 2020. Taxonomic revision of the genus *Prionopelta* Mayr, 1866 (Formicidae: Amblyoponinae) for the Neotropical region. Zootaxa 4821:201–249.

LaPolla, J. S. 2004. *Acropyga* (Hymenoptera: Formicidae) of the world. Contributions of the American Entomological Institute 33:1–130.

Lattke, J. E. 2011. Revision of the New World species of the genus *Leptogenys* Roger (Insecta: Hymenoptera: Formicidae: Ponerinae). Arthropod Systematics and Phylogeny 69:127–264.

Lattke, J. E. 1997. Revision of the genus Apterostigma Mayr (Hymenoptera: Formicidae). Arquivos de Zoologia Museu de Zoologia da Universidade de São Paulo 34:121–221.

Law, S. J., T. R. Bishop, P. Eggleton, H. Griffiths, L. Ashton, and C. Parr. 2020. Darker ants dominate the canopy: Testing macroecological hypotheses for patterns in colour along a microclimatic gradient. Journal of Animal Ecology 89:347–359.

Longino, J. T. 2003. The *Crematogaster* (Hymenoptera, Formicidae, Myrmicinae) of Costa Rica. Zootaxa 151:1–150.

Longino, J. T., and F. Fernández. 2007. Taxonomic review of the genus *Wasmannia*. Memoirs of the American Entomological Institute 80:271–289.

Longino, J. T. 2010. The Ants of Costa Rica website https://ants.biology.utah.edu/AntsofCostaRica.html [Access Date: 25 February 2021]

Longino, J. T. 2012. A review of the ant genus *Adelomyrmex* Emery 1897 (Hymenoptera, Formicidae) in Central America. Zootaxa 3456:1–35.

Longino, J. T. 2013. A revision of the ant genus *Octostruma* Forel 1912 (Hymenoptera, Formicidae). Zootaxa 3699:1–61.

Longino, J. T. 2019. *Pheidole* (Hymenoptera, Formicidae) of Middle American Wet Forest. Zootaxa 4599:1–126.

Longino, J. T., and M. G. Branstetter. 2020. Phylogenomic species delimitation, taxonomy, and 'Bird Guide' identification for the Neotropical ant genus *Rasopone* (Hymenoptera: Formicidae). Insect Systematics and Diversity 4:1–33.

MacKay, W. P. 1993. A review of the new world ant of the genus *Dolichoderus*. Sociobiology 22:1–148.

Mackay, W., and E. Mackay. 2010. Systematics and biology of the New World ants of the genus *Pachycondyla* (Hymenoptera: Formicidae). Lewiston: Edwin Mellen Press.

Ortiz-Sepulveda, C. M., B. Van Bocxlaer, A. D. Meneses, and F. Fernández. 2019. Molecular and morphological recognition of species boundaries in the neglected ant genus *Brachymyrmex* (Hymenoptera: Formicidae): Toward a taxonomic revision. Organisms Diversity & Evolution 19:447–542.

Pacheco, J. A., W. P. Mackay, and J. Lattke. 2013. The systematics and biology of the New World thief ants of the genus *Solenopsis* (Hymenoptera: Formicidae). Lewiston: Edwin Mellen Press.

Salazar, F., F. Reyes-Bueno, D. Sanmartin, and D. A. Donoso. 2015. Mapping continental Ecuadorian ant species. Sociobiology 62:132–162.

Sommer, S. and R. Wehner, 2012. Leg allometry in ants: extreme long-leggedness in thermophilic species. Arthropod Structure & Development 41:71–77.

Parr, C. L., R. R. Dunn, N. J. Sanders, M. D. Weiser, M. Photakis, T. R. Bishop, M. C. Fitzpatrick, X. Arnan, F. Baccaro, and C. R. Brandão. 2017. GlobalAnts: A new database on the geography of ant traits (Hymenoptera: Formicidae). Insect Conservation and Diversity 10:5–20.

Peeters, C., R. A. Keller, A. Khalife, G. Fischer, J. Katzke, A. Blanke, and E. P. Economo (2020). The loss of flight in ant workers enabled an evolutionary redesign of the thorax for ground labour. Frontiers in Zoology 17(1):1–13.

Urbani, C. B., and M. L. de Andrade. 2003. Ant genus *Proceratium* in the extant and fossil record (Hymenoptera: Formicidae). Museo Regionale di Scienze Naturali Monografie 36:1–492.

Weiser, M. D., and M. Kaspari, 2006. Ecological morphospace of New World ants. Ecological Entomology 31:131–142.

Wild, A. L. 2007. Taxonomic revision of the ant genus *Linepithema* (Hymenoptera: Formicidae). University of California Publications in Entomology 126:1–151.

3 STRATIFICATION AND RECOVERY TIME JOINTLY SHAPE ANT FUNCTIONAL RE-ASSEMBLY IN A NEOTROPICAL FOREST

This chapter is currently being prepared for publication.

Author: Philipp O. Hoenle[a]

Affiliation:

[a]Ecological Networks, Department of Biology, Technical University of Darmstadt, Darmstadt, Germany.

3.1 ABSTRACT

Variation in forests structure, such as the successional stage and microhabitat stratification, contributes to maintain the biodiversity of tropical forests. Environmental filtering determines both the community re-assembly during succession and its stratification, resulting in a distinct functional and phylogenetic composition of organisms through time and space. However, it is poorly understood if and how these two environmental filters – forest recovery and stratification – interact with each other. In a chronosequence of a tropical forest in Ecuador, I investigated the recovery trajectory of ant assemblages in three overlapping strata (ground, leaf litter, lower tree trunk) by quantifying 13 traits, functional and phylogenetic diversity. My study included pastures and cacao plantations, secondary forests derived from former agricultural areas between 1 – 34 years of recovery and old-growth forests. Most ant functional traits and phylogenetic diversity across my study plots were distinctly stratified. Community-weighted trait means had complex relationships to recovery time and were shaped by interactions between recovery and stratification. Most trait trajectories converged among strata with increasing recovery time, i.e., differences among strata were most pronounced in plots of ongoing agriculture and decreased towards old-growth forest plots. My study confirms the suspected complex interaction between environmental filters during the functional reassembly in tropical forests. Individual strata are differently affected during recovery, which is a previously underappreciated aspect of re-assembly. I discuss plausible filter mechanisms, which likely arose from both abiotic (e.g., temperature) and biotic (e.g., competition) conditions. Since vertical stratification is prevalent across animal and plant taxa, my results highlight the importance of stratum-specific analysis in dynamic ecosystems and may generalize beyond ant communities. In particular, functional traits with convergent trajectories, i.e., a decreasing extent of stratification with increasing forest age may represent a more general assembly rule in recoverng ecosystems that warrants further research.

3.2 INTRODUCTION

Species co-occuring in local communities often represent a non-random sample of the regional species pool and several ecological theories aim to describe community assembly mechanisms (Diamond 1975, Keddy 1992). These mechanisms are diverse, and include niche differentiation (Macarthur and Levins 1967), dispersal (Hubbell 2011) and stochasticity (Connor and Simberloff 1979, Hubbell 2011). Arguably one of the most central concepts in community assembly is the environmental filter hypothesis, implying that the environment acts as a metaphorical ‘filter’ that selects potential species from the regional pool based on species' specific attributes (i.e., 'traits') (Keddy 1992). Traits mediate the interaction between species and their environment, and thus connect communities to their functional role in ecosystems (de Bello et al. 2021). Subsequently, environmental filters determine community trait diversity, which reflects species' ecological niches (Kraft et al. 2015). Measurement of traits can facilitate comparison across completely different sets of species, enabling the detection of general ecological patterns (Mouchet et al. 2010, de Bello et al. 2021). As more closely related species are often more similar in their ecology and thus their traits compared to distantly related species (i.e., niche conservatism), environmental filters are also reflected in the phylogenetic composition of a community (Kraft et al. 2007). Therefore, phylogenetic studies on communities can capture the signal of filters on traits that were not directly measured (Srivastava et al., 2021).

While environmental filters were traditionally restricted to abiotic factors and are now often used to untangle the relative contribution of biotic interactions versus the abiotic environment (Kraft et al. 2015), I understand a 'filter' here in the broadest sense as any factor that can possibly select from the available species pool, including competitive exclusion (Cadotte and Tucker 2017). A prominent application of the environmental filter concept is the re-assembly of species communities after disturbance or during succession, for example in tropical forests (Davies et al., 2020; Edwards et al., 2014). A fraction of today's tropical landscape is comprised of disturbed forests, often former agricultural areas, which are in recovery towards an old-growth forest state (Crouzeilles et al. 2016, Meli et al. 2017). Studies of the outcomes in functional and phylogenetic diversity generate the opportunity to glimpse into the re-assembly process (Fornoff et al. 2021).

Habitats are comprised of manifold and structurally variable microhabitats, which determine niche availability and have implications for re-assembly. For instance, in lowland tropical rainforest, vertical stratification from lower vegetation to higher canopy areas is pronounced and affects arthropod distribution and abundance (Schulze et al. 2001, Fermon et al. 2005, Basset et al. 2015). Even across smaller scales, such as above and within the litter layer and soil, communities are distinctly stratified (Giller 1996, Widenfalk et al. 2016). Thus, community stratification can be understood as a process determined by environmental filtering. During forest recovery, some previously dominant microhabitats disappear (e.g., dense grass of cattle pastures) while others expand and diversify (e.g., the leaf litter layer; Huang et al. 2017). Forest recovery and other types of ecosystem succession represent a second filter on a community, with substantial effects on the structural complexity and microclimate on a larger habitat scale. However, studies assessing the changes only along a one-dimensional habitat recovery axis are prone to miss important aspects of the re-assembly process that may be invoked by stratification within habitats. To date, only very few studies have tested if and how two gradual environmental filters, such as stratification and forest recovery, interact with each other during community (re)assembly (Fermon et al. 2005, Whitworth et al. 2016). In this study, I use functional traits and phylogenetic diversity to untangle the plausible interaction between stratification and recovery. Several studies indicate that species communities on trees are more heavily affected by habitat degeneration than those on the ground (Klimes et al. 2012, Whitworth et al. 2016, 2019), and I expect that this will be visible in trait diversity and species composition of the lower tree trunk.

In the simplest scenario of a recovering area, species' trait distribution will be filtered by stratification ('stratification hypothesis' Fig. 3.1, A) and/or recovery time ('recovery hypothesis', Fig. 3.1, B). However, recovery trajectories may be highly stratum-specific, i.e., strata are differently affected by recovery time ('interaction hypothesis' Fig. 3.1, C). As forest recovery leads to larger, more heterogeneous strata, I expected that environmental filters lead to a higher degree of stratification with forest age, i.e. more dissimilar the simplest scenario of a recovering area, species' trait distribution will be filtered by stratification ('stratification stratum-specific communities with increasing trait and phylogenetic diversity. To test the interaction between forest recovery and stratification, I use ants as focal organisms. Ants are one of the most abundant insect groups of tropical forests and play a major role in ecosystem functioning (Lach et al. 2010). They display a vast diversity of life histories, from minute subterranean dwellers to conspicuous canopy climbers (Sosiak and Barden 2020). Functional traits of ants have been studied intensively and can be directly linked to certain functions (Gibb et al. 2015, Parr et al. 2017, Law et al. 2020, Sosiak and Barden 2020).

I studied a 34-year forest chronosequence recovery located in the Chocó tropical lowland of North West Ecuador and sampled ant communities in three microhabitats, the leaf litter, ground and tree trunk (henceforth 'strata'). I expect that stratification and forest recovery jointly shape communities, their traits and phylogeny.

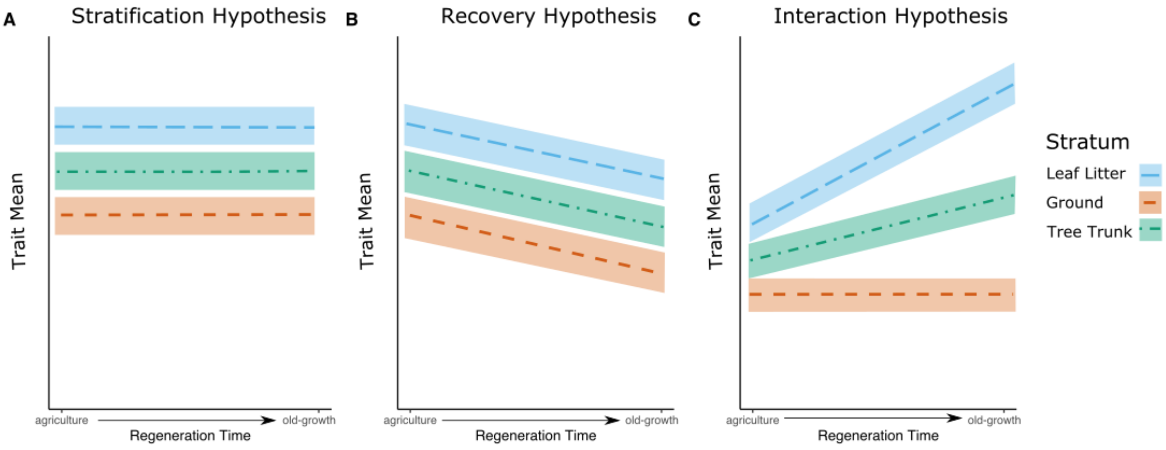

Fig. 3.1 The three main hypotheses for trait trajectories. On the y-axis, a community weighted mean (CWM) for a hypothetical trait is shown. The regression lines each depict the response of this trait to the recovery time on the x-axis. In (A), a trait is differentiated between strata but does not change significantly with recovery time, which I refer to as 'stratification hypothesis'. In (B), a trait is both differentiated among strata and changes with recovery time in a similar manner across the strata, which is the 'recovery hypothesis'. Finally, (C) depicts a trait differentiation and a recovery time effect, which varies among the strata (indicated by a statistically significant interaction between recovery time and stratum), referred to as 'interaction hypothesis'. Here, the trait means diverge to less similar values with recovery time – however, there are several other possible trajectories not depicted here, as for instance traits could also show the opposite pattern (converge).

3.3 MATERIAL AND METHODS

Study site and plot design

My study was conducted at the Reserva Río Canandé (0.5263 N, -79.2129 E) in Ecuador (Esmeraldas Province) in April – June 2018 and February – May 2019. The reserve and surrounding areas contain old-growth rainforests, recovering secondary forests on former pastures or cacao plantations ('recovery areas'), and currently used pastures and cacao plantations ('agricultural areas'). According to interviews with local farmers, land-use is mostly younger than 50 years, and is comprised of small-scale farming in a forest mosaic landscape. Based on the previous work of my supervisor Nico Blüthgen, I selected a total of 61 plots of 40 m × 40 m size including the following categories ('habitat types'): eight cacao plots, eight pasture plots, 12 cacao recovery plots, 17 pasture recovery plots, and 16 old-growth forest plots (as reference; Supplemental Fig. S2.1). All recovery plots are adjacent to forests. Spatial dependence was minimized by haphazardly selection plots and keeping a minimum distance of at least 200 m among plots of the same habitat type. Plot elevation ranged between 127 m and 615 m (Supplement Fig. S2.1). As elevation was weakly correlated with recovery time (Supplement Fig. S2.1), I account for potential influences of elevation by incorporating elevation as fixed effect in all analyses (see Statistical analysis).

My collegues (see Acknowledgements) and I determined recovery age by interviewing local park rangers and farmers and incorporated information of land purchase provided by the Fundación Jocotoco. I assigned each recovery plot the age as the number of years it has been in succession (year after abandonment, range 1 – 34 years). Two types of locally common agriculture (cacao plantations and pastures) were selected from nearby farms. Cacao plantations are typically monocultures, and cacao trees reached a height of approximately four meters. Pasture plots were extensively grazed by various lifestock. Typically, some sparse trees providing shade for livestock. All old-growth forests have, to the best of myknowledge, experienced no logging in recent time.

Ant sampling and identification

With the help of my field assistant Adriana Argoti, I collected ants on each plot with three standardized methods to cover different strata: leaf-litter, epigeal ('ground'), and tree trunk (modified protocol from Agosti et al. 2000). Throughout the rest of the manuscript we will address the methods as their representative stratum (tree trunk sampling: tree trunk; hand sampling: ground; Winkler: leaf litter). Each stratum was represented by five pooled subsamples per plot (except when fewer than five trees where available, see below).

(1) To sample the leaf-litter ant community, I used Winkler extraction. For this, I established a 20 m transect line parallel to one side of the plot. Leaf-litter samples (including topsoil) on an area of 20 cm × 20 cm were collected every 5 m following the transect. Larger twigs and leaves were removed by sifting (1 cm^2 mesh size). Because pastures had no leaf litter, I used a spade to cut out the first five centimeters of the grass turf with the same dimensions. The samples were subsequently pooled per plot and transferred to Winkler bags for 48 hours.

(2) The ground ant assemblage was assessed by standardized hand sampling. I used another transect parallel to the Winkler transect with the same length (20 m) and placed a 1 m^2 sampling subplot every 5 m, where I collected ants with forceps for 5 minutes. The subplots were pooled on plot level.

(3) To sample the tree trunk, I identified the five largest trees in each plot by eye. Using forceps, I collected ants in reachable heights (0 – 2 m) for five minutes per tree, also checking under epiphytes and bark. If there were not enough trees within the pasture plot limit, I collected from adjacent trees in the same pasture. Nevertheless, three of the pastures had fewer than the required five trees, but at least one tree per plot was sampled (n=10 missing trees). In both the tree trunk and ground sampling, I focused on maximizing species numbers by collecting only a few individuals per species (e.g., close to a nest). Tree samples were pooled on plot level.

To avoid a stratum-specific collector bias, the same person carried out all leaf-litter sampling (Adriana Argoti), hand sampling (myself) and tree trunk sampling (myself). Inevitably, each collection method has certain limitations, for instance, Winkler samples may underrepresent large-bodied ant species (Lee and Guénard 2019). Stratum comparisons thus need to be interpreted with care, as each stratum-specific collection method may itself contribute to stratification patterns. I address this by calculating all analyses on incidence data only (see

Statistical Analysis), as collection methods usually are more prone to distort individual numbers than to fail in recording the mere presence of a species.

Specimens were first sorted into morphospecies, and two individuals per morphospecies and sample were mounted. I designated morphospecies and identified the majority of species. The ant expert of Ecuador, David Donoso, contributed to ant species identifications. Because there is a lack of identification literature on Ecuadorian ant species (Salazar et. 2015), I relied primarily on species keys of Costa Rican and Colombian ants (Longino 2007, Fernández et al. 2019). Other taxonomic experts also contributed to several identifications (see Acknowledgements). Voucher specimens are deposited in the MEPN museum collection at Escuela Politécnica Nacional in Quito. The Ministerio de Ambiente de Ecuador issued both the permits for collection (MAE-DNB-CM-2017-0068) and exportation (41-2018-EXPCM- FAU-DNB/MA and 144-2019-EXP-CM-FAU-DNB/MA).

Species composition

Altogether, I collected 183 ant assemblages ('subsamples': 61 plots with 3 strata each). I used the species incidence, i.e. presence/absence of ant species in each subsample for all analyses. All analyses were performed with the software R (R Core Team 2018; Version 3.5.1). The statistical analysis was conducted under close supervision from Nico Blüthgen and Michael Staab. To analyze species composition, I used two-dimensional non-metric multidimensional scaling (NMDS) with Jaccard similarity in the R-package 'vegan' (Oksanen et al. 2010). The dissimilarity matrix was tested for differences in composition between the three strata and with recovery and elevation in a PERMANOVA (function 'adonis' in vegan). Permutations were constrained by collection year. Using the same Jaccard similarity matrix, I also calculated species overlap among strata for each plot.

To visualize if the three strata follow similar trajectories across recovery time and elevation, I ran three separate NMDS on subset of each stratum, and correlated the axes scores with 'recovery time' and 'elevation' in a permutation test applying the function 'envfit'. Each stratum-specific matrix was finally analyzed with a PERMANOVA (constrained by collection year) to test for correlations with elevation and recovery time. All permutation tests used 1000 replicates.

Traits

To test for influences of environmental filters on the ant community, I quantified 13 morphological traits (following Parr et al. 2017; Table 3.1) and investigated their response to microhabitat stratification and forest recovery. The traits relate to ecological attributes and represent classical functional traits (Weiser and Kaspari 2006, Gibb et al. 2015, Parr et al. 2017, Sosiak and Barden 2020). I used a Keyence VHX-5000 (Keyence Deutschland GmmH, Neu-Isenburg, Germany) for trait measurements. I recorded traits of 653 specimens belonging to 240 species (Supplement S2.1 Table S3.1). Because of the high number of species, I measured for more common species (> 10 occurrence) at least three individuals, and for rare species (> 2 occurences) at least one individual. Species with single occurences were common, and traits could not be measured for all singletons (species without traits n=36; 2.5% of total occurences; Supplement S1 Table S3.1). This resulted in an average of 2.7±1.6 SD specimens per species/morphospecies (range 1 – 12). In polymorphic genera (*Azteca*, *Pheidole*, *Tranopelta*, *Camponotus, Solenopsis*) I measured only minor workers. To assess the ants' color lightness, I assigned each specimen a main color, which was based on the color wheel of Parr et al. (2017). The image software GIMP Version 2.10.22 was subsequently used to extract the lightness value for each color-coding following Law et al. (2020).

Table 3.1 List of ant traits that were quantified in this study, and their proposed functional significance. Adapted from Parr et al. (2017).

Trait	**Proposed function**
Weber's length	Closely related to body size and linked to metabolism (Gibb et al. 2018) and microclimate (Kaspari 1993)
Head length	Indicator of diet (Weiser and Kaspari 2006)
Head width	Feeding mode (Weiser and Kaspari 2006)
Mandible length	Length of mandibles relates to diet: longer mandibles = more predatory (Gibb and Cunningham 2013)
Clypeus length	Clypeus linked to sucking ability and liquid-feeding behavior (Davidson et al. 2004)
Scape length	Sensory abilities: longer scapes facilitate following of pheromone trails (Weiser and Kaspari 2006); shorter scapes in complex environments
Pronotum width	Pronotum accommodates neck musculature which is important for digging and feeding (Peeters et al. 2020)
Femur length	Indicative of foraging speed (Feener et al. 1988); thermoregulatory strategy (Sommer and Wehner 2012)
Eye size	Eye size is indicative of food searching behaviour and activity times (Weiser and Kaspari 2006)
Eye position	Related to hunting method (Fowler et al. 1991) or the component of the habitat occupied (Gibb and Parr 2013); Eye position = residual of (Head width – I-O width) with head length
Color lightness	Thermoregulation, sunlight protection (Clusella-Trullaset al. 2007, Law et al. 2020); camouflage (Garcia et al. 2009)
Number of spines	Spines are defensive adaptions (Blanchard et al. 2020)
Sculpture	More sculptured cuticles increase structural integrity and dehydration tolerance (Buxton et al. 2021)

I was interested in trait change independent of body size, and therefore regressed each size-related trait with Weber's length (a proxy of body size) in linear models. I averaged the residuals of these regressions on species level. Based on the averaged species traits and the species incidence matrix, we calculated functional diversity indices and community weighted means (CWMs). Functional diversity indices are calculated for the whole set of traits and result in community-level values, while the trait structure allows for detailed comparisons of single trait trajectories. Thus, the analysis of both results in complementary information on the overall multidimensional trait space, allowing a detailed perspective on trait filtering.

The functional diversity indices were calculated with the R-package 'FD', and result in the following information: FRic, which is a volume measurement of the amount of functional space filled by the community; FEve, which quantifies the regularity with which the functional space is filled by species; Functional Divergence (FDiv), which measures the average distance of species to the centroid of the functional trait space; and finally FDis, which is an estimator of the dispersion of the species in the trait-dimensional space (Villéger et al. 2008, Laliberté and Legendre 2010, Laliberté et al. 2014).

Phylogenetic diversity

Trait measurements will rarely capture the entire trait space of a species, as several traits may be elusive or not be quantifiable. Since many traits are phylogenetically preserved, phylogenetic diversity can be used as a proxy for the overall trait similarity among species (Srivastava et al. 2012, Staab et al. 2021). Thus, phylogenetic diversity can inform on functional re-assembly processes, since environmental filters are expected to create phylogenetically clustered communities. Because my data set contained many ants that could only be assigned to morphospecies, I calculated phylogenetic diversity on the genus level. I used the backbone tree of Economo et al. (2018) as phylogenetic reference tree and pruned the full tree to all 58 ant genera of my species occurrence data using the R-package 'picante' (Kembel et al. 2010). The resulting tree was then transformed into a cophenetic distance matrix, which was subsequently used to calculate the mean pairwise distance as standard effect size of each subsample using the function 'ses.mpd' from 'picante', with an independent swap as a null model (Tucker et al. 2017). Michael Staab provided supervison for this analysis.

Statistical analysis

The main goal of the analysis was to test the possible interaction between the environmental filters of vertical stratification and forest recovery. I therefore tested each of the obtained community metrics (species richness, trait CWMs, functional diversity indices and phylogenetic diversity) in linear mixed effects models (LMEs) against an interaction between recovery time and stratum using the packages 'lme4' (Bates et al. 2007) and 'lmerTest' (Kuznetsova *et al.* 2017). Further, to test if species composition overlap was sensitive to recovery time, I regressed it in a linear mixed effects model against recovery time and elevation.

To allow the incorporation of old-growth forests and agricultural areas into the analysis (even though they are without a formal recovery age), I rank-transformed recovery time. Old-growth forests received the highest rank, agricultural areas the lowest. Because the three collection methods are hard to compare, average species richness differences among these strata might influence some of the community metrics (for instance, FRic is highly correlated with species richness). To minimize this possible relationship, I added species richness to all LMEs as fixed factor (except for the richness model itself). As species richness itself did not change with recovery time (see Supplement Fig. S3.4), differences in species richness could only possibly interfere with the stratification results. Collection year and plot ID were used as crossed random intercepts. Plot ID is always associated with three strata collection events from the same day, while collection year is unique for each plot (either 2018 or 2019).

Depending on the outcome of the LME, I applied further testing. If the fixed factor 'stratum' was significant in an anova on a model, I assessed differences in a pairwise posthoc procedure (Bonferroni-Holm corrected; R-package 'emmeans'; Lenth 2021). Trajectories with statistically significant fixed factor 'stratum' (but without significant interaction or recovery term) were classified as supporting the stratification hypothesis (Fig. 3.1, A). If a community metric changed with recovery time (but without an interaction), I classified it as supporting the recovery hypothesis (Fig. 3.1, B). Note that this can include also metrics with significant stratum term. If an interaction between recovery and stratum was significant in an anova on the model, I classified as support for the 'interaction hypothesis' (Fig. 3.1, C).

If a metric belonged to either the recovery or the interaction hypothesis, I created subsets of each stratum and generated new LMEs with the same model structure (excluding the fixed factor 'stratum' and random factor 'PlotID') to obtain slope estimates for stratum-specific recovery time. This allowed me to assess whether community metrics in each of the strata increased, decreased, or did not change. Finally, I classified the trait mean trajectories, which belonged to the 'interaction hypothesis', in two scenarios. Less overlap in the 95% CIs (from the linear model) of the strata in old-growth forest compared to agriculture was classified as 'divergent', while more overlap was classified as 'convergent'.

Testing for legacy effects (i.e., different pasture or cacao recovery trajectories) required a separate procedure, because the rank-transformed recovery time included old-growth forests, which do not belong to a 'legacy' category. Therefore, I excluded old-growth forests and used a new linear-mixed effect models with the same fixed and random effects structure, but which included the interaction term 'legacy*recovery time'. Residuals of all models met assumptions of normality and homogeneity of variances. For all model residuals, I also performed a test for positive spatial autocorrelation (Moran's I on model residuals; R-package 'ape4'), which was never the case.

3.4 RESULTS

Species composition

I sampled 284 morphospecies across all habitats, belonging to 58 genera (Supplement Table S3.1). I found 2 – 23 ant species per subsample (Fig. 3.4, A), with fewest species found in the leaf litter (Fig 3.2, A). The taxonomic richness was neither related to recovery time ($p=0.12$) nor land-use legacy ($p=0.40$) but increased with elevation (elevation estimate 0.008 ± 0.003, $p=0.004$; Table S3.2). The three collection methods resulted in three well-separated communities (PERMANOVA, $F=6.06$, $R^2=0.06$, $p<0.001$, Fig. 3.2). There was clear stratification, with leaf-litter being most distinct from tree trunks, and ground being intermediate. Species turnover with recovery time was pronounced across all strata (PERMANOVA, all $p<0.001$ and $R^2 >0.36$; Table S3.2; Fig. 3.2). Similarly, elevation influenced turnover except in the leaf litter (PERMANOVA, $F=1.32$, $R^2=0.21$, $p=0.10$; Table S3.2). Ant communities on the tree trunk and ground became more dissimilar to each other with increasing forest recovery time and with elevation (LME recovery time $p=0.005$, elevation $p=0.03$; Table S3.2). Ground and tree trunk species overlap with leaf litter was however stable during recovery (all $p>0.38$; Table S3.2).

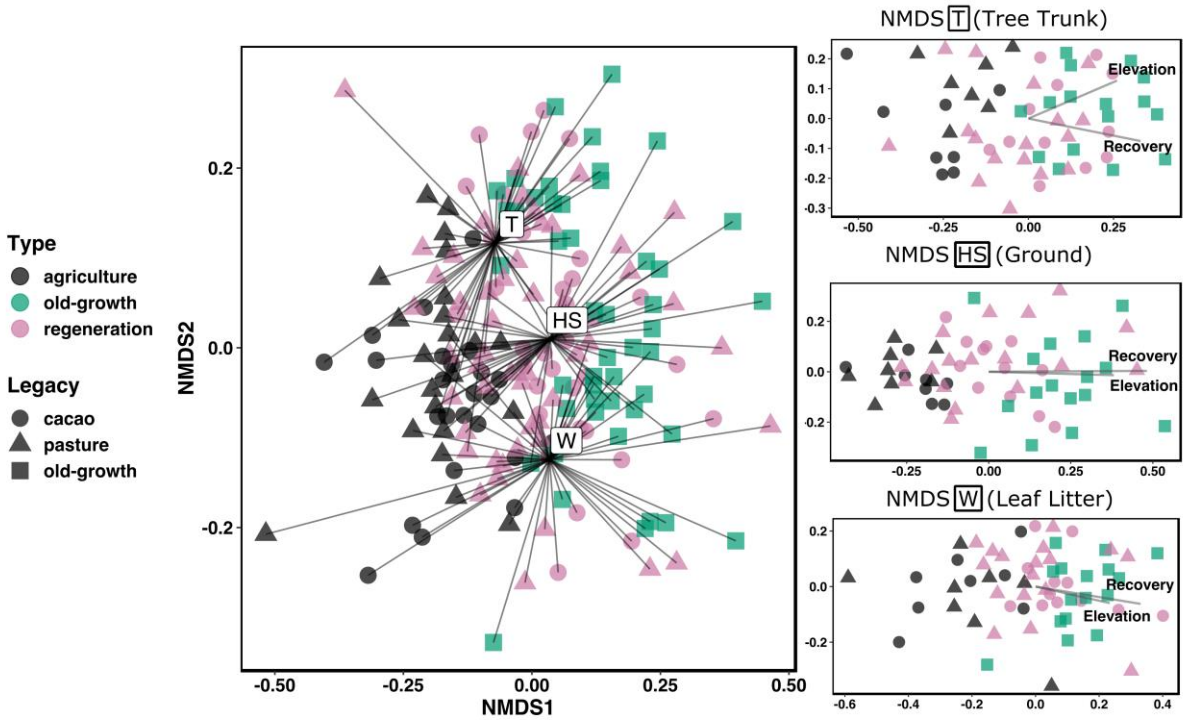

Fig. 3.2 Non-metric multidimensional scaling (NMDS) of species composition for tree trunk (T), ground (HS) and leaf-litter (W). The type 'agriculture' consists of currently used cacao plantations and pastures. The left NMDS (stress = 0.21) shows all strata (subsamples) combined depicting the vertical stratification, while on the right each of the three strata is plotted separately (stress: T = 0.23; HS = 0.19; W = 0.17). The influences of recovery time and elevation on species composition are indicated as grey vectors (all p<0.001; for detailed statistics see Table S3.2). One tree subsample ('T APN01') contained a very dissimilar community that would skew the ordination, which is why it is not shown in the ordination (but included in statistical analyses).

Functional traits

Two of the three trajectory hypotheses were supported by the functional diversity indices, irrespective of land-use legacy, which had no significant effect (Fig. 3.3; Table S3.3). The trajectory of functional dispersion (FDis) was consistent with the 'stratification hypothesis', and was most pronounced in tree trunk communities, followed by ground and leaf litter (Fig. 3.3 A; Table S3.3). Functional divergence (FDiv) was invariant to all factors examined (Table S3.3). However, functional richness and evenness (FRic, FEve) supported the 'interaction hypothesis' (scenario 3) (Fig. 3.3 B, C; Table S3.3). FRic was lowest in the leaf litter and stayed stable during recovery (Fig. 3.3; Table S3.3). Ground FRic decreased with recovery time, while tree trunks remained at the highest values and were stable across recovery time, but they were not significantly different from the ground (Fig. 3.3, B; Table S3.3). Tree trunk communities had the lowest FEve, followed by ground and leaf litter (Fig. 3 C; Table S3.3). While the interaction term was significant in the model, FEve did not change significantly with recovery time in any single stratum (all p>0.13; Table S3.3).

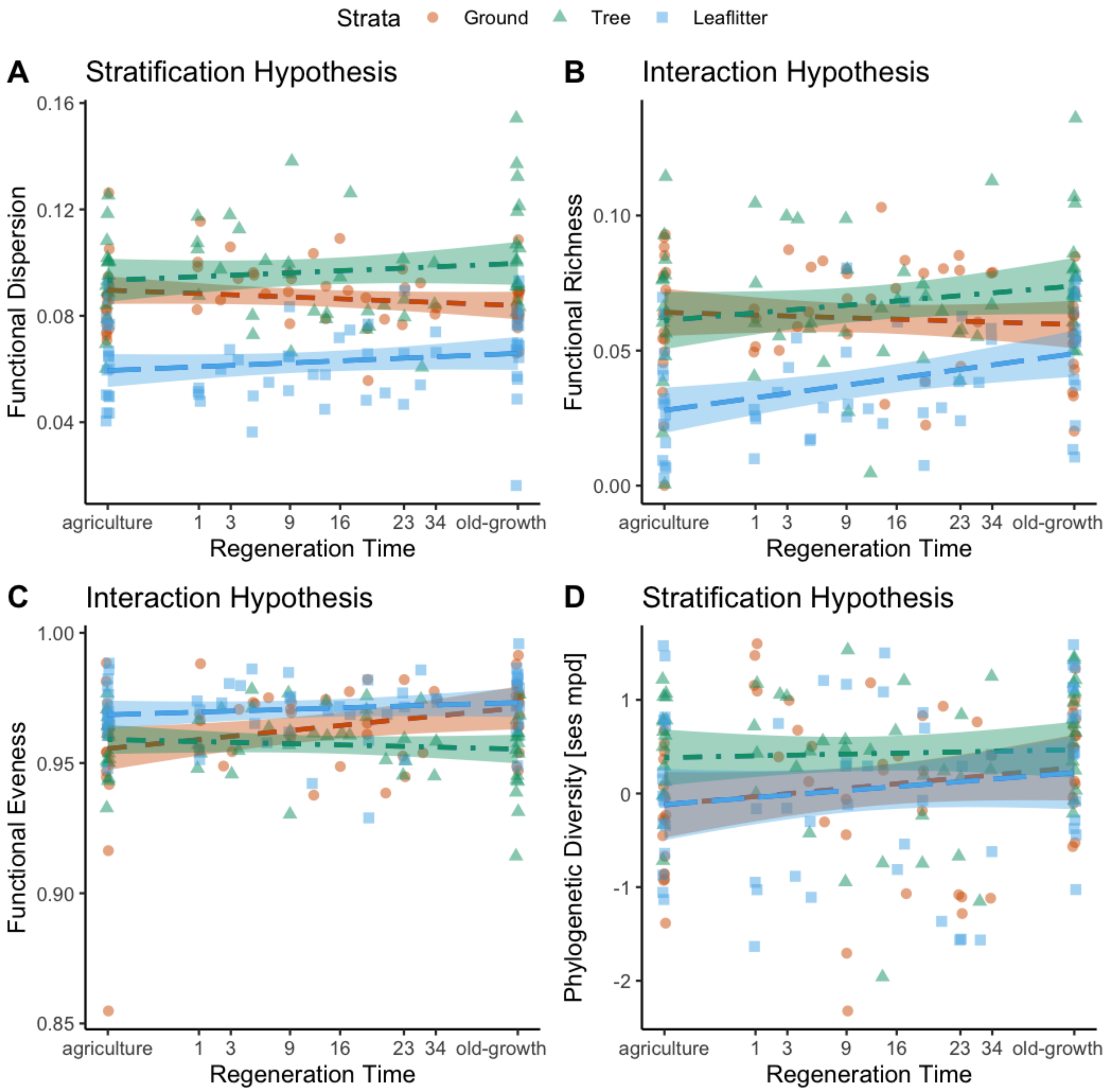

Fig. 3.3 Trajectories of phylogenetic diversity (A) and trait diversity (B-D) that were consistent with the stratification or interaction hypothesis (indicated on top). The regression line and 95% confidence intervals of each stratum are plotted. Colors indicate strata (green = tree trunk; red = ground; blue = leaf litter). For the full statistical models see Supplement Tables S2, S3, S5. The phylogenetic diversity analysis was supervised by Michael Staab.

Among the 13 traits analyzed (correlations among raw traits shown in Fig. S3.2), only the number of spines and femur length were uncorrelated to both stratum and recovery time

(Community weighted means, Table S3.4). Head width showed a trajectory consistent with the stratification hypothesis; sculpture and eye position with the recovery hypothesis; and the remaining eight traits with the interaction hypothesis (Fig. 3.4; Table S3.4). None of the traits were correlated with elevation (all p>0.07; Table S3.4). Legacy only influenced mandible length, however without a significant pairwise contrast (Table S3.4).

Two traits, scape length and Weber's length (Fig. 3.4 A, D; Table S3.4), diverged with recovery time (i.e., strata became more dissimilar), while the remaining five traits converged over time (i.e., strata became more similar): Color lightness, pronotum width, mandible length, clypeus length and eye size (Fig. 4 J, B, F, E, G; Table S3.4). A special case is head length, because its interaction term is significant, but neither the intercept nor stratum differences are (Table S3.4). Thus, it was neither converging nor diverging. As an example, for a diverging trait, the Weber's length CWM (a proxy for body size) is similar among strata at the initial state in the agriculture. Through an increase of Weber's length with recovery time in the tree trunk stratum (slope estimate 6.73±2.72 SE, p=0.02) but not in the ground (slope -2.51±1.79, p=0.16; Table S3.3), both strata become separated over time (Fig. 3.4 A).

In contrast, color lightness had a convergent trajectory. In agriculture, there is a strong differentiation with leaf litter being the lightest assemblages, and ground/tree trunk being darker. Both tree trunks (slope 0.27±0.08, p<0.001) and ground (slope 0.23±0.09, p=0.01) show an increase in color lightness with recovery time, while that of the leaf litter show a slight decrease (slope -0.23±0.09, p=0.01; Table S3.4), thus resulting in more similar color lightness in the older forests.

Phylogenetic diversity

Mean phylogenetic distance values remained similar across the entire chronosequence but exhibited consistent differences among strata, thus supporting the stratification hypothesis (Fig. 3.3 D; Table S3.5). Communities were predominantly random in their phylogenetic structure, however the tree trunk assemblage showed slight overdispersion with higher phylogenetic diversity compared to ground and leaf-litter assemblage (Fig. 3.3 D; Table S3.5).

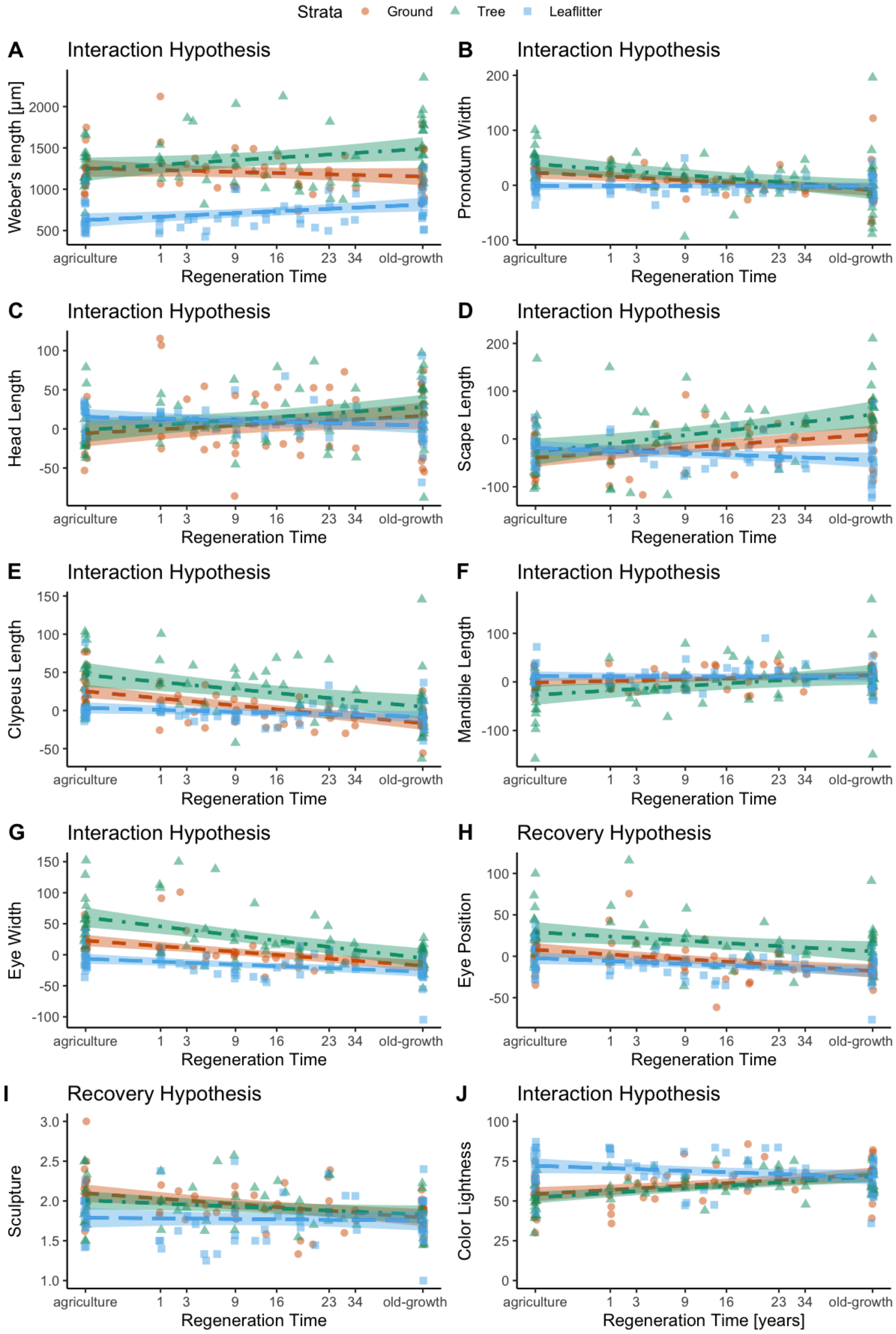

Fig. 3.4 Changes in functional structure across recovery time and strata, which are consistent with the recovery or interaction hypothesis (indicated on top). Weber's Length (A) and Scape Length (D) show diverging patterns, while the rest of the interaction traits show converging patterns. All morphological traits are expressed as residuals of Weber's Length, except color lightness (B; 0-100 scale, with 0=darkest), Weber's Length (H; in micro-meter), and sculpture (A; 0-3, 0 = smooth and shiny and 3 = heavy sculpturing). Strata differences are highlighted with green (tree trunk), red (ground) and leaf litter (blue), and their trajectories to recovery time are plotted from a linear model with 95% CI (Table S3.4).

3.5 DISCUSSION

The re-assembly of an ant community during forest recovery was dynamic and shaped by within-forest stratification. All three strata (leaf litter, ground, lower tree trunk) differed in their re-assembly trajectories, particularly when functional traits were considered, which highlights the complexity of community recovery. Environmental filters influenced the mean trait structure (CWMs) of a large subset of the assessed traits (10 out of 13), which lead to stratum-specific trajectories (interaction hypothesis) for eight out of 13 traits and for two aspects of their functional trait diversity (FRic, FEve). While most trait trajectories were idiosyncratic, I found that – contrary to initial expectations – in the majority of traits the differences across strata became smaller with increasing recovery time, indicating that stratification filters became more similar and/or weaker when forest grew older. Interestingly, this change was masked in ant species richness, phylogenetic diversity and functional dispersion (FDis), which were differentiated among the strata, but neither changed nor interacted with recovery time. Previous research on the role of stratification during forest recovery has been very restricted (Whitworth et al. 2019), and my work incorporates evidence that communities have stratum-specific responses that must be accounted for in biodiversity assessments.

Forest stratification was one of the main drivers of ant community differences in the forest. An estimated half of ant diversity in a tropical forest is found in the vegetation (Klimes et al. 2012, Floren et al. 2014). While my sampling did not include canopies due to logistic constraints, lower tree trunks had a distinct assemblage and comparatively higher phylogenetic diversity, which was likely due to evolutionary distinct lineages that specialized on this stratum (Sosiak and Barden 2020). Many of the more basal lineages of ants are confinded to the soil and litter, while above-ground ants are recruited from relatively few but specious and phylogenetically dispersed lineages (Lucky et al. 2013). In line with the lower phylogenetic diversity, leaf-litter assemblages were comparatively diminished in functional dispersion, and had a higher functional eveness. These patterns suggest that species are filtered towards one or few trait combinations that are well adapted to living in the leaf litter layer, a prominent finding that has previously been described for the trait diversity in stratified soil macroinvertebrate community (Ellers et al. 2018). Stratification filters had pronounced effects on several key functional traits, which are largely in agreement with previous studies (Weiser and Kaspari 2006, Gibb et al. 2015), such as the observed patterns in color lightness (Law et al. 2020), eye size (Schofield et al. 2016) and body size (Silva and Brandão 2010, Sosiak and Barden 2020). Most likely, abiotic filters play a dominant role in invoking community and trait stratification. For example, according to the 'arboreality hypothesis', community stratification on trees mirrors those invoked by elevation, both of which are primarily temperature-driven (Scheffers et al. 2013). Temperature has almost certainly a strong influence on ant vertical stratification, as arboreal ant communties are well-adapted to temperature extremes (Kaspari et al. 2015). On the other hand, there is also prominent evidence that biological filters have a dominant role in structuring ant communities, as competition for limited nesting resources on trees are likely important drivers of community structure (Wittman et al. 2010, Plowman et al. 2020).

I observed strong compositional shifts in the ant communities across all assessed strata with forest recovery, though they were not as pronounced as the differences imposed by stratification. Although I sampled only a fraction of the available microhabitats, it is conceivable that the documented changes are representative of other microhabitats. such as the canopy. Indeed, similar studies in the tropics that employed chronosequences found pronounced species turnover, e.g. in the canopy or underground (Bihn et al. 2010, Schmidt et al. 2013). I expected that due to larger, more diversified microhabitats, species community stratification would increase with recovery time, and this was indeed the case in the comparison between ground and tree communities. Comparisons with leaf litter communities on the other hand did not reflect this change, possibly because they were already composed of very distinct communities in early recovery stages and agriculture.

I expected more evolutionary preserved lineages in the old-growth forests compared to the agricultural areas (Mo et al. 2013, Liu et al. 2016, Edwards et al. 2017). However, phylogenetic diversity was not related to recovery, indicating that during taxonomic turnover with recovery time individual species are replaced by phylogenetically similar species (such as turnover of species in the same genus) or higher clades were replaced by similarly distant lineages. Therefore, ant phylogenetic diversity was more structured by stratification than by recovery.

With the potential to assess environmental effects on the community beyond species identity, the functional trait perspective provides detailed information on the outcome of environmental filters on the average community bauplan (Kraft et al. 2007, Wong et al. 2019, de Bello et al. 2021). In line with the results for phylogenetic diversity, which mirror overall trait similarity, I found that some of the multidimensional functional diversity indices (FDis and FDiv) remained constant during recovery. These findings contradict some previous outcomes of ant functional diversity along disturbance gradients (Rocha-Ortega et al. 2018, Santoandré et al. 2019), but are supported by others (Skarbek et al. 2020). Although not explicitly tested, the close proximity of all plots to old-growth forests might have facilitated the high species richness and functional diversity found in all plots by reducing the environmental filters imposed by dispersal limitation in more fragmented landscapes (Chazdon et al. 2009, Dent and Wright 2009, Lennox et al. 2018).

The relatively stable phylogenetic diversity and trait diversity are opposed to the patterns in the trait structure (CWMs), where almost all traits were related to recovery time. Environmental filtering during forest recovery, thus, shaped ant assemblages predominantly via single trait averages. While resulting trait trajectories were complex, idiosyncratic and stratum-specific, I can approximate trait trajectories in two distinct ways: with recovery time different strata either became more similar (convergence) in average traits (CWMs) or less similar (divergence). While I expected that stratum differences would diverge because forest recovery should lead to a more diversified niche space, the majority of traits converged (5 converge vs. 2 diverge). There are several possible ecological scenarios which may explain the observed patterns. More relaxed stratification filters during forest recovery seem plausible due to abiotic filters, e.g. when leaf litter, ground and lower tree trunks in the understory of an older forest are more similar in their structure, microclimate and light conditions in contrast to pastures and plantations. Indeed, early recovery stages and agricultural areas have a warmer, drier and more fluctuating microclimate due to the lack of a buffering canopy cover present in old-growth forests (del Pliego et al. 2016, De Frenne et al. 2019). Among the traits quantified by me, color lightness and eye size, both being related to light availability, can be attributed to predominantly abiotic filtering (Law et al. 2020). In line with the expectation of relaxed abiotic filtering, both of these traits had converging trajectories with recovery. Further, biotic filters such as competition are hypothesized to be strongly stratum-dependent for ant communities, with more competitive interaction on trees than on the ground (Blüthgen and Stork 2007). If the relative importance of interspecific competition decreases with recovery time, this may result in a more similar functional composition as I observed in my data. However, competitive ability is determined by behavior and not morphological traits, which limits my ability to discriminate biotic versus abiotic filters. Most likely, a mixture of different filters determined the functional re-assembly and were variable between traits.

Mechanisms of community assembly are central to the understanding of the recovery of ecosystems. Here, I show for the first time how stratification is intertwined with re-assembly. While I focus on ant communities, vertical stratification is prevalent across animal and plant taxa (Schulze et al. 2001, Fermon et al. 2005, Laurans et al. 2014, Basset et al. 2015, Chmel et al. 2016). Thus, the relaxed stratum-specific filtering with increasing forest recovery might represent a more general rule for trait patterns that warrants confirmation across different biomes and taxa. My study shows how community (re)assembly can be driven by a complex interplay of environmental filters that lead to unexpected outcomes in the functional structure.

3.6 ACKNOWLEDGEMENTS

I thank Nico Blüthgen for his overarching supervision, installment of study plots and his excellent inputs into statistical analysis. Great thank goes to Michael Staab, without whom I could not have done the statistical analysis, in particular of the phylogenetic diversity. Further, without the outstanding help from Adriana Argoti in the field and the supervision from David Donso the study would not have been possible. Nico Blütghen, Michael Staab and David Donoso also made very valuable comments and improvemets to this manuscript. I thank the Fundacíon Jocotoco and the associated Tesoro Escondido for logistic support and their permission to do research on their forest properties. I thank Martin Schaefer for his engagement in making my research feasible. I would like to acknowledge local support from the park staff in the Canandé and Tesoro Escondido reserve, which made two great field stays possible: Bryan Amayo, Alcides Zombrano, Roberto de la Cruz, Jorge Zambrano, Amado de la Cruz, Yadria Giler, Patricio Encarnación and Vanessa Moreira. Further, I thank Citlalli Morelos-Juárez, Adrian Brückner, Karsten Mody for their kind support during field work, and Matteo Trevisan and Basma Khalid for their help in measuring ant specimens. I thank John Lattke, Roberto J. Guerrero, Rodrigo Feitosa and Jack Longino for identification of several ant species. Ant collecting was supported by EPN Group Project PIGR-19-16, directed by David A. Donso.

I was supported by a scholarship from the German National Academic Foundation.

3.7 REFERENCES

Agosti, D., J. Majer, L. E. Alonso, and T. Schultz. 2000. Ants: standard methods for measuring and monitoring biodiversity. Washington, DC: Smithsonian Institution Press.

Basset, Y., L. Cizek, P. Cuénoud, R. K. Didham, V. Novotny, F. Ødegaard, T. Roslin, A. K. Tishechkin, J. Schmidl, N. N. Winchester, D. W. Roubik, H.-P. Aberlenc, J. Bail, H. Barrios, J. R. Bridle, G. Castaño-Meneses, B. Corbara, G. Curletti, W. Duarte da Rocha, D. De Bakker, J. H. C. Delabie, A. Dejean, L. L. Fagan, A. Floren, R. L. Kitching, E. Medianero, E. Gama de Oliveira, J. Orivel, M. Pollet, M. Rapp, S. P. Ribeiro, Y. Roisin, J. B. Schmidt, L. Sørensen, T. M. Lewinsohn, and M. Leponce. 2015. Arthropod distribution in a tropical rainforest: tackling a four dimensional puzzle. PLOS ONE 10:e0144110.

Bates, D., D. Sarkar, M. D. Bates, and L. Matrix. 2007. The lme4 package. R package version 2:74.

de Bello, F., C. P. Carmona, A. T. Dias, L. Götzenberger, M. Moretti, and M. P. Berg. 2021. Handbook of Trait-Based Ecology: From Theory to R Tools. Cambrige: Cambridge University Press.

Bihn, J. H., G. Gebauer, and R. Brandl. 2010. Loss of functional diversity of ant assemblages in secondary tropical forests. Ecology 91:782–792.

Blanchard, B. D., A. Nakamura, M. Cao, S. T. Chen, and C. S. Moreau. 2020. Spine and dine: A key defensive trait promotes ecological success in spiny ants. Ecology and Evolution 10:5852–5863.

Blüthgen, N., and N. E. Stork. 2007. Ant mosaics in a tropical rainforest in Australia and elsewhere: A critical review. Austral Ecology 32:93–104.

Buxton, J. T., K. A. Robert, A. T. Marshall, T. L. Dutka, and H. Gibb. 2021. A cross-species test of the function of cuticular traits in ants (Hymenoptera: Formicidae). Myrmecological News 31:31–46.

Cadotte, M. W., and C. M. Tucker. 2017. Should environmental filtering be abandoned? Trends in Ecology & Evolution 32:429–437.

Chazdon, R. L., C. A. Peres, D. Dent, D. Sheil, A. E. Lugo, D. Lamb, N. E. Stork, and S. E. Miller. 2009. The potential for species conservation in tropical secondary forests. Conservation Biology 23:1406–1417.

Chmel, K., J. Riegert, L. Paul, and V. Novotný. 2016. Vertical stratification of an avian community in New Guinean tropical rainforest. Population Ecology 58:535–547.

Clusella-Trullas, S., J. H. van Wyk, and J. R. Spotila. 2007. Thermal melanism in ectotherms. Journal of Thermal Biology 32:235–245.

Connor, E. F., and D. Simberloff. 1979. The assembly of species communities: Chance or competition? Ecology 60:1132.

Crouzeilles, R., M. Curran, M. S. Ferreira, D. B. Lindenmayer, C. E. V. Grelle, and J. M. Rey Benayas. 2016. A global meta-analysis on the ecological drivers of forest restoration success. Nature Communications 7:11666.

Davidson, D. W., S. C. Cook, and R. R. Snelling. 2004. Liquid-feeding performances of ants (Formicidae): ecological and evolutionary implications. Oecologia 139:255–266.

Davies, R. W., D. P. Edwards, and F. A. Edwards. 2020. Secondary tropical forests recover dung beetle functional diversity and trait composition. Animal Conservation 23:617–627.

De Frenne, P., F. Zellweger, F. Rodríguez-Sánchez, B. R. Scheffers, K. Hylander, M. Luoto, M. Vellend, K. Verheyen, and J. Lenoir. 2019. Global buffering of temperatures under forest canopies. Nature Ecology & Evolution 3:744–749.

Dent, D. H., and S. J. Wright. 2009. The future of tropical species in secondary forests: a quantitative review. Biological Conservation 142:2833–2843.

Diamond, J. M. 1975. Assembly of Species Communities. In: Ecology and Evolution of Communities. Boston: Havard University Press.

Economo, E. P., N. Narula, N. R. Friedman, M. D. Weiser, and B. Guénard. 2018. Macroecology and macroevolution of the latitudinal diversity gradient in ants. Nature Communications 9:1778.

Edwards, D. P., M. R. Massam, T. Haugaasen, and J. J. Gilroy. 2017. Tropical secondary forest regeneration conserves high levels of avian phylogenetic diversity. Biological Conservation 209:432–439.

Edwards, F. A., D. P. Edwards, T. H. Larsen, W. W. Hsu, S. Benedick, A. Chung, C. Vun Khen, D. S. Wilcove, and K. C. Hamer. 2014. Does logging and forest conversion to oil palm agriculture alter functional diversity in a biodiversity hotspot? Functional diversity and land-use change in Borneo. Animal Conservation 17:163–173.

Ellers, J., M. P. Berg, A. T. C. Dias, S. Fontana, A. Ooms, and M. Moretti. 2018. Diversity in form and function: Vertical distribution of soil fauna mediates multidimensional trait variation. Journal of Animal Ecology 87:933–944.

Feener, D. H., J. R. B. Lighton, and G. A. Bartholomew. 1988. Curvilinear allometry, energetics and foraging ecology: a comparison of leaf-cutting ants and army ants. Functional Ecology 2:509–520.

Fermon, H., M. Waltert, R. I. Vane-Wright, and M. Mühlenberg. 2005. Forest use and vertical stratification in fruit-feeding butterflies of Sulawesi, Indonesia: impacts for conservation. Biodiversity and Conservation 14:333–350.

Fernandez, F., R. J. Guerrero, and T. Delsinne. 2019. Hormigas de Colombia. Bogota: Univ. Nacional de Colombia.

Floren, A., W. Wetzel, and M. Staab. 2014. The contribution of canopy species to overall ant diversity (Hymenoptera: Formicidae) in temperate and tropical ecosystems. Myrmecological News 19:65–74.

Fowler, H. G., L. C. Forti, C. R. F. Brandão, J. H. C. Delabie, and H. L. Vasoncelos. 1991. Ecologia nutricional de formigas. In: Ecologia Nutricional De Insetos. Sao Paulo: Maneto.

Fornoff, F., M. Staab, C.-D. Zhu, and A.-M. Klein. 2021. Multi-trophic communities re-establish with canopy cover and microclimate in a subtropical forest biodiversity experiment. Oecologia 196:289–301.

Garcia, T. S., D. J. Paoletti, and A. R. Blaustein. 2009. Correlated trait responses to multiple selection pressures in larval amphibians reveal conflict avoidance strategies. Freshwater Biology 54:1066–1077.

Gibb, H., and S. A. Cunningham. 2013. Restoration of trophic structure in an assemblage of omnivores, considering a revegetation chronosequence. Journal of Applied Ecology 50:449–458.

Gibb, H. and C. L. Parr. 2013. Does structural complexity determine the morphology of assemblages? An experimental test on three continents. PLOS ONE 8:e64005.

Gibb, H., N. J. Sanders, R. R. Dunn, X. Arnan, H. L. Vasconcelos, D. A. Donoso, A. N. Andersen, R. R. Silva, T. R. Bishop, and C. Gomez. 2018. Habitat disturbance selects against both small and large species across varying climates. Ecography 41:1184–1193.

Gibb, H., J. Stoklosa, D. I. Warton, A. M. Brown, N. R. Andrew, and S. A. Cunningham. 2015. Does morphology predict trophic position and habitat use of ant species and assemblages? Oecologia 177:519–531.

Giller, P. S. 1996. The diversity of soil communities, the poor man's tropical rainforest? Biodiversity and Conservation 5:135–168.

Huang, Y., Y. Ma, K. Zhao, P. A. Niklaus, B. Schmid, and J.-S. He. 2017. Positive effects of tree species diversity on litterfall quantity and quality along a secondary successional chronosequence in a subtropical forest. Journal of Plant Ecology 10:28–35.

Hubbell, S. P. 2011. The Unified Neutral Theory of Biodiversity and Biogeography (MPB-32): Princeton University Press.

Kaspari, M. 1993. Body size and microclimate use in Neotropical granivorous ants. Oecologia 96:500–507.

Kaspari, M., N. A. Clay, J. Lucas, S. P. Yanoviak, and A. Kay. 2015. Thermal adaptation generates a diversity of thermal limits in a rainforest ant community. Global Change Biology 21:1092–1102.

Keddy, P. A. 1992. Assembly and response rules: two goals for predictive community ecology. Journal of Vegetation Science 3:157–164.

Kembel, S. W., P. D. Cowan, M. R. Helmus, W. K. Cornwell, H. Morlon, D. D. Ackerly, S. P. Blomberg, and C. O. Webb. 2010. Picante: R tools for integrating phylogenies and ecology. Bioinformatics 26:1463–1464.

Klimes, P., C. Idigel, M. Rimandai, T. M. Fayle, M. Janda, G. D. Weiblen, and V. Novotny. 2012. Why are there more arboreal ant species in primary than in secondary tropical forests? Journal of Animal Ecology 81:1103–1112.

Kraft, N. J. B., P. B. Adler, O. Godoy, E. C. James, S. Fuller, and J. M. Levine. 2015. Community assembly, coexistence and the environmental filtering metaphor. Functional Ecology 29:592–599.

Kraft, N. J. B., W. K. Cornwell, C. O. Webb, and D. D. Ackerly. 2007. Trait Evolution, Community Assembly, and the Phylogenetic Structure of Ecological Communities. The American Naturalist 170:271–283.

Kuznetsova, A., P.B. Brockhoff, R.H.B. Christensen. 2017. lmerTest Package: Tests in Linear Mixed Effects Models. Journal of Statistical Software 82:1–26.

Lach, L., C. Parr, and K. Abbott. 2010. Ant Ecology. Oxford: Oxford University Press.

Laliberté, E. and P. Legendre. 2010. A distance-based framework for measuring functional diversity from multiple traits. Ecology 91:299–305.

Laliberté, E., P. Legendre, B. Shipley, and M. E. Laliberté. 2014. Package 'FD.' Measuring functional diversity from multiple traits, and other tools for functional ecology. R package version 1.0-12.

Laurans, M., B. Hérault, G. Vieilledent, and G. Vincent. 2014. Vertical stratification reduces competition for light in dense tropical forests. Forest Ecology and Management 329:79–88.

Law, S. J., T. R. Bishop, P. Eggleton, H. Griffiths, L. Ashton, and C. Parr. 2020. Darker ants dominate the canopy: Testing macroecological hypotheses for patterns in colour along a microclimatic gradient. Journal of Animal Ecology 89:347–359.

Lee, R. H., and B. Guénard. 2019. Choices of sampling method bias functional components estimation and ability to discriminate assembly mechanisms. Methods in Ecology and Evolution 10:867–878.

Lennox, G. D., T. A. Gardner, J. R. Thomson, J. Ferreira, E. Berenguer, A. C. Lees, R. Mac Nally, L. E. O. C. Aragão, S. F. B. Ferraz, J. Louzada, N. G. Moura, V. H. F. Oliveira, R. Pardini, R. R. C. Solar, F. Z. Vaz-de Mello, I. C. G. Vieira, and J. Barlow. 2018. Second rate or a second chance? Assessing biomass and biodiversity recovery in regenerating Amazonian forests. Global Change Biology 24:5680–5694.

Lenth, R. V. (2021). emmeans: Estimated Marginal Means, aka Least-Squares Means. R package version 1.5.4. https://CRAN.R-project.org/package=emmeans

Liu, C., B. Guénard, B. Blanchard, Y.-Q. Peng, and E. P. Economo. 2016. Reorganization of taxonomic, functional, and phylogenetic ant biodiversity after conversion to rubber plantation. Ecological Monographs 86:215–227.

Longino, J. T. 2007. Ants of Costa Rica Website. https://ants.biology.utah.edu/AntsofCostaRica.html

Lucky, A., M. D. Trautwein, B. S. Guenard, M. D. Weiser, and R. R. Dunn. 2013. Tracing the rise of ants-out of the ground. PLOS ONE 8:e84012.

Macarthur, R., and R. Levins. 1967. The limiting similarity, convergence, and divergence of coexisting species. The American Naturalist 101:377–385.

Meli, P., K. D. Holl, J. M. Rey Benayas, H. P. Jones, P. C. Jones, D. Montoya, and D. Moreno Mateos. 2017. A global review of past land use, climate, and active vs. passive restoration effects on forest recovery. PLOS ONE 12:e0171368.

Mo, X.-X., L.-L. Shi, Y.-J. Zhang, H. Zhu, and J. F. Slik. 2013. Change in phylogenetic community structure during succession of traditionally managed tropical rainforest in southwest China. PLOS ONE 8:e71464.

Mouchet, M. A., S. Villéger, N. W. H. Mason, and D. Mouillot. 2010. Functional diversity measures: an overview of their redundancy and their ability to discriminate community assembly rules: Functional diversity measures. Functional Ecology 24:867–876.

Oksanen, J., F. G. Blanchet, R. Kindt, P. Legendre, R. B. O'hara, G. L. Simpson, P. Solymos, M. H. H. Stevens, and H. Wagner. 2010. Vegan: community ecology package. R package version 1.17-4. URL http://CRAN. R-project. org/package=vegan.

Parr, C. L., R. R. Dunn, N. J. Sanders, M. D. Weiser, M. Photakis, T. R. Bishop, M. C. Fitzpatrick, X. Arnan, F. Baccaro, and C. R. Brandão. 2017. GlobalAnts: A new database on the geography of ant traits (Hymenoptera: Formicidae). Insect Conservation and Diversity 10:5–20.

Peeters, C., R. A. Keller, A. Khalife, G. Fischer, J. Katzke, A. Blanke, and E. P. Economo. 2020. The loss of flight in ant workers enabled an evolutionary redesign of the thorax for ground labour. Frontiers in Zoology 17:1–13.

del Pliego, P. G., B. R. Scheffers, E. W. Basham, P. Woodcock, C. Wheeler, J. J. Gilroy, C. A. M. Uribe, T. Haugaasen, R. P. Freckleton, and D. P. Edwards. 2016. Thermally buffered microhabitats recovery in tropical secondary forests following land abandonment. Biological Conservation 201:385–395.

Plowman, N. S., O. Mottl, V. Novotny, C. Idigel, F. J. Philip, M. Rimandai, and P. Klimes. 2020. Nest microhabitats and tree size mediate shifts in ant community structure across elevation in tropical rainforest canopies. Ecography 43:431–442.

Rocha-Ortega, M., X. Arnan, J. D. Ribeiro-Neto, I. R. Leal, M. E. Favila, and M. Martínez-Ramos. 2018. Taxonomic and functional ant diversity along a secondary successional gradient in a tropical forest. Biotropica 50:290–301.

Santoandré, S., J. Filloy, G. A. Zurita, and M. I. Bellocq. 2019. Ant taxonomic and functional diversity show differential response to plantation age in two contrasting biomes. Forest ecology and management 437:304–313.

Scheffers, B. R., B. L. Phillips, W. F. Laurance, N. S. Sodhi, A. Diesmos, and S. E. Williams. 2013. Increasing arboreality with altitude: a novel biogeographic dimension. Proceedings of the Royal Society B: Biological Sciences 280:20131581.

Schmidt, F. A., C. R. Ribas, and J. H. Schoereder. 2013. How predictable is the response of ant assemblages to natural forest recovery? Implications for their use as bioindicators. Ecological Indicators 24:158–166.

Schofield, S. F., T. R. Bishop, and C. L. Parr. 2016. Morphological characteristics of ant assemblages (Hymenoptera: Formicidae) differ among contrasting biomes. Myrmecological News 23:129–137.

Schulze, C. H., K. E. Linsenmair, and K. Fiedler. 2001. Understorey versus canopy: patterns of vertical stratification and diversity among Lepidoptera in a Bornean rain forest. Pages 133–152 *in* K. E. Linsenmair, A. J. Davis, B. Fiala, and M. R. Speight, editors. Tropical Forest Canopies: Ecology and Management. Springer Netherlands, Dordrecht.

Silva, R. R., and C. R. F. BrandÃ£o. 2010. Morphological patterns and community organization in leaf-litter ant assemblages. Ecological Monographs 80:107–124.

Skarbek, C. J., M. Noack, H. Bruelheide, W. Härdtle, G. von Oheimb, T. Scholten, S. Seitz, and M. Staab. 2020. A tale of scale: Plot but not neighbourhood tree diversity increases leaf litter ant diversity. Journal of Animal Ecology 89:299–308.

Sommer, S. and R. Wehner. 2012. Leg allometry in ants: extreme long-leggedness in thermophilic species. Arthropod Structure & Development 41:71–77.

Sosiak, C. E., and P. Barden. 2020. Multidimensional trait morphology predicts ecology across ant lineages. Functional Ecology.

Srivastava, D. S., M. W. Cadotte, A. A. M. MacDonald, R. G. Marushia, and N. Mirotchnick. 2012. Phylogenetic diversity and the functioning of ecosystems. Ecology letters 15:637–648.

Staab, M., X. Liu, T. Assmann, H. Bruelheide, F. Buscot, W. Durka, A. Erfmeier, A.-M. Klein, K. Ma, and S. Michalski. 2021. Tree phylogenetic diversity structures multitrophic communities. Functional Ecology 35:521–534.

Tucker, C.M., M.W. Cadotte, S.B. Carvalho, T.J. Davies, S. Ferrier, S.A. Fritz, R. Grenyer, M.R. Helmus, L.S. Jin, A.O. Mooers, S. Pavoine, O. Purschke, D.W. Redding, D.F. Rosauer, M. Winter, and F. Mazel. 2017. A guide to phylogenetic metrics for conservation, community ecology and macroecology. Biological Reviews 92:698–715.

Villéger, S., N. W. Mason, and D. Mouillot. 2008. New multidimensional functional diversity indices for a multifaceted framework in functional ecology. Ecology 89:2290–2301.

Weiser, M. D., and M. Kaspari. 2006. Ecological morphospace of New World ants. Ecological Entomology 31:131–142.

Whitworth, A., C. Beirne, R. Pillco Huarcaya, L. Whittaker, S. J. Serrano Rojas, M. W. Tobler, and R. MacLeod. 2019. Human disturbance impacts on rainforest mammals are most notable in the canopy, especially for larger-bodied species. Diversity and Distributions 25:1166–1178.

Whitworth, A., J. Villacampa, A. Brown, R. P. Huarcaya, R. Downie, and R. MacLeod. 2016. Past Human disturbance effects upon biodiversity are greatest in the canopy; a case study on rainforest butterflies. PLOS ONE 11:e0150520.

Widenfalk, L. A., A. Malmström, M. P. Berg, and J. Bengtsson. 2016. Small-scale Collembola community composition in a pine forest soil – Overdispersion in functional traits indicates the importance of species interactions. Soil Biology and Biochemistry 103:52–62.

Wittman, S. E., N. J. Sanders, A. M. Ellison, E. S. Jules, J. S. Ratchford, and N. J. Gotelli. 2010. Species interactions and thermal constraints on ant community structure. Oikos 119:551–559.

Wong, M. K., B. Guénard, and O. T. Lewis. 2019. Trait-based ecology of terrestrial arthropods. Biological Reviews 94:999–1022.

3.8 SUPPLEMENT

Supplement for Hoenle, P. O.. Stratification and recovery time jointly shape ant functional reassembly in a Neotropical forest. Manuscript in preparation for publication.

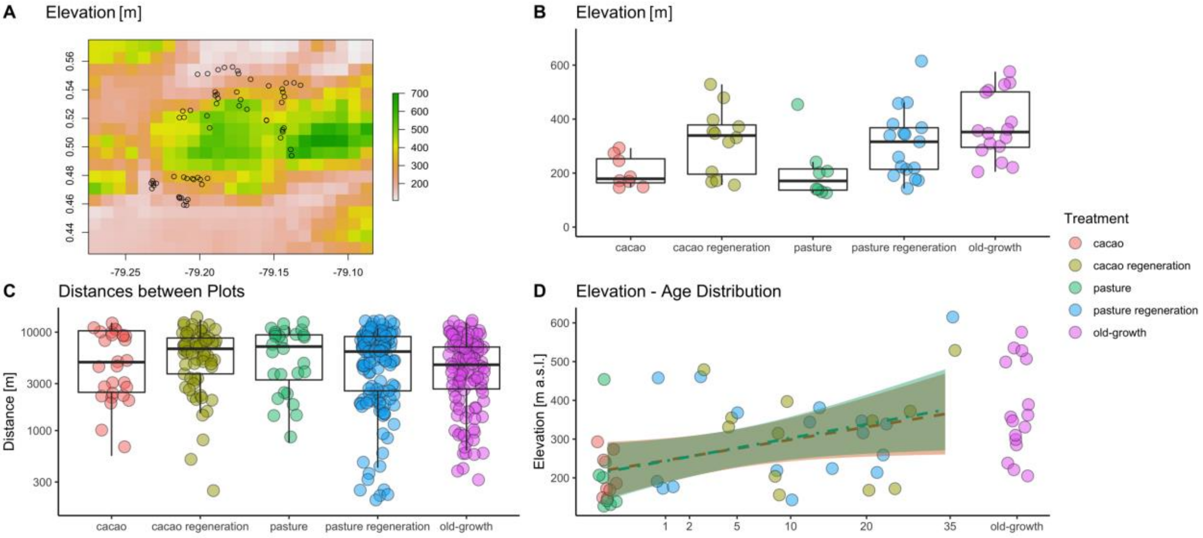

Fig. S3.1 **A**: Map of all plots superimposed on an elevation heatmap of the study area, made with the r-package 'raster' (Hijman 2011: http://raster.r-forge.r-project.org/) **B**: Elevational distribution of each plot category. **C**: Distances between each plot within each category. The y-axis is log-transformed. Mean ± SD distance is 5,799 ± 3,373 m. The shortest inter-category distance is 170 m, the longest is 13,403 m. **D**: Relationship between elevation and recovery time. The two variables are significantly correlated (linear model; F-value = 4.38, $R^2 = 0.18$, p = 0.003), and there is no difference between cacao and pasture land-use legacy (linear model; F-value = 4.38, $R^2 = 0.18$, p = 0.10). Thanks to Nico Blüthgen for his supervision and plot choice.

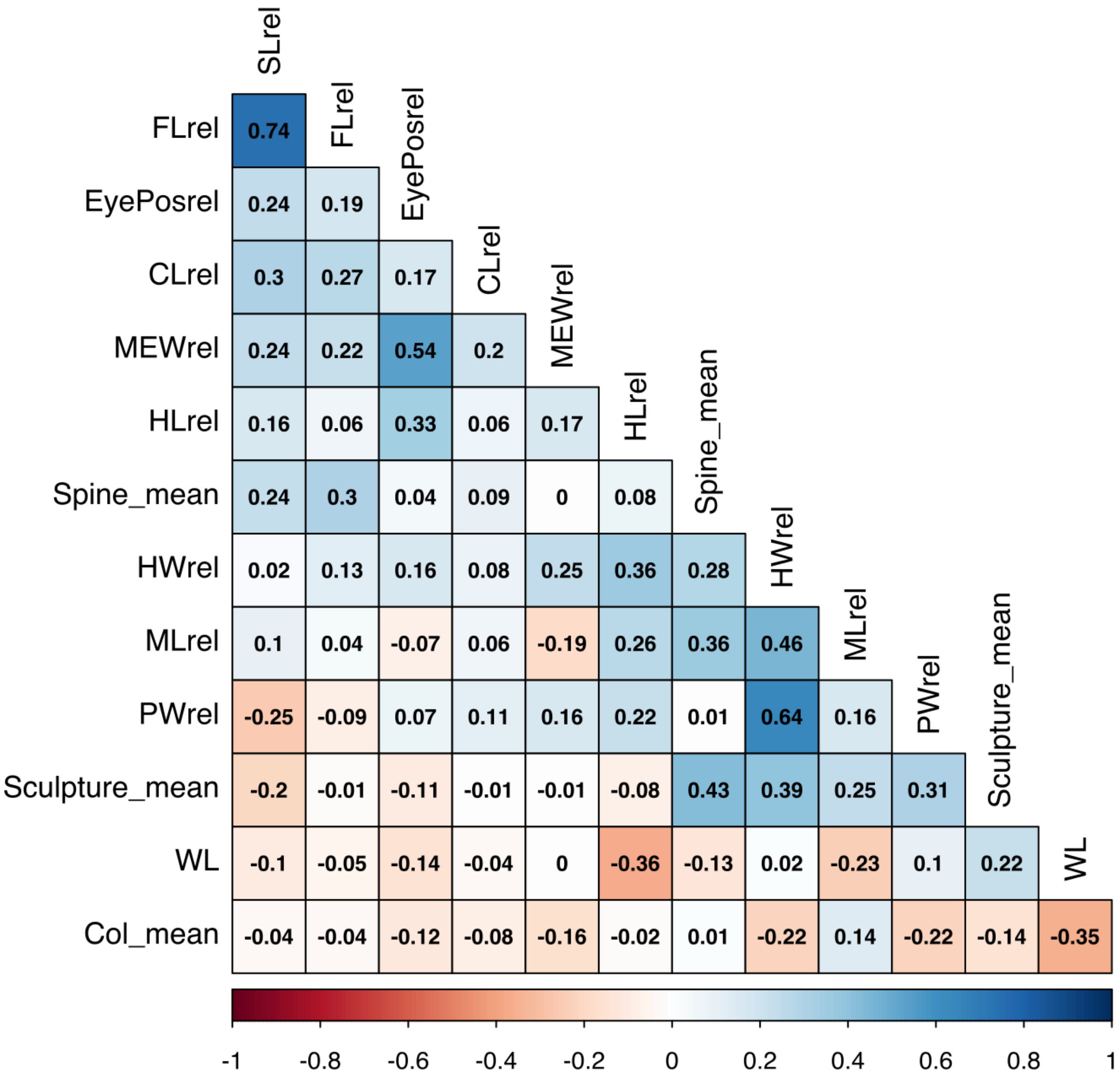

	SLrel	FLrel	EyePosrel	CLrel	MEWrel	HLrel	Spine_mean	HWrel	MLrel	PWrel	Sculpture_mean	WL
FLrel	0.74											
EyePosrel	0.24	0.19										
CLrel	0.3	0.27	0.17									
MEWrel	0.24	0.22	0.54	0.2								
HLrel	0.16	0.06	0.33	0.06	0.17							
Spine_mean	0.24	0.3	0.04	0.09	0	0.08						
HWrel	0.02	0.13	0.16	0.08	0.25	0.36	0.28					
MLrel	0.1	0.04	-0.07	0.06	-0.19	0.26	0.36	0.46				
PWrel	-0.25	-0.09	0.07	0.11	0.16	0.22	0.01	0.64	0.16			
Sculpture_mean	-0.2	-0.01	-0.11	-0.01	-0.01	-0.08	0.43	0.39	0.25	0.31		
WL	-0.1	-0.05	-0.14	-0.04	0	-0.36	-0.13	0.02	-0.23	0.1	0.22	
Col_mean	-0.04	-0.04	-0.12	-0.08	-0.16	-0.02	0.01	-0.22	0.14	-0.22	-0.14	-0.35

Fig. S3.2 Correlation plot of all measured ant traits. Blue indicates a positive, red a negative pairwise correlation (Spearman correlation). Color intensity scales with strength of correlation. FL= Femur length; EyePosrel; relative Eye position; CLrel = relative Clypeus length; MEWrel = relative Maximum Eye width; HLrel= relative head length; Spine_mean = number of spines; HWrel = relative head width; MLrel = relative mandible length; PWrel = relative pronotum width; Sculpture_mean: Sculpture; WL = Weber's Length; Col_mean: Color lightness.

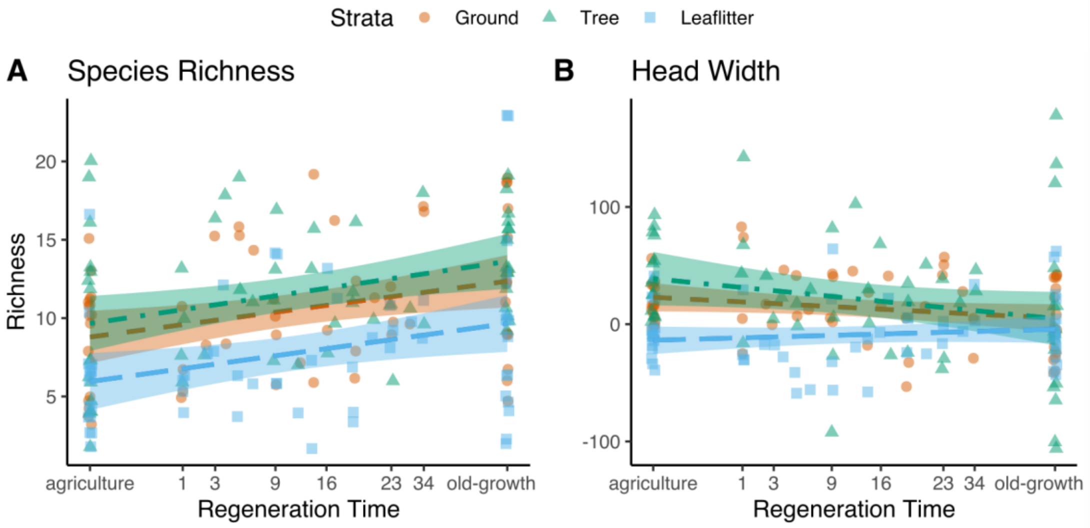

Fig. S3.3 Ant species richness and community weighted mean of head width along the recovery sequence. The regression line and 95% confidence intervals of each stratum are plotted. Colors indicate strata (green = tree trunk; red = ground; blue = leaf litter). Both have a trajectory consistent with the stratification hypothesis. For the full statistical models see Table S3.2 and Table S3.3.

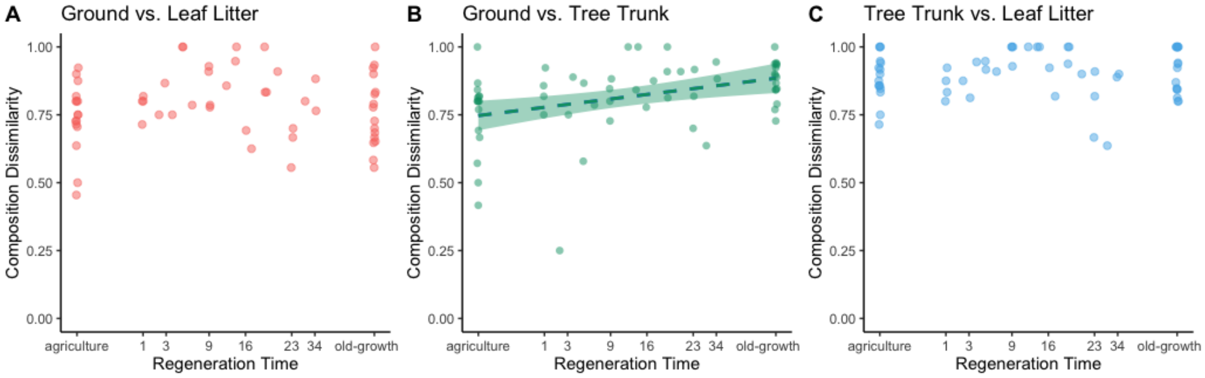

Fig. S3.4 Pairwise comparison of species overlap (as Bray-Curtis Dissimilarity) along recovery time in A) ground vs. leaf litter communities, B) ground vs. tree trunk communities and C) tree trunk vs. leaf litter communities. Only B) was statistically significant (at $p<0.05$) and was plotted with a regression line and 95% CI. For the full models see Supplement Table S3.2.

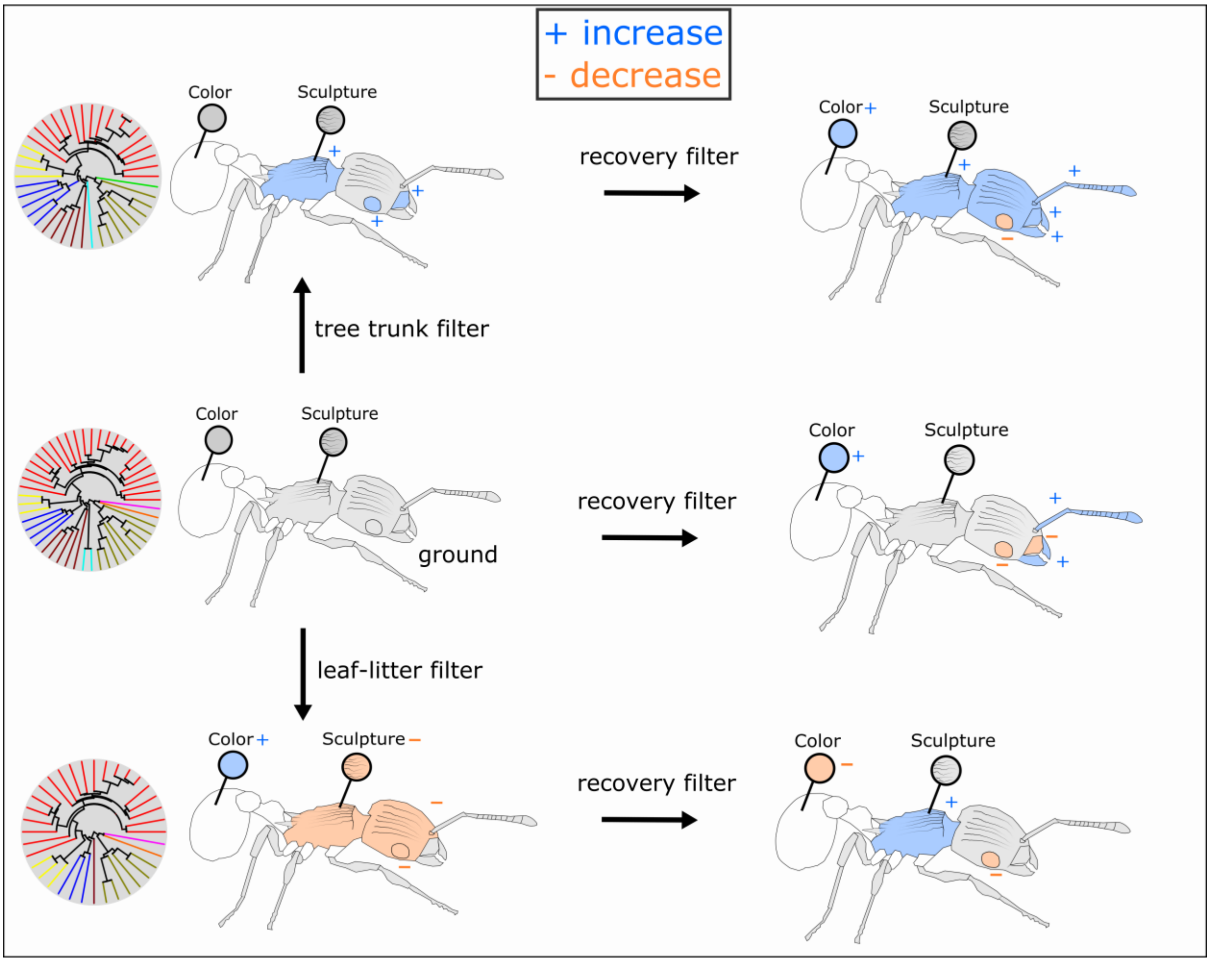

Fig. S3.5. Morphological and phylogenetic differences between the three strata and induced morphological changes with recovery time. The middle ant on the left side represents the ground assemblage, which serves as comparison baseline for the tree and leaf-litter community. Phylogenetic trees show all genera found per stratum, with colors indicating subfamily affiliation (same color = same subfamily). On the ants' body, grey areas indicate traits that were measured, but did not change (either between stratum: upper left & lower left; or induced by recovery, all ants at to the right). Blue-colored traits indicate a significant increase, while orange indicates a significant decrease. Three body parts are represented by two different trait measurements (mesosoma: Weber's length and pronotum width; Head: head length and head width; Eye: Eye size and Eye positioning). If any of these trait means were significant, I colored the whole part. Legs indicate changes in femur length, spines the amount of spines, mandibles the mandible length, clypeus the clypeus length, and the antenna the scape length. Note that on the left side, only significant differences between either tree trunk and ground or leaf-litter and ground are highlighted, i.e. not those between tree and leaf-litter.

Table S3.1 Species list of the ants collected during this study. In total, 284 species were collected. They are sorted alphabetically within subfamilies. Further given are the sum of occurences for each stratum and the number of individuals measured for the trait analysis.

Species	n measured	Leaf litter	Ground	Tree
Amblyoponinae				
Prionopelta amabilis	4	5	0	0
Prionopelta modesta	4	8	5	0
Dolichoderinae				
Azteca sp. A	2	0	0	2
Azteca sp. B	0	0	0	1
Azteca sp. C	2	0	0	2
Azteca sp. D	0	0	0	1
Azteca sp. E	2	0	0	1
Azteca sp. F	2	0	0	1
Azteca sp. G	0	0	0	1
Azteca sp. H	0	0	0	1
Azteca sp. I	2	0	0	4
Azteca sp. J	0	0	0	1
Azteca sp. K	0	0	1	1
Azteca sp. L	1	0	0	1
Azteca sp. O	0	0	0	1
Azteca sp. P	1	0	0	2
Azteca sp. Q	0	0	0	1
Dolichoderus baenae	2	0	1	5
Dolichoderus cf. *bispinosus*	2	0	0	3
Dolichoderus cf. *validus*	2	0	1	2
Dolichoderus lamellosus	2	0	0	1
Dolichoderus laurae	0	0	0	1
Linepithema piliferum	3	2	7	6
Linepithema tsachila	3	0	1	3
Tapinoma ramulorum inrectum	6	0	0	4
Tapinoma sp. A	0	0	0	1
Tapinoma sp. C	4	0	1	3
Dorylinae				
Eciton burchellii	2	0	1	2
Eciton lucanoides	3	0	1	0
Neivamyrmex sp. A	1	0	1	0
Ectatomminae				

Ectatomma goninion	0	1	3	0
Ectatomma ruidum	4	7	34	24
Ectatomma tuberculatum	3	0	0	13
Gnamptogenys annulata	2	0	1	2
Gnamptogenys banksi	0	0	1	0
Gnamptogenys cf. *brunnea*	4	0	2	3
Gnamptogenys cf. *enodis*	0	0	1	0
Gnamptogenys concinna	1	0	0	1
Gnamptogenys continua	1	1	0	0
Gnamptogenys extra	2	1	1	1
Gnamptogenys haenschi	2	1	1	0
Gnamptogenys horni	3	0	5	0
Gnamptogenys minuta	1	1	1	0
Gnamptogenys nr. *banski*	2	0	1	0
Gnamptogenys porcata	4	0	1	20
Gnamptogenys regularis	1	0	0	1
Gnamptogenys sulcata	4	0	0	4
Gnamptogenys tornata	2	2	1	1
Typhlomyrmex pusillus	2	1	1	0
Typhlomyrmex rogenhoferi	0	0	0	1
Typhlomyrmex sp. A	0	0	1	0
Formicinae				
Acropyga cf. *guianensis*	4	2	0	2
Acropyga fuhrmanni	2	0	1	2
Brachymyrmex cavernicola	2	0	4	0
Brachymyrmex cf. *australis*	7	8	4	10
Brachymyrmex cf. *termitophilus*	2	0	1	2
Brachymyrmex pictus	6	4	2	7
Brachymyrmex sp. A	4	1	5	8
Brachymyrmex sp. B	1	0	0	2
Camponotus cf. *brettesi*	0	0	0	1
Camponotus cf. *senex*	2	0	0	2
Camponotus novogranadensis	5	0	1	7
Camponotus sericeiventris	4	0	0	5
Camponotus sp. A	0	0	0	1
Camponotus sp. B	0	0	0	1
Myrmelachista sp. B	0	0	0	1
Nylanderia cf. *guatemalensis*	5	5	6	9
Nylanderia sp. A	1	0	0	1
Nylanderia sp. B	3	0	1	1
Nylanderia sp. C	2	3	0	0

Nylanderia sp. D	2	3	2	0
Nylanderia sp. F	2	0	0	1
Nylanderia sp. G	0	0	0	1
Nylanderia steinheili complex	3	9	13	20
Heteroponerinae				
Acanthoponera minor	2	0	0	3
Acanthoponera PH1	0	0	0	1
Myrmicinae				
Acromyrmex cf. *octospinosus*	3	0	4	4
Acromyrmex cf. *volcanus*	2	0	0	4
Adelomyrmex sp. A	2	1	1	0
Apterostigma carinatum	3	0	2	14
Apterostigma chocoense	2	1	1	0
Apterostigma sp. A	3	1	1	0
Atta cephalotes	0	3	0	0
Cardiocondyla emeryi	0	0	1	0
Cardiocondyla minutior	1	1	1	0
Carebara brevipilosa	2	0	1	0
Cephalotes cf. *peruviensis*	0	0	0	1
Cephalotes cf. *umbraculatus*	0	0	0	1
Crematogaster arcuata	2	0	1	2
Crematogaster brasiliensis	2	0	0	3
Crematogaster carinata	4	0	0	9
Crematogaster cf. *flavomicrops*	3	0	3	7
Crematogaster crinosa complex	4	0	2	9
Crematogaster curvispinosa	4	1	1	9
Crematogaster limata	4	0	3	12
Crematogaster longispina	4	2	6	11
Crematogaster nigropilosa	4	0	3	13
Crematogaster raptor	2	0	0	1
Crematogaster sotobosque	4	2	5	1
Crematogaster sp. A	0	0	0	1
Crematogaster tenuicula	2	0	4	3
Cyphomyrmex castagnei	4	1	5	3
Cyphomyrmex cf. *bicarinatus*	4	3	8	0
Cyphomyrmex cf. *cornutus* sp. A	4	1	9	21
Cyphomyrmex cf. *cornutus* sp. B	2	1	2	0
Cyphomyrmex cf. *cornutus* sp. C	0	0	0	1
Cyphomyrmex costatus	4	0	5	0
Cyphomyrmex longiscapus	2	0	0	4

Cyphomyrmex nr. *rimosus* sp. A	4	2	10	6
Cyphomyrmex nr. *rimosus* sp. B	3	0	5	3
Cyphomyrmex nr. *salvini* sp. B	4	1	7	4
Cyphomyrmex nr. *salvini* sp. C	4	6	4	0
Eurhopalothrix xibalba	0	0	1	0
Hylomyrma montana	2	2	0	0
Lachnomyrmex cf. *haskinsi*	1	0	1	0
Lenomyrmex foveolatus	4	2	2	2
Megalomyrmex bidentatus	1	0	0	2
Megalomyrmex incisus	2	1	0	0
Megalomyrmex leoninus group sp. A	2	0	0	3
Megalomyrmex leoninus group sp. B	0	0	1	0
Megalomyrmex leoninus group sp. C	12	0	9	7
Megalomyrmex modestus group sp. A	4	0	1	6
Megalomyrmex sp. A	1	1	0	0
Monomorium floricola	4	5	1	1
Mycecopurus tardus	1	0	1	0
Mycetomoellerius isthmicus	3	2	11	0
Mycetomoellerius sp. A	1	0	1	0
Mycetomoellerius sp. B	1	0	1	0
Nesomyrmex asper	0	0	0	1
Octostruma cf. *amrishi*	4	17	9	0
Octostruma cf. *gymnogon*	0	0	1	0
Octostruma cf. *onorei*	0	1	0	0
Octostruma stenoscapa	2	3	2	0
Paratrachymyrmex bugnioni	1	0	0	1
Paratrachymyrmex cornetzi	2	1	3	0
Pheidole cf. *anastasii*	2	1	0	3
Pheidole cf. *boliviana*	1	0	0	1
Pheidole cf. *cataphracta*	1	0	0	1
Pheidole cf. *excubitor*	2	0	2	0
Pheidole cf. *flavens*	3	2	2	26
Pheidole cf. *harrisonfordi*	4	28	11	1
Pheidole cf. *hazenae*	1	0	0	1
Pheidole cf. *jaculifera*	4	1	9	0
Pheidole cf. *simonsi*	2	0	1	2
Pheidole cf. *tennantae*	2	1	0	1
Pheidole cf. *unicornis*	0	0	1	0
Pheidole cf. *verricula*	0	0	1	0
Pheidole colobopsis	5	1	4	0
Pheidole dilligens group sp. A	2	0	2	1
Pheidole dilligens group sp. B	1	0	1	0

Pheidole ectatommoides	2	0	2	0
Pheidole fallax group sp. A	1	0	0	1
Pheidole fallax group sp. C	2	0	1	0
Pheidole fallax group sp. D	1	0	0	3
Pheidole fallax group sp. E	3	1	3	0
Pheidole fallax group sp. F	4	0	5	1
Pheidole fallax group sp. G	4	0	7	2
Pheidole fallax group sp. I	2	0	2	0
Pheidole fallax group sp. K	2	0	1	1
Pheidole flavens group sp. A	1	1	0	0
Pheidole flavens group sp. D	2	0	0	4
Pheidole flavens group sp. E	1	0	0	1
Pheidole flavens group sp. G	3	0	0	4
Pheidole flavens group sp. H	2	2	2	0
Pheidole flavens group sp. L	3	2	3	0
Pheidole flavens group sp. M	2	1	1	0
Pheidole flavens group sp. N	2	2	1	0
Pheidole flavens group sp. O	0	0	0	1
Pheidole flavens group sp. P	2	1	2	0
Pheidole flavens group sp. Q	1	0	0	1
Pheidole flavens group sp. R	3	0	0	3
Pheidole flavens group sp. S	1	0	0	1
Pheidole flavens group sp. T	2	1	0	0
Pheidole flavens group sp. U	1	0	0	1
Pheidole flavens group sp. V	2	0	0	3
Pheidole flavens group sp. W	1	0	1	0
Pheidole flavens group sp. Z	1	0	0	1
Pheidole gauthieri	2	0	1	2
Pheidole guyasana	3	2	7	0
Pheidole nitella	3	8	16	6
Pheidole nr. *ajax*	2	0	0	1
Pheidole nr. *exquisita*	2	1	1	0
Pheidole nr. *onyx*	6	2	4	5
Pheidole nr. *specularis*	4	3	3	1
Pheidole perpusilla	2	0	0	3
Pheidole perpusilla group sp. A	2	0	0	3
Pheidole perpusilla group sp. B	1	0	0	1
Pheidole rhinomontana	3	2	4	2
Pheidole rugiceps	4	5	9	0
Pheidole sensitiva	2	0	1	0
Pheidole tristis group sp. A	1	0	0	1
Pheidole tristis group sp. B	1	0	1	0

Pheidole ulothrix	4	0	1	9
Pheidole vorax	2	0	0	1
Pheidole zeteki	4	6	3	1
Rogeria cf. *belti*	4	19	13	1
Rogeria cf. *leptonana*	0	0	1	0
Rogeria gibba	2	2	5	1
Rogeria inermis	2	0	1	2
Rogeria scandens	0	0	0	1
Rogeria sp. A	2	0	0	1
Sericomyrmex cf. *amabilis*	8	5	11	0
Solenopsis bicolor	6	3	1	4
Solenopsis cf. *brevicornis*	5	21	4	5
Solenopsis cf. *stricta*	2	1	4	0
Solenopsis cf. *zeteki*	4	0	5	5
Solenopsis geminata	4	3	9	3
Solenopsis modesta group lump	11	26	10	10
Solenopsis sp. A	7	8	5	0
Solenopsis sp. B	4	3	4	0
Solenopsis sp. C	2	2	0	0
Solenopsis sp. D	2	1	2	0
Solenopsis sp. E	2	1	2	0
Solenopsis sp. F	3	3	2	2
Solenopsis subterranea	2	4	0	0
Stenamma schmidti	4	4	8	1
Strumigenys biolleyi	3	3	0	2
Strumigenys cascanteae	1	0	0	1
Strumigenys denticulata	6	11	1	0
Strumigenys eggersi	3	7	2	0
Strumigenys fridericimuelleri	2	1	0	1
Strumigenys gundlachi	4	11	1	1
Strumigenys gundlachi group sp. A	1	0	0	1
Strumigenys lalassa	2	2	0	1
Strumigenys longispina	3	0	6	0
Strumigenys louisianae	4	5	11	1
Strumigenys myllorhapha	2	2	1	0
Strumigenys nigrescens	1	0	0	1
Strumigenys oconitrilloae	1	0	0	1
Strumigenys schulzi	1	0	0	1
Strumigenys sp. A (=*S. ayersthey*)	0	0	1	0
Strumigenys spathula	1	0	1	0
Strumigenys trinidadensis	2	0	0	2
Tranopelta gilva	4	7	1	12

Wasmannia auropunctata	7	36	35	40
Wasmannia sigmoidea	3	7	3	2
Paraponerinae				
Paraponera clavata	1	0	0	5
Ponerinae				
Anochetus diegensis	2	1	1	0
Anochetus mayri	2	0	3	0
Anochetus simoni	3	3	4	1
Hypoponera cf. *distinguenda*	5	6	6	1
Hypoponera cf. *parva*	3	2	5	1
Hypoponera sp. A	4	10	13	2
Hypoponera sp. B	3	6	10	1
Hypoponera sp. D	1	1	0	0
Hypoponera sp. E	2	4	1	0
Hypoponera sp. F	2	2	1	1
Hypoponera sp. G	2	2	2	0
Hypoponera sp. I	2	0	0	4
Hypoponera sp. J	0	1	0	0
Hypoponera sp. K	5	22	15	1
Hypoponera sp. L	4	3	4	12
Hypoponera sp. N	0	1	0	0
Leptogenys cf. *punctaticeps*	1	0	0	1
Leptogenys sp. B	2	0	1	1
Leptogenys sp. C	2	0	1	1
Odontomachus bauri	5	4	17	16
Odontomachus chelifer	3	0	4	1
Odontomachus hastatus	3	0	0	5
Odontomachus meinerti	2	0	1	1
Odontomachus sp. A	1	0	0	2
Pachycondyla harpax	4	6	22	8
Pachycondyla impressa	2	0	0	1
Platythyrea angusta	1	0	1	0
Platythyrea prizo	2	0	0	2
Pseudoponera cf. *succedanea*	2	1	2	3
Pseudoponera stigma	3	1	0	3
Rasopone (=Mayaponera) arhuaca	2	2	2	0
Neoponera apicalis	3	0	0	9
Neoponera bugabensis	0	0	0	1
Neoponera carinulata	4	0	0	12
Neoponera laevigata	2	0	0	1

Neoponera striatinodis	2	0	0	2
Neoponera villosa	2	0	1	6
Proceratiinae				
Discothyrea sexarticulata	0	1	0	0
Proceratium convexiceps	0	0	1	0
Pseudomyrmecinae				
Pseudomyrmex boopis	3	0	5	8
Pseudomyrmex gracilis group sp. A	2	0	0	3
Pseudomyrmex oki	1	0	1	2
Pseudomyrmex pallidus group sp. A	2	0	0	1
Pseudomyrmex pallidus group sp. B	1	0	0	1
Pseudomyrmex spiculus	1	0	0	1
Pseudomyrmex subater	0	0	0	1

Table S3.2 Statistical results for analysis on species richness from Fig. S3.3 A and species composition from Fig. 3.2. The table shows results from PERMANOVA, envit vectors and linear mixed effects models (LME). The anova in parentheses indicates an anova test on the model for significance. When testing for legacy effects I used a dataset without old-growth forests (see methods). Significant p-values are highlighted in bold. Nico Blüthgen and Michael Staab provided supervision on the statistical analysis.

Composition Dissimilarity: HS vs. T

- LME	*Estimates*	*SE*	*p*
Intercept	0.7768	0.0484	**<0.0001**
Elevation[m]	-0.0001	0.0002	0.5655
Richness	0.0035	0.0039	0.3746
Recovery Time	0.0027	0.0001	**0.0029**
- Legacy (anova)			0.4498
- Legacy * Recovery Time (anova)			0.7088

Composition Dissimilarity: HS vs. W

- LME	*Estimates*	*SE*	*p*
Intercept	0.8057	0.0360	**<0.0001**
Elevation[m]	0.0003	0.0001	**0.0163**
Richness	-0.0020	0.0031	0.5360
Recovery Time	-0.0007	0.0008	0.3892
- Legacy (anova)			0.3241
- Legacy * Recovery Time (anova)			0.4325

Composition Dissimilarity: T vs. W

- LME	*Estimates*	*SE*	*p*
Intercept	0.9092	0.0266	**<0.0001**
Elevation[m]	<0.0001	0.0001	0.7870
Richness	0.0012	0.0020	0.5710
Recovery Time	0.0002	0.0005	0.7230
- Legacy (anova)			0.3241
- Legacy * Recovery Time (anova)			0.4325

Species Richness

- LME	*Estimates*	*SE*	*p*
Intercept	6.5560	1.6816	**0.0307**
Elevation [m]	0.0080	0.0027	**0.0042**
Recovery Time	0.0461	0.0301	0.1278
- Marginal R^2 / Conditional R^2	0.2286/ 0.3879		

- Stratum*Recovery Time (anova)			0.9747
- Legacy(anova)			0.4004
- Legacy*Recovery Time (anova)			0.1777
- Stratum (anova)			**0.0256**
- contrast estimate (Holm-adj.)			
Ground - Tree	-1.0656	0.6823	0.1210
Ground - Leaf litter	2.7705	0.6823	**0.0002**
Tree - Leaf litter	3.8361	0.6823	**<0.0001**
Species Composition Tree Trunk			
- PERMANOVA	*R2*	*F*	*p*
Elevation [m]	0.0312	1.974	**0.0002**
Recovery Time	0.0364	2.301	**<0.0001**
Species Composition Leaf litter			
- PERMANOVA	*R2*	*F*	*p*
Elevation [m]	0.0207	1.3158	0.0954
Recovery Time	0.0428	2.7236	**<0.0001**
Species Composition Ground			
- PERMANOVA	*R2*	*F*	*p*
Elevation [m]	0.0292	1.9066	**0.0032**
Recovery Time	0.0495	3.2307	**<0.001**

Table S3.3 Model outputs for the functional diversity indices, which are shown in Fig. 3.3, A-C. The table shows linear mixed effects model (LME) results and subsequent post-hoc tests. For each functional diversity index, I indicated if its trajectory was consistent with the stratification or interaction hypothesis. The anova in brackets indicates an anova test on the model. If 'Stratum' was significant in the anova, I applied a contrast as post-hoc procedure to test specifically between the strata. If recovery time or an interaction was significant in the LME, I tested the recovery trajectory of each subset separately ('Recovery subset models'). When testing for legacy effects I used a dataset without old-growth forests (see methods). Significant p-values are highlighted in bold. Nico Blüthgen and Michael Staab provided supervision on the statistical analysis.

Functional Divergence			
-LME	*Estimates*	*SE*	*p*
Intercept	0.7968	0.0192	**<0.0001**
Elevation [m]	<0.0001	<0.0001	0.687
Recovery Time	0.0004	0.0005	0.420
Richness	-0.0018	0.0012	0.119
Marginal R^2 / Conditional R^2	0.0308/ 0.0308		
- Legacy (anova)			0.8463
- Legacy* Recovery Time (anova)			0.9459
- Stratum (anova)			0.6305
- Stratum*Recovery Time (anova)			0.7863
Functional Richness: Interaction Hypothesis			
- LME	*Estimates*	*SE*	*p*
Intercept	0.0040	0.0055	**<0.0001**
Elevation [m]	<0.0001	1.202e-05	0.2156
Recovery Time	-0.0003	0.0001	0.0214
Richness	0.0034	0.0033	**<0.0001**
- Marginal R^2 / Conditional R^2	0.250/ 0.3578		
- Legacy (anova)			0.1337
- Legacy*Recovery Time (anova)			0.0699
- Stratum (anova)			**<0.0001**
- Stratum*Recovery Time (anova)			**0.0171**
-contrast estimate (Holm-adj.)			
Ground - Tree	-0.0016	0.0032	0.6238
Ground - Leaf litter	0.0156	0.0033	**<0.0001**
Tree - Leaf litter	0.0171	0.0035	**<0.0001**
- Recovery subset models			
Tree subset	<0.0001	<0.0001	0.8173
Leaf litter subset	0.0002	0.0002	0.1322

Ground subset	-0.0003	0.0001	**0.0328**

Functional Eveness: Interaction Hypothesis

- LME	*Estimates*	*SE*	*p*
Intercept	0.9437	0.0048	**<0.0001**
Elevation [m]	<0.0001	<0.0001	0.2886
Recovery Time	0.0002	0.0001	**0.0433**
Richness	0.0008	0.0003	**0.0048**
- Marginal R^2 / Conditional R^2	0.2070/ 0.2070		
- Legacy (anova)			0.2775
- Legacy * Recovery Time (anova)			0.4675
- Stratum (anova)			**0.0100**
- Stratum*Recovery Time (anova)			**0.0269**
-contrast estimate (Holm-adj.)			
Ground - Tree	0.0072	0.0028	**0.0108**
Ground - Leaf litter	-0.0094	0.0029	**0.0032**
Tree - Leaf litter	-0.0165	0.0031	**<0.0001**
- Recovery subset models			
Tree subset	-0.0001	0.0001	0.2315
Leaf litter subset	-0.0001	0.0001	0.3425
Ground subset	0.0003	0.0002	0.1280

Functional Dispersion: Stratification Hypothesis

- LME	*Estimates*	*SE*	*p*
Intercept	**0.0869**	**0.0057**	**<0.0001**
Elevation [m]	- <0.0001	<0.0001	0.8419
Recovery Time	-0.0002	0.1217	0.2041
Richness	0.0005	0.0003	0.1147
- Marginal R^2 / Conditional R^2	0.4573/ 0.4992		
- Legacy (anova)			0.3996
- Legacy * Recovery Time (anova)			0.2226
- Stratum (anova)			**<0.0001**
- Stratum*Recovery Time (anova)			0.1609
- contrast estimate (Holm-adj.)			
Ground - Tree	-0.0092	0.0028	**0.0013**
Ground - Leaf litter	0.0226	0.0029	**<0.0001**
Tree - Leaf litter	0.0318	0.0030	**<0.0001**

Table S3.4 Model output for the trait community weighted mean trajectories, which are shown in Fig. 3.4. For each trait, I indicated if its trajectory was consistent with the stratification or interaction hypothesis. The anova in brackets indicates an anova test on the model. If 'Stratum' was significant in the anova, I applied a contrast as post-hoc procedure to test specifically between the strata. If recovery time or an interaction was significant in the LME, we tested the recovery trajectory of each subset separately ('Recovery subset models'). When testing for legacy effects I used a dataset without old-growth forests (see methods). Significant p-values are highlighted in bold. Nico Blüthgen and Michael Staab provided supervision on the statistical analysis.

Head Width CWM: Stratification Hypothesis

- LME	*Estimates*	*SE*	*p*
Intercept	28.6321	13.9148	0.0603
Elevation [m]	-0.0043	0.0273	0.8763
Recovery Time	-0.3512	0.3028	0.2477
Richness	-0.1502	0.7494	0.8414
- Marginal R^2 / Conditional R^2	0.1362/ 0.2074		
- Legacy (anova)			0.1197
- Legacy*Recovery Time (anova)			0.1625
- Stratum (anova)			**0.0001**
-Stratum*Recovery Time (anova)			0.0526
- contrast estimate (Holm-adj.)			
Ground - Tree	-7.9736	6.9097	0.2508
Ground - Leaf litter	23.4133	7.1953	**0.0029**
Tree - Leaf litter	31.3869	7.4905	**0.0002**

Sculpture CWM: Recovery Hypothesis

- LME	*Estimates*	*SE*	*p*
Intercept	2.2848	0.0868	**< 2e-16**
Elevation [m]	-0.0004	0.0002	0.0757
Recovery Time	-0.0049	0.0022	**0.0238**
Richness	-0.0077	0.0051	0.1313
- Marginal R^2 / Conditional R^2	0.1410/ 0.1791		
- Legacy (anova)			0.8631
- Legacy * Recovery Time (anova)			0.9489

- Stratum (anova)			**0.0007**
- Stratum*Recovery Time (anova)			0.0990
- Recovery subset models			
Tree Recovery Time	<0.0001	0.0022	0.9973
Leaf litter Recovery Time	-0.0025	0.0026	0.3517
Ground Recovery Time	-0.0038	0.0022	0.0811
- contrast estimate (Holm-adj.)			
Ground - Tree	0.0168	0.0491	0.7300
Ground - Leaf litter	0.1937	0.0491	**0.0007**
Tree - Leaf litter	0.1769	0.0491	**0.0025**

Eye Position CWM: Recovery Hypothesis

- LME	*Estimates*	*SE*	*p*
Intercept	12.5731	7.2302	0.0841
Elevation [m]	0.0151	0.0170	0.3793
Recovery Time	-0.5956	0.1786	**0.0011**
Richness	-0.3387	0.4210	0.4222
- Marginal R^2 / Conditional R^2	0.3020/ 0.3752		
- Legacy (anova)			0.4466
- Legacy * Recovery Time (anova)			0.7341
- Stratum (anova)			**0.0002**
- Stratum*Recovery Time (anova)			0.6021
- contrast estimate (Holm-adj.)			
Ground - Tree	-22.7456	3.8967	**<0.0001**
Ground - Leaf litter	6.2510	4.0981	0.1297
Tree - Leaf litter	28.9966	4.3043	**<0.0001**
- Recovery subset models			
Ground Recovery Time	-0.5316	0.1679	**0.0025**
Leaf litter Recovery Time	-0.4398	0.1461	**0.0040**
Tree Recovery Time	-0.5397	0.2527	**0.0370**

Color CWM: Interaction Hypothesis

- LME	*Estimates*	*SE*	*p*
Intercept	47.6032	3.4072	**<0.0001**
Elevation [m]	0.0016	0.0077	0.8333
Recovery Time	0.2261	0.0791	**0.0050**

Richness	0.4892	0.1906	**0.0112**
- Marginal R^2 / Conditional R^2	0.2863/ 0.3963		
-Stratum (anova)			**<0.0001**
- Stratum*Recovery Time (anova)			**<0.0001**
- Legacy (anova)			0.0550
- Legacy*Recovery Time (anova)			0.0744
- contrast estimate (Holm-adj.)			
Ground - Tree	2.1554	1.6951	0.2060
Ground - Leaf litter	-9.4887	1.7740	**<0.0001**
Tree - Leaf litter	-11.6442	1.8551	**<0.0001**
- Recovery subset models			
Ground Recovery Time	0.2267	0.0871	**0.0118**
Leaf litter Recovery Time	-0.2422	0.0920	**0.0109**
Tree Recovery Time	0.2722	0.0762	**0.0007**

Pronotum Width CWM: Interaction Hypothesis

- LME	*Estimates*	*SE*	*p*
Intercept	36.0498	10.3645	**0.0012**
Elevation [m]	0.0091	0.0262	0.7304
Recovery Time	-0.63841	0.2478	**0.0111**
Richness	-1.0910	0.5599	0.0534
- Marginal R^2 / Conditional R^2	0.1859/ 0.4189		
- Legacy (anova)			0.1362
- Legacy*Recovery Time (anova)			0.3068
- Stratum (anova)			**<0.0001**
- Stratum* Recovery Time (anova)			**0.0016**
- contrast estimate (Holm-adj.)			
Ground - Tree	-9.7953	4.7780	**0.0433**
Ground - Leaf litter	11.6867	5.0238	**0.0433**
Tree - Leaf litter	21.4820	5.2755	**0.0013**
- Recovery subset models			
Ground Recovery Time	-0.3791	0.2108	0.0774
Leaf litter Recovery Time	-0.0503	0.1593	0.7531
Tree Recovery Time	-1.1354	0.3717	**0.0034**

Scape Length CWM: Interaction Hypothesis

- LME	*Estimates*	*SE*	*p*
Intercept	-0.6435	0.1608	**0.0002**

Elevation [m]	0.0006	0.0035	0.9867
Recovery Time	0.9251	0.3949	**0.0203**
Richness	1.951	0.9511	**0.0433**
- Marginal R^2 / Conditional R^2	0.2332/ 0.2332		
- Stratum* Recovery Time (anova)			**<0.0001**
- Stratum (anova)			0.0792
- Legacy (anova)			0.4491
- Legacy* Recovery Time (anova)			0.6334
- Recovery subset models			
Ground Recovery Time	0.8860	0.3744	**0.0214**
Leaf litter Recovery Time	-0.5900	0.3286	0.0779
Tree Recovery Time	1.4972	0.5679	**0.0108**

Clypeus Length CWM: Interaction Hypothesis

- LME	*Estimates*	*SE*	*p*
Intercept	44.2905	8.4672	**<0.0001**
Elevation [m]	-0.0087	0.0182	0.6337
Recovery Time	-0.8019	0.2069	**0.0002**
Richness	-1.1781	0.5002	**0.0205**
- Marginal R^2 / Conditional R^2	0.2799/ 0.2987		
- Legacy (anova)			0.4223
- Legacy * Recovery Time (anova)			0.4712
- Stratum (anova)			**<0.0001**
- Stratum*Recovery Time (anova)			**0.0214**
- contrast estimate (Holm-adj.)			
Ground - Tree	-22.6480	4.81238	**<0.0001**
Ground - Leaf litter	9.9380	5.03184	0.0505
Tree - Leaf litter	32.586	5.2578	**<0.0001**
- Recovery subset models			
Ground Recovery Time	-0.698	0.1714	**0.0001**
Leaf litter Recovery Time	-0.2732	0.1471	0.0686
Tree Recovery Time	-0.7623	0.3043	**0.0152**

Head Length CWM: Interaction Hypothesis

- LME	*Estimates*	*SE*	*p*
Intercept	-13.0733	11.1391	0.2424
Elevation [m]	0.0086	0.0263	0.7444

Recovery Time	0.4439	0.2751	0.1086
Richness	0.2089	0.6478	0.7475
- Marginal R^2 / Conditional R^2	0.0659/ 0.1689		
- Legacy (anova)			0.6153
- Legacy*Recovery Time (anova)			0.8816
- Stratum (anova)			0.0504
- Stratum*Recovery Time (anova)			**0.0230**
- Recovery subset models			
Ground Recovery Time	0.2773299	0.3493535	0.4306
Leaf litter Recovery Time	-0.2819231	0.2113474	0.1875
Tree Recovery Time	0.75100227	0.31975011	**0.0223**

Weber's Length CWM: Interaction Hypothesis

- LME	*Estimates*	*SE*	*p*
Intercept	1278.6596	119.5524	**0.0017**
Elevation [m]	0.0279	0.1794	0.8769
Recovery Time	-1.9746	1.9847	0.3212
Richness	-0.9566	4.9423	0.8468
- Marginal R^2 / Conditional R^2	0.5067/ 0.6169		
- Legacy (anova)			0.4688
- Legacy*Recovery Time (anova)			0.1015
- Stratum (anova)			**<0.0001**
- Stratum*Recovery Time (anova)			**0.0078**
- contrast estimate (Holm-adj.)			
Ground - Tree	-162.9934	45.1853	**0.0005**
Ground - Leaf litter	485.6714	46.9930	**<0.0001**
Tree - Leaf litter	648.6648	48.8640	**<0.0001**
- Recovery subset models			
Ground Recovery Time	-2.5107	1.7920	0.1667
Leaf litter Recovery Time	3.9682	1.7579	**0.0279**
Tree Recovery Time	6.7283	2.7224	**0.0165**

Mandible Length CWM: Interaction Hypothesis

- LME	*Estimates*	*SE*	*p*
Intercept	-4.9406	10.7036	0.6457
Elevation [m]	-0.0114	0.0240	0.6371
Recovery Time	0.3502	0.2644	0.1871

Richness	0.3615	0.6309	0.5684
- Marginal R^2 / Conditional R^2	0.1203/ 0.1526		
- Legacy (anova)			**0.0391**
- contrast estimate (Holm-adj.)			
cacao - pasture	9.98	5.44	0.0744
- Legacy*Recovery Time (anova)			0.1656
- Stratum (anova)			**0.0007**
- Stratum*Recovery Time (anova)			**0.0238**
- contrast estimate (Holm-adj.)			
Ground - Tree	12.6941	6.0236	0.0744
Ground - Leaf litter	-5.9885	6.3192	0.3451
Tree - Leaf litter	-18.6826	6.6227	**0.0167**
- Recovery subset models			
Ground Recovery Time	0.4283	0.1772	**0.0189**
Leaf litter Recovery Time	-0.1192	0.2082	0.5693
Tree Recovery Time	0.9527	0.4272	**0.0297**

Maximum Eye Width CWM: Interaction Hypothesis

- LME	*Estimates*	*SE*	*p*
Intercept	33.7688	8.7952	**0.0002**
Elevation [m]	0.0124	0.0202	0.5435
Recovery Time	-0.8937	0.2177	**<0.0001**
Richness	-0.6791	0.5158	0.1897
- Marginal R^2 / Conditional R^2	0.4629/ 0.4994		
- Legacy (anova)			0.1073
- Legacy*Recovery Time (anova)			0.5820
- Stratum (anova)			**<0.0001**
- Stratum*Recovery Time (anova)			**0.0024**
- contrast estimate (Holm-adj.)			
Ground - Tree	-25.4758	4.8628	**<0.0001**
Ground - Leaf litter	21.4291	5.1101	**0.0001**
Tree - Leaf litter	46.9049	5.3635	**<0.0001**
- Recovery subset models			
Ground Recovery Time	-0.8681	0.1821	**<0.0001**
Leaf litter Recovery Time	-0.6701	0.1588	**8.5896**
Tree Recovery Time	-1.2897	0.3160	**0.0001**

Spines CWM

- LME	*Estimates*	*SE*	*p*
Intercept	**1.3140**	**0.2365**	**<0.0001**
Elevation [m]	-0.0004	0.0005	0.412
Recovery Time	-0.0060	0.0059	0.306
Richness	0.01441	0.0140	0.304
- Marginal R^2 / Conditional R^2	0.0396/ 0.0427		
- Legacy (anova)			0.2315
- Legacy * Recovery Time (anova)			0.4655
- Stratum (anova)			0.6004
- Stratum*Recovery Time (anova)			0.9315
- Stratum (anova)			0.1921

Femur Length CWM

- LME	*Estimates*	*SE*	*p*
Intercept	-4.2872	21.4078	0.842
Elevation [m]	-0.0209	0.0468	0.656
Recovery Time	-0.8496	0.5325	0.112
Richness	1.6126	1.2648	0.20
- Marginal R^2 / Conditional R^2	0.1847/ 0.1847		
- Legacy (anova)			0.5596
-Legacy*Recovery Time (anova)			0.8826
- Stratum (anova)			0.1136
- Stratum*Recovery Time (anova)			0.9055

Head Width CWM: Stratification Hypothesis

- LME	*Estimates*	*SE*	*p*
Intercept	28.6321	13.9148	0.0603
Elevation [m]	-0.0042	0.0273	0.8764
Recovery Time	-0.3512	0.3028	0.2477
Richness	-0.1502	0.7494	0.8414
- Marginal R^2 / Conditional R^2	0.1362/ 0.2074		
- Legacy (anova)			0.1197
- Legacy*Recovery Time (anova)			0.1625
- Stratum (anova)			**0.0001**

-Stratum*Recovery Time (anova)			0.0526
- contrast estimate (Holm-adj.)			
Ground - Tree	-7.9736	6.9097	0.2508
Ground - Leaf litter	23.4133	7.1953	**0.0029**
Tree - Leaf litter	31.3869	7.4905	**0.0002**

Table S3.5 Model output for the phylogenetic diversity trajectory from Fig. 3.3 D, which was consistent with the stratification hypothesis. The anova in brackets indicates an anova test on the model. Because 'Stratum' was significant in the anova, I applied a contrast as post-hoc procedure to test specifically between the strata. When testing for legacy effects I used a dataset without old-growth forests (see methods). Significant p-values are highlighted in bold. Nico Blüthgen and Michael Staab provided supervision on the statistical analysis.

Phylogenetic Diversity: Stratification Hypothesis			
- LME	*Estimates*	*SE*	*p*
Intercept	0.0408	0.2766	0.8839
Elevation [m]	0.0002	0.0006	0.7159
Recovery Time	0.0103	0.0063	0.1065
Richness	-0.0031	0.0157	**0.0467**
- Marginal R^2 / Conditional R^2	0.0806/ 0.1099		
- Legacy (anova)			0.5089
- Legacy*Recovery Time (anova)			0.6479
- Stratum (anova)			**0.0498**
- contrast estimate (Holm-adj.)			
Ground - Tree	-0.3934	0.1461	**0.0195**
Ground - Leaf litter	0.1027	0.1525	0.4933
Tree - Leaf litter	0.4961	0.1586	**0.0076**

4 *ODONTOMACHUS DAVIDSONI* SP. NOV. (HYMENOPTERA, FORMICIDAE), A NEW CONSPICUOUS TRAP-JAW ANT FROM ECUADOR

This chapter was published in the journal “Zookeys”: doi.org/10.3897/zookeys.948.48701

Authors:

Philipp O. Hoenle[a1], John E. Lattke[b1], David A. Donoso[c], Christoph von Beeren[a], Michael Heethoff[a], Sebastian Schmelzle[a], Adriana Argoti[d], Luis Camacho[e], Bernhard Ströbel[f], Nico Blüthgen[a]

Affiliations:

[a] Ecological Networks, Department of Biology, Technical University of Darmstadt, Darmstadt, Germany.

[b] Departamento de Zoologia, Universidade Federal do Paraná, Curitiba, Brazil.

[c] Departamento de Biología, Escuela Politécnica Nacional, Quito, Ecuador.

[d] Escuela de Ciencias Biológicas, Pontificia Universidad Católica del Ecuador, Quito, Ecuador.

[e] Department of Zoology, University of British Columbia,Vancouver, Canada.

[f] University of Applied Sciences, Darmstadt, Germany.

Author contributions

NB & DD supervised the study and provided logistic support. PH, AA, LC did the field work. PH, DD, CvB & JL wrote the manuscript. CvB performed genetic analyses. PH, DD & JL performed morphological analysis and species description. MH, SS & BS performed 3D scans and worked on the models. All authors read and approved the manuscript.

4.1 ABSTRACT

One of the largest species in its genus, *Odontomachus davidsoni* Hoenle, Lattke & Donoso **n.sp.** is described from workers and queens collected at lowland forests in the Chocó-Darién bioregion in coastal Ecuador. The workers are characterized by their uniform red coloration, their large size (16-18 mm body length), and their frontal head striation that reaches the occipital margin. We provide DNA barcodes (*COI*) and high resolution 2D images of the type material, as well as an updated key for the Neotropical species of *Odontomachus*. In addition, we present, for the first time in a species description, a three-dimensional digital model of the worker holotype and a paratype queen scanned with DISC3D based on photogrammetry. Findings of large and conspicuous new species are uncommon around the world and suggest that these Ecuadorian rainforests may conceal many more natural treasures that deserve conservation.

Resumen

Describimos una especie nueva, entre las más grandes conocidas del género *Odontomachus*. La nueva especie, *Odontomachus davidsoni* Hoenle, Lattke & Donoso **n. sp.**, es descrita a partir de obreras y reinas recolectadas en bosques de tierras bajas en la bioregión Chocó-Darién de la costa del Ecuador. Las obreras se caracterizan por su coloración rojiza uniforme, su grande tamaño (largo del cuerpo 16 -18 mm), y la estriación del frente cefálico que alcanza el margen occipital. Proveemos códigos de barras de DNA (*COI*) e imágenes 2D de alta resolución para el material tipo y así como una guía de identificación actualizada para las especies neotropicales del género *Odontomachus*. Por primera vez en una descripción de especies, se proveen imágenes 3D de un escáner fotogramétrico DISC3D. Los hallazgos de especies grandes y conspicuas son poco comunes alrededor del mundo y sugieren que estos bosques lluviosos ecuatorianos pueden contener muchos más tesoros naturales que merecen ser conservados.

4.2 INTRODUCTION

Members of the genus *Odontomachus* Latreille, 1804 are among the most conspicuous and recognizable ants of the subfamily Ponerinae. All members of the genus exhibit trap jaws, a character shared with the sister genus *Anochetus* Mayr, 1861 (Schmidt and Shattuck 2014) and several other unrelated genera (Larabee and Suarez 2014). Trap jaws are long, slender mandibles that are mainly used for predation and secondarily in some taxa to catapult the ant into the air as a predator escape response (Larabee and Suarez 2015). Trap jaws function via a special clamping mechanism with the mandibles opening at a 180 degree angle and snap shut at high speeds upon physical contact with mechanosensory hairs (Gronenberg et al. 1993, Gronenberg 1995). *Odontomachus* typically comprises medium- to large-sized ants with a pantropical distribution including subtropical regions. The genus currently contains a total of 72 species (Bolton 2018), with the highest diversity found in the Neotropics and South-East Asia (Larabee et al 2016, Guenard et al 2017, Matos-Maraví et al. 2018).

Ecuador, with at least 18 *Odontomachus* species (Salazar et al. 2015), is among the countries showing the highest species diversity recorded for this genus. In general, Ecuadorian biodiversity is comparatively high, because the country comprises three vastly distinct bioregions: the Amazon basin in East Ecuador, the Chocó-Darién bioregion in the North-West, and the Tumbesian drylands in the South of the country which are divided by the Andes, one of the highest mountain chains in the world (Salazar and Donoso 2013, Salazar et al. 2015). While ants of the Ecuadorian Amazon have received some attention (e.g. Donoso et al. 2009, Wilkie et al. 2010), ant research is severely lacking in the highly threatened areas of the Chocó-Darién (Donoso and Ramón 2009, Donoso 2017) and in the southern drylands (Dominguez et al. 2016, Lattke et al. 2016). Notably, the Chocó-Darién is home for several large and rare *Odontomachus* species, including *O. mormo* Brown, 1976, and *O. cornutus* Stitz, 1933, both of which are only known from few collections (Rodriguez 2008). Since Brown's (1976) global revision of the genus, the taxonomy of the New World species has remained relatively stable, with one additional species described in the United States (Deyrup and Cover 2004) and none for the Neotropics except for *O. scalptus* Brown, 1978, from Tena, in the Ecuadorian Amazon.

We describe a surprisingly large new species, i.e. *O. davidsoni* Hoenle, Lattke & Donoso **n. sp.**, from the Ecuadorian Chocó-Darién region that rivals in size *O. mormo*, previously considered the largest species of New World *Odontomachus*. We use morphological and genetic analyses to distinguish it from other *Odontomachus* species and use, for the first time in insect taxonomy, textured 3D-models to present a digital version of the holotype, a queen and several other specimens.

4.3 MATERIALS AND METHODS

Sampling and geographic origin

Specimens of *O. davidsoni* were collected and observed in field trips to the Reserva Río Canandé in Ecuador (Esmeraldas Province) from February 2018 to April 2019. We searched for specimens by walking through the forest and examining the vegetation and recently fallen trees. Alate queens were collected with light traps directly located at the Ecolodge of the Reserve. We collected exclusively by hand, and specimens were preserved in vials containing 96% ethanol. Photographs of living specimens were taken with a Nikon D5300 camera body (Nikon Corp., Tokio, JP) and a Laowa 60mm f2.8 2x macro lens (Venus Optics, Hefei, China). The Ministerio de Ambiente de Ecuador issued the permits for collection (MAE-DNB-CM-2017-0068) and exportation (41-2018-EXP-CM-FAU-DNB/MA and 144-2019-EXP-CM-FAU-DNB/MA).

Photogrammetry

The worker holotype, two worker paratypes and one paratype queen were mounted with water soluble insect glue on the tip of an insect needle and imaged using the Darmstadt Insect Scanner (DISC3D, Ströbel et al. 2018). Specimens were imaged with extended depth of field (EDOF) using calibrated stacks of 19 images with 4 megapixels (Ströbel et al. 2018). EDOF images were taken from 398 viewing angles (in total 7562 images were recorded) and used for photogrammetric reconstruction and texturing in PhotoScan Professional 1.4.5. (Agisoft LLC, St. Petersburg, Russia) with the highest quality settings and visibility consistent mesh generation. Polygons corresponding to the insect pin were removed from the resulting mesh and the mesh was slightly smoothed (with a factor of 0.5). In addition, the holotype and queen models were textured using the "average" option resulting in 5000 x 5000 pixel texture maps. Textures were sharpened and cleaned in Adobe® Photoshop® CS6 13.0 (Adobe Inc., San Jose, CA, USA). We furthermore provide videos with added light effects created with Blender® (Blender Foundation; Amsterdam, NL; Supplemental files S1 and S2).

Additional stacking pictures were taken with a Canon EOS 7D with a MPE 65mm lens (Canon, Tokio, Japan) and a Keyence VHX-5000 (Keyence Deutschland BmH, Neu-Isenburg, Germany) with a Z20 lens. Stacking pictures were assembled with Helicon Focus Version 7 (Helicon Soft Ltd., Kharkiv, Ukraine) software, and further edited with Adobe Photoshop CS6 13.0 (Adobe Inc., San Kaso, CA, USA).

Morphological Data

Morphological measurements of three workers (the holotype and 2 paratypes) and one alate queen were performed using 3D-models embedded in PDF files obtained with DISC3D. The measurements obtained through such models are more precise and reproducible than traditional ocular micrometer measurements, partly since parallax errors are avoided (see Ströbel et al. 2018). Measurements were taken with Adobe Acrobat Reader DC (version 11.0.23; Adobe Inc., San Jose, CA, USA) following the definitions described in MacGown et al. (2014) and Brown (1976), with the exception of head and petiole height measurements (see definitions below). As Brown (1976) already recognized, heads of *Anochetus* and *Odontomachus* can have a relatively trapezoid or more rectangular shape in frontal view, which is a reliable indicator to help differentiate between species. To discern between these shapes, we included the head ocular width (HoW – synonym with HW in other studies, e.g. MacGown et al. 2014) and head vertexal width (HvW, see below). We measured two paratype workers with a binocular with measuring eyepiece only (see Supplement S3). The morphological values given in the species description however solely derive from measurements of the 3D scan of workers (n=3) and queen (n=1) for reasons of consistency. All measurements are given in millimeters.

Additional to the measurements we give a detailed morphological description of *Odontomachus davidsoni* **n.sp.**. The morphological terminology, including those of surface sculpturing, is based on definitions found in Wilson (1955), Harris (1979) and Keller (2011.)

Measurement definitions

HL Head length. Maximum length of head in full-face view, excluding mandibles, measured from anteriormost point of clypeal margin to midpoint of a line across the posterior margin.

HoW Head ocular width. Maximum width of head at ocular prominence in full-face view, measured in the same plane as HL.

HvW Head vertexal width. Width of head at vertex in full-face view, measured in the same plane as HL. An imaginary line is drawn parallel to the cephalic posterior margin and perpendicular lines are extended anterad to where the posterolateral cephalic curve meets the lateral cephalic margin.

ML Mandible length. The straight-line length of mandible at full closure, measured in the same plane as HL, from mandibular apex to anterior clypeal margin.

SL Scape length. Maximum chord length of antennal scape in dorsal view excluding basal constriction.

EL Eye length. Maximum length of eye as measured normally in oblique view of the head to show full surface of eye.

MsL Mesosoma length. Maximum length of mesosoma, measured in lateral view, a diagonal line from the cervical shield to the posterolateral propodeal edge.

PrW Pronotum width. Maximum width of pronotum in dorsal view.

PtW Petiole width. Maximum width of petiole in dorsal view.

PtL Petiole length. Maximum length of petiole in lateral view.

PtH Petiole height. Direct linear distance from the apex of petiolar needle to ventral subpetiolar process measured in the same plane as PtL.

FL Femur length. Maximum length of hind femur.

CI Cephalic index. HW/HL × 100.

SI Scape index. SL/HW × 100.

MI Mandible index. ML/HL × 100

Molecular analyses

We sequenced the classical mitochondrial barcode region for animals, a 658 base pair (bp) region of the *cytochrome oxidase subunit I* gene (*COI*), for two *O. davidsoni* **n.sp.** specimens and six specimens of six additional *Odontomachus* species (*O. erythrocephalus* Emery, 1840, *O. mormo*, *O. chelifer* (Latreille, 1802), *O. meinerti* Forel, 1805, *O.* c.f. *mayi* Mann, 1912, *O. hastatus* (Fabricius, 1804)*;* see Supplemental file S4 for collection data). Specimens were identified by PH. We used whole specimens for non-destructive DNA extraction using the Qiagen 96 DNeasy Blood & Tissue Kit (Quiagen, Venlo, Netherlands) following the standard protocol with one exception: we shortened the protein lysis step to 2h-3h to avoid any damaging of the specimens, which keeps specimens intact and in good condition so as to serve as morphological vouchers (e.g., von Beeren et al. 2016). We amplified *COI* using the primer combination LCO1490 / HCO2198 (Folmer et al. 1994). PCRs were set up as described previously by von Beeren et al. (2016). Purification and sequencing of PCR products in forward and reverse direction were outsourced to Macrogen

Europe B.V. (Amsterdam, Netherlands). The laboratory information management system Geneious Prime 2019.1.3 was used to process and analyse sequences (https://www.geneious.com).

To evaluate whether *COI* can be used as reliable species discriminator for *O. davidsoni* **n. sp.** we further included available data of published *COI* sequences of Neotropical *Odontomachus* species. For this, we analyzed *Odontomachus COI* sequences from the New World. We downloaded 264 published *COI* sequences by using the following search terms in the Barcode of Life database system (www.boldsystems.org; search criteria: Odontomachus; "United States"; USA; Mexico; Cuba; Haiti; "Dominican Republic"; "Puerto Rico"; "British Virgin Islands"; Montserrat; "Antigua and Barbuda"; Dominica; "St Lucia"; Barbados; Grenada; "Trinidad and Tobago"; Guatemala; Honduras; Belize; "El Salvador"; Nicaragua; "Costa Rica"; Panama; Colombia; Venezuela; Ecuador; Guyana; Suriname; "French Guiana"; Brazil; Peru; Bolivia; Paraguay; Chile; Argentina; Uruguay"; accessed on 15th of May 2019).

Published and newly acquired data from this study were then analyzed together. We first performed several quality checks. Sequences lacking species identifications, sequences containing ambiguous bases, and sequences smaller than 400bp were sorted out. We then used the MUSCLE algorithm (Edgar 2004) to align *COI* sequences and, on this basis, sorted out additional sequences which showed gaps and/or additional bases in the sequence alignment. No apparent stop codons were detected in the analyzed *Odontomachus* dataset. Finally, we extracted unique sequences (or *COI* haplotypes) from the dataset resulting in 94 distinct *COI* sequences of 16 *Odontomachus* species. For eight of those specimens lateral habitus images were uploaded to BOLD. BOLD process IDs of sequences are given in Supplemental file S5.

We used a neighbor-joining (NJ) tree as simple clustering approach of DNA barcode data to depict genetic differences and to examine the reliability of *COI* as possible molecular identifier of *O. davidsoni* **n.sp.** Note that it was not our goal to evaluate whether *COI* can serve as a reliable identification character in the entire genus. We thus did not define species boundaries in other *Odontomachus* species based on intraspecific p-distance thresholds and barcoding gaps as it is often done so in other barcoding studies. Except for our own identifications (see above) we used and relied on species identifications that were deposited together with *COI* sequences in GenBank. The NJ tree was analyzed in MEGA 10.0.5 (Kumar et al. 2018) based on p-distances with pairwise deletion of missing data. P-distances simply give the proportion of bases that differ in pairwise sequence comparisons. Metadata of the NJ tree are given in Supplemental file S6 as newick formatted file.

4.4 RESULTS

Key to Neotropical *Odontomachus* species

This key is a modification of the keys of Rodriguez (2008) and Brown (1976), both of which contain many additional helpful figures as well as detailed morphological descriptions. Please note that this key does not include the species native to the USA such as the Florida endemic *O. relictus* Deyrup & Cover, 2004, for which we recommend using the key of MacGown et al. (2014).

From the Rodriguez (2008) key only the herewith described *O. davidsoni* **n.sp.** is added as new. However, the classification of *Odontomachus brunneus* has been cleared up. Originally, it was thought to be distributed in South and Central America, but it is now clear that it is restricted to the Southern USA, and previous material that has been identified as such probably belongs to *O. ruginodis* Smith, 1937 (MacGown et al. 2014).

For easy identification, we recommend to point mount workers of *Odontomachus* by bending the tip of the point and gluing it to the pleura so as to leave the space between the hind coxae exposed. This is because the metasternal process is an important identification characteristic and it might be obscured otherwise.

English key:

1

- Petiole pedunculate to subpedunculate, in lateral view the anterodorsal margin of the gaster forms a single convexity that ascends posterad at approximately 45° (Fig.4.1, A) 2

- Petiole sessile, not subpendunculate, in lateral view the anterodorsal margin of the first gaster segment forming a much steeper slope (>45°) with a more or less distinct vertical anterior face (Fig. 4.1, B) 4

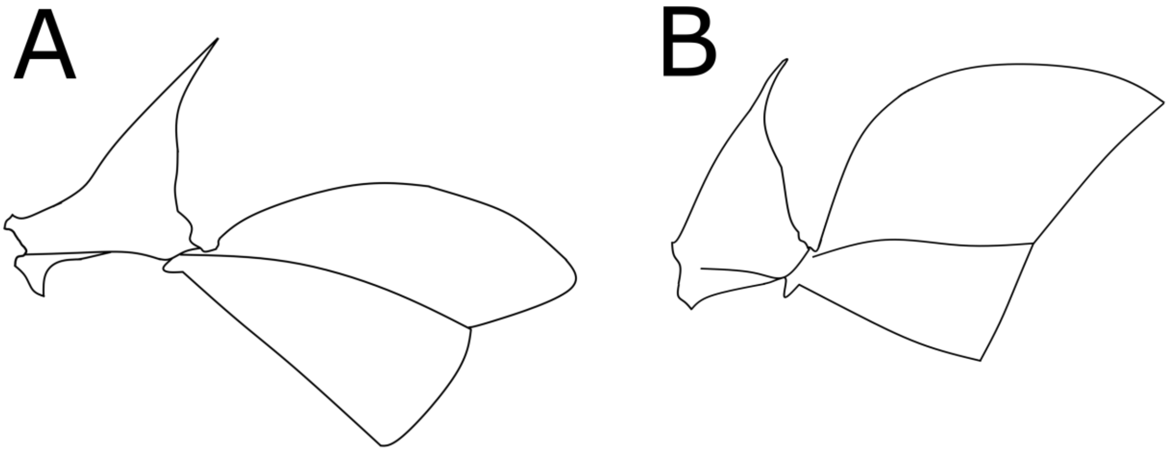

Fig. 4.1 Lateral view of petiole and first gaster segment of *O. hastatus* (left) and *O. bauri* (right).

2(1)

- Dorsal surface of the head with deep striation that reaches to the nuchal collar; color uniform ferruginous to dark red *davidsoni* **n.sp.**

-Posterior third to half of dorsal surface of head smooth and shining; color variable 3

3(2)

- Without metasternal process; mesonotum almost hairless; larger body size (HL > 4 mm). Ground living *mormo*

- With metasternal process; dorsal surface of mesonotum covered in small erect setae; smaller body size (HL < 3.8 mm). Arboreal *hastatus*

4(1)

- Dorsal surface of head distinctly striate to or nearly to the nuchal carina 5

- Posterior third to half of dorsal surface of head smooth and shining, or nearly so 22

5(4).

- Disc (dorsal surface) of first gastric segment predominantly smooth, punctulate, alutaceous, or reticulate; striation absent, or if present, mixed with other sculpture and distinct only on the posterior half of the disc 6

- Disc of first gastric segment distinctly and evenly striate over its entire surface, at least as seen from dorsal view 17

6(5)

-Mesonotum longitudinally striate *yucatecus* Brown, 1976

-Mesonotum prevailingly transversely striate 8

7(5)

- Head more or less bright red (frontal area often infuscate), contrasting with blackish-brown body and yellow legs; size medium *erythrocephalus*

- Color combination otherwise; if head is distinctly red, then trunk is red also, or legs are dark 8

8(7)

- Sternum immediately in front of and between metathoracic coxae produced as a slender, acute pair of teeth or spines; disc of first gastric segment densely and finely shagreened and pubescent, usually opaque; body brown, legs yellow to brown *haematodus* (Linnaeus, 1758)

- Sternum in front of metathoracic coxae with a low transverse ridge, sometimes notched in the middle or bilobed, but not produced as acute, paired teeth 9

9(8)

- Petiole predominantly smooth and shiny, with the anterior border erected or slightly convex, and the apex produced into a large spine with posterior orientation; head, mesosoma and petiole with a clear red coloration and the gaster dark brown *insularis* Guérin-Méneville, 1844

- Petiole differently shapes, color combination varies 10

10(9)

- Anterior face of petiolar node as seen from the side rising steeply from anterior margin, then passing through an obtuse angle into a long section concave in outline to the root of the apical spine; labial palpi 4-merous *bradleyi* Brown, 1976

- Petiole differently shaped 11

11(10)

- Metasternal process like an arc with or without middle division; petiole smooth or a little striate, with both the anterior and posterior margin convex; the petiolar spine forms gradually, without clear distinction from petiole

cf. *brunneus* Patton, 1894 (Possibly *Odontomachus ruginodis. O. brunneus* is apparently restricted to southeastern US. The status of the Central and South American populations comparable with *O. brunneus* need to be established.)

- Metasternal process absent, bilobed or triangular; petiole differently shapes or if both sides convex, with a clear differentiation of the spine from the rest of the petiole 12

12(11)

- Metasternal process absent 13

- Metasternal process bilobed or triangular 14

13(12)

- Black coloration; Node of petiole with a pair of prominent posterolateral tumosities at about mid-height and without striation; apex as seen from side abruptly narrowed to an axially erect, acute tooth *biumbonatus* Brown, 1976

- Node of petiole without paired posterolateral tumosities; Posterior face of petiole less concave, with short petiolar spine (0.1 mm) *clarus* Roger, 1861

14(12)

- Anterior margin of petiole at least weakly convex 15

- Anterior margin of petiole basal of the node concave or straight 16

15(14)

- Metasternal process completely bilobed; color generally dark *bauri* Emery, 1892

- Metasternal process formed by an obtuse wide lobe followed by a transverse flange which is produced into a triangular process; usually light color *biolleyi* Forel, 1809

16(14)

-Petiole strongly transversely striate, with a clearly differentiated spine; small species (TL 8.6-9.35 mm) *ruginodis*

- Petiole without or only weak striation and with spine not clearly differentiated from the petiole; large species (TL 12 mm) *laticeps* Roger, 1861

17(5)

- First gaster segment with only one type of sculpturation, which is either punctulate or striate 18

- First gaster segment with a combination of punctulate and reticulate sculpturation 21

18(17)

- First gaster segment punctulate on its entire surface *opaciventris* Forel, 1899

- First gaster segment striate on most of its surface, at least in dorsal view 19

19(18)

- Transverse striation patterns on the gaster; large and slender *chelifer* (Latreille, 1802)

- Longitudinal striation on the dorsal gaster surface 20

20(19)

- Mesonotum strongly convex, but broadly sulcate and longitudinally striate on at least the anterior half near midline *caelatus* Brown, 1976

- Mesonotum gently but evenly convex, transversely striate *laticeps*

21(17)

- Mesonotum with longitudinal striation *scalptus* Brown, 1978

- Mesonotum with transverse striation *meinerti* Forel, 1805

22(4)

- Ocular prominences each produced anterolaterally into a stout, acute, oblique, toothlike process *cornutus*

- Ocular prominences bluntly rounded, as usual 24

23(22)

- Antennal scapes very short, not reaching posterior border of head in full-face view; very small species with broad head *spissus* Kempf, 1962

- Antennal scapes surpassing posterior border of head viewed full-face 24

24(23)

- Apex of mandible with only 2 large teeth (intercalary tooth lacking) *allolabis* Kempf, 1974

- Apex of mandible with 3 teeth 25

25(24)

- Mesepisternum with a prominent, narrowly rounded anteroventral lobe projecting conspicuously on each side when trunk is viewed from above *mayi*

- Mesepisternum with at most a low, inconspicuous convexity on its anteroventral margin 26

26(25)

-Petiole clearly differentiated spine; larger species (HL>2.8 mm *affinis* Guérin-Méneville, 1844

-Both faces of petiole converge into a thick spine that is flattened laterally; smaller species (HL<2.8 mm) *panamensis* Forel, 1899

Spanish key:

1

- Pecíolo en vista lateral pedunculado a semi-pedunculado, el perfil anterodorsal del primer segmento del gáster forma una convexidad contínua con una pendiente de aproximadamente 45° (Fig. 4.1, A) 2

- Pecíolo sésil, no semi-pedunculado, el perfil anterior del primer segmento del gáster relativamente vertical y bien diferenciado del perfil dorsal, con una pendiente mayor de 45° (Fig. 4.1, B) 4

2(1)

- Superficie dorsal de la cabeza con estrías que llegan hasta la carena nucal, color ferruginoso *davidsoni* **n.sp.**

- Superficie dorsal de la cabeza con estrías que tan sólo ocupan de la mitad a dos tercios de la región anterior de la cabeza, color es variable 3

3(2)

- Espacio entre las coxas posteriores liso, sin proceso ni estrías; mesonotum casi sin pelos; gran tamaño (LC > 4 mm). Hormiga del suelo *mormo*

- Espacio entre las coxas posteriores con un proceso bilobulado y siempre estriado; mesonotum con muchos pelos; más pequeña (LC < 3.8 mm). Hormiga arbórea. *hastatus*

4(1)

- Superficie dorsal de la cabeza con estrías que llegan hasta la carena nucal o muy cerca de ésta 5

- Superficie dorsal de la cabeza con estrías que tan sólo ocupan de la mitad a dos tercios de la región anterior de la cabeza 22

5(4).

-Primer segmento del gaster predominantemente liso y brillante, opaco o suavemente reticulado 6

- Primer segmento del gaster con escultura que puede ser de un sólo tipo o una mezcla de varios (estríado, punteado, estríado- punteado) 17

6(5).

- Mesonoto estríado longitudinalmente *yucatecus*

- Mesonoto estríado transversalmente 7

7(6)

- Cabeza de color rojo claro que contrasta con cuerpo marrón oscuro a negro y extremidades amarillas *erythrocephalus*

- Diferente combinación de color; si la cabeza es rojo claro, entonces el mesosoma debe ser también rojo o las extremidades de un color oscuro; o la cara anterior del pecíolo es recta o cóncava 8

8(7)

-Metaesterno, exactamente entre las coxas posteriores posee un par de espinas o dientes agudos; primer segmento del gaster reticulado, usualmente opaco; cuerpo marrón, extremidades de color amarillo a marrón *haematodus*

-Metasterno sin o con proceso, el cual puede ser bilobulado, dividido en la mitad o redondeado 9

9(8)

-Pecíolo predominantemente suave y brillante, con borde anterior recto o ligeramente convexo, el ápice de éste se estrecha formando una espina larga, delgada que está dirigida posteriormente; cabeza, mesosoma y pecíolo de color rojo claro y gaster marrón oscuro *insularis*

-Pecíolo de diferente forma; combinación de color variada 10

10(9)

-Cara anterior del nodo peciolar se levanta casi verticalmente desde el margen anterior, luego pasa por un ángulo obtuso a una sección larga y cóncava que forma una espina apical *bradleyi*

-Pecíolo con forma diferente ^ 11

11(10)

-Proceso metasternal como un arco con o sin división en el medio; pecíolo suavemente o poco estríado, la cara anterior es convexa, al igual que la posterior; la espina del pecíolo se va formando gradualmente, lo cual hace que no sea claramente diferenciada de éste

cf. *brunneus* (Posiblemente se trata de *O. ruginodis. O. brunneus* aparentemente esta restringida al sureste de los EEUU. El estatus de las poblaciones centro y suramericanas que son comparables con *O. brunneus* aún esta por definirse.

-Proceso metasternal ausente, bilobulado o triangular; pecíolo con diferente forma o si ambos lados son convexos hay una espina claramente diferenciada del resto del pecíolo 12

12(11)

- Proceso metasternal ausente 13

-Proceso metasternal bilobulado o triangular 14

13(12)

- Color negro; nodo del pecíolo con un par de prominencias posterolaterales y sin estrías; ápice en vista lateral se estrecha hasta formar un diente agudo axialmente erguido *biumbonatus*

- Color claro; nodo del pecíolo sin prominencias o si las posee tiene estrías; cara posterior del pecíolo al menos débilmente cóncava, la espina peciolar es corta (0.1mm) *clarus*

14(12)

-Cara anterior del pecíolo al menos débilmente convexa 15

-Parte anterior basal del nodo peciolar cóncava o recta 16

15(14)

- Proceso metasternal completamente bilobado; color oscuro generalmente *bauri*

- Proceso metasternal formado por un lóbulo ancho obtuso, seguido de un reborde transverso que se observa como un proceso de forma triangular; color claro generalmente *biolleyi*

16(14)

-Pecíolo fuertemente estríado transver- salmente, presenta una espina claramente diferenciada, especies pequeñas (8.6- 9.35mm) *ruginodis*

- Pecíolo sin estrías o suavemente estríado, la espina no está claramente diferenciada del pecíolo, especies grandes (TL 12 mm) *laticeps*

17(5)

- Primer segmento del gaster con un sólo tipo de escultura, que puede ser punteada o estriada 18

- Primer segmento del gaster con una combinación de escultura punteada y reticulada 21

18(17)

- Primer segmento del gaster punteado a lo largo de toda su superficie *opaciventris*

- Primer segmento del gaster estríado a lo largo de toda su superficie, al menos en vista dorsal 19

19(18)

- Estrías transversales curvas en el gaster; especies grandes y delgadas *chelifer*

- Estrías longitudinales en el dorso del gaster 20

20(19)

- Mesonoto fuertemente convexo, pero fuertemente surcado y estríado longitudinalmente al menos en la mitad del área de la parte *caelatus*

- Mesonoto suave pero uniformemente convexo, estríado transversalmente *laticeps*

21(17)

- Mesonoto estríado longitudinalmente *scalptus*

- Mesonoto estríado transversalmente *meinerti*

22(4)

- Prominencias oculares con un proceso agudo, oblicuo a manera de diente *cornutus*

- Prominencias oculares redondeadas 23

23(22)

- Escapos antenales muy cortos que no alcanzan el borde posterior de la cabeza *spissus*

- Escapos antenales sobrepasan el borde posterior de la cabeza 24

24(23)

-Dos dientes grandes en el ápice de la mandíbula *allolabis*

- Tres dientes en el ápice de las mandíbulas 25

25(24)

- Mesepisterno con un lóbulo anteroventral redondeado y prominente que se proyecta a los lados del mesosoma en vista dorsal *mayi*

- Mesopleura con una convexidad inconspicua en su margen anteroventral 26

26(25)

-Pecíolo convexo en ambas caras, con una espina delgada claramente diferenciada; más grande (LC>2.8 mm) *affinis*

- Pecíolo con ambas caras convexas, las cuales convergen en una espina gruesa y aplanada lateralmente; más pequena (LC<2.8 mm) *panamensis*

Museum abbreviations

The collection abbreviation is taken from Evenhuis (2020). The specimens used in this study are deposited at the following institutions:

DZUP: Department of Zoology, Universidade Federal do Paraná, Curitiba, Brazil

MCZ: Havard Museum of Comparative Zoology, Cambrigde, Massachusetts, USA

MEPN: Museo de Colecciones Biológicas Gustavo Orcés, Escuela Politécnica Nacional, Quito, Ecuador

RBINS: Royal Belgium Institute of Natural Sciences, Brussels, Belgium

QCAZ: Zoology Museum at the Pontifical Catholic University of Ecuador, Quito, Ecuador

Odontomachus davidsoni **n. sp.**

Hoenle, Lattke & Donoso, new species

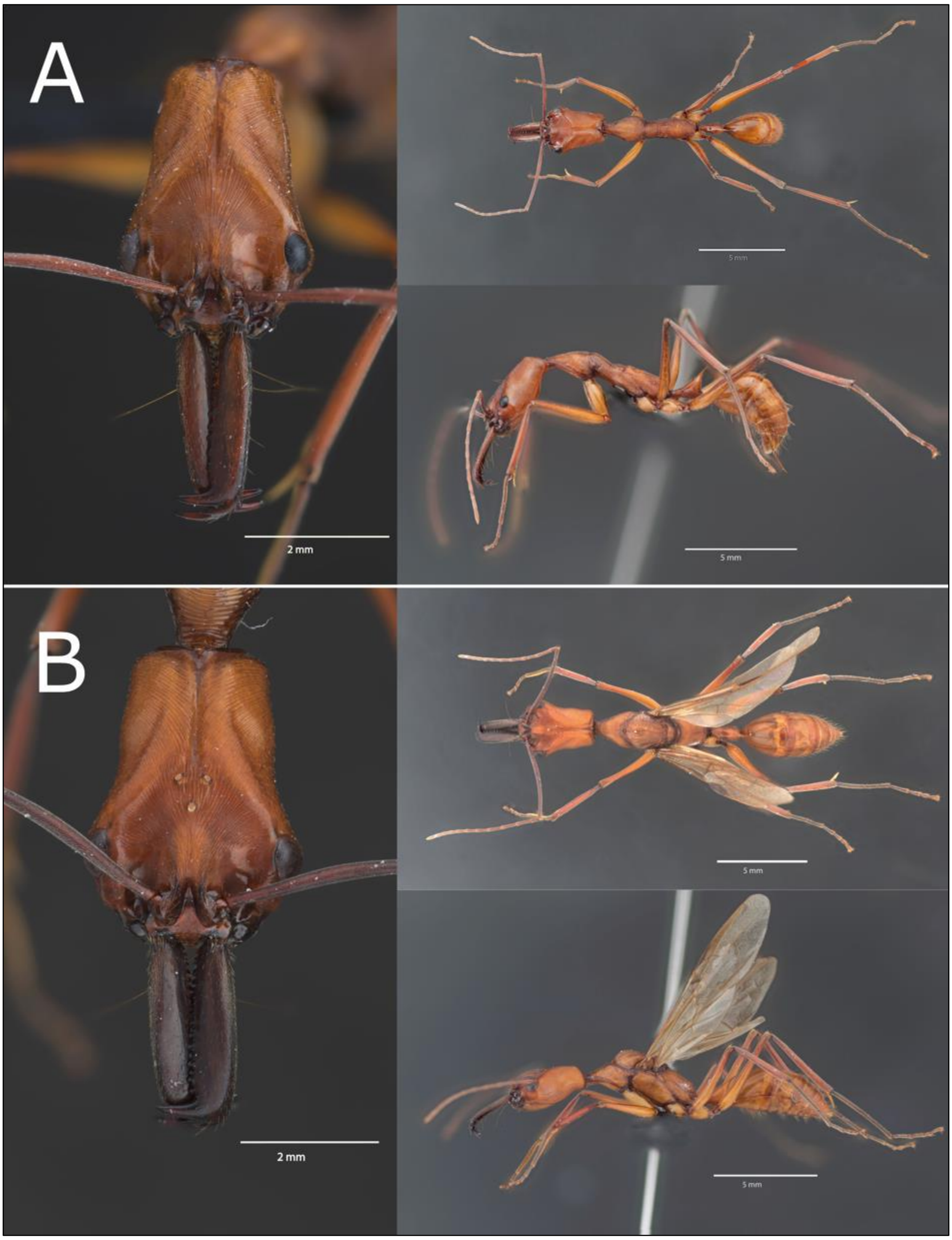

Fig. 4.2 *Odontomachus davidsoni* Hoenle, Lattke & Donoso **n.sp.** stacking pictures. A: Worker paratype (specimen PE23_01) B: Queen paratype (specimen PE24_01). Additional pictures in Supplemental file S7. Scale bars: 2 mm (left); 5 mm (right)

Fig. 4.3 Screenshots of the 3D models of *Odontomachus davidsoni* **n.sp.**. Top: 3D scan of *Odontomachus* holotype (PE39_01). Bottom: 3D scan of queen (PE24_01). Additional 3D models of two more paratypes in Supplemental file S8.

Type material examined

Complete list of localities in Supplemental file S9. Unique museum specimen identifiers are given in brackets after each specimen identification code.

Type locality.

ECUADOR• Esmeraldas, Reserva Río Canandé; 0.5281°N, 79.2070°W; ca 330 m; 21 February 2019; P. Hoenle & G. Villagomez leg.; collection code PE39; single worker near large fig tree in mature forest

Holotype specimen.

ECUADOR• 1 worker; Esmeraldas, Reserva Río Canandé; 0.5281°N, 79.2070°W; ca 330 m; 21 February 2019; P. Hoenle & G. Villagomez leg.; collection code PE39; single worker near large fig tree in mature forest; specimen code PE39_01; [MEPN5074]

Paratype workers.

ECUADOR• 3 workers; Esmeraldas, Reserva Rio Canande; 0.5252°N, 79.2079°W; ca 320 m; 04 February 2019; P. Hoenle & A. Argoti leg.; collection code PE23; hand sampling on Cecropia tree, same location as Odonto_Phil; specimen codes PE23_01, PE23_02, PE,_23_03; [MCZ-ENT00731935]

ECUADOR• 2 workers; Esmeraldas, Reserva Río Canandé; 00.5263°N, 79.2117°W; ca 310 m; 06 February 2019; P. Hoenle leg.; collection code PE25; workers on recently large, fallen tree; specimen codes PE25_01, PE25_02; [RBINS IG 34167]

ECUADOR• 4 workers; Esmeraldas, Reserva Río Canandé; 0.5238°N, 79.2130°W; ca 330 m; 11 February 2019; P. Hoenle leg.; collection code PE36; nest in fallen branch in secondary forest (former cacao plantation); specimen codes PE36_01[RBINS IG 34167]; PE36_02, PE36_03, PE36_04; [MEPN_5075]

ECUADOR• 4 workers; Esmeraldas, Reserva Río Canandé; 0.5252°N, 79.2079°W; ca 320 m; 29 May 2018; P. Hoenle & A. Argoti leg.; collection code Odonto_Phil; hand sampling on Cecropia tree. Same colony as PE23; One point-mounted worker ;specimen code: Odon_Phil_02 [DZUP 548819], (BOLD ID: ODECU002-19) and one point-mounted worker with the same locality data but collected on 20 May 2018, specimen code Odon_Phil_01 [DZUP 548820]; (BOLD ID: ODECU001-19); Two workers mounted with permanent glue on top of needle specimen codes Odon_Phil_3, Odon_Phil_4; [PH private collection]

Paratype queens.

ECUADOR• 2 queens; Esmeraldas, Reserva Río Canandé; 0.5263°N, 79.2129°W; ca. 340 m; 25 January 2019; P. Hoenle leg.; collection code PE24; 2 alate queens, ex. light trap at the Río Canandé station, 8 pm.; specimen codes PE24_01 [MCZ-ENT00731935], PE24_02 [MEPN_5076]

ECUADOR• 1 queen; Esmeraldas, Reserva Río Canandé; 0.5263°N, 79.2129°W; ca. 340 m; 13 April 2019; P. Hoenle leg.; collection code PE87, 1 alate queen, ex. light trap at the Río Canandé station, 9 pm.; specimen code PE87_01; [RBINS IG 34167]

ECUADOR• 1 queen; Esmeraldas, Reserva Río Canandé; 0.5263°N, 79.2129°W; ca 340 m; 09 May 2018; P. Hoenle & A. Argoti leg.; collection code Odon_Phil_queen; ex. light trap at Canandé Lodge; specimen code Odon_Phil_queen_01; [PH private collection]

ECUADOR• 1 queen; Esmeraldas, Kumanii Lodge near Cotocachi-Cayapas Reserve; 0.7539°N, -78.9208°W; ca 40 m; 14 April 2006; L. Camacho leg.; ex. light tap; [QCAZI 15167]

Specimens used for 3D scan: 1 Holotype worker (PE39_01), 1 paratype worker (PE23_01), 1 paratype worker (PE36_01), 1 paratype queen (PE24_01)

Specimens used for DNA barcoding: Paratype workers DZUP 548819 (BOLD ID: ODECU002-19) & DZUP 548820 (BOLD ID: ODECU001-19)

Diagnosis of workers

Measurements (n=3): HL 3.91-4.09, HoW 2.67-2.76, HvW 1.65-1.74, ML 2.62-2.70, SL 4.22-4.43, EL 0.62-0.71, MsL 6.00-6.20, PrW 1.49-1.57, PtW 0.59-0.64, PtL 1.53-1.57, PtH 2.20-2.23, FL 5.28-5.37, CI 67.48-68.53, SI 158.05-160.74, MI 65.28-69.05.

Long (TL > 17 mm), but slender, ferruginous to yellow brown body with striae on cephalic dorsum from antennal insertions to vertex, mandible with over 15 pre-apical teeth and denticles, pronotal dorsum with concentric to transverse striae. Petiole strongly pedunculate with posteriorly inclined apical spine, gaster smooth and shining.

Description of the holotype worker

Head elongate in dorsal view, anterior and posterior margins approximately of same width, posterior cephalic margin mostly transverse; head widest across eyes, at anterior one-third of head length; lateral cephalic margin posterior to eye sinuous. Median furrow deep, extends anterad to antennal fossa where it fades; occipital ridge distinctly delineated by antennal fossa, extending posteromedially, joining broad ridge that runs parallel to median furrow. Extraocular furrow broad and shallow, temporal prominence broad and weakly elevated. Cephalic surface with well-defined striae that diverge posterad from between frontal carina, reaching vertex, striae fade away on most of lateral cephalic surface with some striae reaching posteroventral cephalic surface. Ocular ridge smooth closest to eye and striate towards cephalic median region. Cephalic dorsal surface anterad of eye and between eye and antennal sclerite mostly smooth. Scape slender and slightly arched, SL longer than HL, scape widest just anterad of mid length, finely punctulate; funicular segment elongate and slender, segment I half as long as segment II.

Median clypeus mostly smooth and shining, posteriorly projecting as flattened triangular surface between frontal carina; carina defines narrow elevated region that descends posteriorly and extends to antennal fossa; frontal carina narrow, width not greater than scape width; carina steeply elevated over posteromedian clypeal surface. Ventral cephalic surface mostly smooth and shining. Labium drop-shaped, anteroventral surface very convex, PF 4,4. Buccal cavity with lateral hypostomal tooth. Mandibular masticatory margin with basal row of six denticles and eleven blunt triangular, relatively short teeth apicad of denticles. One or more teeth closest to apex may be broken. Mandibular apex tridentate, ventral tooth with basal tooth. Mandibular dorsal surface mostly smooth, with sparse piligerous punctulae, but dorsolaterally with abundant punctulae, ventral surface smooth and shining.

Pronotal dorsum with concentric striation that become progressively transverse and elongate medially towards posterior margin, in lateral view striae appear anteriorly transverse, medially curving and U-shaped, posteriorly oblique to almost vertical. Posterolateral pronotal margin with short convex lobe. Mesosoma relatively slender and elongate, in lateral view pronotal dorsal margin straight to weakly convex, forming a posteriorly ascending slope, mesonotum anterior margin slightly higher than posterior pronotal margin, mesonotal dorsal margin mostly straight to weakly convex, descending to metanotal groove. Dorsal mesosomal margin between metanotal sulcus and metanotal spiracle forms brief convexity, propodeal anterodorsal margin brief and convex, dorsal margin mostly straight, three times longer than declivity, declivity forms blunt obtuse angle with dorsal margin. Propleuron mostly smooth and shining with narrow transverse band of sparse weak rugulae anteriorly and posteriorly.

Mesonotum with transverse striae that extend uninterrupted laterally to anepisternum and ventrally to mesosternum, katepisternum mostly smooth and shining except for sparse striae anteriorly and posteroventrally. Bulla of metathoracic spiracle semispherical, weakly sculpted, opening shaped as transverse slit. Propodeum and metanotum transversely striate.

Mesometapleural suture distinct, propodeal- metapleural suture weakly impressed. No carina or visible suture between mesopleuron and mesosternum, mesosoma in hypothetical cross-section at mid-length forms relatively uniform ovoid. Mesosternum with median longitudinal region raised as low and broad convex ridge; metasternal process bidentate, teeth short and blunt. Propodeal spiracle slit-shaped, transverse to oblique, not elevated.

Petiole in lateral view slightly pedunculate, node shaped as posteriorly sloping cone with acute apical needle, anterior node margin weakly convex, posterior margin vertical, straight to weakly convex; anteroventral process prominent, triangular; node smooth and shining. Abdominal tergite 3 in lateral view with anterodorsal margin forming single convexity to posterior margin, ascending posterad at approximately 45°; ventral margin of tergite 3 briefly concave at prora, then broadly convex and mostly at the same level as prora. Constriction between abdominal segments 3 and 4 weak to negligible; gaster smooth and shining.

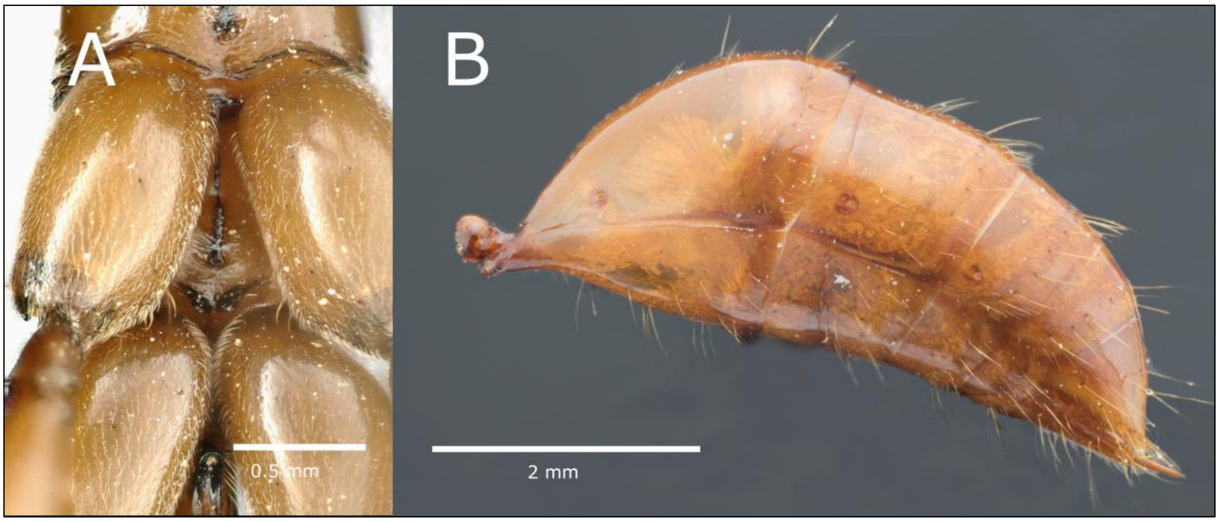

Fig. 4.4 *Odontomachus davidsoni* ventral picture of metasternal process (specimen: Odon_Phil_3) and lateral image of gaster (specimen Odon_Phil_4).

Coxae mostly smooth with abundant minute piligerous punctulae, punctulae denser on tibiae. Protibial apex with single seta, spur with basal translucent lamella. Probasitarsus with row of short, stiff hairs and parallel row of short setae opposite spur. Meso and metatibial apex each with two spurs, one pectinate, one simple; each also with 3 setae, each seta widely separated from each other. Body pilosity generally short and scattered with little pubescence; dorsal surface with few standing hairs: one on head where antennal fossa and nuchal carina almost meet, few on gastral sterna. Head and mandibular dorsum with sparse appressed pubescence, hairs straight on mandible and arched on head. Mandibular ventral surface next to masticatory margin with row of five flagellate long hairs plus two long trigger hairs at base. Scape with dense appressed pubescence, no standing hairs. Mesosoma with sparse appressed to subdecumbent small hairs, node with longer hairs; gaster mostly with sparse short, appressed to decumbent hairs with suberect hairs towards posterior end of gaster. Mandible and other bucal appendages, antenna, tibiae, and tarsi ferruginous brown to brown. Body mostly ferruginous to brownish yellow, head dark anterad and gaster darker posterad; trochanters and apex of femora tend to be darker.

Queen.

Measurements (n=1): HL 4.30, HoW 3.8, HvW 1.99, ML 2.87, SL 4.46, EL 0.75, MsL 6.78, PrW 2.22, PtW 0.79, PtL 1.68, PtH 2.40, FL 5.46, CI 71.63, SI 144.81, MI 66.74

Mesosoma developed for wings, head with three ocelli. Queen with larger dimensions than worker: HoW > 3.3; MsL > 6.5; PrW >1.9 mm., otherwise similar.

Male. Unknown.

Etymology.

The species epithet is a patronym in genitive case honoring Stuart Carleton Davidson, the founder of Clyde's Restaurant Group, Washington, D.C. Stuart had a lifelong interest in our environment, and would have loved this amazing ant.

Comparison to similar species

Odontomachus davidsoni most closely resembles *O. hastatus* by sharing a relatively large size, a red to brown color, a head which has in dorsal view a great difference between ocular and vertexal width, a relatively slender habitus, a bilobed metasternal process (Fig. 4.4, A), and a pedunculate petiole with a posterior inclining node topped by a long dorsal needle. Together with *O. mormo* both species also share an evenly convex anterior margin of abdominal tergite III that in lateral view ascends posterad at an approximate 45° angle (Fig. 4.4, B).

Compared to *O. hastatus*, *O. davidsoni* is clearly larger: The HL range of *O. hastatus* is 2.81 - 3.67 mm (Brown 1976) versus 3.91 - 4.09 mm. Further, it has coarse striae throughout the dorsal cephalic surface, whereas the striae on *O. hastatus* are fine and limited to the area between the frontal carina and the antennal fossa, not extending to the occipital ridge. The pronotum in *O.*

hastatus frequently presents smooth and shining areas on the pronotal disc or its sides, where it is always striate in *O. davidsoni.*

While the body size of *O. davidsoni* is similar to *O. mormo* (HL 4.14 - 4.36 (Brown (1976)), both species can be clearly distinguished by the striation pattern on the head: The striation in *O. mormo* does not reach the occipital ridge and there is instead a large and shiny area on the cephalic dorsum, while in *O. davidsoni* the entire cephalic dorsum is covered in coarse striae. Further, *O. mormo* does not possess a metasternal process, while *O. davidsoni* has a rounded bilobed metasternal process. *O. mormo* is almost hairless on the entire dorsal body surface including the petiole, whereas *O. davidsoni* body possesses a few appressed to decumbent hairs on the mesonotum, and many long erect hairs on the petiole. Overall, *O. mormo* has a more brownish coloration (very similar to *O. chelifer*), in contrast to the red coloration in *O. davidsoni.*

When using the key to Neotropical *Odontomachus* species by Rodriguez (2008) this species will be taken easily to couplet 13 , whereupon it will not fit any of the two alternatives: *O. ruginodis* nor *O. laticeps*. It is clearly larger than *O. ruginodis*, which also differs in its dark brown color, sessile petiole, and a very short stubby petiolar needle. *O. laticeps* is smaller, dark brown, with a sessile and relatively erect petiole bearing a shorter dorsal needle. Using the identification key in Brown (1976: 111), or the key in Antwiki (2015), this species is easily taken to couplet 14 where it becomes stuck as it fits neither alternative: *O. bauri* nor *O. laticeps*. Both of these ants are much smaller, dark brown, have a sessile, erect petiolar node with a relatively shorter dorsal needle, and the anterior dorsal margin of abdominal tergite III in lateral view is mostly vertical.

Molecular analyses

We successfully amplified DNA barcodes of two *Odontomachus davidsoni* workers, a 569 bp fragment and a 668 bp fragment (GenBank accession numbers MN454765 and MN454766, respectively). The two specimens came from the same nest and had identical sequences. *Odontomachus davidsoni* barcodes were clearly distinguishable from *COI* sequences of other *Odontomachus* species (Fig. 4.5) as indicated by the minimum interspecific p-distance of 0.09 in pairwise comparisons (range of p-distances in 94 pairwise comparisons: 0.09 - 0.14; Fig. 4.5). A search in the BOLD identification database for the closest sequence match yielded similar results of 90.76% and 90.67% sequence similarity to *O. chelifer* (private, not published yet) and *O. hastatus* (GenBank accession number: KU504889), respectively (accession date: 28.05.2019).

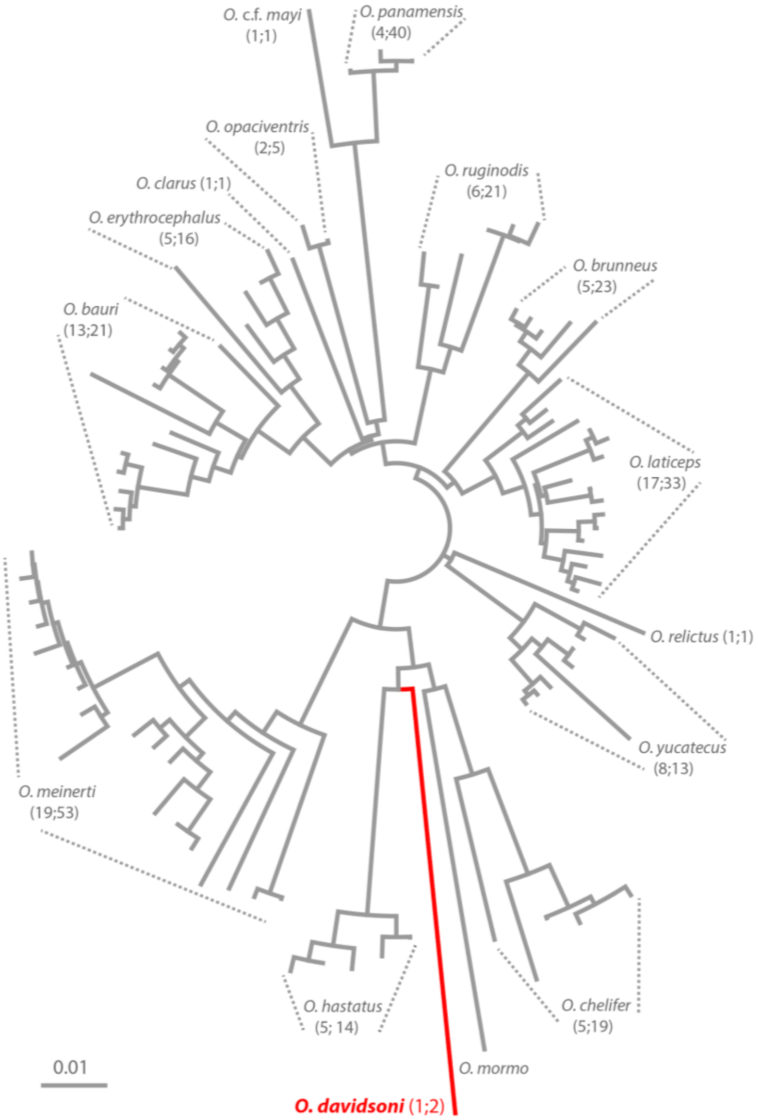

Fig. 4.5 Neighbor-joining (NJ) tree of *Odontomachus COI* sequences. The NJ tree is based on p-distances (scale bar). First digit in parentheses gives the number of identified *COI* haplotypes of a given species and the second one the total number of available *COI* sequences for this species. GenBank accession numbers and Newick tree file are given in Supplemental files S6.

Biology and Distribution

Workers of *O. davidsoni* were only found in the Río Canandé Reserve and its neighboring reserve Tesoro Escondido (Fig. 4.6). Alate queens were collected with light traps in April 2006 (Kumanii Lodge, Cotocachi-Cayapas Reserve, leg. Camacho), April and June 2018, as well as in February, March and April 2019 (Canandé Lodge, Río Canandé Reserve, leg. Hoenle). In 2018 and 2019 we frequently visited a tree in a selectively logged area of the Canandé Reserve where a few workers of the species were spotted. Foraging workers were observed predominantly during nighttime between 8 pm and 11 pm. On at least five occasions during day time (i.e. between 9 am and 5 pm) the plot was visited, but only once foraging workers were observed. Although their exact nest position was not detected, workers were predominantly foraging on a liana attached to a *Cecropia* tree. The tree had a diameter of 63 cm at breast height and an estimated height of 20 m. Workers could be observed walking straight up on it until they were out of sight in a height of approx. 10 m. Workers were never seen foraging on the ground, and we thus assume that they primarily forage in the canopy. Workers were observed to sit still on the surface of leaves with their mandibles open, probably waiting to ambush prey (Fig. 4.7).

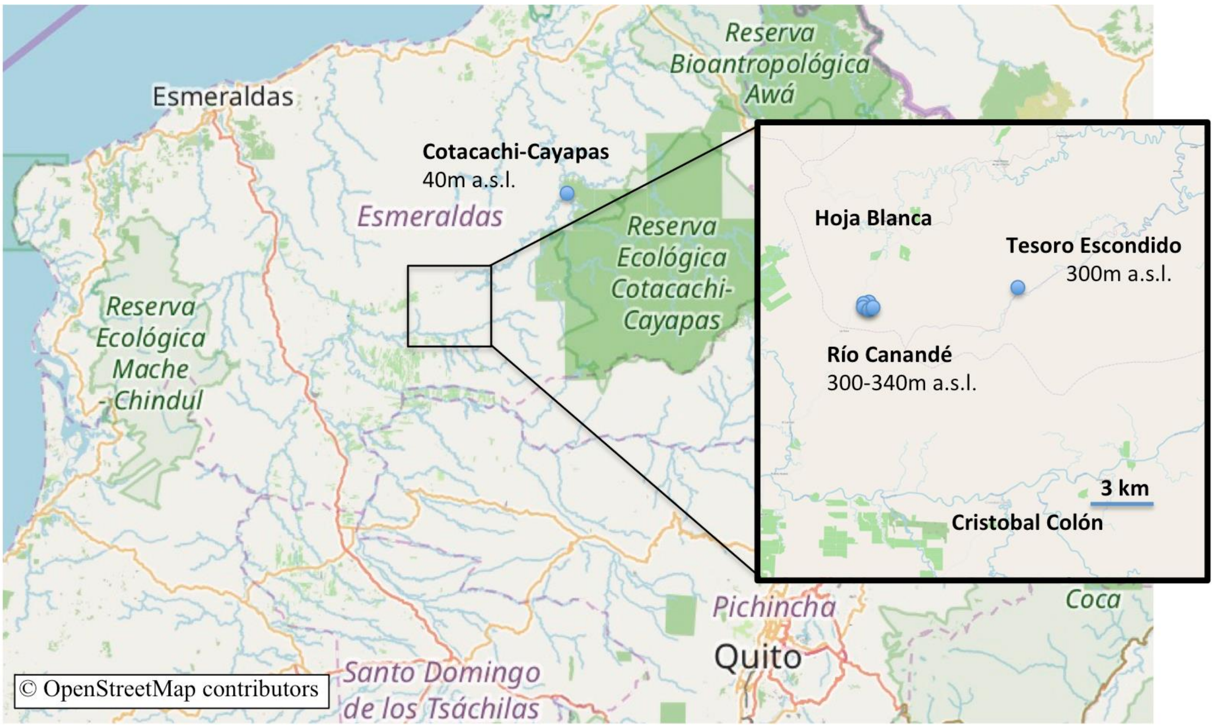

Fig. 4.6 *Odontomachus davidsoni* collection sites. Blue dots show collection sites in Esmeraldas Province (Ecuador) within the reserves Río Canandé, Tesoro Escondido and Cotacachi-Cayapas.

On the 11th of February 2019 we collected what looked like a complete nest in a fallen branch (Fig. 4.8; GPS data: 0.5238°N, 79.2130°W). The nest contained one dealate queen and 18 workers, as well as brood in all development stages (Fig. 4.9). We assume that this colony was not fully grown because it contained no alates (despite other colonies having alates at this time). The single nest entry was located under a bromeliad (Fig. 4.8, A). We opened all parts of the nest with a machete, revealing a 40cm long tubular chamber within the center of the branch (Fig. 4.8, B.). It does not look like the ants themselves carved it, but it was probably a pre-existing cavity.

Fig. 4.7 *Odontomachus davidsoni* worker sitting on a leaf in its natural habitat.

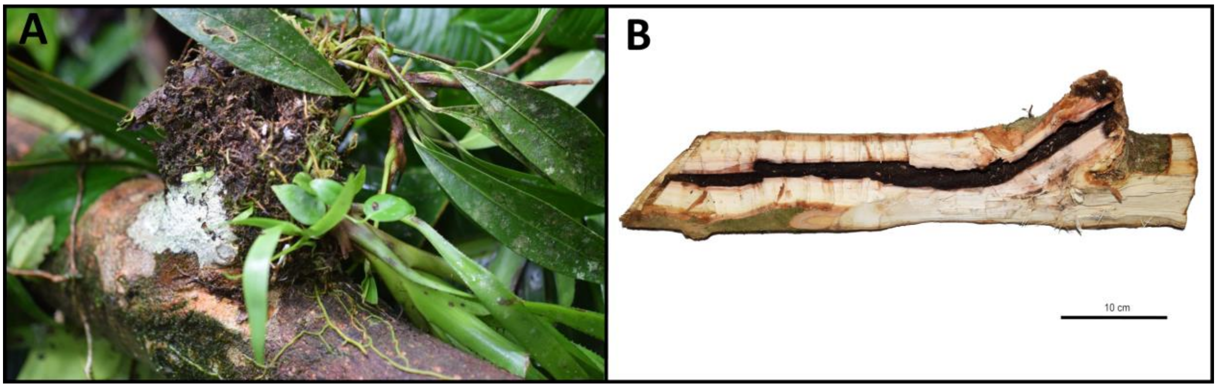

Fig. 4.8 Nest of *Odontomachus davidsoni* **A**: Nest found under natural conditions with bromeliad covering the nest entrance. **B**: Nest architecture visible after opening a fallen tree branch with a machete. Scale bar: 10 cm.

We kept the colony for three months (11th February - 15th April 2019) for further observations. The colony accepted various smaller insects as food, including flies, crickets and termites. However, insects larger than 2 cm (e.g. large cicadas, moths, large crickets) were usually not accepted. Furthermore, the colony had *ad libitum* access to sugar water which was frequently visited. In accordance with field observations, the colony showed most activity during nighttime. No recruitment to offered food resources was observed. Due to the possibly threatened status of this ant species, the colony was released at the end of our observation time on a tree bromeliad nearby the Canandé lodge.

Fig. 4.9 Colony of *O. davidsoni.* This colony was kept in the field laboratory after taking it out from the twig nest (Fig. 4.8). The sole dealate queen is marked with a red arrow.

4.5 DISCUSSION

We here formally described the species *Odontomachus davidsoni*. It is morphologically and genetically different from any other of the New World *Odontomachus* species. It rivals in size *O. mormo*, the largest known *Odontomachus* in the Americas, but the dark brown color, more sessile and robust petiole, mostly smooth cephalic dorsum, and lack of a metasternal process in *O. mormo* will easily permit the distinction between the two species. Unfortunately, there are few measurements available for gauging the dimensions of *O. mormo* (Brown 1976: 118; Rodriguez 2008: 156) but it seems safe to affirm that together with *O. chelifer* these species share the position as the largest known *Odontomachus* in the Americas.

Sequence similarities of *COI* barcodes suggested that *O. davidsoni* might be most closely related to *O. hastatus*, *O. mormo* and *O. chelifer*. However, more informative phylogenetics/-genomics analyses are necessary to draw robust conclusions. This is because a single mitochondrial locus does not allow us to reliably infer phylogenetic relationships and because our species coverage is incomplete (10 Neotropical *Odontomachus* species do not possess published barcodes). Morphological characters suggest that *Odontomachus davidsoni* is most closely related to *Odontomachus hastatus*, which shares the arboreal and nocturnal foraging lifestyle (Camargo and Oliveira 2011, Rodrigues and Oliveira 2014). The species are easily separated by the lack of striation at the occipital margin in *O. hastatu*s and the uniform red coloration of *O. davidsoni*. Both species seem to live in sympatry: our closest record of *O. hastatus* is in a linear distance of approximately 727 m to *O. davidsoni* (390 m vs. 300 m elevation, respectively). Other *Odontomachus* species found in the vicinity are *O. mormo*, *O. chelifer*, *O. bauri*, *O. erythrocephalus* and *O. meinerti* (PH, pers. obs.), which highlights the high local species richness in the reserve.

Our species description is accompanied by 3D scans of three workers and a queen (Fig. 4.3, Supplemental file S8). This offers morphological details of the new species to the reader and the ability to take exact trait measurements. 3D imaging techniques, and in particular micro-computed X-ray tomography (μCT), are becoming more frequently used in taxonomy and functional morphology, including studies on ants (Faulwetter et al. 2013, Akkari et al. 2015; Garcia et al. 2017, Sarnat et al. 2017, Staab et al. 2018). Garcia et al. (2017) provided a comprehensive overview of the benefits and caveats of μCT scans for such purposes. The 3D scans used in our study were produced via photogrammetry. This technique has some advantages as well as disadvantages over μCT scans, e.g. it is comparatively inexpensive and requires little manual work, but it provides no internal structure and has a comparatively low spatial resolution (Ströbel et al. 2018). The resulting surface model can thus lack taxonomically important structural features such as the head striation in the case *of O. davidsoni*. On the other hand, the resulting 3D surface models are texturized, thus also providing information on specimen color, which is lacking in μCT scans. A further disadvantage of DISC3D scans is that structures that are obscured in the physical specimen, e.g. through leg positioning or characters laying underneath the glue, are not recovered in a resulting 3D model. Overall, we argue that the 3D scans are a good addition to the traditional morphological description and stacking images by providing valuable 3D models that everyone can easily access and use for reliable trait measurements. Additionally, the 398 EDOF images, that the 3D models are based on, allow for an even more detailed inspection of the specimens in comparison to the texture on the 3D model.

The new species was discovered in the Chocó-Darién bioregion in Ecuador - probably one of the most biodiverse regions on earth, and at the same time one of the most threatened ones (Dinerstein 1995, Olson and Dinerstein 1998, Myers et al. 2000). Research in this region is scarce, with many undescribed endemic species still awaiting scientific discovery and description (Donoso et al. 2009). The fact that a large and conspicuous ant like the herein described trap-jaw ant *O. davidsoni* remained unknown to science until now suggests that a hidden diversity remains to be discovered in this region. Similar to other biodiversity hotspots, increasing deforestation and conversion of forests to agriculture threatens the biodiversity of the Chocó-Darién bioregion, bearing the risk that many endemic and even yet undescribed species become extinct before being detected. With the description of a new, conspicuous trap-jaw ant, probably endemic to the region, we hope to provide additional reasons to protect this threatened biodiversity hotspot.

Conclusion. Odontomachus davidsoni is a noteworthy discovery in a vastly understudied and highly threatened area - the Chocó-Darién region of Ecuador. We sincerely hope that conservation efforts will continue and expand to protect this unique and important biodiversity hotspot.

4.6 ACKNOWLEDGEMENTS

We thank the Fundacíon Jocotoco and the associated Tesoro Escondido for logistic support and their permission to do research on their forest properties. We like to thank especially the local support from the park staff in the Canandé and Tesoro Escondido reserve, that made the field collection easier and made two great field stays possible: Bryan Amayo, Alcides Zombrano, Roberto de la Cruz, Jorge Zambrano, Amado de la Cruz, Yadria Giler, Patricio Encarnación and Vanessa Moreira.

The species name was auctioned for a good cause at the anniversary of the Rainforest Trust, and we like to thank them and the highest bidder for this opportunity to aid in the conservation efforts and research in the Chocó area.

We would like to thank Brian L. Fisher as well as three reviewers for helpful comments on the manuscript.

We acknowledge support by the German Research Foundation and the Open Access Publishing Fund of Technische Universität Darmstadt.PH was supported by a scholarship from the German National Academic Foundation.

CvB received funding from the German Research Foundation (DFG: BE 5177/4-1 & BE 5177/4-2). SS was funded by the German Federal Ministry of Education and Research (BMBF), project NOVA (05K2016 / 05K16RDD).

List of Supplemental files:

Downloadable from the publication online: https://doi.org/10.3897/zookeys.948.48701

S1: Video of *Odontomachus davidsoni* holotype 3D model

S2: Video of *Odontomachus davidsoni* queen paratype 3D model

S3: Table with measurements

S4: DNA barcode information

S5: BOLD barcodes

S6: NJ tree

S7: Additional detail images of *O. davidsoni*

S8: Additional 3D scans of two more paratype workers

S9: Table of localities

4.7 REFERENCES

Akkari, N., H. Enghoff, and B.D. Metscher. 2015. A new dimension in documenting new species: high-detail imaging for Myriapod taxonomy and first 3D cybertype of a new millipede species (Diplopoda, Julida, Julidae). PLOS ONE 10:e9135243.

Antwiki. 2015. Key to *Odontomachus* of the New World. Accessed 17.IX.2018. http://www.antwiki.org/wiki/index.php?title=Key_to_Odontomachus_of_the_New_World&oldid=398024

Bolton, B. 2018. An online catalog of the ants of the world. Accessed 20.XI.2018. http://antcat.org

Brown, W. L. Jr .1976. Contributions toward a reclassification of the Formicidae. Part VI. Ponerinae, tribe Ponerini, subtribe Odontomachiti. Section A. Introduction, subtribal characters. Genus *Odontomachus*. Studia Entomologica 19:67–171.

Camargo, R. X. and P. S. Oliveira. 2012. Natural history of the Neotropical arboreal ant, *Odontomachus hastatus*: nest sites, foraging schedule, and diet. Journal of Insect Science 12:1–9.

Deyrup, M., and S. Cover. 2004. A new species of *Odontomachus* ant (Hymenoptera: Formicidae) from inland ridges of Florida, with a key to *Odontomachus* of the United States. Florida Entomologist, 87:136–144

Dinerstein, E.A. .1995. Conservation Assessment of the Terrestrial Ecoregions of Latin America and the Caribbean. Washington, D.C.: World Bank.

Dominguez, D. F., M. Bustamante, R. A. Albuja, A. Castro, J. E. Lattke, and D. A. Donoso. 2016. COI barcodes for ants (Hymenoptera: Formicidae) of drylands in the south of Ecuador. Ecosistemas 25:76–78.

Donoso, D. A., F. Salazar, F. Maza, R. E. Cárdenas, and O. Dangles. 2009. Diversity and distribution of type specimens deposited in the Invertebrate section of the Museum of Zoology QCAZ, Quito, Ecuador. Annales de la Société Entomologique de France 45:437–454.

Donoso, D. A. and G. Ramón. 2009. Composition of a high diversity leaf litter ant community (Hymenoptera: Formicidae) from an Ecuadorian pre-montane rainforest. Annales de la Société Entomologique de France 45:487–499.

Donoso, D. A. 2017. Tropical ant communities are in long-term equilibrium. Ecological Indicators 83:515–523.

Edgar, R.C. 2004. MUSCLE: multiple sequence alignment with high accuracy and high throughput. Nucleic Acids Research 32:1792–1797.

Evenhuis, N. L. 2020. The insect and spider collections of the world website. Available at: http://hbs.bishopmuseum.org/codens/ [Last accessed: 20/02/2020].

Faulwetter, S., A. Vasileiadou, M. Kouratoras, T. Dailianis, and C. Arvanitidis. 2013. Micro-computed tomography: Introducing new dimensions to taxonomy. ZooKeys 264:1–45.

Folmer, O., M. Black, W. Hoeh, R. Lutz, and R .Vrijenhoek. 1994. DNA primers for amplification of mitochondrial cytochrome c oxidase subunit I from diverse metazoan invertebrates. Molecular Marine Biology and Biotechnology 3:294–299.

Garcia, F. H., G. Fischer, C. Liu, T. L. Audisio, G. D. Alpert, B. L. Fisher, and E. P. Economo. 2017. X-Ray microtomography for ant taxonomy: An exploration and case study with two new *Terataner* (Hymenoptera, Formicidae, Myrmicinae) species from Madagascar. PLOS ONE 12:e0172641.

Gronenberg, W., J. Tautz, and B. Hölldobler. 1993. Fast trap jaws and giant neurons in the ant *Odontomachus*. Science 262:561–563.

Gronenberg, W. 1995. The fast mandible strike in the trap-jaw ant *Odontomachus*. Journal of Comparative Physiology A 176:399–408.

Guenard, B., M. Weiser, K. Gomez, N. Narula, and E. P. Economo. 2017. The Global Ant Biodiversity Informatics (GABI) database: a synthesis of ant species geographic distributions. Myrmecological News 24:83–89.

Harris, R.A. 1979. A glossary of surfacing sculpturing. Occasional papers in Entomology, State of California, Department of Food and Agriculture 28:1–31.

Keller, R.A. 2011. A phylogenetic analysis of ant morphology (Hymenoptera: Formicidae) with special reference to the poneromorph subfamilies. Bulletin of the American Museum of Natural History 355:1–90.

Kumar, S., G. Stecher, M. Li, C. Knyaz, and K. Tamura. 2018. MEGA X: Molecular Evolutionary Genetics Analysis across computing platforms. Molecular Biology and Evolution 35:1547–1549.

Larabee, F. J., and A. Suarez. 2014. The evolution and functional morphology of trap-jaw ants (Hymenoptera: Formicidae). Myrmecological News 20:25–36.

Larabee, F.J., and A. Suarez. 2015. Mandible-powered escape jumps in trap-jaw ants increase survival rates during predator-prey encounters. PLOS ONE 10:e0124871.

Larabee, F. J., B. L. Fisher, C. A. Schmidt, P. Matos-Maraví, M. Janda, and A. V. Suarez. 2016. Molecular phylogenetics and diversification of trap-jaw ants in the genera *Anochetus* and *Odontomachus* (Hymenoptera: Formicidae). Molecular Phylogenetics and Evolution 103:143–154.

Lattke, J., M. Vélez, and M. Aguirre. 2016. Survey of ants in dry forests of southwestern Ecuador (Hymenoptera: Formicidae). Sociobiology 63:909–918.

MacGown, J.A., B. Boudinot, M. Deyrup, and D. M. Sorger. 2014. A review of the Nearctic *Odontomachus* (Hymenoptera: Formicidae: Ponerinae) with a treatment of the males. Zootaxa 3802:515–552.

Matos-Maraví, P., N. J. Matzke, F. J. Larabee, R. M. Clouse, W. C. Wheeler, D. M. Sorger, A. V. Suarez, and M. Janda. 2018. Taxon cycle predictions supported by model-based inference in Indo-Pacific trap-jaw ants (Hymenoptera: Formicidae: Odontomachus). Molecular Ecology 27:4090–4107.

Myers, N., R. A. Mittermeier, C. G. Mittermeier et al. 2000. Biodiversity hotspots for conservation priorities. Nature 403:853–858.

Olson, D. M., and E. Dinerstein. 1998. The Global 200: a representation approach to conserving the Earth's most biologically valuable ecoregions. Conservation Biology 12:502–15.

Rodrigues, P. A. P., and P. S. Oliveira. 2014. Visual navigation in the Neotropical ant *Odontomachus hastatus* (Formicidae, Ponerinae), a predominantly nocturnal, canopy-dwelling predator of the Atlantic rainforest. Behavioural Processes 109:48–57.

Rodriguez, J. 2008. Género *Odontomachus* Latreille. pp. 148 – 170 in Jiménez, E., F. Fernández, T. M. Arias, and F.H. Lozano-Zambrano (eds.) Sistemática, biogeografía y conservación de las hormigas cazadoras de Colombia. Bogotá: Instituto de Investigación de Recursos Biológicos Alexander von Humboldt.

Salazar, F., and D. A. Donoso. 2013. New ant (Hymenoptera: Formicidae) records for Ecuador deposited at the Carl Rettenmeyer ant collection in the QCAZ Museum. Boletín Técnico 11, Serie Zoológica 8-9:151–177.

Salazar, F., F. Reyes-Bueno, D. Sanmartin, and D. A. Donoso. 2015. Mapping continental Ecuadorian ant species. Sociobiology: 62:132–162.

Sarnat, E. M., N. R. Friedman, G. Fischer, B. Lecroq-Bennet, and E. P. Eonomo. 2017. Rise of the spiny ants: diversification, ecology and function of extreme traits in the hyperdiverse genus Pheidole (Hymenoptera: Formicidae). Biological of the Linnean Society 122:514–538.

Schmidt, C. A., and S. O. Shattuck. 2014. The higher classification of the ant subfamily ponerinae (Hymenoptera: Formicidae), with a review of ponerine ecology and behavior. Zootaxa 3817:001–242.

Staab, M., F. H. Garcia, C. Liu, Z. H. Xu, and E. P. Economo. 2018. Systematics of the ant genus *Proceratium* Roger (Hymenoptera, Formicidae, Proceratiinae) in China – with descriptions of three new species based on micro-CT enhanced next-generation-morphology. ZooKeys: 137–192.

Ströbel, B., Schmelzle, S., Blüthgen, N., and Heethoff, M. 2018 An automated device for the digitization and 3D modelling of insects, combining extended-depth-of-field and all-side multi-view imaging. ZooKeys 759:1–27.

von Beeren, C., Y. Maruyama, and D.J.C. Kronauer. 2016. Cryptic diversity, high host specificity and reproductive synchronization in army ant associated *Vatesus* beetles. Molecular Ecology 25:990–1005.

Wilkie, K. T. R., A. L. Mertl, and J. F. A. Traniello. 2010. Species Diversity and Distribution Patterns of the Ants of Amazonian Ecuador. PLOS ONE 5:e13146.

Wilson, E. O. 1955. A monographic revision of the ant genus *Lasius*. Bulletin of the Museum of Comparative Zoology 113:1–204.

5 A NEW SPECIES GROUP OF *STRUMIGENYS* (HYMENOPTERA, FORMICIDAE) FROM ECUADOR, WITH A DESCRIPTION OF ITS MANDIBLE MORPHOLOGY

This chapter was published in the Journal “Zookeys”: doi.org/10.3897/zookeys.1036.62034

Authors:

Douglas B. Booher[1,2*], Philipp O. Hoenle[3*]

* Authors contributed equally.

Affiliations:

[1]Yale Center for Biodiversity and Global Change, 165 Prospect Street, New Haven, CT 06520-8106, USA

[2]Georgia Museum of Natural History, 101 Cedar Street, Athens, GA 30602

[3]Ecological Networks, Department of Biology, Technical University of Darmstadt, Darmstadt, Germany.

Author contributions

PH did the field work. PH & DB wrote the manuscript. DB performed morphological analysis and species description. All authors read and approved the manuscript.

5.1 ABSTRACT

Strumigenys is one of the most diverse ant genera in the world and arguably the most morphologically diverse — exhibiting an exceptional range of mandible shape and function. Here we describe a new species, *Strumigenys ayersthey* **sp. nov.**, discovered in the Chocó region of Ecuador. With two morphological characters we show that this species is a morphologically unique outlier among *Strumigenys* globally, having predominately smooth and shining cuticle surface sculpturing and long trap-jaw mandibles. Using µCT scans, we produced 3D images of the worker ant and static images to examine and compare mandible articular morphologies with most morphologically similar members of the *mandibularis* species-group. Cuticular, pilosity, and articular mandible morphological differences supports placing the new species in its own new species-group.

5.2 INTRODUCTION

Ecuador has one of the highest animal and plant species richness of any country, both in terms in of species per area and total species richness (Sierra et al. 2002). This unusually high diversity is due to the three vastly distinct bioregions within Ecuador: the Amazon basin in eastern Ecuador, the Chocó-Darién bioregion in the northwest, and the Tumbesian drylands in the southern portion of the country (Sierra et al. 2002). Of these, the areas west of the Andes have been the least studied, and particularly the Chocó-Darién is a hotspot for new, previously unknown ant species (Donoso and Ramón 2009, Donoso et al. 2009, Salazar and Donoso 2013, Salazar et al. 2015, Donoso 2017, Hoenle et al. 2020). The *Strumigenys* fauna of Ecuador currently includes 51 species (Salazar et al. 2015), several of which are endemic (e.g. *Strumigenys madrigalae* Lattke & Aguirre 2015). Here, we report the finding of another likely endemic *Strumigenys* species from the Ecuadorian Chocó, contributing to a better understanding of this hyperdiverse region.

Strumigenys is one of the most diverse ant genera known with currently 852 extant and four fossil species, and is present on all continents except Antarctica (Guénard et al. 2017, Bolton 2020). Over the past two decades this genus received a lot of taxonomic attention but given the amount of recent species descriptions it is certain that many species are still waiting to be discovered (e.g. Booher et al. 2019, Sarnat et al. 2019, Dong and Kim 2020). *Strumigenys* are comparatively small ants (most < 4 mm) and are primarily litter dwelling although there are a few arboreal species (Bolton 2000). Most species assessed for diet are specialist predators of entomobryomorph Collembola (springtails), which may have led them to evolve a range of peculiar mandible forms to facilitate predation of fast-moving prey (Wesson and Wesson 1939, Wilson 1953, Masuko 1984, Dejean 1985, Brown and Wilson 1995, Masuko 2009, Lattke et al. 2018, Gray et al. 2019, Booher et al. 2021). Most spectacular, many *Strumigenys* possess trap-jaws —fast-snapping mandibles that function via a power amplified latch-mediated spring-actuation (LaMSA) (Booher et al. 2021, Ilton et al. 2018, Longo et al. 2019) — akin to a biological mousetrap (Gronenberg 1996, Larabee and Suarez 2014). Performance and evolution of the trigger and latch system has been studied in detail, however there has been little attention given to additional undefined mandibular morphology that may contribute to the stability of trap-jaw movement in *Strumigenys* and other trap-jaw ants (Gronenberg 1996, Larabee et al. 2018, Booher et al. 2021). Within *Strumigenys,* the LaMSA mechanism has evolved independently multiple times, with each evolution convergent in morphology, function, and performance (Booher et al. 2021). However, the morphological variation in articular surfaces and articular processes involved in mandible movement across *Strumigenys* with or without LaMSA is morphologically variable and not well understood (Booher, unpublished data, Silva and Feitosa 2019). Here, we construct and define the single species *ayersthey* species-group, describe the mandible articular morphology in detail within the description of the previously unknown *S. ayersthey* **sp. nov.**, and compare it to that of morphologically similar members of the *S. mandibularis* species-group to support species-group separation.

5.3 MATERIALS AND METHODS

Sampling and geographic origin

The specimen of *Strumigenys ayersthey* **sp. nov.** was collected during a field trip to the Reserva Río Canandé in Ecuador (Esmeraldas Province) in May 2nd 2018 (Fig. 5.1). The reserve belongs to the Chocó-Darién bioregion, and is characterized by evergreen tropical forest with a wet season from January to March, and a dry season from September to December. The reserve contains low- to mid-elevation forest spanning a range of approximately 200 to 600 m. The specimen was collected in old-growth forest, along the ridge of small plateau at 507 m elevation. We generated the distribution map with SimpleMappr (Shorthouse 2010). The specimen was collected alive by hand, and later preserved in a vial containing 96% ethanol. The Ministerio de Ambiente de Ecuador issued the permits for collection (MAE-DNB-CM-2017-0068) and exportation (41-2018-EXP-CM-FAU-DNB/MA).

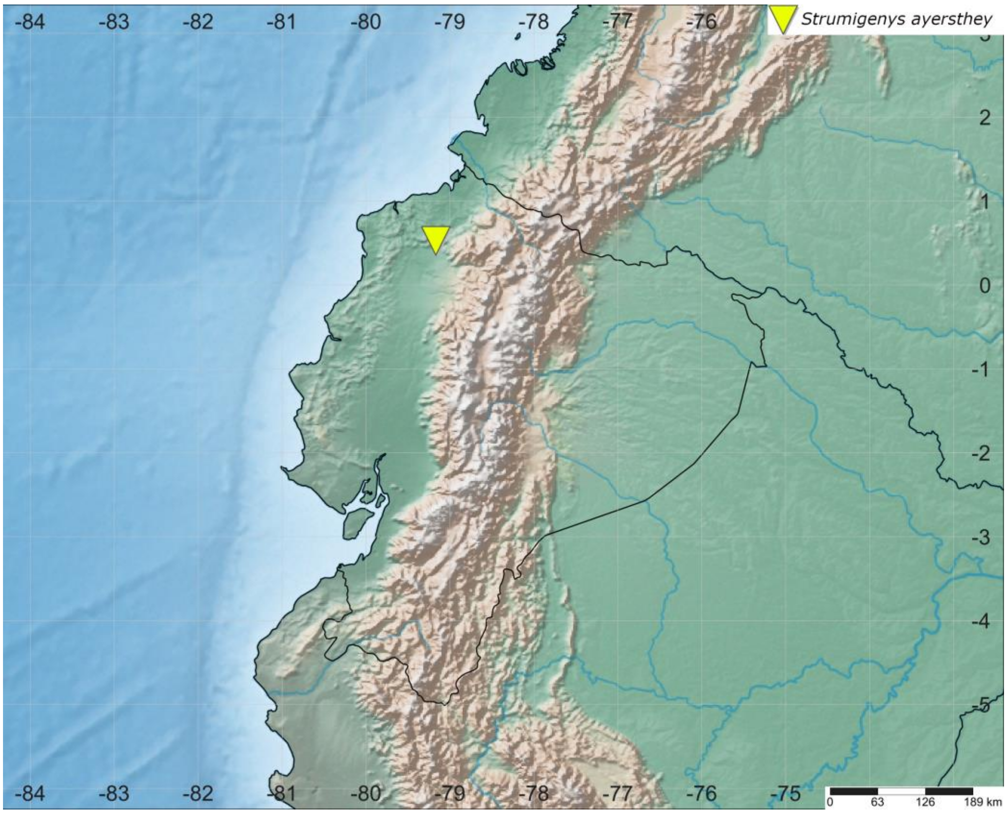

Fig. 5.1 Location of the holotype collection of *S. ayersthey* **sp. nov.** in Ecuador (Reserva Río Canandé, Esmeraldas Province).

Photos

We took stacking images with a Canon EOS 7D with a MPE 65mm lens (Canon, Tokyo, Japan). We used Helicon Focus Version 7 (Helicon Soft Ltd., Kharkiv, Ukraine) to focus stack multiple images, and added a scale and brightness adjustments with Adobe Photoshop CS6 13.0 (Adobe Inc., San Kaso, CA, USA). All images presented are available online and can be viewed on AntWeb (Antweb 2020), where it can be identified by a specimen-level code affixed to the pin.

Synchrotron X-Ray micro-computed-tomography (SRµCT) scan

The SRµCT scan of the sample was recorded at P05 at PETRA III, Deutsches Elektronen-Synchrotron DESY in Hamburg, Germany. We used absorption contrast tomography with an energy of 11 keV, a sample-detector distance of 20 mm, and a magnification of 9.97 resulting in an effective pixel size of 0.642 µm. The dataset has been cropped, positioned, and visualized in VGStudio MAX 3.0 (build 109953; Volume Graphics GmbH, Heidelberg, Germany). Amira 5.6 (FEI Visualization Sciences Group, Mérignac Cedex, France) was used to digitally remove the cardboard the specimen was glued onto and to make a surface model of the scan data. Fiji (Schindelin et al. 2012) was then used to convert the resulting surface model to U3D.

Morphological Data

The measurements, indices, and morphological terminology used in species-group definitions and species descriptions in this study are based on Bolton (2000), and the mandible articular terminology is based on two studies (Table 3.1) (Silva and Feitosa 2019, Richter et al. 2019). We compared anologous terms for these studies, and added our own terminology for features that were not included in these studies in best agreement with terminology already in use. Measurements were taken using the measurement application of the LAS-X Leica software using a Leica IC90 E digital camera and Leica M165 C microscope with either a 1.0x or 1.6x PLANAPO objective. Measurements and indices are presented as a single value mean of three independent measures; measurements are expressed in millimeters to three decimal places. Global morphological mandible index data were assimilated by DBB (Booher et al. 2021). Specimens were identified without head surface sculpture visually from species imaged and hosted on AntWeb (Antweb 2020). The data was plotted with JMP® version 15.0.0 statistical software. Softening specimens and visual confirmation of trap-jaw mechanisms through visual manipulations of specimen were done as described in Booher et al. (2020). For this study, we examined mandible morphology in the following *mandibularis*-group species: *S. planeti* casent0873025, *S. biolleyi* casent0747760, *S. cordovensis* casent0609666, and *S. smithi* from Ecuador in author DB's collection.

Measurement definitions

HL Head length. Maximum length of head in full-face view, excluding mandibles, measured from anterior most point of clypeal margin to midpoint of a line across the posterior margin.

HW Head width. Maximum width of head in full-face view, measured in the same plane as HL.

ML Mandible length. The straight-line length of mandible at full closure, measured in the same plane as HL, from mandibular apex to anterior clypeal margin.

PW Pronotum width. Maximum width of pronotum in dorsal view.

SL Scape length. Length of antennal scape excluding the basal condylar bulb.

FL Femur length. Maximum length of hind femur.

EL Eye length. Maximum length of eye as measured in oblique view of the head to show full surface of eye.

TL Total body length

WL Weber's Length

CI Cephalic index. HW/HL × 100.

SI Scape index. SL/HW × 100.

MI Mandible index. ML/HL × 100

5.4 RESULTS

Key to Strumigenys ayersthey

1 Head in full face view absent of sculpture, smooth and shining; mandible relatively long MI 65; pilosity consisting of nearly uniform sub-erect to erect filiform setae…***Strumigenys ayersthey*** **sp. nov.** (Ecuador).

- Without combination of characters above...**Start with couplet 1 Bolton (2000) Key to Nearctic and Neotropical *Strumigenys.***

Strumigenys ayersthey sp. nov.

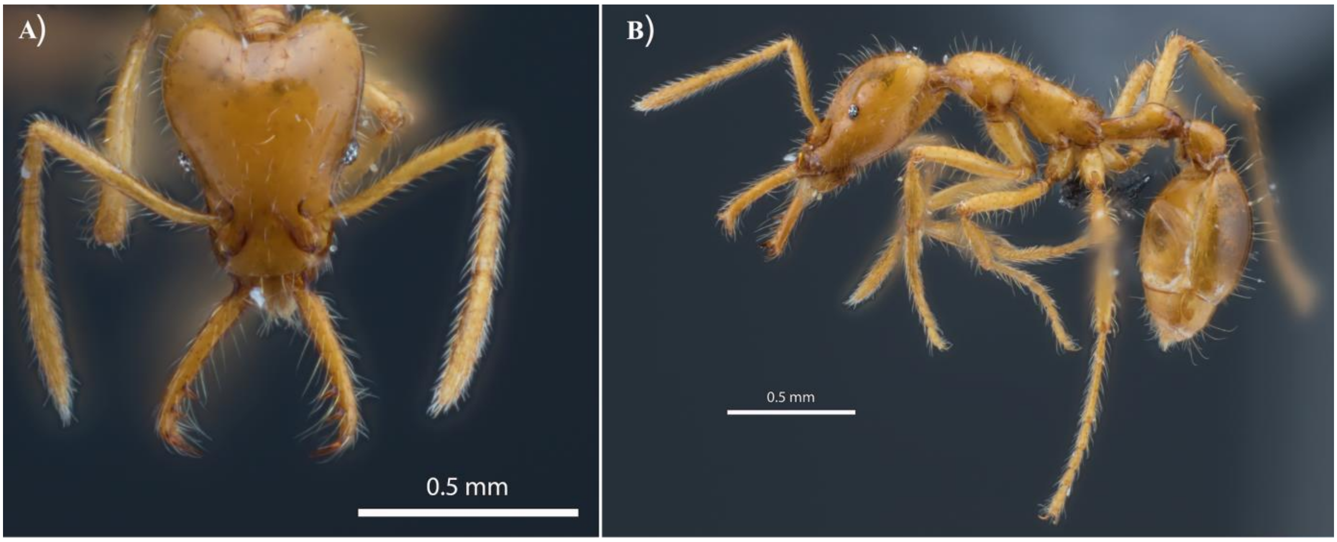

Fig. 5.2 Images of **A** head in full-face view and **B** profile of Holotype specimen of *Strumigenys ayersthey* **sp. nov.** (CASENT0875770) [MEPN].

Fig. 5.3 3D scan of *Strumigenys ayersthey* **sp. nov.** assembled by μCT.

Strumigenys ayersthey-group

The *ayersthey* group contains one member and exhibits most morphological resemblance to the *mandibularis*-group (Bolton 2000), from which it is most easily separated by differences in sculpture and pilosity. *Strumigenys ayersthey* **sp. nov** has little to no sculpture anywhere on its body and has only fine simple to flagellate setae, whereas *mandibularis* species-group members are predominately sculptured and not shining with mostly decumbent to appressed apically expanded or flattened setae. Also separating these two groups are morphological differences in dorsal articular processes of mandibles, in *S. ayersthey* **sp. nov.** these processes project from the dorsal surface at the base of each mandible without distinct lamellate lateral edges. In *mandibularis* species-group members, these processes arise from laterally expanded lamella at the base of mandibles that are continuous with the dorsal surface of each mandible. *Strumigenys ayersthey* **sp. nov.** can be distinguished from all other *Strumigenys* species by shining sculpture and MI 65, other *Strumigenys* predominately lacking sculpture and shining have MI < 40 (Fig. 5.4). The following diagnosis is adapted and expanded from the *mandibularis* species-group diagnosis (Bolton 2000).

Table 5.1 Comparison of morphological features of *Strumigenys ayersthey* **sp. nov.** with those described in *Strumigenys* spp. (Silva and Feitosa 2019), and the Myrmicine ant *Wasmannia affinis* (Richter et al. 2019). *S. ayersthey* **sp. nov.** has several features previously not reported but may be shared with many other *Strumigenys*. Presence refers to the reporting of each morphological feature: S – *Strumigenys* including *S. ayersthey*, SA – only reported in this publication in *S. ayersthey*, W – reported in *Wasmannia affinis.*

abbreviation					
This study	Silva & Feitosa 2019	Richter et al. 2019	presence	definition	Figure
aba	NA	apab	SA&W	apodeme attachment location of the abductor muscle	Fig. 5.6
ada	NA	apad	SA&W	apodeme attachment location of the adductor muscle	Fig. 5.6
clp	clp	cl	S&W	clypeus	Fig. 5.5
dfc	NA	dma (of head)	SA&W	dorsal mandibular articular surface of clypeus	Fig. 5.5
dmap	dmap	dma (of mandible)	S&W	dorsal articular process of mandible	Figs. 5.5, 5.6
lbp	lplb	lbrp	S&W	labral articular process	Fig. 5.5, 5.6
lbh	NA	NA	SA	labral hood of basal mandibular process insertion	Fig. 5.5
lbm	labrum	lbr	S&W	labrum	Fig. 5.5
lmap	lmap	abs (abductor swelling)	S&W	lateral articular process of mandible	Figs. 5.5, 5.6
md	mandible	mandible	S&W	mandible	Fig. 5.5
vmap	vmap	vma (of mandible)	S&W	ventral articular process of mandible	Figs. 5.5, 5.6
vpc	NA	NA	SA	ventral articular process of clypeus	Fig. 5.5
lmah	NA	absa (of head)	S&W	articular area of the abductor swelling	NA
vmah	NA	vma (of head)	S&W	ventral mandibular articulation	NA
bpm	bpm	NA	S	basal process of mandible	Figs. 5.5, 5.6

Strumigenys ayersthey species-group: Diagnosis of worker

- Bulla of femoral gland not easily visible but appears as a faint streak along the medial dorsal surface.
- Scape not dorsally flattened SI 110
- Apical fork of mandible with one well-developed intercalary tooth. Mandible with two conspicuous acute preapical teeth; both about the same length. Preapical dentition not crowded near apex. MI 65.
- Anterior clypeal margin usually shallowly convex.
- Leading edge of scape usually with all setae standing and directed toward apex of the scape. Scape slender, the subbasal curve extremely shallow; relatively long, SI 110
- Preocular carina in profile short, terminating before level of eye.
- Upper margin of the antennal scrobe not sharply defined behind level of eye.
- Ventrolateral margin of head continuous and not obviously concave in front of eye.
- Postbucal impression absent.
- Propodeum with minute teeth with a lower propodeal tooth-like lobe at base of declivity that is slightly less developed than the upper propodeal tooth, the two linked by a lamella.
- Ventral surface of petiole with spongiform tissue.
- Pilosity. Pronotal humeral setae flagellate and indistinguishable from neighboring background pilosity of similarly shaped simple standing to flagellate setae. Standing setae on head and mesosoma not differentiated from ground pilosity, abundant and simple to flagellate.
- Sculpture. Head and mesosoma predominantly or entirely free of sculpture and shining, usually with a smooth area on mesopleuron.
- Basal process of mandible arises dorsally with a locking angle estimated between 180 and 200°
- Dorsal articular process of mandibles bluntly pointed arising evenly from the dorsal surface without a distinct lateral lamella.
- Basal mandibular process arising in dorsal most plane of mandibles.
- Processes of clypeus present as a pair of small tooth like laminar ridges each positioned between the basal mandibular and dorsal articular processes of mandibles in closed position.

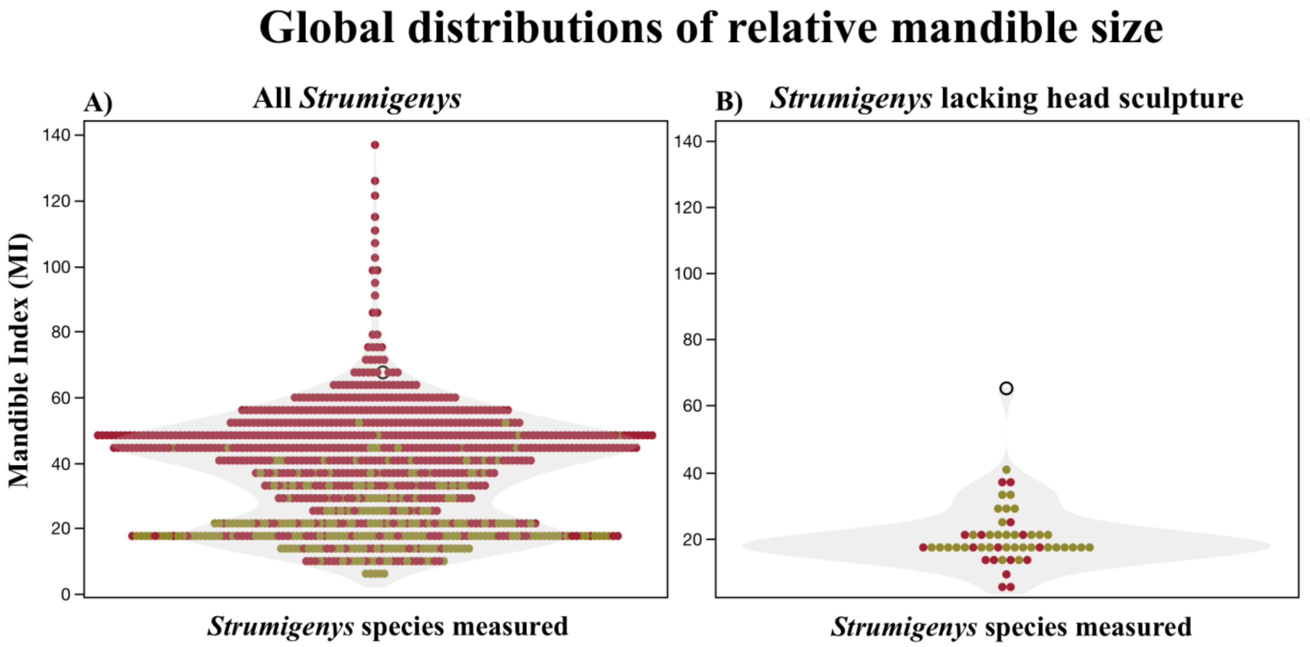

Fig. 5.4 Comparisons of MI among *Strumigenys* spp. **A** Accounts of 961 species and morphospecies globally representing all species-groups **B** MI of 52 *Strumigenys* identified as not smooth and shining cuticular surface of the head in full frontal view. Light yellow points are species without trap-jaws, dark red points are those with trap-jaws. *S. ayersthey* **sp. nov.** is marked with an open black circle and possesses trap-jaw mandible morphology.

Type material examined

Holotype worker: Ecuador: Esmeraldas Province, Reserva Río Canandé, 2 May 2018, Elevation 507m, 0.5263, -79.1682, Part of diversity study Hoenle & Blüthgen plot F1N31, hand-sampling on forest floor in primary forest, specimen broke in several parts, leg. P. Hoenle. Specimen identifier code (casent0875770), deposited at [MEPN] (Museo de Colecciones Biológicas Gustavo Orcés, Escuela Politécnica Nacional, Quito, Ecuador).

Holotype worker measurements (n = 1): HL = (0.609); HW = (0.480); ML = (left = 0.383, right = 0.411), the left mandible is slightly shorter than the right mandible; PW = (0.303); SL = (0.530); FL = (0.568); EL = (0.07); WL = (0.683); CI = (78.82); MI = (65.19); SI = (110.42).

Description

Strumigenys ayersthey **sp. nov.**

Mandibles with five teeth; two preapical teeth, apicodorsal and apicoventral teeth, and an intercalary tooth. The two preapical teeth are well developed and spiniform with nearly equal lengths and are longer than the width of the mandible where they arise (first preapical tooth = 0.056, second preapical tooth = 0.050). These teeth are located in the apical third of mandible and separated by a distance approximately equal their length (0.051). Apicodorsal (0.78) and apicoventral (0.73) teeth spiniform and of nearly equal length and with a well-developed intercalary tooth (0.38) arising just above the apicoventral tooth. Basal portion of mandible with four processes, three articular processes (dorsal, lateral, and ventral articular processes) and a latching process (basal mandibular process; Fig. 5.5). The dorsal articular process extends posteriorly from the basal dorsal surface without a distinct lateral ridge and terminating as a small bulbous point. The ventral articular process extends from the latero-posterior basal portion of the mandible as a dorsal to ventral cuticular ridge from and is continuously connected to the lateral articular process. The lateral articular process is dilated, with the medial portion extending laterally away from a line drawn vertically from the posterior-most positions of the dorsal and ventral processes. In full face view, the lateral articular process appears as a lateral bulge below the dorsal ridge of the dorsal articular process and shadows the ventral process (Fig. 5.6). The dorsal area between the basal process and dorsal articular process is indented and when mandibles are closed the process of the clypeus extends into this cavity (Fig 5.5).

Clypeus about 1.5 times as wide as long. Eye apparent (0.070) with 15-16 pigmented ommatidia. Scape sub-cylindrical with shallowly curved subbasal bend. Ventrolateral margin of head in front of eye not sharply defined, strongly indented or concave. Postbucal impression absent. Preocular carina and upper margin of the antennal scrobe in profile short, terminating anterior of eye.

Mesosoma shallowly and gradually impressed between pronotum and propodeum. Declivity of propodeum with two bluntly rounded triangular teeth that are just longer than the lamella connecting them (upper tooth = 0.062, lower tooth = 0.50, lamella at shallowest point between = 0.046).

In profile view, bulla of propodeal spiracle located at dorsal-most position of propodeum with propodeal spiracle opening facing postero-dorsally and forming lateral bulges that disrupt the outline in dorsal view. Spiracle opening much narrower than EL (.022). Petiolar node longer (0.127) than wide (0.113). Postpetiolar disc longer (0.185) than wide (0.153.). First gastral tergite with no basigastral costulae past the limbus.

Sculpture. Head, and rest of body smooth and shining and without obvious sculpture other than piligrous punctations where setae arise. Basigastral sculpture limited to costulae within the limbus and do not extend onto the surface of the first gastral tergite.

Pilosity. The background pilosity of all surfaces (mandibles, head, mesosoma, petiole, postpetiole, abdomen, and legs) are covered in evenly spaced simple to subflagellate erect to suberect setae that vary in length and are apically pointed. Head without differentiated apicoscrobal setae and leading edge of scape also without differentiated setae, pilosity of scape on all surfaces consists of short erect simple setae tending to point towards apex, none are recurved as to point to the base, and scape pilosity is similar to those elsewhere on head. Differentiated longer subflagellate to flagellate setae are limited to a pair straddling the midline on the anterior margin of clypeus that extend over mandibles when closed, a lateral pair on pronotal shoulders, a pair arising from ventral portion of propodeal spiracle, one to two pairs on the dorsum of petiole, and postpetiole. The majority of pilosity on gaster consist of slightly longer subflagellate setae than those on mesosoma.

Spongiform appendages. Length of lateral lobe of petiole weakly developed and visible only as a thin carinae along posterior third of node; expanded as a thin cuticular flange just behind the node in dorsal view. Subpetiolar flange developed as a thin cuticular narrow flange deepest posteriorly (0.046). Lateral lobes of postpetiole distinct and separated from the anterior flange of the post petiolar disc and do not connect posteriorly leaving a medial posterior gap along the posterior portion of disc (most easily seen in dorsal view). In profile, ventral lobe of postpetiole also weakly-developed (0.053 in depth) and much narrower than the exposed height of postpetiolar node (0.149).

Color. Yellow uniform light reddish brown.

Queen and male unknown.

Etymology

Many cultures have recognized a spectrum of genders between and beyond the binary of male and female. However, by following a rule exampled in the International Code of Nomenclature (ICZN 1999) for how to name species after individuals, one might conclude only binary gender assignments possible when assigning new species names derived from Latin. Dubois (2007) provides clarification to this rule stating that there is no need to amend or Latinize personal names – and therefore no need to assign gender. In contrast to the traditional naming practices that identify individuals as one of two distinct genders, we have chosen a non-Latinized portmanteau honoring the artist Jeremy Ayers and representing people that do not identify with conventional binary gender assignments – *Strumigenys ayersthey*. The 'they' recognizes non-binary gender identifiers in order to reflect recent evolution in English pronoun use - 'they, them, their' and address a more inclusive and expansive understanding of non-neutral gender identification. *Strumigenys ayersthey* **sp. nov.** is thus inclusively named in honor of Jeremy Ayers for the multitude of humans among the spectrum of gender who have been unrepresented under traditional naming practices. Jeremy was a multifaceted and beloved Athens-based (GA, USA) artist and activist whose humanity and achievements defied the limits of categorized classification. Jeremy brought an intellectual and playful, Pan-like curiosity to every aspect of his life. He was a writer, philosopher, painter, musician, activist, photographer, gardener, and exploder of boundaries who transformed the culture that surrounded him. His deep appreciation of the variety and minute details of the natural world astounded all who knew him. In the spirit of Jeremy, we also propose that the -they suffix can be used for singular honorific names of non-binary identifiers in compliance with the ICZN.

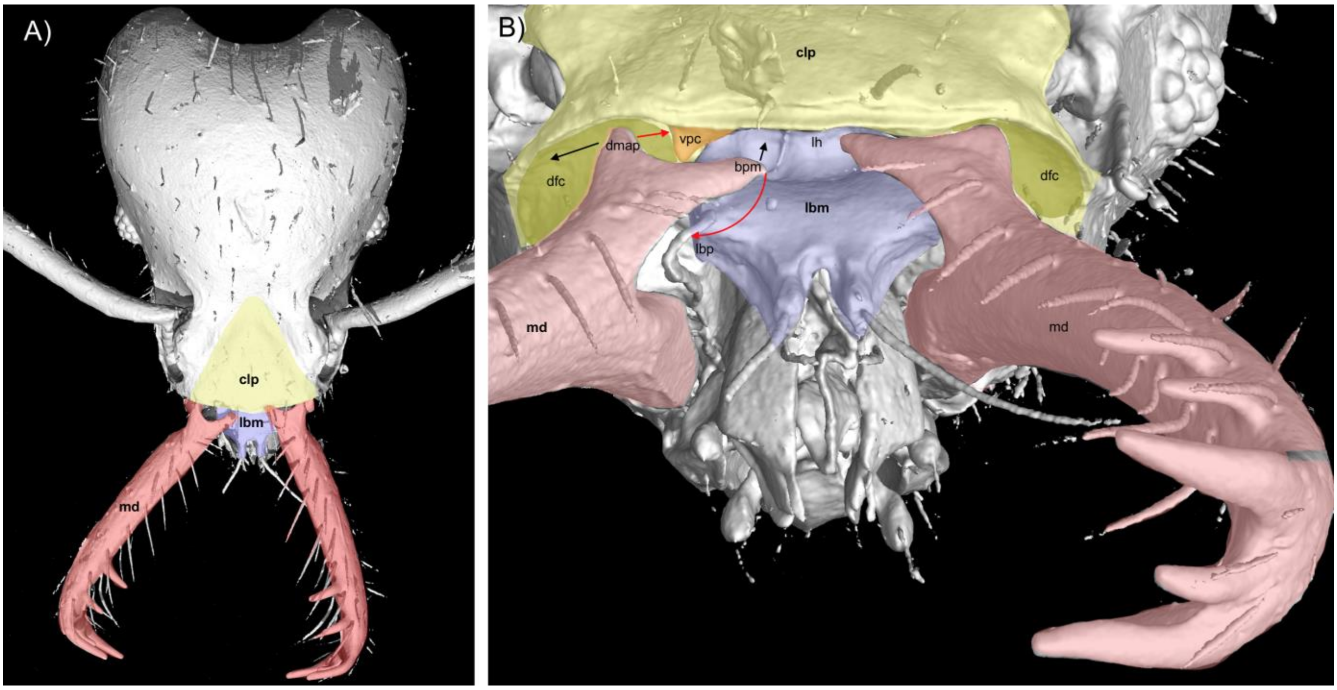

Fig. 5.5 Colorized µCT surface renders of the head of *S. ayersthey* **sp. nov. A** Head in full face view and **B** view from apex of mandibles looking towards base of mandibles. Black arrows represent closing motions and red arrows represent opening motions of mandibles. Abbreviations: **bpm** – basal process of mandible, **clp** – clypeus (yellow), **dfc** – dorsal articular surface of oral cavity (green), **dmap** – dorsal articular process of mandible, **lbp** – labral articular process, **lh** – labral hood, **lbm** – labrum (lavender), **md** – mandible (red), **vmap** – ventral articular process of mandible, **vpc** – ventral articular process of clypeus in orange. As the mandibles open towards latched position, the labrum (lbm) hinges upwards such that the basal mandibular process (bmp) latches into the complementary pocket of the labrum (lbp) and the dorsal articular process of the mandible (dmap) articulates freely within the dorsal articular surface of the oral cavity (dfc) around the ventral process of the clypeus (vpc). The

labral hood (lh) and the ventral processes of the clypeus (vpc) forms a pair of pockets housing the basal mandibular process (bmp) of each mandible.

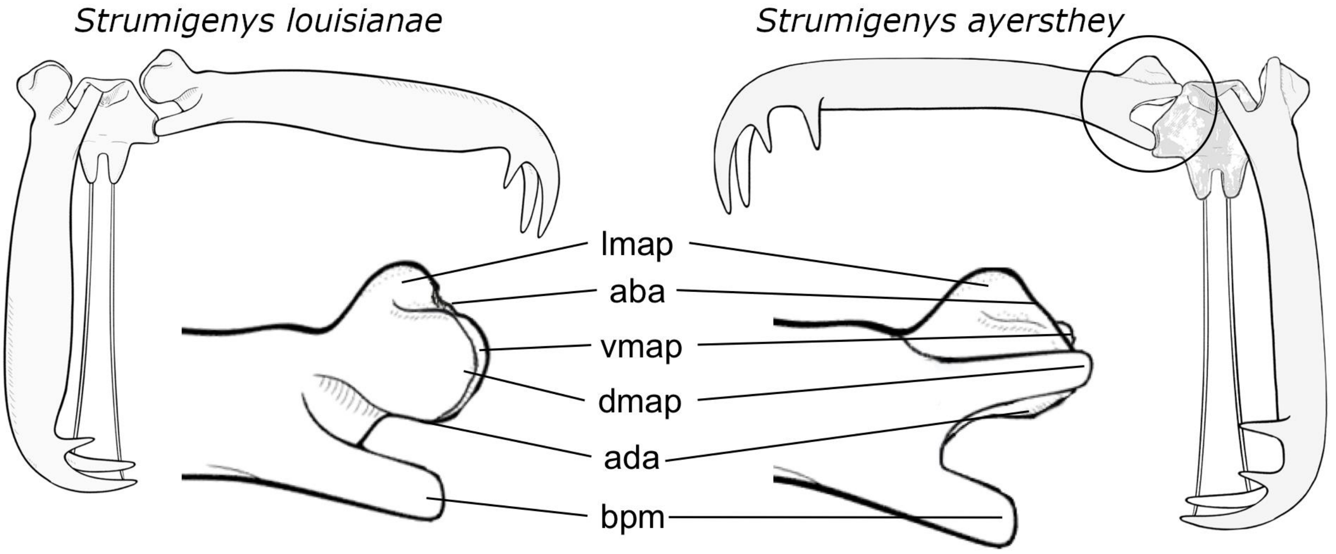

Fig. 5.6 Comparison of the mandibles between *S. louisianae* (left) and *S. ayersthey* **sp. nov.** (right). Abbreviations: **aba** – apodeme attachment location of the abductor muscle, **ada** – apodeme attachment location of the adductor muscle, **bpm** – basal process of mandible, **dmap** – dorsal articular process of mandible, **lmap** – lateral articular process of mandible, **vmap** – ventral articular process of mandible. Illustrations adapted from Booher et al. (2021).

5.5 DISCUSSION

As morphological convergence is rampant among *Strumigenys* morphotypes (short or long mandible species) it is difficult to determine by morphology alone how species are related (Ward et al. 2014). However, within biogeographic regions, species-groups of morphologically similar *Strumigenys* species are often phylogenetically most closely related (Booher 2021). As such, morphological species-groups are relevant and useful for identification as well as evolutionary research (Booher et al. 2021). In the construction of *Strumigenys* morphological species-groups, differences in the position, presence, and shape of pilosity are of major importance. For example, the direction and shape of hairs along the clypeal margin and along the leading edge of the scape separates several Nearctic species-groups e.g., *pulchella, ornata,* and *talpa* groups (Bolton 2000). Similarly, slight differences in sculpturing help to identify similar species, but major differences in sculpture (i.e., having sculpture present across most cuticular surfaces compared to no sculpture) do not occur among species within any *Strumigenys* species-group. We further justify the formation of a new single species-group with differences in basal mandibular morphology from most morphologically similar *mandibularis*-group members.

The general mandibular morphology of LaMSA *Strumigenys* has been well described with the base of the mandible having three articular processes; the dorsal and ventral articulatory processes are responsible for holding mandibles in place during movement and a third lateral process is attached via apodemes to opening muscles (Fig. 5.6) (Silva and Feitosa 2019), alternatively termed the abductor swelling of the mandible or 'atala' (Richter et al. 2019, Richter et al. 2020). Although articular morphology of mandibles has been described in LaMSA *Strumigenys* and more generally in the more typical ant genera *Wasmannia* (Richter et al. 2019), *Formica*, and *Brachyponera* (Richter et al. 2020), there has not yet been a comparison in morphological features between them and there are a few important differences associated with the derived morphology of trap-jaws in *Strumigenys* (Table 5.1). Most morphological features in *S. ayersthey* have homologous features shared with other ants, however there are a few features that are not shared or have not been previously reported and are worth discussing. A most apparent difference is the dorsal articulation of the mandible and head. In what is described in *Wasmannia* and other ants, mandibles are tightly connected to the head capsule with primary and secondary joints, with the "secondary joint (dmah-dmap) formed by a ventrolateral longitudinal smooth elongation of the clypeus… which articulates with a smooth dorsolateral area on the mandibular base" (Richter 2019). In *S. ayersthey* **sp. nov.**, this secondary joint is not connected to the head and the dmap moves freely within the dfc. We hypothesize that in contrast to typical ants, the clypeal articular process present in *S. ayersthey* helps to stabilize dorsal mandible articular movement. A second morphological feature important to note, is the derived labral hood (lh) present in *S. ayersthey.* This dorsal expansion of the basal area of the labrum is highly sclerotized, hypothesized to reduce damage from self-piercing and over-rotation, and is common to trap-jaw *Strumigenys* (Booher et al. 2021). We provide a table of mandible terminology (Table 5.1), however a more extensive comparative study across ants is needed to truly understand homology of mandible morphology.

Less prominent morphological features differ between trap-jaw *Strumigenys* and mandible dentition have been used as focal distinguishing characters between species groups. *Strumigenys ayersthey,* although most similar to members of the *mandibularis*-group, the dorsal articular process of the mandible differs in shape with *mandibularis*-group species. In members of *mandibularis* species-group the dorsal articular process arises from a laterally extending dorsal surface forming a shelf like lamellate ridge at the basal portion of the mandible. In dorsal view, this lamellate process overhangs the lateral articular process obscuring most of it from view. In *S. ayersthey* **sp. nov.**, the lateral corner of the dorsal articular surface is gradually rounded and does not form a lamellate margin. Additionally, in the only species with a detached mandible that could be visually inspected by us (*S. planeti*) the posteriormost articular surface of the dorsal process contained three small bulbous points connected by indented lamellae, wherein *S. ayersthey* **sp. nov.** there is a single bulbous articular point. Therefore, *S. ayersthey* **sp. nov.** is an exceptional morphological outlier and a rare addition to the hyperdiverse genus *Strumigenys*. It does not fit cleanly into any of Bolton's species-groups, nor can existing species-group definitions envelope this species with minor changes — hence, we placed it as the only member of a new species-group. We find morphological articular structure of mandibles are important taxonomic characters and should be investigated in future taxonomic works in this genus.

Our species description includes a µCT 3D render of the holotype worker, and its surface model is freely available for download (Supplement 1). This offers any reader virtual morphological details of the new species and the ability to view morphological features at all angles. 3D imaging techniques, and in particular micro-computed X-ray tomography (µCT), are being frequently used in taxonomy and functional morphology, particular in ants (Faulwetter et al. 2013, Akkari et al. 2015, Garcia et al. 2017, Sarnat et al. 2017, Staab et al. 2018). For *Strumigenys*, they already lead to detailed morphological analysis, and µCT scans of Fijian *Strumigenys* have even been suggested as a tool for teaching with augmented reality (Sarnat et al. 2019). In our case, the µCT scan facilitated additional descriptions of mandibular morphology and function of *S. ayersthey* **sp. nov.**.

The discovery of *Strumigenys ayersthey* **sp. nov.** advanced our understanding of the global morphology of this genus: It's unique combination of almost no surface sculpturing and long trap-jaw mandibles make it stand out among nearly a thousand other *Strumigenys* species. Because of *S. ayersthey* **sp. nov.** unusual morphology, information about its general biology could prove to be valuable. However, subsequent attempts in obtaining more specimens at the previous location with Winkler traps in 2019 have failed, and a large ecological ant study in the Canandé reserve did not reveal any more specimens. *Strumigenys ayersthey* **sp. nov.** can therefore be considered as rare. The discovery of such an unusual rare ant highlights the importance of scientific exploration and conservation of the Chocó region in Ecuador, which is at the same time one of the most biodiverse and threatened areas on our planet (Dinerstein et al. 1995, Olson and Dinerstein 1998, Myers et al. 2000).

5.6 ACKNOWLEDGEMENTS

We thank the Fundacíon Jocotoco and the associated Tesoro Escondido for logistic support and their permission to do research on their forest properties. First, we like to thank Adriana Argoti and Adrian Brückner for help during field collection. We are grateful for the local support from the park staff in the Canandé and Tesoro Escondido reserve, that made the field collection easier and made two great field stays possible: Bryan Amayo, Alcides Zombrano, Roberto de la Cruz, Jorge Zambrano, Amado de la Cruz, Yadria Giler, Patricio Encarnación and Vanessa Moreira.

We thank musician and artist Michael Stipe for contributing to the etymology writing in honor of a hero to many and dear friend to those that knew him, Jeremy Ayers. We further thank the support from the LGBTQIA+ and gender dynamic community, for which we hope this species furthers pride. Additional thanks to Adrienne Truscott for input and suggestions.

Further, we like to thank Sebastian Schmelzle for providing and editing the µCT scans. We thank Roberto Keller for comments on the functional aspects of the trap-jaw, and James Trager for his Latin expertise. We thank Christoph von Beeren for the use of his photostacking equipment. David Donoso, Martin Schäfer and Nico Blüthgen provided supervision and logistic support for the studies in Ecuador, and without them this discovery would not have been possible.

The SRµCT data of the single *Strumigenys ayersthey* **sp. nov.** specimen was acquired within the project NOVA (**N**etwork for **O**nline **V**isualization and synergistic **A**nalysis of tomographic data) funded by the German Federal Ministry of Education and Research (05K16VKB) within the call for proposals "Erforschung kondensierter Materie an Großgeräten" 2016-2019. We thank the proposers of the NOVA project Michael Heethoff (Technische Universität Darmstadt), Vincent Heuveline (Heidelberg University), and Jürgen Becker (Karlsruhe Institute of Technology). We thank the associated partners of the NOVA project Felix Beckmann from the Helmholtz-Zentrum Geesthacht, and Andreas Kopmann and Wolfgang Mexner from the Karlsruhe Institute of Technology. We acknowledge DESY (Hamburg, Germany), a member of the Helmholtz Association HGF, for the provision of experimental facilities. Parts of this research were carried out at PETRA III and we would like to thank Jörg Hammel and Fabian Wilde for assistance in using the experimental station at P05 and reconstruction of the data.

Finally, we are grateful for the suggestions from two anonymous reviewers and Brian L. Fisher, which substantially improved the manuscript.

We acknowledge support by the Open Access Publishing Fund of Technische Universität Darmstadt. PH was supported by a scholarship from the German National Academic Foundation.

5.7 REFERENCES

Akkari N., H. Enghoff, and B. D. Metscher. 2015. A new dimension in documenting new species: high-detail imaging for Myriapod taxonomy and first 3D cybertype of a new millipede species (Diplopoda, Julida, Julidae). PLOS ONE 10:e9135243.

AntWeb. Version 8.45.1. California Academy of Science, online at https://www.antweb.org. [Accessed on 21 November 2020]

Booher, D. B., J. C. Gibson, C. Liu, J. T. L. Longino, B. L. Fisher, M. Janda, N. Narula, E. Toulkeridou, A. S. Mikheyev, A. V. Suarez, E. P. Economo. 2021. Functional innovation promotes diversification of form in the evolution of an ultrafast trap-jaw mechanism in ants. PLOS Biology. 19(3):e3001031.

Booher, D. B., M. M. Prebus, and D. Lubertazzi. 2019. A taxonomic revision of the *Strumigenys nitens* and *simulans* groups (Hymenoptera: Formicidae), two Caribbean radiations of leaf litter ants. Zootaxa 4656:335–358.

Bolton, B. 2000. The ant tribe Dacetini. Memoirs of the American Entomological Institute 65: 1–1028.

Bolton, B. 2020. An online catalog of the ants of the world. http://antcat.org [Accessed on 16 July 2020]

Brown, W. L. and E. O. Wilson. 1959. The evolution of the dacetine ants. The Quarterly Review Biology 34:278–294.

Dinerstein, E. A., D. M. Olsen, D. J. Graham, A. L. Webster, S. A. Primm, M. P. Bookbinder, and G. Ledec. 1995. Conservation assessment of the terrestrial ecoregions of Latin America and the Caribbean. Washington, DC: The World Bank.

Dong, M. S., and S. K. Kim. 2020. A taxonomic study on the genus *Strumigenys* Smith, 1860 (Hymenoptera: Formicidae) from Korea with a description of new species. Asian Myrmecology 12:e012001.

Donoso, D. A., F. Salazar, F. Maza, R. E. Cárdenas, and O. Dangles. 2009. Diversity and distribution of type specimens deposited in the Invertebrate section of the Museum of Zoology QCAZ, Quito, Ecuador. Annales de la Société Entomologique de France 45:437–454.

Donoso, D. A., and G. Ramón. 2009. Composition of a high diversity leaf litter ant community (Hymenoptera: Formicidae) from an Ecuadorian pre-montane rainforest. Annales de la Société Entomologique de France 45:487–499.

Donoso, D. A. 2017. Tropical ant communities are in long-term equilibrium. Ecological Indicators 83:515–523.

Dubois, A. 2007. Genitives of species and subspecies nomina derived from personal names should not be emended. Zootaxa 1550:49–68.

Faulwetter, S., A. Vasileiadou, M. Kouratoras, T. Dailianis, and C. Arvanitidis. 2013. Micro-computed tomography: Introducing new dimensions to taxonomy. ZooKeys 264:1–45.

Garcia, F. H., G. Fischer, C. Liu, T. L. Audisio, G. D. Alpert, B. L. Fisher, and E. P. Economo. 2017. X-Ray microtomography for ant taxonomy: An exploration and case study with two new

Terataner (Hymenoptera, Formicidae, Myrmicinae) species from Madagascar. PLOS ONE 12:e0172641.

Guénard, B., M. Weiser, K. Gomez, N. Narula, and E. P. Economo. 2017. The Global Ant Biodiversity Informatics (GABI) database: a synthesis of ant species geographic distributions. Myrmecological News 24:83–89.

Gray, K. W., S. P. Cover, R. A. Johnson, and C. Rabeling. 2018. The dacetine ant *Strumigenys arizonica*, an apparent obligate commensal of the fungus-growing ant *Trachymyrmex arizonensis* in southwestern North America. Insectes Sociaux 65:401–410.

Gronenberg, W., J. Tauz, and B. Hölldobler. 1993. Fast trap jaws and giant neurons in the ant *Odontomachus*. Science 262:561–563.

Gronenberg, W. 1996. The trap-jaw mechanism in the dacetine ants *Daceton armigerum* and *Strumigenys* sp. Journal of Experimental Biology 199:2021–2033.

Hoenle, P. O., J. E. Lattke, D. A. Donoso, C. von Beeren, M. Heethoff, S. Schmelzle, A. Argoti, L. Camacho, B. Ströbel, N. Blüthgen. 2020. *Odontomachus davidsoni* sp. nov (Hymenoptera: Formicidae), a new conspicuous trap-jaw ant from Ecuador. Zookeys 948:75–105.

ICZN [International Commission on Zoological Nomenclature] 1999. International code of zoological nomenclature. Fourth Edition. London: The International Trust for Zoological Nomenclature.

Ilton, M., M. S. Bhamla, X. Ma, S. M. Cox, L. L. Fitchett, Y. Kim, J. Koh, D. Krishnamurthy, Y.-C. Kuo, F. Z. Temel, A. J. Crosby, M. Prakash, G. P. Sutton, R. J. Wood, E. Azizi, S. Bergbreiter, and S. N. Patek. 2018. The principles of cascading power limits in small, fast biological and engineered systems. Science 360:eaao1082.

International Code of Nomenclature. 2020., 5th edition, Arcticle 31.1, https://www.iczn.org/the-code/the-international-code-of-zoological-nomenclature/the-code-online/ [Accessed on 20 November 2020]

Larabee, F. J., A. A. Smith, and A. V. Suarez. 2018. Snap-jaw morphology is specialized for high-speed power amplification in the Dracula ant, *Mystrium camillae*. Royal Society Open Science:181447.

Larabee, F. J., and A. V. Suarez (2014) The evolution and functional morphology of trap-jaw ants (Hymenoptera: Formicidae). Myrmecological News 20:25–36.

Lattke, J. E., T. S. R. Da Silva, and T. Delsinne. 2018. Taxonomy and natural history of *Strumigenys thaxteri* Wheeler and *Strumigenys reticeps* (Kempf) (Hymenoptera: Formicidae). Zootaxa 4438:137–147.

Lattke, J. E. and Aguirre, N. 2015. Two new *Strumigenys* F. Smith (Hymenoptera: Formicidae: Myrmicinae) from montane forests of Ecuador. Sociobiology 62:175–180.

Longo, S. J., S. M. Cox, E. Azizi, M. Ilton M., J. P. Olberding, R. St. Pierre, and S. N. Patek. 2019. Beyond power amplification: latch-mediated spring actuation is an emerging framework for the study of diverse elastic systems. Journal of Experimental Biology 222:jeb197889

Masuko, K. 1984. Studies on the Predatory Biology of Oriental Dacetine Ants (Hymenoptera, Formicidae) .1. Some Japanese Species of *Strumigenys*, *Pentastruma*, and *Epitritus*, and a

Malaysian *Labidogenys*, with Special Reference to Hunting Tactics in Short-Mandibulate Forms. Insectes Sociaux 31:429–451.

Masuko, K. 2009. Studies on the predatory biology of Oriental dacetine ants (Hymenoptera: Formicidae) II. Novel prey specialization in *Pyramica benten*. Journal of Natural History 43:825–841.

Myers, N., R. A. Mittermeier, C. G. Mittermeier, et al. 2000. Biodiversity hotspots for conservation priorities. Nature 403:853–858.

Olson, D. M., and E. Dinerstein. 1998. The Global 200: a representation approach to conserving the Earth's most biologically valuable ecoregions. Conservation Biology 12:502–15.

Richter, A., F. H. Garcia, R. A. Keller, J. Billen, E. P. Economo, and R. G. Beutel. 2020. Comparative analysis of worker head anatomy of *Formica* and *Brachyponera* (Hymenoptera: Formicidae). Arthropod Systematics & Phylogeny 78:133–170.

Richter, A., R. A. Keller, F. B. Rosumek, E. P. Economo, F. H. Garcia, and R. G. Beutel. 2019. The cephalic anatomy of workers of the ant species *Wasmannia affinis* (Formicidae, Hymenoptera, Insecta) and its evolutionary implications. Arthropod Structure & Development 49:26–49.

Salazar, F., and D. A. Donoso. 2013. New ant (Hymenoptera: Formicidae) records for Ecuador deposited at the Carl Rettenmeyer ant collection in the QCAZ Museum. Boletín Técnico 11, Serie Zoológica 8-9:151–177.

Salazar, F., F. Reyes-Bueno, D. Sanmartin, and D. A. Donoso. 2015. Mapping continental Ecuadorian ant species. Sociobiology 62:132–162.

Sarnat, E. M., F. Hita Garcia, K. Dudley, C. Liu, G. Fischer, and E. P. Economo. 2019. Ready species one: exploring the use of augmented reality to enhance systematic biology with a revision of Fijian *Strumigenys* (Hymenoptera: Formicidae). Insect Systematics and Diversity 3:6:1–43.

Sarnat, E. M., N. R. Friedman, G. Fischer, B. Lecroq-Bennet, and E. P. Economo. 2017. Rise of the spiny ants: diversification, ecology and function of extreme traits in the hyperdiverse genus *Pheidole* (Hymenoptera: Formicidae). Biological of the Linnaean Society 122:514–538.

Schindelin, J., I. Arganda-Carreras, E. Frise, V. Kaynig, M. Longair, T. Pietzsch, S. Preibisch, C. Rueden, S. Saalfeld, B. Schmid, J.-Y. Tinevez, D. J. White, V. Hartenstein, K. Eliceiri, P. Tomancak, and A. Cardona. 2012. Fiji: an open-source platform for biological-image analysis. Nature Methods 9:676–682.

Shorthouse, D. P. 2010. SimpleMappr, an online tool to produce publication-quality point maps. https://www.simplemappr.net. Accessed July 03, 2020.

Sierra, R., F. Campos, and J. Chamberlin. 2002. Diversity conservation priorities: ecosystem risk and representativeness in continental Ecuador. Landscape and Urban Planning 59:95–110.

Silva, T. S. R. and R. M. Feitosa. 2019. Using controlled vocabularies in anatomical vocabulary: a case study with *Strumigenys*. Arthropod Structure & Development 52:100877.

Staab, M., F. H. Garcia, C. Liu, Z. H. Xu, and E. P. Economo. 2018. Systematics of the ant genus *Proceratium* Roger (Hymenoptera, Formicidae, Proceratiinae) in China – with descriptions of three new species based on micro-CT enhanced next-generation-morphology. ZooKeys 770:137–192.

Ward, P. S., S. G. Brady, B. L. Fisher, and T. R. Schultz. 2014. The evolution of myrmicine ants: phylogeny and biogeography of a hyperdiverse ant clade (Hymenoptera: Formicidae). Systematic Entomology 40:61–81.

Wesson, L. G. and R. G. Wesson. 1939. Notes on *Strumigenys* from southern Ohio, with descriptions of six new species. Psyche 46:91–112.

Wilson, E. O. 1953. The Ecology of Some North American Dacetine Ants. Annals of the Entomological Society of America 46:479–495.

6 GENERAL DISCUSSION

Considering the severe consequences of the ongoing biodiversity crisis (United Nations Environment Programme 2021), it is of major importance to better understand the recovery potential of tropical forests. I addressed this global problem in my present PhD thesis by studying the recovery potential and dynamics of a disturbed tropical forest in Ecuador – located in the biodiversity hotspot of the Chocó-Magdalena-Tumbes region. As the remaining old-growth forests are consistently shrinking, understanding the recovery potential of agricultural areas is of particular importance for conservation management. Further, this setting provided an ideal opportunity to study faunistic re-assembly processes and advance ecological knowledge. Hence, one of the main questions of my thesis was whether former agricultural areas converge towards old-growth forests, and thus sufficiently preserve biodiversity and sustain ecosystem function within a reasonable timeframe.

As presented in my first study, a fast recovery of the communities was indeed the case, at least from the viewpoint of the ants in the specific study area. I collected clear evidence for a rapid recovery of ant communities in terms of species composition and functional trait composition. Levels of old-growth forests were reached within less than four decades. Given the ants' key role in the ecosystem, their quick recovery likely indicates similar potential of other arthropods, which makes up the largest fraction of biodiversity in tropical areas (Stork 2018, Andersen 2019). Natural forest regeneration in the Chocó seems to have good chances to succeed, thus contributing to sustain high biodiversity, including the long-term survival of many endemic species. My thesis focused on ants, however, and such a fast recovery time does not necessarily apply to the forest as whole. For instance, plant community recovery takes considerably longer, as the old-growth forests contain many hundred years old trees with long generation times (Chazdon 2003, Curran et al. 2014, Meli et al. 2017). The conductance of many more exhaustive studies on long-term recovery dynamics of other animals and plants will be challenging, but necessary.

A key question that remains is how applicable my findings are for the Chocó region at large and for tropical rainforests in general. There are several hypothesis explaining why the study area shows a relatively high level of resistance and resilience: Land use was rather small both in scale and intensity, and it had occurred over relatively short time periods. Therefore, soil impoverishment, which can delay recovery (Pascarella et al. 2000, Holl and Zahawi 2014), was probably not pronounced. Resilience was likely boosted by the close distance to regenerating and old-growth forests, promoting rapid dispersal of forest animals and plants into early recovery sites, as proximity to old-growth forests generally aids forest recovery (Chazdon et al. 2009, Dent and Wright 2009, Wijdeven and Kuzee 2017). Previous studies demonstrated that the recovery potential is lower in areas where land-use is much older and includes large-scale agricultural practices (Crouzeilles et al. 2016). In the Chocó, more intensive agricultural practices such as oil palm plantations have a strong foothold with virtually no remaing forest area just on the Southern side of the Canandé reserve, most likely making these areas less suitable for natural forest recovery.

Regarding the influence of former land-use, my thesis supports previous findings that land-use legacies play an important role in determining the recovery potential (Crouzeilles et al. 2016, Meli et al. 2017). Former cacao plantations had a slight recovery advantage over former pastures, which might be explained by the fact that cacao plantations already offered a heterogeneous litter environment and a "canopy". Noteworthy, there is potential to enhance recovery potential of agricultural land use, for instance, by integrating cacao trees in forest patches instead of planting cacao monocultures – a cultivation method known as agroforestry (Delabie et al. 2007). For forest recovery projects, knowledge on these aspects need to be considered when choosing which areas have the best recovery potentials and should thus be primarily protected.

In my second chapter, I outlined the broad recovery patterns of an ant fauna. However, not every forest stratum necessarily underlies the same recovery processes, and my second study gave a detailed comparison of the re-assembly process of different forest strata (ground, leaf-litter, tree trunk). The ant communities were highly stratified in their species composition and their functional traits throughout the chronosequence. By assessing trait structure and trait diversity on stratum level, I was able to study the effects of potential environmental filters, which selects the ant communities via their functional traits (de Bello et al. 2021). Most of the trait recovery trajectories were determined by a statistical interaction of both the recovery and stratification. In other words, each stratum had its own distinct filter processes, and a given functional trait (e.g., eye size) did not necessarily follow the same recovery pattern in each stratum. Intriguingly, strata became more similar to each other in their functional structure with regeneration time, which means that stratification filters became either weaker or more similar over time. It is difficult to infer what these filters fundamentally consist of, but I briefly outlined some ideas in the discussion of this study. The most parsimonious explanation to me is that microclimatic filters play the strongest role in shaping the communities, because early recovery stages and agricultural areas have a warmer, drier and more fluctuating microclimate due to the lack of a buffering canopy cover present in old-growth forests (del Pliego et al. 2016, De Frenne et al. 2019). According to this hypothesis, all strata developed a more similar microclimate with increasing recovery age, selecting for functionally similar ant communities. Future investigation will reveal whether this pattern constitutes a general pattern of forest recovery, or whether it is a more idiosyncratic pattern of ant/arthropod communities. Ecologists only began to study and understand how stratification processes drive forest recovery (Klimes et al. 2012, Whitworth et al. 2016, 2019), and my second study outlined some first steps into this direction. Our research shows that acknowledging the complex three-dimensional structure of the forest can be helpful in uncovering underlying recovery processes.

Like in most large-scale ecological studies on arthropods of tropical rainforests, our collection efforts resulted in a long list of species, and provided several notable species records for the region. For instance, the large and arboreal ant species *Platythyrea prizo* was, for the first time, recorded for Ecuador (Fig. 6.1, Guenard et al. 2017). The Canandé is home to a plethora of unique, poorly known ant species with diverse ecologies and behaviors, creating a lot of potential for future investigations (some examples are given in Fig. 6.1). Many specimens of the collection remain to be identified to the species level because their taxonomy is not well resolved and existing species keys are incomplete. For instance, the species rich genera *Solenopsis*, *Hypoponera* and *Pheidole* have only received rudimentary work in this part of the Neotropics. This lack of a taxonomic framework hinders identification, and it demonstrates that we still know very little about the number of ant species, including the number of endemics and threatened species, in many tropical forests. My established ant collection will hopefully provide a valuable resource for future research in the Chocó. A promising approach to facilitate species determination is DNA barcoding, which has proven to be a successful tool in untangling difficult ant groups in Ecuador and the Atlantic rainforest (Delsinne et al. 2012, Hanisch et al. 2017).

Taxonomy is the backbone of biology by providing the basic vocabulary for all organismal research (Wilson 2017). Studies in scientific disciplines such as community ecology and biodiversity research are thriving - disciplines that rely greatly on a taxonomic framework for species identifications. I thus consider the two taxonomic studies in this thesis valuable resources for future work as they contribute to the knowledge of the endemic Chocó ant fauna. In both taxonomic studies, we used state-of-the art 3D visualization of specimens, which has several important benefits. The virtual 3D models have the advantage of conferring spatial information that is otherwise not available through the standard stacking pictures. Since the scans are easily and freely available, they might considerably reduce the need of taxonomists to access museum specimens in person. This will facilitate the exchange of morphological information as well as taxonomy in regions with limited access to funding. A digital twin of the species can also not be destroyed, as, for instance, so many important biological specimens have been during the destructive fire of the National museum of Brazil in 2018 (Escobar 2018). For *Odontomachus davidsoni*, we used the DISC-3D scanner, a newly developed 3D insect scanner at the TU Darmstadt, which works via photogrammetry (Ströbel et al. 2018). This was the first time 3D models of this new scanner were used in a species description. The DISC-3D models do not provide internal structures like micro-CT scans, but it provides real colors from photos and is considerably cheaper and easier to use, and I believe it has promising taxonomic applications for future work.

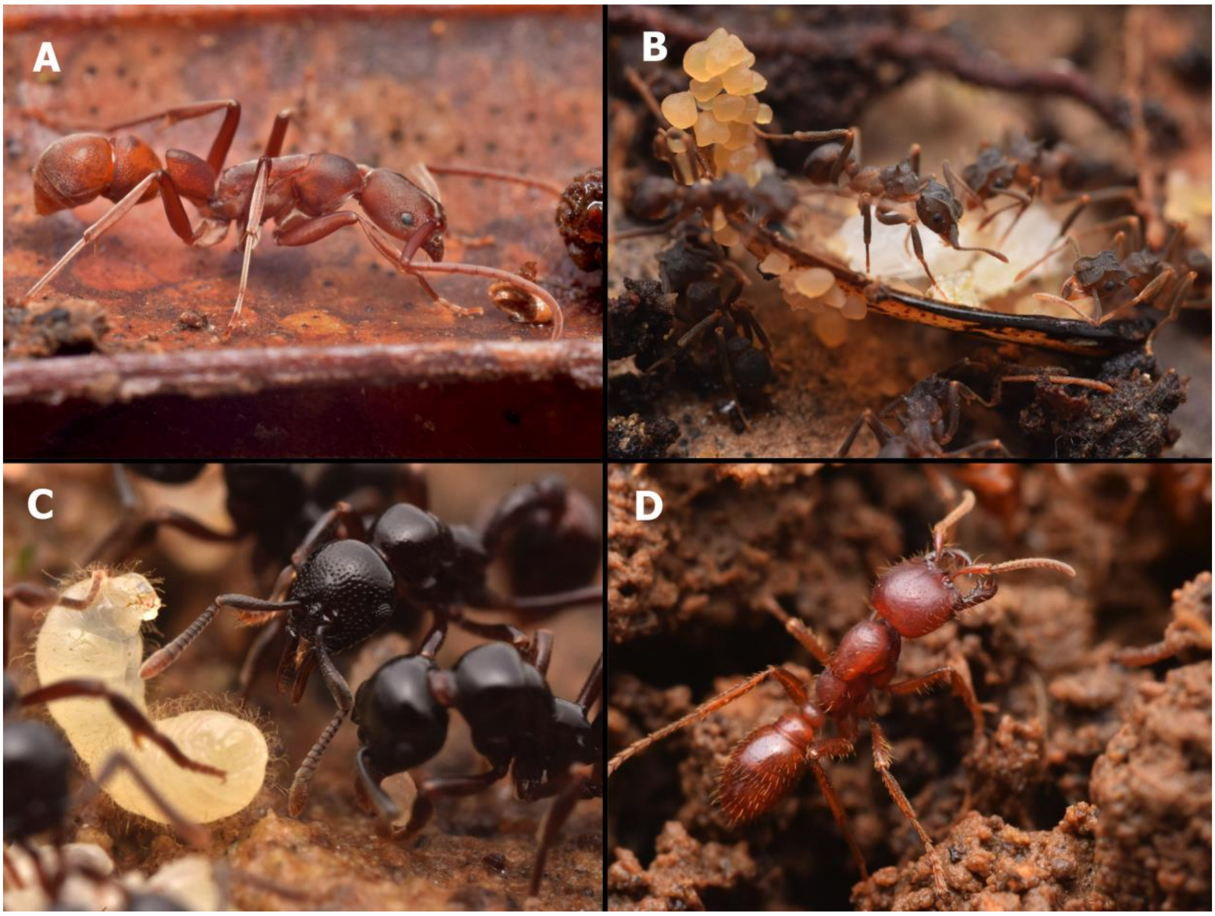

Fig. 6.1 Notable ant species observed in the Reserva Canandé, Ecuador. A) *Platythyrea prizo*, a rare arboreal ant that was for the first time collected in Ecuador. B) *Cyphomyrmex cornutus* nest. This species lives in a mutualistic symbiosis with a yeast fungus (white pebbles on the picture). C) *Lenomyrmex foveolatus*. These cryptic ant species built their nests near streams, and have only very rarely been collected. I uncovered several nests during my studies. Nothing is known about their biology. D) *Cheliomyrmex andicola* is an unusual species of army ant. The falcate mandibles are used to cut carrion and earthworms. Colonies are hard to find, as they mostly have a subterranean lifestyle.

The description of the two new species had implications beyond given these species a name. Both are easily recognizable, and do not resemble any previously known species. The new *Odontomachus davidsoni* is one of the largest species of its genus in South America, and, compared to its relatives, stands out through its red coloration. If such an obvious ant has not been noticed for so long the question arises of how many more species are still awaiting to be discovered. The Chocó is indeed a hotspot for unusual *Odontomachus* trap-jaw ants. For instance, it is also the home to the largest *Odontomachus* species, *Odontomachus mormo* (Fernández et al. 2019). The knowledge of the life history of this and other *Odontomachus* species is very sparse. I was able to also provide valuable information of *O. davidsoni*'s nesting habits and behavior, helping to better understand the biology of these ants.

Without protecting the Chocó rainforest, such unique ant species might go extinct so that future naturalists will no longer have the chance to discover and observe them. While *O. davidsoni* is locally not rare, it has so far only been detected in the Reserva Canandé, Tesoro Escondido and the Reserva Cotacachi-Cayapas, and the surrounding region is severely under threat by deforestation. I my opinion, *O. davidsoni* could even have potential as a flagship species for conservation efforts, because of its charming trap-jaws and exceptional large size for an ant. Flagship species are used to raise public awareness and interest to fund conservation areas, though the approach of flagship species has been debated (Walpole and Leader-Williams 2002, Seddon and Leech 2008). As long as conservation NGOs are transparent in how they distribute donations and protect threatened areas as whole, I see no problem for the use of flagship species (e.g., McGowan et al. 2020). My colleagues and I got the great opportunity by the NGO Jocotoco to auction the name of the undescribed ant for conservation purposes, and it resulted in a quite large bid (ca. 10'000 US-$), which subsequently drew attention in the Ecuadorian media. While certainly not every species will get the chance to be used for conservation fund raising, the discovery of *O. davidsoni* is an ideal example for an unusual way in which taxonomy can contribute to conservation.

The second species I described is *Strumigenys ayersthey*, an exceptional outlier within the hyperdiverse genus *Strumigenys*. The life history and behavior of this species remains entirely unknown and my attempts at finding more specimens failed, even though I went to its exact collection site several times. While over a hundred specimens belonging to the genus *Strumigenys* were collected during the collection effort for all my studies, only one belonged to the new species. Therefore, *S. ayersthey* is either a very rare species or it is not well collectable via the conventional collection methods (e.g., entirely subterranean species). Its mandibular morphology is, however, exceptional and therefore of interest for evolutionary considerations. We included a detailed functional description of its trap-jaw mechanisms by using modern 3D visualization. The 3D scan of *Strumigenys ayersthey* was assembled via micro-CT, a technique that has successfully been applied in ant morphology before (e.g., Sarnat et al. 2016, Hita Garcia et al. 2017) and resulted in both surface scans and insights into inner structures. The use of the 3D scans was pivotal in accurately describing the complex clypeal-mandibular structures of this small ant. The application of micro-CT for taxonomy and for functional morphology is promising and already lead to important insights into the functional evolution of *Strumigenys* and other ants (Sarnat et al. 2016, Booher et al. 2021).

However, the functional morphology of most trap-jaw ants is unknown so that our study provides a valuable resource for future comparative approaches. Such studies in *Strumigenys* will be necessary to elucidate the evolutionary and functional implications of, for instance, the clypeal tooth detected in *S. ayersthey*. It would be important to observe its mandible closure *in vivo*, as the functional mandible closure hypothesis outlined here is only based on comparative morphology, which certainly has its limitations. *S. ayersthey* is a rather small species and it is probably neither interesting to the general public as flagship species nor important for ecosystem functioning, given its extreme rarity. However, its odd morphology sparks interest for functional, providing a more complete picture on the global morphospace of *Strumigenys*.

To summarize, the present thesis highlights the forest recovery potential of an ant community in a landscape of former agricultural areas and old-growth forest patches. I demonstrated that the ant fauna of disturbed areas recovered relatively quickly, so that recovering agricultural sites can provide a suitable habitat for many endangered species. Ant communities were highly stratified, and their reassembly process was stratum-specific. Both the ecological and the taxonomic approaches synergistically contributed to a better understanding of the ant biodiversity in the Chocó, and the process of community and morphologists functional reassembly. A plethora of fascinating ant species remains to be discovered and described. Ecuador has potential to remain an inspiration for many coming generations of explorers and scientists, but only if its biodiversity is treated as the national treasure that it represents.

6.1 REFERENCES

Andersen, A. N. 2019. Responses of ant communities to disturbance: Five principles for understanding the disturbance dynamics of a globally dominant faunal group. Journal of Animal Ecology 88:350–362.

Booher, D. B., J. C. Gibson, C. Liu, J. T. Longino, B. L. Fisher, M. Janda, N. Narula, E. Toulkeridou, A. S. Mikheyev, A. V. Suarez, and E. P. Economo. 2021. Functional innovation promotes diversification of form in the evolution of an ultrafast trap-jaw mechanism in ants. PLOS Biology 19:e3001031.

Chazdon, R. L. 2003. Tropical forest recovery: legacies of human impact and natural disturbances. Perspectives in Plant Ecology, Evolution and Systematics 6:51–71.

Chazdon, R. L., C. A. Harvey, O. Komar, D. M. Griffith, B. G. Ferguson, M. Martínez-Ramos, H. Morales, R. Nigh, L. Soto-Pinto, and M. Van Breugel. 2009. Beyond reserves: A research agenda for conserving biodiversity in human-modified tropical landscapes. Biotropica 41:142–153.

Chazdon, R. L. 2014. Second growth. Chicago: University of Chicago Press.

Crouzeilles, R., M. Curran, M. S. Ferreira, D. B. Lindenmayer, C. E. V. Grelle, and J. M. Rey Benayas. 2016. A global meta-analysis on the ecological drivers of forest restoration success. Nature Communications 7:11666.

Curran, M., S. Hellweg, and J. Beck. 2014. Is there any empirical support for biodiversity offset policy? Ecological Applications 24:617–632.

De Bello, F., C. P. Carmona, A. T. Dias, L. Götzenberger, M. Moretti, and M. P. Berg. 2021. Handbook of trait-based ecology: from theory to R tools. Cambrige: Cambridge University Press.

De Frenne, P., F. Zellweger, F. Rodríguez-Sánchez, B. R. Scheffers, K. Hylander, M. Luoto, M. Vellend, K. Verheyen, and J. Lenoir. 2019. Global buffering of temperatures under forest canopies. Nature Ecology & Evolution 3:744–749.

Delabie, J. H., B. Jahyny, I. C. do Nascimento, C. S. Mariano, S. Lacau, S. Campiolo, S. M. Philpott, and M. Leponce. 2007. Contribution of cocoa plantations to the conservation of native ants (Insecta: Hymenoptera: Formicidae) with a special emphasis on the Atlantic Forest fauna of southern Bahia, Brazil. Biodiversity and Conservation 16:2359–2384.

Delsinne, T., G. Sonet, Z. T. Nagy, N. Wauters, J. Jacquemin, and M. Leponce. 2012. High species turnover of the ant genus *Solenopsis* (Hymenoptera : Formicidae) along an altitudinal gradient in the Ecuadorian Andes, indicated by a combined DNA sequencing and morphological approach. Invertebrate Systematics 26:457–469.

Dent, D. H., and S. J. Wright. 2009. The future of tropical species in secondary forests: a quantitative review. Biological Conservation 142:2833–2843.

Escobar, H. 2018. In a 'foretold tragedy,' fire consumes Brazil museum. Science 361:960–960.

Fernández, F., R. J. Guerrero, and T. Delsinne. 2019. Hormigas de Colombia. Bogota: Univ. Nacional de Colombia.

Guenard, B. S., M. D. Weiser, K. Gomez, N. Narula, and E. P. Economo. 2017. The Global Ant Biodiversity Informatics (GABI) database: synthesizing data on the geographic distribution of ant species (Hymenoptera: Formicidae). Myrmecological News 24: 83–89.

Hanisch, P. E., P. D. Lavinia, A. V. Suarez, D. A. Lijtmaer, M. Leponce, C. I. Paris, and P. L. Tubaro. 2017. Mind the gap! Integrating taxonomic approaches to assess ant diversity at the southern extreme of the Atlantic Forest. Ecology and Evolution 7:10451–10466.

Hita Garcia, F., G. Fischer, C. Liu, T. L. Audisio, G. D. Alpert, B. L. Fisher, and E. P. Economo. 2017. X-Ray microtomography for ant taxonomy: An exploration and case study with two new *Terataner* (Hymenoptera, Formicidae, Myrmicinae) species from Madagascar. PLOS ONE 12:e0172641.

Holl, K. D., and R. A. Zahawi. 2014. Factors explaining variability in woody above-ground biomass accumulation in restored tropical forest. Forest Ecology and Management 319:36–43.

Klimes, P., C. Idigel, M. Rimandai, T. M. Fayle, M. Janda, G. D. Weiblen, and V. Novotny. 2012. Why are there more arboreal ant species in primary than in secondary tropical forests? Journal of Animal Ecology 81:1103–1112.

McGowan, J., L. J. Beaumont, R. J. Smith, A. L. M. Chauvenet, R. Harcourt, S. C. Atkinson, J. C. Mittermeier, M. Esperon-Rodriguez, J. B. Baumgartner, A. Beattie, R. Y. Dudaniec, R. Grenyer, D. A. Nipperess, A. Stow, and H. P. Possingham. 2020. Conservation prioritization can resolve the flagship species conundrum. Nature Communications 11:994.

Meli, P., K. D. Holl, J. M. Rey Benayas, H. P. Jones, P. C. Jones, D. Montoya, and D. Moreno Mateos. 2017. A global review of past land use, climate, and active vs. passive restoration effects on forest recovery. PLOS ONE 12:e0171368.

Pascarella, J. B., T. M. Aide, M. I. Serrano, and J. K. Zimmerman. 2000. Land-use history and forest regeneration in the Cayey Mountains, Puerto Rico. Ecosystems 3:217–228.

del Pliego, P. G., B. R. Scheffers, E. W. Basham, P. Woodcock, C. Wheeler, J. J. Gilroy, C. A. M. Uribe, T. Haugaasen, R. P. Freckleton, and D. P. Edwards. 2016. Thermally buffered microhabitats recovery in tropical secondary forests following land abandonment. Biological Conservation 201:385–395.

Sarnat, E. M., G. Fischer, and E. P. Economo. 2016. Inordinate Spinescence: Taxonomic Revision and Microtomography of the *Pheidole cervicornis* Species Group (Hymenoptera, Formicidae). PLOS ONE 11:e0156709.

Seddon, P. J., and T. Leech. 2008. Conservation short cut, or long and winding road? A critique of umbrella species criteria. Oryx 42:240–245.

Stork, N. E. 2018. How many species of insects and other terrestrial arthropods are there on earth? Annual Review of Entomology 63:31–45.

Ströbel, B., S. Schmelzle, N. Blüthgen, and M. Heethoff. 2018. An automated device for the digitization and 3D modelling of insects, combining extended-depth-of-field and all-side multi-view imaging. ZooKeys 759:1–27.

United Nations Environment Programme. 2021. Making Peace with Nature: A scientific blueprint to tackle the climate, biodiversity and pollution emergencies. Nairobi. https://www.unep.org/resources/making-peace-nature

Walpole, M. J., and N. Leader-Williams. 2002. Tourism and flagship species in conservation. Biodiversity and Conservation 11:543–547.

Whitworth, A., C. Beirne, R. Pillco Huarcaya, L. Whittaker, S. J. Serrano Rojas, M. W. Tobler, and R. MacLeod. 2019. Human disturbance impacts on rainforest mammals are most notable in the canopy, especially for larger-bodied species. Diversity and Distributions 25:1166–1178.

Whitworth, A., J. Villacampa, A. Brown, R. P. Huarcaya, R. Downie, and R. MacLeod. 2016. Past human disturbance effects upon biodiversity are greatest in the canopy; a case study on rainforest butterflies. PLOS ONE 11:e0150520.

Wijdeven, S. M., and M. E. Kuzee. 2017. Seed availability as a limiting factor in forest recovery processes in Costa Rica. Restoration Ecology 8:414–424.

Wilson, E. O. 2017. Biodiversity research requires more boots on the ground. Nature Ecology & Evolution 1:1590–1591.

ACKNOWLEDGEMENTS

This PhD would not have been possible – or, at least would've been so much worse – if it were not for the many people that inspired and supported me during these almost 4 years of research. The breakout of a global pandemic in early 2020 did not make things easier and lead to re-organization of my topics, and I was not able to finish some parts of my research. It's mostly thanks to the incredible support I received that I was finished my PhD with content and without larger delays.

First, I want thank those who were directly involved in the studies of this thesis:

Nico Blüthgen, who did an incredible job as a supervisor. I sincerely enjoyed working under your supervision, and your key insights that resulted from fruitful discussions have been of paramount importance to bascially all the scientific works presented here. Thank you for giving me your time and labspace, and also the very much fun field trips to Ecuador!

David Donoso, the ant person of Ecuador. I am super lucky to have such an amazing collaborator from Ecuador who shares my passion!

Adriana Argoti, thank you for doing an incredible job as field assisstent. I would've been very lost in Ecuador without your support, and not just during field work but during all Ecuador-related problems may it be sickness, permits, or angry farmers.

Michael Staab, I thank you for being the person I could always talk to in Darmstadt. Your broad knowledge in ecology and statistical experience was very valuable and I appreciated the time you sacrificied for my sometimes mundane problems. Plus, your own fascination for ants made you a perfect companion at the TU Darmstadt!

Christoph von Beeren, the human myrmecophile. I think you deserve not just a paragraph but whole book of acknowledgements. I am very grateful that you gave me the opportunity to work in Darmstadt and Costa Rica with army ants for my Master, and then later gave me so much support in writing with my thesis, and lab work. You are one of the most essential ingredients of this thesis.

Doug Booher, I thank you a lot for your help with the description of *Strumigenys*. Without you, surely this ant would be still without name.

John Lattke, thank you for your incredible taxonomic expertise and the always very friendly input. It was a pleasure to work with you.

I sincerely thank the 3D scanner team of Darmstadt consisting of Bernhard Ströbel, Sebastian Schmelzle and Michael Hetthoff. The scans improved the taxonomic works by a large margin, and I am very grateful for this lucky opportunity.

Also, my gratefulness extendends to the teams of Jocotoco and Tesoro Escondido. In particular, I thank Martin Schäfer, Michael Moens, Citlalli Morelos-Juárez, Efraim Cepeda, Yadria Giler, and so many more, for their constant help. All my field stays were an incredible experience, and I am grateful for the help during field work. The many parabiologists and park rangers have all contributed a lot to this thesis: Bryan Amayo, Alcides Zombrano, Roberto de la Cruz, Jorge Zambrano, Amado de la Cruz, Miguel Marcias, Patricio Encarnación, Vanessa Moreira, and many more.

An important part of my thesis was supported by the all the people in the lab of Darmstadt. I am grateful for the warm welcome and the good coffee, so that I had a relaxed and enjoyable work environment. Thanks especially to Andrea Hilpert, Karin Römer, Karen Pederson, Fernando

Villagomez, Nadja Simons, Katja Wehner, Genieve Walther, among others. A great thank you goes to my two Bachelor students, Matteo Trevisan and Basma Khalid, for their help in measuring ant specimens. Further, I express my sincere thanks to Karsten Mody and Adrian Brückner both for their scientific input as well as their guidance in the field.

I am very grateful and indepted to the support of the Deutsche Studienstiftung. Without their financial and ideational support, this research would not have been possible.

I thank my friend circle at my old university in Würzburg. After almost 4 years in Darmstadt, I still feel more at home in Würzburg than anywhere else. Thank you for organizing so many amazing parties (including my birthdays), and having engaged scientific discussion, and sometimes both at the same time: In particular, Patrick Kohl, Benjamin Rutschmann, Fabian Bötzl, Mathias Reese, Nils Schuhmacher, Justine Vasynghel, Cassandra Vogel, Daniel Villalobos, Cristina Ganuza Vallejo...! And so many more.

I thank Gemma Nydia Villagomez from all my heart for her lovely and never-ending support, conservations and fun field trips! My life would have been so much duller without your smile.

Finally, I am very grateful to my family; My father Jürgen Hönle for his constant support and allowing me to follow my ant dreams and Kung for making such delicious german-thai crossover food. I also am very grateful for the support from my brother Jonas, my sister Tabea and my brother-in-law Maurice. I thank my little niece Ellie for giving me a fun time and making me smile.

EHRENWÖRTLICHE ERKLÄRUNG

Ich erkläre hiermit ehrenwörtlich, dass ich die vorliegende Arbeit entsprechend den Regeln guter wissenschaftlicher Praxis selbstständig und ohne unzulässige Hilfe Dritter angefertigt habe.

Sämtliche aus fremden Quellen direkt oder indirekt übernommenen Gedanken sowie sämtliche von Anderen direkt oder indirekt übernommenen Daten, Techniken und Materialien sind als solche kenntlich gemacht. Die Arbeit wurde bisher bei keiner anderen Hochschule zu Prüfungszwecken eingereicht.

Ort, Datum

……………………………………………………………………

Philipp Hönle

CURRICULUM VITAE

Philipp Otto Hoenle

Date of Birth: 06.07.1992

Place of Birth: Leonberg

Nationality: German

Adress:

Bessunger Str. 14

64347 Griesheim, Germany

philipp.hoenle92@gmail.com

Education

2015 Bachelor of Science Biology, University of Würzburg

Thesis: „Optimal trail choice and learning in the Matabele Ant *Megaponera analis* (Fabr.)". Supervisor: Prof. K.E. Linsenmair; grade: 1.7 [grade system: 1 best – 5 worst]

2018 Master of Science Biology, University of Würzburg

Thesis: „Diet specialization in Neotropical army ants". Advisors: Dr. Brigitte Fiala & Dr. Christoph von Beeren; grade: 1.0

Since **2018**: PhD (in progress), Technical University of Darmstadt

Thesis Topic: Ant Recovery Dynamics in Ecuador. Advisors: Prof. Dr. Nico Blüthgen & PD Dr. Michael Heethoff

Interests & skills

Science Communication

Since 2010 Admin and Co-Founder of the German interest group "Eusozial", which manages an internet forum interested in ant biology and ant keeping (eusozial.de)

Since 2018 Editor of the Myrmecological News Blog, an online outlet of the international journal "Myrmecological News". For this I conduct interviews, post photoblog contributions and help in the editing process (blog.myrmecologicalnews.org)

Science Videos

Several of my videos were used for television shows:

- '1, 2 oder 3' Famous German Television Show for children; channel ZDF (2018)
- 'Wer weiß denn sowas?' Quiz show; channel: ARD (2017)
- 'Ziyology', Discovery Channel Canada (2017)

- ‘La terre vue du Coeur’ (Earth from the Heart), documentary of Jane Losa Films Québec (2018)

- ‘True facts: Army ant riders’ documentary by YT personality ‘ze frank’, currently 2.1 mio views (2020) (https://www.youtube.com/watch?v=p16g5IVCdeE)

Macrophotography

Several of my photographs were used in scientific publications (e.g., Molecular Ecology, PeerJ) as well as in the following media outlets:

- Royal Society Publishing Photo Contest, Honourable Mention for the picture “Army Ant Intruder” (2018; https://royalsociety.org/journals/publishing-activities/photo-competition/2018-winners-runners-up/behaviour)

- Several photoblogs published at the Myrmecological News Blog:
  Ant course 2018 (co-written with Mark Wong) https://blog.myrmecologicalnews.org/2018/10/16/ant-course-2018/

- Photographic journey to the Ants of Ecuadorian Chocó
  https://blog.myrmecologicalnews.org/2019/06/19/a-photographic-journey-to-the-ants-of-the-ecuadorian-choco/

- A short photographic trip to the Ants of Northern Italy
  https://blog.myrmecologicalnews.org/2019/11/13/a-short-photographic-trip-to-northern-italy/

- A photographic glimpse into Brazils ant diversity
  https://blog.myrmecologicalnews.org/2020/02/19/a-photographic-glimpse-into-brazils-ant-diversity/

- Ants among Mesoamerican ruins
  https://blog.myrmecologicalnews.org/2020/09/30/ants-among-mesoamerican-ruins/

Field experience & Volunteering

Malaysia

09/2013 – 04/2014

Internship on the behaviour & conservation of pig-tailed macaques (macaca-nemestrina.org)

08/2016 – 10/2016

Research on the odd interaction of two ant species in a mimicry system: *Polyrhachis rufipes* and *Gnamptogenys menadensis*

Ivory Coast

08/2015 – 11/2015

Fieldwork for my Bachelor thesis on the behavior of the Matabele Ant *Megaponera analis*.

First preliminary ant collection of the Comoé NP

Internship for the Comoé Chimpanzee Conservation Project (https://www.facebook.com/comoechimpanzeecp)

Costa Rica

02/2017 – 04/2017

Field work for my Master thesis on the diet of Neotropical army ants

Internship on the colony integration mechanisms of army ant associates

Ecuador

01/2018 – 04/2018

02/2019 – 05/2019

09/2021 – 10/2021

Field work for my PhD thesis in the Río Canandé Reserve

Attendend Courses

2015 European Ant Course, Center for Social Evolution, Copenhagen, Denmark

2016 Asian Myrmecology Workshop, UP Diliman, Manila, Philippines

2018 The Ant Course, California Academy of Sciences, French Guiana

2019 Social Evolution Course, Center for Social Evolution, Copenhagen, Denmark

Presentations

2017 Hoenle, P.O., von Beeren, C., Fiala, B. Diet specialization in army ants. Presentation at the meeting of the International Union for the Study of Social Insects (IUSSI) 2017, Kloster Schöntal, Deutschland

2019 Hoenle, P.O., von Beeren, C., Donoso, D., Lattke, J., Blüthgen, N. A conspicous new species of *Odontomachus* trap-jaw ants from Ecuador. Poster at the Simpósio de Mirmecologia, Belo Horizonte, Brazil.

Scholarships

2014 PROMOS: Program for the increase of mobility of students from German universities, granted by the German Academic Exchange Service (DAAD)

2018 PhD Scholarship of the German Academic Scholarship Foundation

Teaching

2017 Co-Instructor for Insect Taxonomy & Biology, University of Würzburg

2018 Supervising the Bachelor thesis: „Ant Traits across a land-use gradient in Ecuador", TU Darmstadt

2019 Lecture and seminar for master students: "Ants and their important ecological role", TU Darmstadt

Awards

2011 Jugend Forscht (youth research) regional competition, 2nd place

Topic: ‚Koloniegründung der Stöpselkopfameise Camponotus truncatus unter verschiedenen Bedingungen' (Colony foundation of the truncated ant Camponotus truncatus)

2012 Biology graduate Award

For outstanding achievements in the biology subject during the German high school (Abitur), awarded by the VBio Rheinland-Pfalz

2017 IUSSI: Best Student Talk, 3rd place

For the presentation at the Central European Meeting oft he IUSSI (International Union for the Study of Social Insects), Kloster Schöntal, Germany.

2020 OTS Kimberly G. Smith Award for Outstanding Student Paper, Honorable Mention For the paper Hoenle et al. (2019) 'Species-level predation network uncovers high prey specificity in a Neotropical army ant community'

Publications

Scientific

- **Hoenle, P.O.**, Frank, E.T.F., Linsemair, K.E. (2018) Optimal path choice in the termite hunting ant *Megaponera analis*. Journal of Experimental Biology 221: doi:10/jeb.1242/174854

- Brückner, A., **Hoenle, P.O.**, von Beeren, C. (2018) Comparative chemical analysis of army ant mandibular gland volatiles (Formicidae: Dorylinae) PeerJ 6:e5319; doi: 10.7717/peerj.5319

- **Hoenle, P.O.**, Blüthgen, N., Brückner, A., Kronauer, D.J.C., Fiala, B., Donoso, D.A., Smith, A., Ospina Jara, B., von Beeren, C. (2019) Species-level predation network uncovers high prey specificity in a Neotropical army ant community. Molecular Ecology 28(9): 2423-2440

- **Hoenle, P.O.**, Lattke, J., Donoso, D., von Beeren, C., Heethoff, M., Schmelzle, S., Argoti, A., Camacho, L., Ströbel, B., Blüthgen, N. (2020) *Odontomachus davidsoni* sp. nov. (Hymenoptera, Formicidae), a new conspicuous trap-jaw ant from Ecuador. Zookeys 948: 75-105

- **Hoenle, P. O.**, Booher, B. (2021) A new species-group of *Strumigenys* (Hymenoptera, Formicidae) from Ecuador, with a highlighted description of its mandible morphology. Zookeys 1036: 1-9

- von Beeren C., Blüthgen N., **Hoenle P.O.**, Pohl S., Brückner A., Tishechkin A.K., Maruyama M., Brown B.V., Hash J.M., Hall W.E., Kronauer D.J.C. (2021). A remarkable legion of guests: Diversity and host specificity of army ant symbionts. Molecular Ecology, https://doi.org/10.1111/mec.16101

- von Beeren C., Brückner A., **Hoenle P.O.**, Ospina-Jara B., Kronauer D.J.C., & Blüthgen N. (2021). Multiple phenotypic traits as triggers of host attacks towards ant symbionts: body size, morphological gestalt, and chemical mimicry accuracy. Frontiers in Zoology 18:46; https://doi.org/10.1186/s12983-021-00427-8

- **Hoenle P.O.**, Donoso, D., Argoti, A., Staab, M., von Beeren, C. & Blüthgen, N. (accepted). Rapid ant community re-assembly in a Neotropical forest: recovery dynamics and land-use legacy. Ecological Applications

- **Hoenle P.O.**, Staab, M., Donoso, D., Argoti, A., & Blüthgen, N. (in prep). Stratification and recovery time jointly shape ant functional re-assembly in a Neotropical forest.

Popular Science

- **Hoenle, P.O.** (2010) Auf den Spuren der Ameisen – eine Suche nach den familiären Krabblern in Thailand. ZAG Phoenix 1(1): 28-46 (Translation: On the trail of the ants – a search for the familiar critters in Thailand)

- **Hoenle, P.O.** (2013) Ameisen im Terrarium – Die Vielfalt des Superorganismus. Bugs, das Wirbellosenmagazin 1(4): 14-19 (Translation: Ants in Terrariums – the Diversity of the Superorganism)

- **Hoenle, P.O.** (2013) Schnappkieferameisen der Gattung Myrmoteras – Beobachtungen und Haltungserfahrungen. Bugs, das Wirbellosenmagazin 1 (4): 26-29 (Translation: Trap-jaw ants of the genus Myrmoteras – Observations and Keeping Experiences)